UFMG
UNIVERSIDADE FEDERAL
DE MINAS GERAIS

Doctoral Thesis

New methods for consensus in multiagent systems

Novos métodos para consenso em sistemas multiagentes

by **Heitor Judiss Savino**

supervised by
Prof. Dr. Fernando de Oliveira Souza
Prof. Dr. Luciano Cunha de Araújo Pimenta

Graduate Program in Electrical Engineering
Universidade Federal de Minas Gerais
Belo Horizonte, MG – Brazil
September 30, 2016

UNIVERSIDADE FEDERAL DE MINAS GERAIS
Graduate Program in Electrical Engineering

NEW METHODS FOR CONSENSUS IN MULTIAGENT SYSTEMS

NOVOS MÉTODOS PARA CONSENSO EM SISTEMAS MULTIAGENTES

Doctoral thesis presented to the Graduate Program in Electrical Engineering of the Federal University of Minas Gerais in partial fulfillment of the requirements for the degree of Doctor in Electrical Engineering.

Tese de doutorado apresentada ao Programa de Pós-Graduação em Engenharia Elétrica da Universidade Federal de Minas Gerais como requisito parcial para a obtenção do grau de Doutor em Engenharia Elétrica.

Heitor Judiss Savino

Advisor: Prof. Dr. Fernando de Oliveira Souza
Co-Advisor: Prof. Dr. Luciano Cunha de Araújo Pimenta

Thesis Committee:

Reinaldo Martinez Palhares	Prof. Dr., UFMG
Bruno Vilhena Adorno	Prof. Dr., UFMG
Valter Júnior de Souza Leite	Prof. Dr., CEFET-MG/Divinópolis
Leonardo Amaral Mozelli	Prof. Dr., UFSJ/Ouro Branco

Belo Horizonte, MG – Brazil

September 30, 2016

UNIVERSIDADE FEDERAL DE MINAS GERAIS
Graduate Program in Electrical Engineering

NEW METHODS FOR CONSENSUS IN MULTIAGENT SYSTEMS

Doctoral thesis presented to the Graduate Program in Electrical Engineering of the Federal University of Minas Gerais in partial fulfillment of the requirements for the degree of Doctor in Electrical Engineering.

Approved in September 30, 2016:

Fernando de Oliveira Souza,
Prof. Dr., Advisor

Luciano Cunha de Araújo Pimenta,
Prof. Dr., Co-Advisor

Reinaldo Martinez Palhares,
Prof. Dr., UFMG

Bruno Vilhena Adorno,
Prof. Dr., UFMG

Valter Júnior de Souza Leite,
Prof. Dr., CEFET-MG/Divinópolis

Leonardo Amaral Mozelli,
Prof. Dr., UFSJ/Ouro Branco

Aos meus pais.

Acknowledgments

I can't think of a better example to show the results that can be obtained from a multiagent system than this thesis itself. Many contributions and many inputs, with a lot of exchange in information, discussions, and... consensus. My main role during these four years was to manage all this rich information from all the people who collaborated with me, and give it a direction, which is summarized next in this final text. Therefore, I have many people to thank. Without all of them, this work would have never been possible.

I would like to thank, initially, to my academic advisors Prof. Fernando Souza and Prof. Luciano Pimenta. I'm very lucky to be supervised by these two extraordinary professors. I will always be grateful for being received by them as a student. I have learned so much with our discussion on many topics, and I appreciate all the opinions I have heard from them, and for being heard by them with so much esteem.

I must thank all the professors in the Graduate Program in Electrical Engineering at UFMG, their directions in so many valued topics were of great importance for the development of this work. I owe special thanks to Professor Reinaldo Palhares for receiving me in his laboratory when I wasn't even a graduate student at UFMG, and for introducing me to the professors who would come to be my advisors. I would also like to thank all the advices, friendly and professional talks I've had with Prof. Leonardo Torres, Prof. Eduardo Mazoni, Prof. Luis Aguirre, Prof. Benjamim Menezes, Prof. Guilherme Pereira, Prof. Guilherme Raffo, Prof. André Paim, Prof. Ricardo Adriano, Prof. Rodney Saldanha, and many others in UFMG. Every word I've heard from you had great impact in me, both professionally and personally.

A special thanks goes to Professor Bruno Adorno, who initiated the collaboration with MIT and included me as part of this project. I really appreciate all I've learned with him, and I'll always have the memory of working together with him and Professor Luciano Pimenta in the laboratories of MIT as one of my most valuable experiences. In the same line, I would like to thank Professor Julie Shah for opening the doors of the Interactive Robotics Group (IRG) to me, and making me feel so welcome to this excellent group. Her feedbacks and the trust put on me and the work of our UFMG team has made possible

the collaboration and the results presented in this text, with many future results to come. To the IRG members Abhi, Alex, Ankit, Been, Brad, Chongjie, Monaco, Claudia, Jessie, Joe, Jorge, Keren, Kyle, Lindsay, Matthew, Michael, Pem, Ramya, Rebecca, and Vaibhav, thank you for all the pleasant talks and making me feel like we have always known each other. I've learned so much from you, and I've really enjoyed all of our meetings and retreats, "tenquiu".

To the members of DIFCOM during these years in UFMG, Anna Paula, Carlos, Fulvia, Klenilmar, Guilhermão, Antoniel, Wagner, Sajad, Tiago, Ramon, and Daniel, and colleagues of the PPGEE, Reza, Roozbeh, Diana, Fred, Lucas (Alemão), Ana, Rafael, Ernesto, and Brenner, thank you all for being so supportive and for sharing this experience with me. I have enjoyed so much your company through these years and I wish you all great success in all of your plans. A special thanks to Anna Paula for being my first partner in consensus problems and to Antoniel for playing a role of thesis reader. I also thank to the groups MACRO and CORO, at UFMG for the space and support provided for the development of this work.

Without the support of my family and friends I would probably have never started this graduate study. Thus, thanks to my mother Marina, my father Nestor, my brothers Bruno and Beto, and my sister Silvina. Thanks to the family who received me as one of their own in Belo Horizonte, Edmundo, Elcy, Julia, Else, Luiz, Maria Clara, Luiz Mario, Helen, Camila, Jojô, Zé, and Junior. And thanks to my Brazilian friends in Boston, Ivo, Paulo, Mayara, Marisa, and Erica. Each of you has made this journey a bit more pleasant.

Finally, I would like to thank the Brazilian agency CNPq for the economical support provided during my years at UFMG and during my exchange program at MIT, to MISTI MIT-Brazil Program, and to the Brazilian agency CAPES.

Not everyone can become a great artist, but a great artist can come from anywhere.
Ratatouille

Abstract

Consensus refers to achieving an agreement on a variable of interest on all the agents in a multiagent system by sharing and/or acquiring information within other agents. Its applications are given in the field of multiagent systems that work cooperatively by sharing information in a networked manner. Many problems such as formation control, flocking, and platoon, can be addressed using consensus-based approaches. Additionally, as communication and processing rely on processes subject to time-delays, the analysis of the delays is of major importance for networked applications, as it may cause great impact in the system's response, avoiding or enabling consensus and consequently the execution of the task. The starting point of the methodology is the translation of the consensus problem into a stability problem, thus analyzed with the vast theory for linear systems. The impacts of delays in communication and input delays are presented to show the importance of analyzing the delays in intervals considering lower and upper bounds for time-varying delays. Thereby, results considering the analysis of consensus with the considered bounds are presented by means of sufficient conditions described by linear matrix inequalities (LMIs), using Lyapunov-Krasovskii theory. Failures in the communication links, changes in the agents arrangement, or obstructions on sensing are described by switching topologies, modeled as Markov jump linear systems, with uncertain transition rates. In order to increase the delay margins or improve convergence rate of the system, a method for the design of the coupling strengths is presented, also by means of LMIs. Finally, single-order consensus is applied in real-world problems in cooperative robotics, based on the extension of consensus on dual quaternions, which describe the pose of rigid-bodies adequately. Through all the text, examples are presented to show the performance of the methods with application-oriented problems.

Keywords: Consensus, time-delay, Lyapunov-Krasovskii, multiagent systems, LMI, Markov Jump linear systems, switching topology, coupling strengths, cooperative robotics, pose, dual quaternions.

Resumo

Consenso se refere a atingir um acordo em uma determinada variável de interesse em todos os agentes de um sistema multiagente por meio da troca/aquisição de informações com os demais agentes. Suas aplicações são dadas no campo de sistemas multiagentes que operam de forma cooperativa por meio da troca de informações em rede. Vários problemas como controle de formação, enxame, rebanho e comboio, podem ser tratados utilizando-se abordagens de consenso. Além disso, dado que a comunicação e o processamento da informação dependem de processos sujeitos a atrasos no tempo, a análise destes é de grande importância para aplicações em rede, dado que podem causar grande impacto na resposta do sistema, evitando ou permitindo atingir consenso e consequentemente a execução da tarefa. O ponto de partida da metodologia utilizada é a tradução do problema de consenso em problema de estabilidade, sendo então analisado com a ampla teoria de sistemas lineares. O impacto dos atrasos de comunicação ou entrada são apresentados para mostrar a importância de analisar o atraso considerando intervalos com limites inferiores e superiores para atrasos variantes no tempo. Com isto, resultados considerando a análise de consenso com os limites impostos são apresentados por meio de condições suficientes descritas por desigualdades matriciais lineares (LMIs), usando a teoria de Lyapunov-Krasovskii. Falhas nos enlaces de comunicação, mudanças no arranjo dos agentes ou obstruções nos sensores são descritas pelo chaveamento da topologia de rede, modelado como um sistema linear sujeito a saltos markovianos com taxas de transição incertas. De modo a aumentar as margens de atraso ou melhorar a taxa de convergência do sistema, é apresentado um método para o projeto dos ganhos de acoplamento nos enlaces entre os agentes, também baseado em LMIs. Finalmente, o problema de consenso em agentes de primeira ordem é aplicado em problemas reais de robótica cooperativa, baseando-se na extensão de consenso utilizando quatérnios duais, que descrevem a pose de corpos rígidos adequadamente. Ao longo do texto são apresentados exemplos para mostrar o desempenho dos métodos com problemas centrados em aplicações.

Palavras-chave: Consenso, atraso no tempo, Lyapunov-Krasovskii, sistemas multiagentes, LMI, saltos markovianos, topologia chaveada, ganhos de acoplamento, robótica cooperativa, pose, quatérnios duais.

List of Figures

List of Tables

List of Symbols

$\mathbb{R}$ Set of Real Numbers.

$\mathbb{N}$ Set of Natural Numbers.

$\mathbb{Z}$ Set of Integer Numbers.

$\mathbb{H}$ Set of Quaternions.

$\mathbb{E}$ Expectancy.

$\mathcal{H}$ Set of Dual Quaternions.

M^T Transpose of a matrix M.

$\dot{x}(t)$ First time-derivative of $x(t)$.

$\ddot{x}(t)$ Second time-derivative of $x(t)$.

$\mathcal{G}$ Simple Directed Graph.

I_n Identity Matrix of size n.

1_n Column-vector of ones with size n.

0_n Column-vector of zeros with size n.

0 Zero matrix with appropriate dimension.

$\otimes$ Kronecker Product

$M > 0$ Denotes a Positive Definite Matrix M.

$M < 0$ Denotes a Negative Definite Matrix M.

$M^\dagger$ Moore-Penrose pseudoinverse of M.

$\min(x, y, ..., z)$ Returns the minimum value of the arguments.

$\text{sign}(x)$ Returns sign of the argument x.

$\emptyset$ Empty set.

$\det(M)$ Determinant of a matrix M.

$\boldsymbol{x}$ Denotes a quaternion.

$\underline{\boldsymbol{x}}$ Denotes a dual quaternion.

$|\cdot|$ Module operator.

$||\cdot||$ Norm operator.

$*$ In a matrix represents a symmetric, transpose, element.

$\lambda_i\{\cdot\}$ The i-th eigenvalue of a matrix.

$\lambda_{\max}\{\cdot\}$ The maximum eigenvalue of a matrix.

$\lambda_{\min}\{\cdot\}$ The minimum eigenvalue of a matrix.

$\text{diag}\{d_1, \ldots, d_n\}$ Diagonal matrix with elements $d_1, \ldots, d_n$ in the main diagonal.

$\sup\{\cdot\}$ Supremum element in a set.

$\mathcal{F}$ Reference frame.

$G \ltimes H$ Denotes the semidirect product of a group G by a group H.

$A_{\square}$ The index $\square$ denotes an arbitrary subindex for matrix A.

List of Abbreviations

LMI Linear Matrix Inequality.

BMI Bilinear Matrix Inequality.

MJLS Markov Jump Linear System.

LKF Lyapunov-Krasovskii Functional.

Contents

Chapter 1

Introduction

There is a growing interest in systems composed of multiple agents that work cooperatively by sharing information in a networked manner. This growth is mainly given due to the recent advances in communication systems, with the ease to enable digitally controlled devices to work connected in a network. In addition to the reduction in size and cost of electromechanical devices and the boost in computational power, networked systems have become an increasingly recurrent scenario. This kind of systems is referred to as multiagent system, i.e. a system composed of several distributed parts, sharing information and working cooperatively in order to accomplish a common objective (Tanenbaum and Van Steen, 2007). In fact, one of the most important attributes of an intelligent system is the ability to communicate. Communicating and sharing information allows an agent to distribute/cooperate in tasks. The distribution of tasks makes the multiagent system robust to failures and endows intelligent group behavior. In addition, it mainly allows the execution of tasks that a single agent would not be able to accomplish, e.g. the transportation of heavy duty loads. Some cutting-edge applications of multiagent systems can be highlighted in topics like Internet of Things (Greengard, 2015), Cloud Computing (Ruparelia, 2016), and Cloud Robotics, referred to as one of the 10 breakthrough technologies for the year 2016 (Schaffer, 2016).

One of the ongoing topics covered by the theory of multiagent systems is called consensus. The meaning of consensus problem is to make all the agents in a multiagent system achieve an agreement on a variable of interest, assuming that each agent is able to share and/or acquire information within a subset of other agents, called neighbors. Applications of consensus are found in many practical fields, such as traffic jams in communication networks (Li et al., 2011b), formation of autonomous mobile agents (Ren, 2007), page ranking (Ishii and Tempo, 2014), robotics (Hatanaka et al., 2015), etc. Many other results are summarized by Cao et al. (2013). Next section covers an overview and part of the history of this topic.

1.1 History

Consensus problem has its origins in statistics, in the decades of 1960 and 1970. At that time, the main concern was with the problem of social learning process, and some methods were presented to describe how a group of individuals reach an agreement about a common goal. This problem was discussed by many authors, among those it can be referred the works of Eisenberg and Gale (1959), Stone (1961), Norvig (1967), and Winkler (1968). The work of DeGroot (1974) can be highlighted, it once described a group of individuals acting together as a team, in which each individual had its own subjective probability distribution regarding the opinion about some given parameter. The author described a model on how the team achieves a common subjective probability distribution through the exchange of information and the combination of the individuals' beliefs by weighting and averaging the opinions, deprived of taking any new information from the environment.

Later on, with the advent of coordinated multiagent systems, one of the major problems was the one of establishing distributed control laws based on the information exchanged between the agents, such that an agreement could be achieved on a common value of a given variable of interest. Seminal results emerged in physics (Vicsek et al., 1995) and distributed algorithms (Lynch, 1996), borrowing the main ideas of consensus originated in the field of statistics regarding the exchange of information between the agents.

The work of Vicsek et al. (1995) described the self-ordered motion of a system composed of multiple particles. At each time step, each particle assumed the average direction of neighboring particles in a given distance radius, introducing in multiagent systems the concept of neighborhood and the interaction with neighbors only. This inspiration came from parallel advances in the field of biology and computer graphics, in the biological description of the function of fish schools (Partridge, 1982), and from the behavioral models of flocks, herds and schools for computer graphic simulations in the work by Reynolds (1987).

At the end of the 90's, the problem of flight formation arose as one of the enabling technologies for the 21^{st} century. The purpose was to extend the control of a single spacecraft to the control of a group of it, flying in a particular designated arrangement. Some authors like the ones by Wang et al. (1999), Mesbahi and Hadaegh (1999), and Mesbahi and Hadaegh (2001) considered the leader-following model, and the latter can be emphasized by the usage of the graph interpretation of the problem and also the derivation of control laws based on Linear Matrix Inequalities (LMIs).

The problem of formation control was being addressed at the same time in the field

of robotics. Research was focused on the extension of motion planning algorithms to the control of multiple robots in a distributed manner, as pointed by Wang and Beni (1988) and Sugihara and Suzuki (1990). The purpose was to enable a group of robots to cooperate in order to accomplish a global task under the government of a protocol (a distributed algorithm), executed individually by each robot. These simple protocols borrowed ideas from Cellular Automata (Neumann and Burks, 1966), in which global complex tasks can be accomplished with the cooperation between many agents with the execution of simple individual rules. Some of the results refer to the formation of circular patterns (Tanaka, 1992), and, further, to more general geometric patterns (Suzuki and Yamashita, 1999).

Within all the theoretical advances, it was noted that the control architecture of a multiagent system is strongly affected by the corresponding sensing and communication topology (Mesbahi and Hadaegh, 2001; Mesbahi, 2002). At that point, Fax and Murray (2002) and Jadbabaie et al. (2003) applied the algebraic theory of graphs to write the relationship between neighboring agents as presented in the work of Vicsek et al. (1995). Henceforth, the network topology could be described algebraically, inheriting terms from graph theory like: directed, when the information flow can be unidirectional; or undirected, when the flow is bidirectional. This algebraic approach assisted on better understanding the impacts of the topology and model the multiagent dynamics, and many other results emerged, such as the ones by Olfati-Saber and Murray (2003), Olfati-Saber and Murray (2004), Ren and Beard (2005), etc. The present work makes use of this algebraic approach.

1.1.1 Consensus in Robotics

Some recent works have considered the problem of consensus in robotic networks composed of multiple mobile manipulators, in which the objective might be to achieve a common configuration on the joints in order to execute some tasks, like grasping or carrying an object. The work by Cheng et al. (2008) considered the uncertainties in the model of the manipulators and showed an adaptive consensus protocol to reach consensus on the joints. Hou et al. (2009) considered also the presence of external disturbances. In the work of Ge and Dongya (2014) the problem of consensus is treated using robust control techniques. Most of these works have dealt with Euler-Lagrange models, and some have also considered a model description that uses quaternions to represent orientation (Aldana et al., 2015). Additionally, the application of dual quaternions is of great interest since complex systems can be easily modeled with dual quaternions using a whole-body approach (Adorno, 2011).

An interesting use of consensus-based algorithms in robotics is for solving decentralized formation control problems as in the work by Schwager et al. (2011). In fact, several tasks

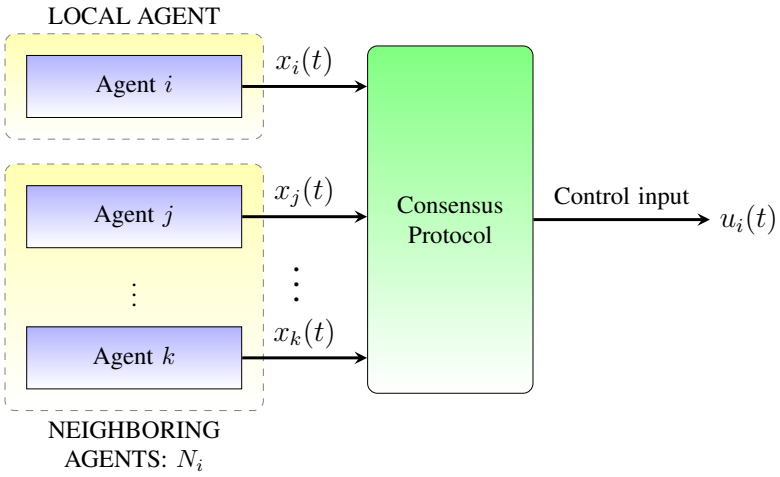

Figure 1.1: Block diagram for the consensus protocol.

may benefit from solutions of formation control, such as cooperative load transportation to move flexible payloads (Bai and Wen, 2010). Besides, rigid formation problems have also been considered by Mou et al. (2014) and Sun et al. (2015).

Next section presents and describes the application of consensus protocol with an introductory example.

1.2 Consensus Protocol

In the literature, the distributed control law devised to drive the agent states to consensus is commonly denominated as consensus protocol. The protocol provides the agent's control input and is usually based on the difference between the agent's own state and the states of its neighbors. Figure 1.1 illustrates the application of the consensus protocol by an arbitrary agent i in a multiagent system. The neighboring agents of i are represented by the set N_i, such that $j, \ldots, k \in N_i$. The agent's local state is represented by $x_i(t) \in \mathbb{R}$ and the state of a neighboring agent j or k is represented by $x_j(t) \in \mathbb{R}$ or $x_k(t) \in \mathbb{R}$, respectively. The protocol is any function taking into account the agent's local state and all the states of its neighbors $f_i = (x_i, x_j, \ldots, x_k)$, $j, \ldots, k \in N_i$, and is executed locally by each agent. The protocol returns the control input $u_i(t) \in \mathbb{R}$ for an agent i. The most prevailing consensus protocol in the literature is the linear consensus protocol introduced by Olfati-Saber and Murray (2003), given by

$$u_i(t) = -\sum_{j \in N_i} a_{ij}(x_i(t) - x_j(t)), \tag{1.1}$$

where a_{ij} is the gain related to the information from agent j to agent i, for all $j \in N_i$.

Consider, as an example, a group of individuals discussing the height of a building they

want to build, as shown in Figure 1.2. The blue individual (agent 1) wants a building with a height of 26m, the pink individual (agent 2) wants a height of 20m, and the green one (agent 3) suggests 12m. Therefore, the initial conditions of this problem are $x_1(0) = 26$, $x_2(0) = 20$, and $x_3(0) = 12$. The next step is to define the network topology and the gains a_{ij} related to the communication links. If the individuals can only talk to the immediate neighbors the information flow can be defined as in Figure 1.2, where agent 2 can listen to both agents 1 and 2, with $a_{21} = a_{23} = 1$, and the others can only listen to agent 2, $a_{12} = 1$ and $a_{32} = 1$. With this information, protocol (1.1) can be applied, and one can consider that the assumption that each individual opinion varies continuously according to

$$\dot{x}_i(t) = u_i(t). \tag{1.2}$$

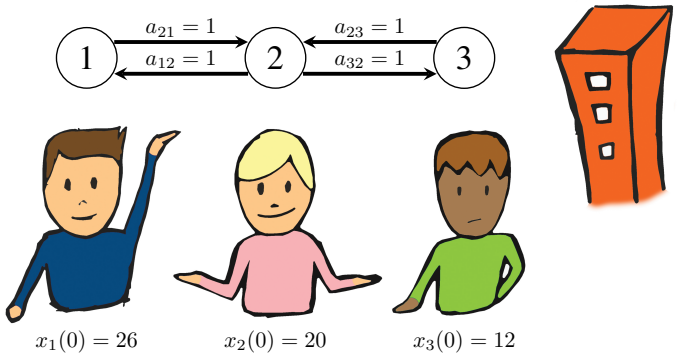

Figure 1.2: Individuals consensus problem.

With these parameters defined, a simulation is carried out to show the evolution of the individuals' opinions as consensus is reached, presented in Figure 1.3. The representation of the agents' states along time presented in Figure 1.3 will be widely used in this text to show whether consensus is achieved or not. From this figure the final value and the time spent to achieve consensus can be assessed. For this example, the individuals reach a consensus that the height of the building to be constructed is the consensus value as time goes to infinity $\lim_{t\to\infty} x_i(t) \approx 19.3$m.

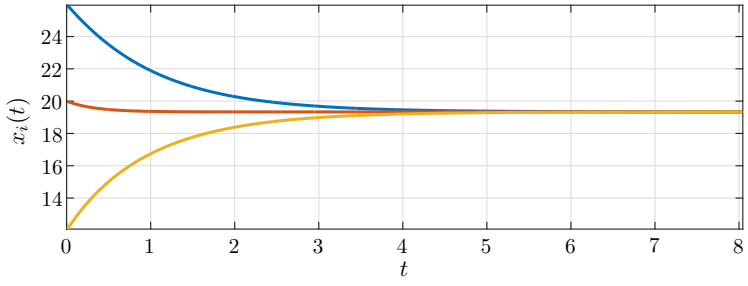

Figure 1.3: Individuals' opinions reaching consensus.

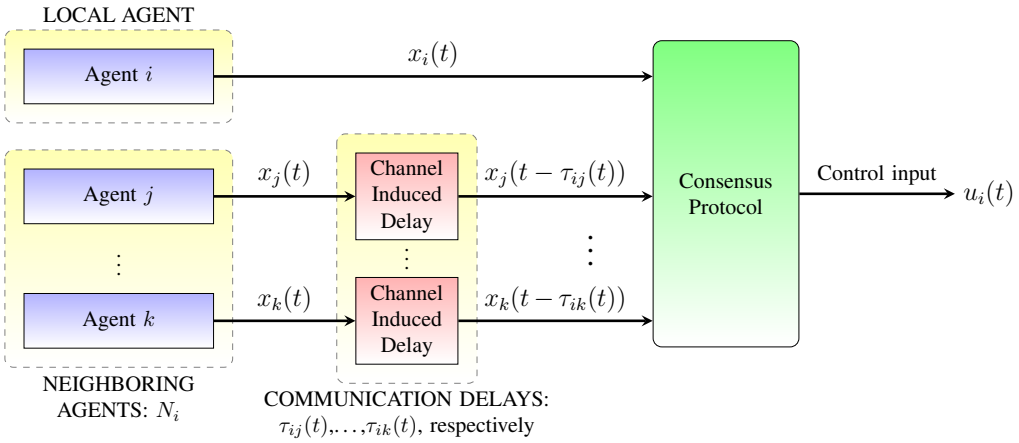

Figure 1.4: Block diagram for the consensus protocol with communication delays.

More recently, the topic of consensus has been considered to deal with a variety of scenarios. Major concerns have been in the consideration of real issues arising from the application of communication networks, specifically time-delays and switching topologies. An overview with the implications of delays is presented in the next section.

1.3 Time-delay in Consensus Protocol

In practice, time-delays are always present in the agents' interactions. This is mainly given due to computational and physical limitations in information processing, transmission channels, time-response of actuators, etc. The presence of delays has a great impact on consensus problems as it can make the system oscillate or diverge about the variable of interest (Lin et al., 2009). Based on this fact, many works have dealt with consensus problems subject to different forms of time-delays.

The class of delays given by the time spent by an agent i to acquire information from an agent j —or the time spent to carry information from the j-th agent to the i-th agent— which can arise naturally due to physical characteristics of communication channels or sensing, is called communication delay. This delay can be represented by $\tau_{ij}(t)$, and essentially indicates how old is the information that agent i has from agent j, at the instant of time t when agent i is locally running the consensus protocol. The occurrence of communication delays is illustrated in Figure 1.4, where the consensus protocol has access to the local agent's state $x_i(t)$ instantly, but the states of the neighboring agents j to k are delayed by $\tau_{ij}(t)$ and $\tau_{ik}(t)$, i.e $x_j(t-\tau_{ij}(t))$ and $x_k(t-\tau_{ik}(t))$, respectively. Additionally, communication delays can exist and be different for each neighboring agent, as the agents j and k can be subject to different delays $\tau_{ij}(t) \neq \tau_{ik}(t)$.

Results from Moreau (2004) showed that a multiagent system composed of individuals

with a *single integrator dynamics* as in (1.2) is able to achieve consensus regardless of communication delays, as long as the information from one of the agents can reach all the other agents. This network constraint will be presented later as the existence of a directed spanning tree in the graph that describes the communication topology. Consensus is achieved by applying the linear consensus protocol introduced by Olfati-Saber and Murray (2003), by writing (1.1) with the communication delays $\tau_{ij}(t)$ as

$$u_i(t) = -\sum_{j \in N_i} a_{ij}(x_i(t) - x_j(t - \tau_{ij}(t))). \tag{1.3}$$

To illustrate the effects of communication delays in agents whose dynamics are described by (1.2) subject to protocol (1.3), the same parameters and initial conditions for the example in the previous section are considered in a simulation, with the addition of a very large communication delay $\tau_{ij} = \tau = 10$s, $\forall j \in N_i$. The state trajectories are shown in Figure 1.5, showing the tendency of the agents to achieve consensus. As expected from Moreau (2004), the communication time-delay did not prevent the agents to achieve consensus, but did affect convergence time when compared to Figure 1.3. Some results will be presented in the next chapters showing that communication delays can indeed prevent consensus achievement for more complex dynamics.

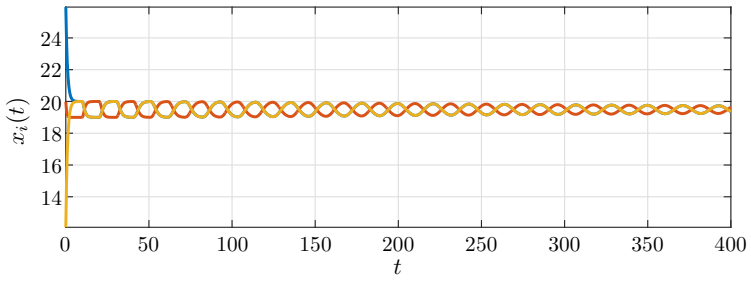

Figure 1.5: Consensus with very large communication delay.

Another common type of time-delay is the one in the control inputs, given by the time-response of actuators and information processing. This is called input delay and is represented by $\tau_i(t)$. It is locally present in agent i and affects the action of the controller, representing how much time it takes for the control action to be executed. The occurrence of input delays is illustrated in Figure 1.6, where the protocol has access to all the states instantaneously, but its action is delayed by $\tau_i(t)$. This effect acts at instant of time t, for agent i, as if all the states where delayed by $\tau_i(t)$, with $x_i(t - \tau_i(t))$ and $x_j(t - \tau_i(t))$. The input delays can also exist and be different for each agent, such that each i-th agent is subject to a different delay $\tau_i(t)$.

Considering the input delays $\tau_i(t)$ into (1.1), the effect of the consensus protocol in

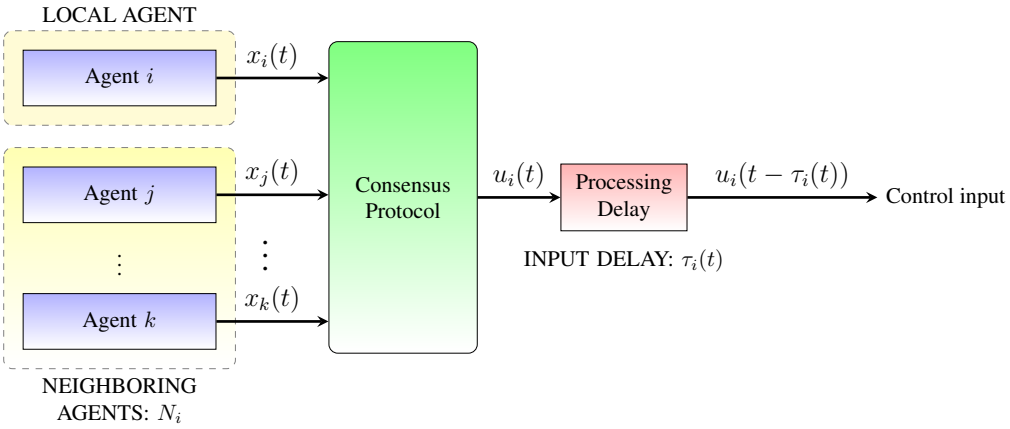

Figure 1.6: Block diagram for the consensus protocol with input delays.

Figure 1.6 is given by

$$u_i(t) = -\sum_{j \in N_i} a_{ij}(x_i(t-\tau_i(t)) - x_j(t-\tau_i(t))). \tag{1.4}$$

The analysis of multiagent systems with delayed consensus protocols as (1.3) and (1.4) are held in order to find the delay margins that allow consensus. Accordingly, consensus with time-delays has been treated under many perspectives and many results can be found in the works by Olfati-Saber and Murray (2003), Olfati-Saber and Murray (2004), Moreau (2005), Ren and Beard (2005), Lin et al. (2008), Bliman and Ferrari-Trecate (2008), and Sakurama and Nakano (2015), for example.

For the same previous example, considering all the agents with the same delay $\tau_i = \tau$, the maximum input delay $\tau^{\max}$ that would allow consensus according to Olfati-Saber and Murray (2004) is $\tau^{\max} = 0.5236$. Figure 1.7 shows a simulation with an input delay $\tau = 0.55$, greater than the margin $\tau^{\max}$, to verify and show that consensus is not achieved.

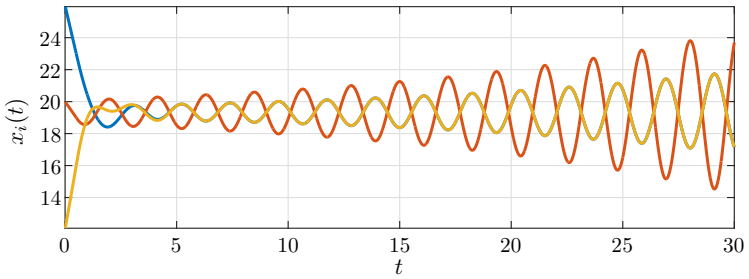

Figure 1.7: Input delay higher than upper margin preventing consensus.

Since Moreau (2004) showed that communication delays do not prevent consensus for single integrator dynamics, most of the results in the literature deal only with input delays. Some of these considerations are summarized next.

Considering the consensus protocol with input delays, Lin et al. (2008) obtained a sufficient condition for directed networks including also external disturbances and model uncertainties. Bliman and Ferrari-Trecate (2008) extended the work of Olfati-Saber and Murray (2003) for time-delays to the cases with time-varying topologies, showing analytical necessary and/or sufficient conditions to reach consensus. Kecai et al. (2011) and Zhang et al. (2011) studied differentiable and nonuniform time-varying delays, where the delays can be time-varying satisfying $0 \leq \tau_{ij}(t) \leq \tau_{ij}^{\max}$ and also be different for each communication link. Some authors, like Sun and Wang (2009) and Xi et al. (2013), considered the possibility of nonuniform and also non-differentiable time-varying delays, such that the variation of the delay is unknown. These results were limited to agents with single integrator dynamics

Results considering time delay and second-order integrator dynamics can be found in the work of Pan et al. (2014), which shows necessary conditions for constant and uniform time delays for undirected networks. For directed networks, Yu et al. (2010) shows some sufficient results.

To contextualize and highlight the different classes of multiagent systems that will be addressed in the text, next section covers some examples of multiagent systems with first-order dynamical systems with an example in formation control, second-order dynamics with an example in flocking, and high-order dynamics applied to the control of vehicles in a platoon.

1.4 First-order Dynamics

First-order dynamics agents are referred to agents with a single integrator, with the consensus protocol acting directly on the agent's "velocity". The dynamics of this kind of agent is given by (1.2) and repeated here for convenience:

$$\dot{x}_i(t) = u_i(t). \tag{1.5}$$

This agent dynamics can be considered in the kinematic control of multiple wheeled or aerial vehicles, with the state x_i given as a position in the space and controlled directly by velocity v_i, where $\dot{x}_i = v_i$, with $v_i = u_i$. Note that in this case each axis in the tridimensional space is considered to be independent to each other, such that an omnidirectional agent can act separately in each variable.

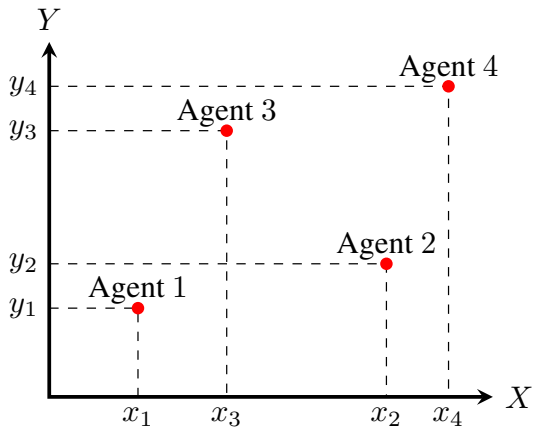

Figure 1.8: Agents placement in the two-dimensional plane.

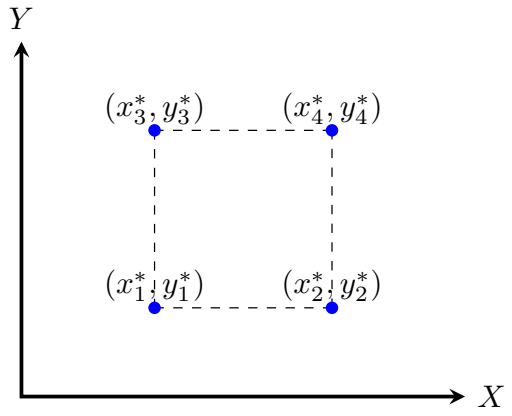

Figure 1.9: Desired agents' formation.

1.4.1 Consensus-based Formation

One of the most prevailing applications on multi-vehicle systems is the formation problem. The purpose is that the agents collectively maintain a prescribed geometry, considering decentralized control and prior knowledge of the desired formation shape. The desired shape can be either set by a centralized reference or programmed on each agent. Finally, the system is able to achieve formation anywhere in the space, depending on the negotiation among the team members.

To illustrate this problem in a consensus-based approach, consider holonomic vehicles able to move in a two-dimensional space. The state of each agent is described by the coordinates (x_i, y_i), $\forall i$, with respect to the X and Y axis, according to Figure 1.8.

Next, the desired agents' positions are drawn in an arbitrary position in the space respecting the desired relative positions. Figure 1.9 shows the desired agents' formation represented by the blue dots, and coordinates (x_i^*, y_i^*), $\forall i$.

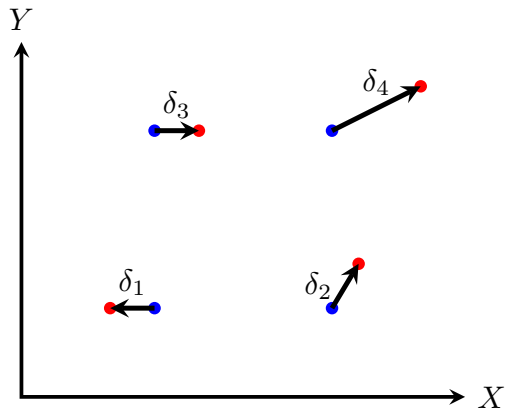

Figure 1.10: Distance δ_i to the formation position.

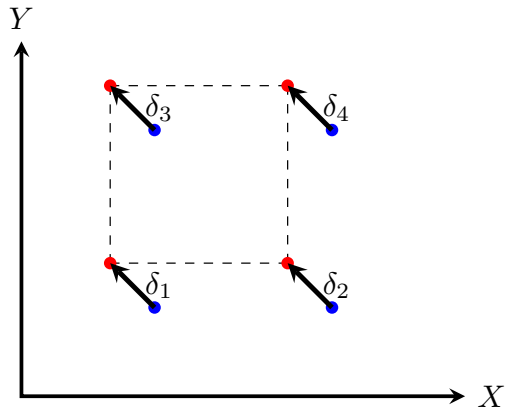

Figure 1.11: Consensus on the distance – formation.

The consensus-based approach to keep formation is that all the agents must achieve consensus on the displacement between the reference of the desired formation and the actual position. The displacement vector $\delta_i \in \mathbb{R}^2, \forall i$, in Figure 1.10, represents this error, with

$$\delta_i = \begin{bmatrix} x_i - x_i^* \\ y_i - y_i^* \end{bmatrix}. \tag{1.6}$$

Following the results presented by Ren (2007), formation is achieved when the agents achieve consensus on δ_i. Figure 1.11 shows the case when the agents have achieved the squared desired formation in a different part of the two-dimensional plane, showing equal displacement vectors δ_i.

Thus, the consensus protocol to achieve formation is $u_i \in \mathbb{R}^2$,

$$u_i(t) = -\sum_{j \in N_i} a_{ij}(\delta_i(t) - \delta_j(t)), \tag{1.7}$$

which can be separated in X and Y parts, considering the two parts of equation (1.6)

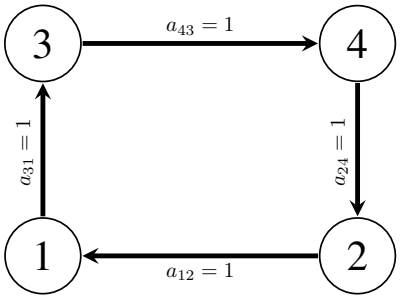

Figure 1.12: Network topology represented as a graph.

given by $\delta_{x,i} = x_i(t) - x_i^*$ and $\delta_{y,i} = y_i(t) - y_i^*$, yielding

$$u_{x,i}(t) = -\sum_{j \in N_i} a_{ij} \big(\underbrace{(x_i(t) - x_i^*)}_{\delta_{x,i}} - \underbrace{(x_j(t) - x_j^*)}_{\delta_{x,j}} \big), \tag{1.8}$$

$$u_{y,i}(t) = -\sum_{j \in N_i} a_{ij} \big(\underbrace{(y_i(t) - y_i^*)}_{\delta_{y,i}} - \underbrace{(y_j(t) - y_j^*)}_{\delta_{y,j}} \big), \tag{1.9}$$

such that the agents are controlled by inputs which are velocities given by

$$v_x(t) = u_{x,i}(t), \tag{1.10}$$

$$v_y(t) = u_{y,i}(t), \tag{1.11}$$

where $v_x(t)$ and $v_y(t)$ are the velocities on X and Y axis, respectively, and are independently set.

A simulation is carried out to illustrate the formation problem. Considering the state of each agent given by

$$q_i(t) = \begin{bmatrix} \delta_{x,i}(t) \\ \delta_{y,i}(t) \end{bmatrix}, \tag{1.12}$$

with initial conditions considered $q_1(0) = [-1 \;\; 0.5]^T$, $q_2(0) = [2 \;\; 0]^T$, $q_3(0) = [-0.5 \;\; 1]^T$, and $q_4(0) = [-1 \;\; 1]^T$, and given that the desired formation is a square given by $(x_1^*, y_1^*) = (0, 0)$, $(x_2^*, y_2^*) = (1, 0)$, $(x_3^*, y_3^*) = (0, 1)$, and $(x_4^*, y_4^*) = (1, 1)$. The communication network is such that agent 1 receives information from agent 2 ($a_{12} = 1$), agent 2 receives information from agent 4 ($a_{24} = 1$), agent 4 receives information from agent 3 ($a_{43} = 1$), and agent 3 receives information from agent 1 ($a_{31} = 1$). The network topology describing this information flow can be graphically represented by the graph in Figure 1.12.

The state trajectories are shown in Figure 1.13. Figure 1.13a shows the convergence for the state variable $\delta_{x,i}(t)$ and Figure 1.13b for $\delta_{y,i}(t)$, both converging approximately at $t = 5s$. Additionally, the trajectories of the agents in the two-dimensional plane XY are illustrated in Figure 1.14. The initial state $q_i(0)$ is represented at the initial position (x_i, y_i) of each agent, and trajectories are represented as continuous lines reaching the

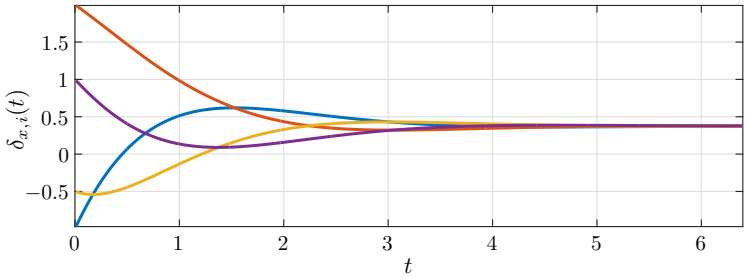

(a) State trajectories for $\delta_{x,i}(t)$ for all agents.

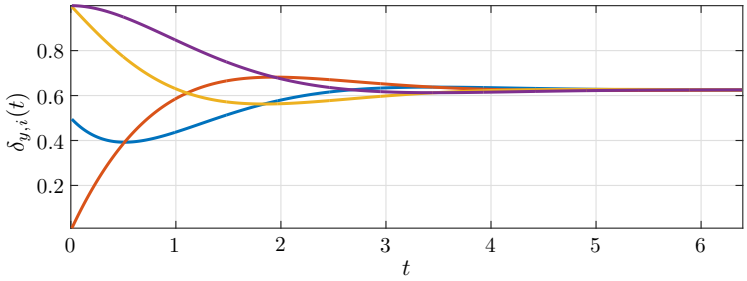

(b) State trajectories for $\delta_{y,i}(t)$ for all agents.

Figure 1.13: State trajectories for first-order agents formation.

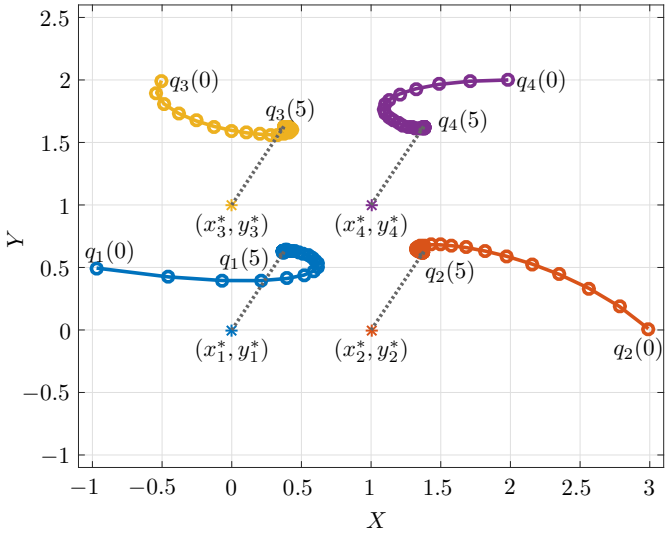

Figure 1.14: Simulated state trajectories for single-order agents achieving formation.

approximately stationary state $q_i(5)$ at time $t = 5s$, with circles representing the position (x_i, y_i) at time-steps of $0.02s$. The dashed lines represent the final displacements between the agents and the reference positions $(x_1^*, y_1^*) = (0, 0)$, $(x_2^*, y_2^*) = (1, 0)$, $(x_3^*, y_3^*) = (0, 1)$, and $(x_4^*, y_4^*) = (1, 1)$, which are represented by asterisks.

1.5 Second-order Dynamics

Some agents are assumed to obey a second-order model to describe its dynamics. This model is suitable for mechanical systems controlled through acceleration (force or torque). For example, thrust-propelled vehicles (Wang, 2016), or more generally agents that can be feedback linearized as double integrators, as it will be presented next.

A second-order integrator agent is given by the state variables $x_i \in \mathbb{R}$ and $\dot{x}_i \in \mathbb{R}$, which can represent, for example, position and velocity, respectively. The dynamics is given such that

$$\ddot{x}_i(t) = u_i(t), \tag{1.13}$$

where the control input represents an "acceleration".

An example from Ren and Atkins (2007) is presented to illustrate the description of a non-holonomic mobile robot with second-order dynamics. The equations of motion are given by

$$\dot{x}_i = v_i \cos(\theta_i), \tag{1.14}$$
$$\dot{y}_i = v_i \sin(\theta_i), \tag{1.15}$$
$$\dot{\theta}_i = \omega_i, \tag{1.16}$$
$$m_i \dot{v}_i = F_i, \tag{1.17}$$
$$J_i \dot{\omega}_i = T_i, \tag{1.18}$$

where (x_i, y_i) is the position of the robot center, θ_i is the orientation, v_i is the linear velocity, ω_i is the angular velocity, m_i is the mass, J_i is the moment of inertia, F_i is the force, and T_i is the torque applied to the robot. An illustration for this agent is given in Figure 1.15a.

Next, to avoid the issue introduced by the non-holonomic constraints, a point (x_{hi}, y_{hi}) at a distance d_i off the wheel axis as in Figure 1.15b is considered in order to define the outputs:

$$\begin{bmatrix} x_{hi} \\ y_{hi} \end{bmatrix} = \begin{bmatrix} x_i \\ y_i \end{bmatrix} + d_i \begin{bmatrix} \cos(\theta_i) \\ \sin(\theta_i) \end{bmatrix}. \tag{1.19}$$

Let

$$\begin{bmatrix} F_i \\ T_i \end{bmatrix} = \begin{bmatrix} \frac{1}{m_i}\cos(\theta_i) & -\frac{d_i}{J_i}\sin(\theta_i) \\ \frac{1}{m_i}\sin(\theta_i) & \frac{d_i}{J_i}\cos(\theta_i) \end{bmatrix}^{-1} \begin{bmatrix} u_{xi} + v_i\omega_i \sin(\theta_i) + d_i\omega_i^2 \cos(\theta_i) \\ u_{yi} - v_i\omega_i \cos(\theta_i) + d_i\omega_i^2 \sin(\theta_i) \end{bmatrix}, \tag{1.20}$$

where u_{xi} and u_{yi} are the acceleration inputs, related to the velocities v_{xi} and v_{yi}, of x_{hi} and y_{hi}, respectively, as in Figure 1.15b. Thus, the following sets of equations are

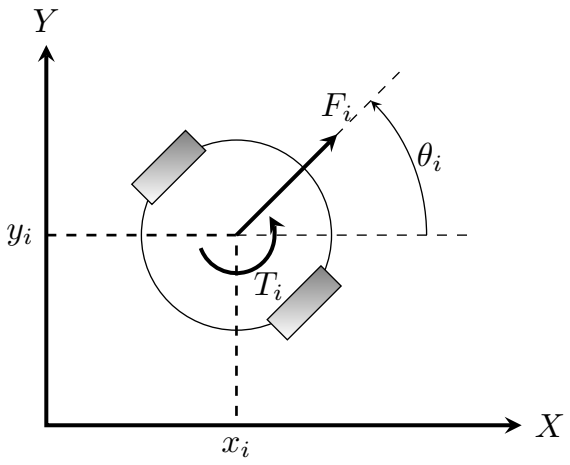

(a) Mobile robot controlled by force and torque.

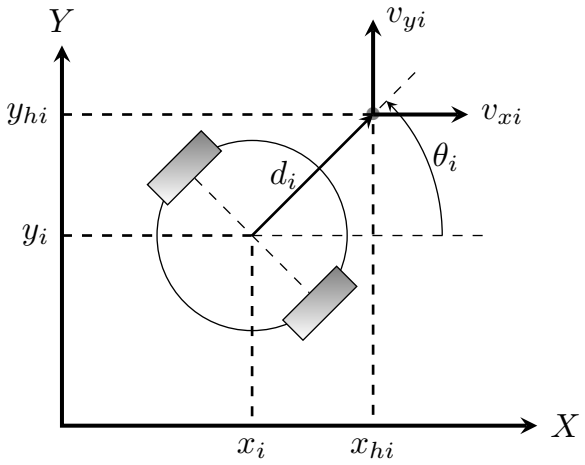

(b) Mobile robot with a reference point off wheel axis for linearization.

Figure 1.15: Linearization of second-order agent.

obtained:

$$\dot{x}_{hi} = v_{xi}, \tag{1.21}$$

$$\dot{v}_{xi} = u_{xi}, \tag{1.22}$$

$$\dot{y}_{hi} = v_{yi}, \tag{1.23}$$

$$\dot{v}_{yi} = u_{yi}. \tag{1.24}$$

Finally, the pairs of equations (1.21)–(1.22) and (1.23)–(1.24) are in the form of (1.13), and thus the system can be analyzed as second-order integrator agents and consensus-based results can be applied.

A second-order consensus protocol that can lead the system in (1.13) to consensus is

proposed by Ren and Atkins (2007) and can be written as

$$u_i(t) = -\sum_{j\in N_i} a_{ij}\left(\alpha_2(x_i(t) - x_j(t)) + \alpha_1(\dot{x}_i(t) - \dot{x}_j(t))\right), \tag{1.25}$$

where α_1 and α_2 are the gains in the consensus protocol related to each state variable.

1.5.1 Consensus-based Flocking

A framework similar to the one applied in formation control problem can be used in order to describe flocking for second-order integrator dynamics. In flocking, the objective is that the agents keep a relative distance between each other, and achieve same orientation. It means keeping formation and achieving consensus in the velocity. The first part —keeping formation— can be handled by defining the displacement to a predefined desired formation (x^*_{hi}, y^*_{hi}) for each agent. Thus, analogously to (1.6), the error displacement is defined as

$$\delta_{hi} = \begin{bmatrix}\delta_{x,hi}\\ \delta_{y,hi}\end{bmatrix} = \begin{bmatrix}x_{hi} - x^*_{hi}\\ y_{hi} - y^*_{hi}\end{bmatrix}. \tag{1.26}$$

Taking the time-derivative of $\delta_{x,hi}$ and $\delta_{y,hi}$, it is easy to see that $\dot{\delta}_{x,hi}(t) = \dot{x}_{hi}(t) = v_{xi}(t)$ and $\dot{\delta}_{y,hi}(t) = \dot{y}_{hi}(t) = v_{yi}(t)$, as x^*_{hi} and y^*_{hi} are constants. Therefore, the dynamics of each agent can be described as in (1.21)–(1.24). The pair of equations (1.21)–(1.22) is decoupled from the pair (1.23)–(1.24), such that each pair can be independently analyzed analogously to (1.13).

Thus, the protocol (1.25) that can drive the agents to consensus is applied as

$$u_{xi}(t) = -\sum_{j\in N_i} a_{ij}\left(\alpha_2(\delta_{x,hi}(t) - \delta_{x,hj}(t)) + \alpha_1(v_{x,i}(t) - v_{x,j}(t))\right), \tag{1.27}$$

$$u_{yi}(t) = -\sum_{j\in N_i} a_{ij}\left(\alpha_2(\delta_{y,hi}(t) - \delta_{y,hj}(t)) + \alpha_1(v_{y,i}(t) - v_{y,j}(t))\right). \tag{1.28}$$

A simulation is carried out to illustrate this problem, considering $\alpha_1 = \alpha_2 = 1$, the state of each agent given by

$$q_i(t) = \begin{bmatrix}\delta_{x,hi}(t)\\ v_{xi}(t)\\ \delta_{y,hi}(t)\\ v_{yi}(t)\end{bmatrix}, \tag{1.29}$$

with initial conditions $q_1(0) = [-1 \quad 0.5 \quad 2 \quad 0]^T$, $q_2(0) = [2 \quad 0 \quad 1 \quad 0.5]^T$, and $q_3(0) = [0 \quad -0.5 \quad -1 \quad 0.5]^T$, and given that the desired formation is a triangle given by $(x^*_{h1}, y^*_{h1}) = (0, 0)$, $(x^*_{h2}, y^*_{h2}) = (1/2, 0)$, and $(x^*_{h3}, y^*_{h3}) = (1/4, \sqrt{2}/4)$. It is considered that all the

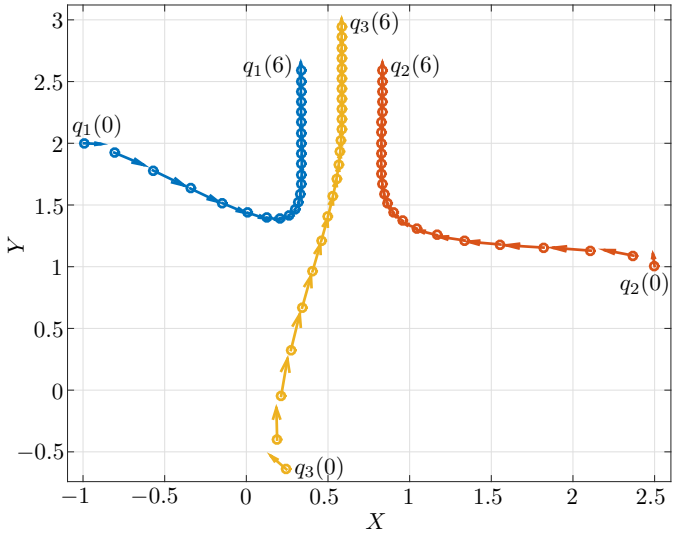

Figure 1.16: Initial states $q_i(0)$ and trajectories in the plane XY.

agents can communicate with each other, i.e. can send to and receive information from all the other agents, representing a fully connected communication network.

The trajectories of the agents in the two-dimensional plane XY is illustrated in Figure 1.16 for a running time of $6s$. The initial state $q_i(0)$ is represented at the initial position (x_{hi}, y_{hi}) of each agent. At each time interval of $0.25s$, a snapshot is represented with the circle representing the position (x_{hi}, y_{hi}), and an arrow indicating the velocity (v_{xi}, v_{yi}). At time $t = 6s$ the agents are represented by $q_i(6)$ already performing flocking behavior.

Finally, the state trajectories for this example are shown in Figure 1.17. Figure 1.17a shows that the velocity $v_{yi}(t)$ achieves consensus around $t = 4s$. Additionally, the state variable $\delta_{y,hi}(t)$ in Figure 1.17b also achieves consensus while still varying as a ramp, since it is integrating $v_{yi}(t)$. The velocity $v_{xi}(t)$ in Figure 1.17c is also shown to achieve consensus at the same time. Note that $\delta_{x,hi}(t)$ in Figure 1.17d achieves consensus, but, differently from $\delta_{y,hi}(t)$, has ramp slope close to zero, since $v_{xi}(t)$ converges to a value close to zero.

1.6 High-order Dynamics

Many agents can be described as high-order integrator dynamics, which is comprised by any input-state linearizable system, e.g. speed control (Xia et al., 2012), and power generators (Rigatos et al., 2014).

An example is presented for the longitudinal dynamics of a ground vehicle, including

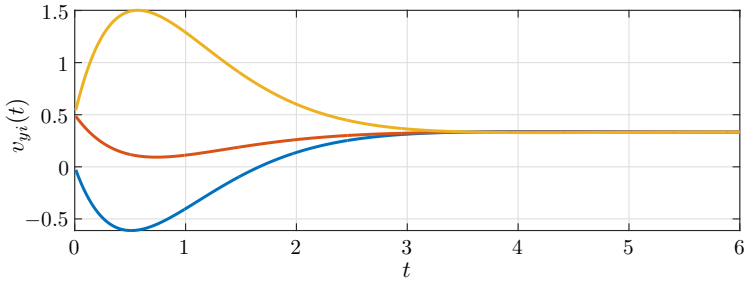

(a) State trajectories for $v_{yi}(t)$ for all agents.

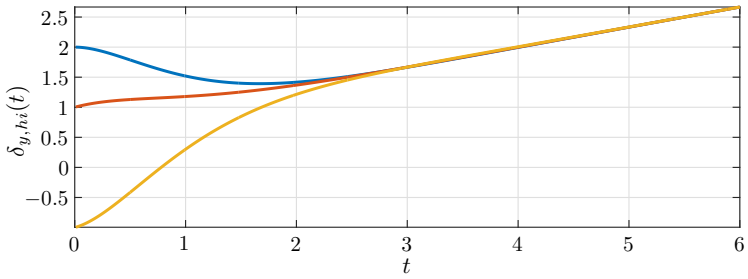

(b) State trajectories for $\delta_{y,hi}(t)$ for all agents.

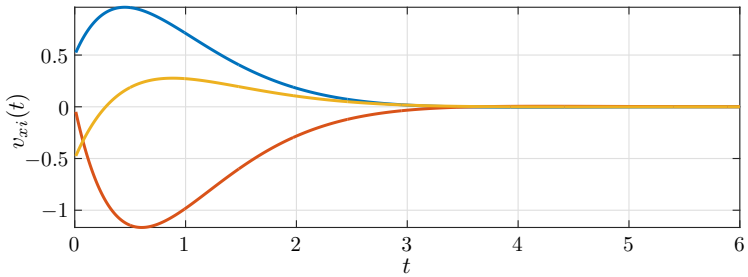

(c) State trajectories for $v_{xi}(t)$ for all agents.

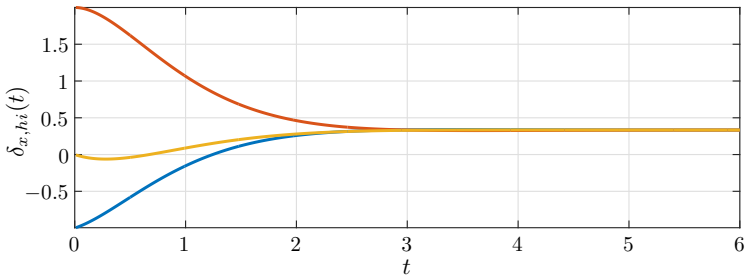

(d) State trajectories for $\delta_{x,hi}(t)$ for all agents.

Figure 1.17: State trajectories for second-order agents.

engine, drive line, brake system, aerodynamics drag, tire friction, rolling resistance, and gravitational force, with the following assumptions extracted from Zheng et al. (2016) (Swaroop et al., 1994; Xiao and Gao, 2011; Li et al., 2011a, 2013):

- The tire longitudinal slip is negligible, and the powertrain dynamics are lumped into a first-order inertial transfer function;
- The vehicle body is considered to be rigid and symmetric;
- The influence of pitch and yaw motions is neglected;
- The driving and braking torques are controllable inputs.

With these considerations, the following simplified but still nonlinear longitudinal dynamics of a vehicle i can be obtained (Zheng et al., 2016):

$$\dot{s}_i(t) = v_i(t) \tag{1.30}$$

$$\dot{v}_i(t) = \frac{1}{m_i}\left(\eta_i \frac{T_i(t)}{R_i} - C_i v_i^2 - m_i g f\right) \tag{1.31}$$

$$\iota_i \dot{T}_i(t) + T_i(t) = T_{i,des}(t), \tag{1.32}$$

where $s_i(t)$, $v_i(t)$ denote the position and velocity, m_i is the vehicle mass, C_i is the lumped aerodynamic drag coefficient, g is the acceleration due to gravity, f is the coefficient of rolling resistance, $T_i(t)$ denotes the actual driving/braking torque, $T_{i,des}(t)$ is the desired driving/braking torque, ι_i is the inertial delay of vehicle longitudinal dynamics, R_i denotes the tire radius, and η_i is the mechanical efficiency of driveline.

Zheng et al. (2016) use the output position to linearize the nonlinear model by making

$$T_{i,des}(t) = \frac{1}{\eta_i}(C_i v_i(2\iota_i \dot{v}_i + v_i) + m_i g f + m_i u_i) R_i, \tag{1.33}$$

where u_i is the new input signal after linearization, such that the linear model for the vehicle longitudinal dynamics

$$\eta_i \dot{a}_i(t) + a_i(t) = u_i(t), \tag{1.34}$$

where $\dot{a}_i(t) = v_i(t)$ denotes the acceleration. Finally, the third-order state space model can be written as (Xiao and Gao, 2011; Zheng et al., 2016)

$$\begin{bmatrix} \dot{s}_i(t) \\ \dot{v}_i(t) \\ \dot{a}_i(t) \end{bmatrix} = \begin{bmatrix} 0 & 1 & 0 \\ 0 & 0 & 1 \\ 0 & 0 & \frac{-1}{\iota_i} \end{bmatrix} \begin{bmatrix} s_i(t) \\ v_i(t) \\ a_i(t) \end{bmatrix} + \begin{bmatrix} 0 \\ 0 \\ \frac{1}{\iota_i} \end{bmatrix} u_i(t). \tag{1.35}$$

With this model at hand, the platoon problem is presented as an application of consensus.

1.6.1 Consensus-based Platooning

The objective in a platoon problem is to make all vehicles move at the same speed while maintaining a desired inter-vehicle spacing policy. The platoon problem has a long history and has recently attracted extensive research interests. Some overviews can be seen in the works by Tsugawa (2002), Li et al. (2015), and Jia et al. (2016).

A platoon can be viewed as a group of agents, i.e. vehicles, and the problem may be described similarly to the consensus-based formation problem, to achieve consensus on three variables: the distance from the current position to a pre-defined position; the speed; and the acceleration. The following state variables are thus defined

$$\begin{bmatrix} \tilde{s}_i(t) \\ v_i(t) \\ a_i(t) \end{bmatrix} = \begin{bmatrix} s_i(t) - s_i^* \\ v_i(t) \\ a_i(t) \end{bmatrix}, \tag{1.36}$$

with s_i^* defined similarly to x_i^* in Equation (1.6) for the formation problem. Hence, the vehicles can achieve platoon with a distance policy δ_{ij} as shown in Figure 1.18 which can be defined from s_i^* and s_j^* as

$$\delta_{ij} = s_i^* - s_j^*. \tag{1.37}$$

Figure 1.18 shows an example where each vehicle can measure the distance only to the vehicle in front of itself with a_{ij} describing these neighboring vehicles.

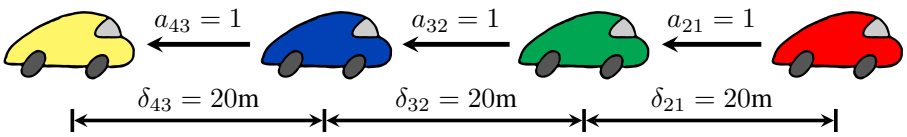

Figure 1.18: Platooning problem.

A consensus protocol that can drive the agents to consensus is

$$u_i(t) = -\sum_{j \in N_i} a_{ij} \left(\alpha_3(\tilde{s}_i(t) - \tilde{s}_j(t)) + \alpha_2(v_i(t) - v_j(t)) + \alpha_1(a_i(t) - a_j(t)) \right), \tag{1.38}$$

which replacing $\tilde{s}_i(t)$ from (1.36) yields

$$u_i(t) = -\sum_{j \in N_i} a_{ij} \left(\alpha_3(s_i(t) - s_j(t) - (s_i^* - s_j^*)) + \alpha_2(v_i(t) - v_j(t)) + \alpha_1(a_i(t) - a_j(t)) \right), \tag{1.39}$$

with δ_{ij} from (1.37), the consensus protocol can be written equivalently as

$$u_i(t) = -\sum_{j \in N_i} a_{ij} \left(\alpha_3(s_i(t) - s_j(t) - \delta_{ij}) + \alpha_2(v_i(t) - v_j(t)) + \alpha_1(a_i(t) - a_j(t)) \right), \tag{1.40}$$

and $s_i(t) - s_j(t)$ can be assessed by a sensor located in front of vehicle i to measure the distance to vehicle j.

The group of vehicles represented in Figure 1.18 is simulated in order to show the state evolution as the agents achieve platoon formation. The agents are indexed as follows, the rightmost red vehicle is agent 1, the green is agent 2, the blue one is agent 3, and finally agent 4 refers to the leftmost yellow car. The desired distance between each pair of cars is $\delta_{43} = \delta_{32} = \delta_{21} = 20\text{m}$.

Note that the red vehicle receives no information from any other agent and therefore is considered the leader. Its velocity thus remains constant, as the control input from the consensus protocol is zero. Additionally, all the agents are expected to achieve consensus on the velocity and acceleration defined by the leader.

The initial conditions are considered as follows: $s_1(0) = 200\text{m}$, $s_2(0) = 150\text{m}$, $s_3(0) = 90\text{m}$, and $s_4(0) = 20\text{m}$ are the initial positions in relation to an inertial reference; all the initial velocities are considered to be $v_1(0) = v_2(0) = v_3(0) = v_4(0) = 10\text{m}/s$; and all the accelerations are considered initially null, i.e $a_1(0) = a_2(0) = a_3(0) = a_4(0) = 0\text{m}/s^2$. For the spacing distances defined as $\delta_{43} = \delta_{32} = \delta_{21} = 20\text{m}$, it can be defined the desired formation-like parameters as $s_1^* = 60\text{m}$, $s_2^* = 40\text{m}$, $s_3^* = 20\text{m}$, and $s_4^* = 0\text{m}$.

A simulation is carried-out to show that the analysis of the vehicle dynamics (1.35) with the consensus protocol (1.38) can be applied to guarantee platoon considering gains $\alpha_1 = 1$, $\alpha_2 = 2$, and $\alpha_3 = 1$ as designed by Zheng et al. (2016). Figure 1.19 shows the evolution of the space distance between two adjacent cars. The simulation carried out shows that the vehicles manage to achieve the desired distance of 20m between the cars.

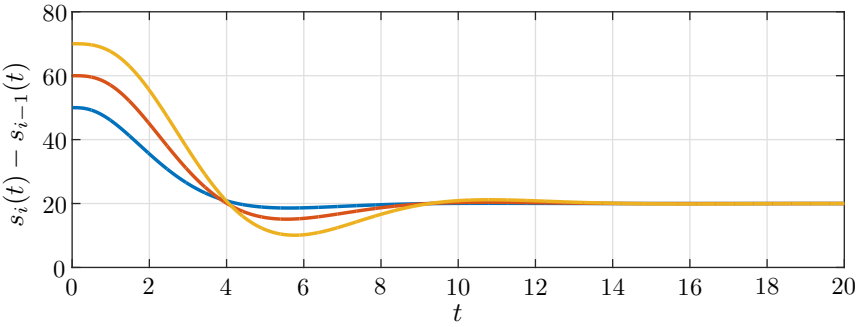

Figure 1.19: Spacing between the vehicles for $i = 1, 2, 3$.

Additionally, the state variables in (1.36) are shown in Figure 1.20 as the agents achieve consensus, converging to the blue line related to agent 1, red front car in Figure 1.18. All the states reach consensus, with the $\lim_{t\to\infty} a_i(t) = 0$ in Figure 1.20c, $\lim_{t\to\infty} v_i(t) = 10$

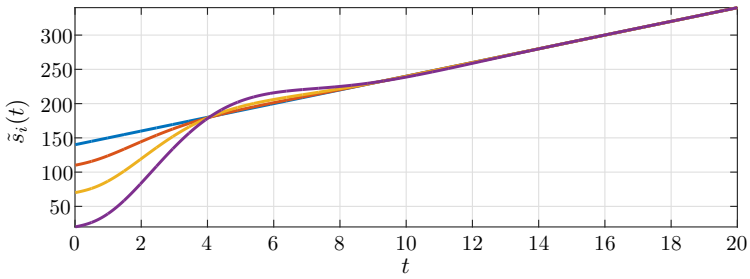

(a) State trajectories for $\tilde{s}_i(t) = s_i(t) - s_i^*$ for all agents.

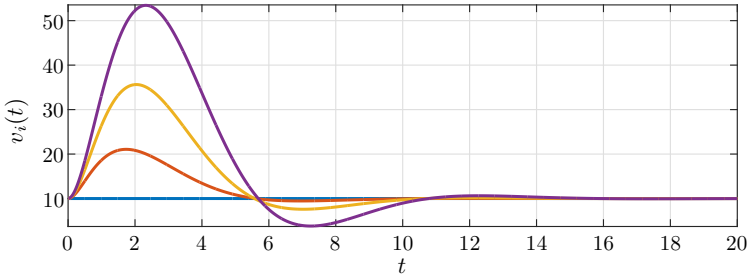

(b) State trajectories for $v_i(t)$ for all agents.

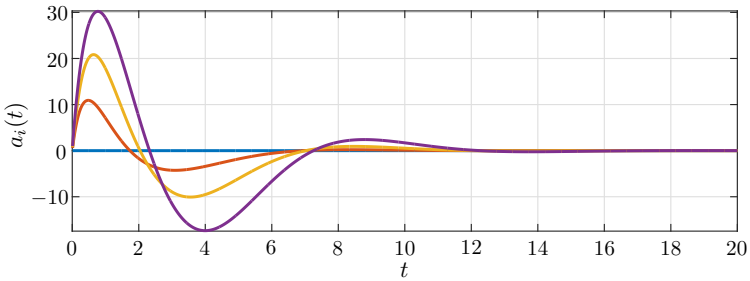

(c) State trajectories for $a_i(t)$ for all agents.

Figure 1.20: State trajectories for vehicles longitudinal dynamics.

and constant in Figure 1.20b, and $\tilde{s}_i(t)$ varying as a ramp with slope given by the velocity in Figure 1.20a.

1.7 Overview of this Thesis and Contributions

The examples presented for formation control, flocking, and platoon, show some of the many classes of problems and dynamics of agents that can be addressed using consensus-based approaches. In fact, consensus can be applied in many problems in distributed control or multiagent systems. Additionally, as communication and signal processing relay on processes that can introduce delays, its analysis in multiagent systems is of major importance for networked application, as the delays can cause degradation of the system dynamics (Figure 1.5) and lead to instability (Figure 1.7), preventing consensus and consequently the execution of the task that is under analysis. Therefore, in the remaining of this text the results for consensus will be presented considering time-delays.

In Chapter 2, it is presented a transformation that allows consensus problems with communication and input delays to be analyzed as stability problems. Additional lemmas used throughout this thesis are also presented in that chapter.

An analysis of the impacts of delays in communication or input-delays will be presented in Chapter 3 showing that for different values of constant time-delays, the introduction of the delays can either prevent or enable consensus. It shows the importance of analyzing delays in different intervals of variation. The presented results are exact, i.e. necessary and sufficient. Part of these results were published by Savino et al. (2015) and are also applied here to communication delays.

Next, results considering the analysis of consensus with the considered bounds of time-varying delays is presented in Chapter 4. The presented results are sufficient but less conservative than others in the literature. This chapter generalizes the results published by Savino et al. (2013), Savino et al. (2014b), Savino et al. (2014a), and Savino et al. (2016b), and extends the results to the application in communication delays.

Analysis of switching topologies, which can be due to failures in the communication channels causing the drop of communication links, is presented in Chapter 5. This is a reprint of the result published by Savino et al. (2016a), which also generalizes dos Santos Junior et al. (2014) and dos Santos Junior et al. (2015). The result is also applied to communication delays.

The design of the coupling strengths between the agents related to the weights a_{ij} assigned to the communication links is presented in Chapter 6. These results are presented by Savino et al. (2016c), a book chapter to be published on the series of Advances in Delays and Dynamics, edited by Springer.

An analysis of single-order consensus applied to rigid bodies with an application in cooperative robotics is shown in Chapter 7. It summarizes the results obtained during the exchange program at the Interactive Robotics Groups in the Massachusetts Institute of Technology. These results follow the lines of the work published by Brito et al. (2015).

Finally, the text ends with the conclusions.

The contributions of this Thesis are summarized next:

- An alternative way to write the Laplacian matrix of a graph in Lemma 2.2 which simplifies the design of the coupling strengths by showing all the weights in a diagonal matrix $\mathcal{W}$.

- An extension of the tree-type transformation of consensus into a stability problem for high-order dynamics in Section 2.2, which gives the disagreement systems (2.49) for communication delays and (2.72) for input delays.

- The analysis of consensus on intervals of time-delays for agents described by chain of integrators in Theorem 3.1 for communication and Theorem 3.2 for input delays. It is also shown that a multiagent system with agents given by single-order integrator can achieve consensus independent of the communication delay (Corollary 3.1), as expected from previous results in the literature. The system can also be independent of the communication delay for second-order integrator dynamics if the gains in the consensus protocol are properly adjusted (Corollary 3.2), and for higher-order the delays can either improve or degrade the systems behavior according to the interval of time-delay, according to Theorem 3.1. Likewise, the effects of input-delays always degrade the systems performance for first- and second-order integrators, showing an upper bound for the delay margins in Corollaries 3.3 and 3.4, respectively. For higher-orders, like the communication delays, input delays can also improve or degrade performance according to its interval (Theorem 3.2). This analysis shows that the impact of time-delays, either allowing or preventing consensus, depends on the interval on which the time-delay belongs. Thus, consensus with time-delays have to be analyzed on intervals, which is the assumption made for the domain of the time-delays in the next results.

- An LMI method for the analysis of consensus with time-delays is presented for both communication and input delays in Theorem 4.1. The delays are assumed to belong to an interval described by a lower and upper bound in order to analyze the delays on intervals. The result also presents a guaranteed exponential convergence rate for consensus and is related to the time needed to approach consensus. The proposed method is shown to perform better than related results in the literature.

- An extension of the analysis method to deal with switching topologies is presented and a sufficient condition to show consensus is given in Theorem 5.1. The switching behavior is described as a Markov Chain with uncertain parameters, which can describe uncertainties in the model of the transition rates, and also consider time-delays given on intervals.

- The design of the coupling strengths is done with LMI methods in order to increase performance according to a convergence rate in Theorem 6.1, for fixed topologies. It can also be applied to allow greater margins of time-delays, as presented for switching topologies in Theorem 6.2.

- A result for rigid-body pose consensus is presented to the application of dual quaternions to describe the pose. New mappings between the derivative of the logarithm

of a quaternion, or a dual quaternion, and the derivative of the quaternion itself, or dual quaternion, are given in Theorems 7.1 and 7.2, respectively. Then, a direct extension for consensus in dual quaternions is show in Theorem 7.3, and the extension to consensus on the pose is given in Theorem 7.4 and to consensus-based formation is given in Theorem 7.5. The results are applied to practical examples using mobile manipulators.

Chapter 2

Background for Analyzing Consensus as Stability

This chapter presents how to transform a consensus problem into a stability one, which is necessary for the development of the results to be presented in the following chapters. The representation of the network topology with graphs is followed by the description of the dynamics of multiagent systems with communication delays, input delays, and free of delay as a special case. The chapter is finished with some important lemmas.

2.1 Algebraic Graph Theory

The information flow of a multiagent system is modeled using the algebraic theory of graphs as first proposed by Fax and Murray (2002) and Jadbabaie et al. (2003). An example of this representation has been introduced in the previous chapter (see Figure 1.2). A more detailed example is presented here in Figure 2.1a, where an undirected graph is used to model the interactions of four agents. An undirected graph refers to communication networks with two-way communication links, i.e. if node 1 is able to receive information from node 2, then node 2 also receives information from node 1, and the same is valid for all the other nodes in Figure 2.1a. Additionally, in undirected networks, the coupling strengths a_{ij}, equivalent to the weights associated to each neighbor j of an agent i, obey $a_{ij} = a_{ji}$.

An undirected network is a special case of a directed network, presented in Figure 2.1b. In a directed network, it is not necessary for two agents sharing a link to have bidirectional communication. As seen in Figure 2.1b, node 2 receives information from node 3, but the opposite is not true. The same happens for the links between nodes 3 and 4, and nodes 4 and 2. The two-way communication link as in undirected networks is still possible, as shown for nodes 1 and 2, but, it is not necessary that the two coupling strengths to be

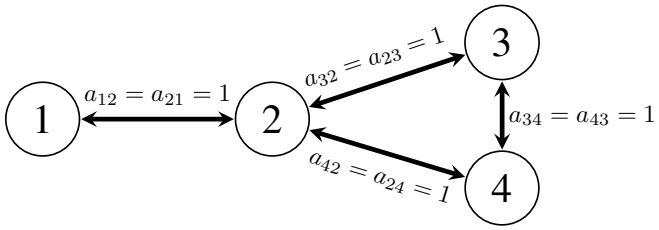

(a) Undirect graph.

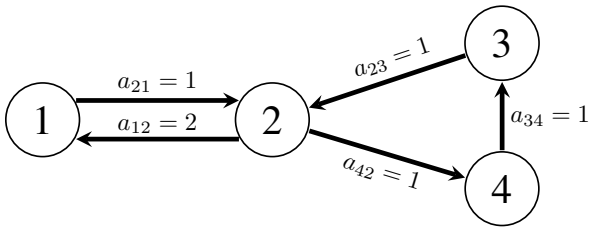

(b) Directed graph.

Figure 2.1: Example of graphs.

equal, e.g. $a_{21} = 1$ and $a_{12} = 2$.

This text makes use of directed graphs, which can also represent undirected graphs. Additionally, directed graphs can also model leader-following multiagent systems. This is the case if $a_{12} = 0$ in Figure 2.1b, which implies that agent 1 receives no information from any other agent. An example of a leader following system was presented for platooning in Figure 1.18.

A simple directed graph is denoted by $\mathcal{G}(\mathcal{V}, \mathcal{E}, \mathcal{A})$, where $\mathcal{V}$ represents the set of m vertices (or nodes) ordered and labeled as $v_1, ..., v_m \in \mathcal{V}$, $\mathcal{E}$ represents the set of directed edges connecting the nodes and dictating the direction of the information flow, given by $e_{ij} = (v_i, v_j)$, where the first element v_i is the parent node (tail) and the second element v_j is the child node (head). No multiple edges or graph loops are allowed. The Adjacency Matrix $\mathcal{A} = [a_{ij}]$ associated with graph $\mathcal{G}$ assigns a real non-negative value to each edge e_{ij}, according to

$$a_{ij} \begin{cases} = 0, & \text{if } i = j \text{ or } \nexists\ e_{ji}, \\ > 0, & \text{if and only if } \exists\ e_{ji}. \end{cases} \tag{2.1}$$

Additionally, it is defined the Degree Matrix $\mathcal{D} = [d_{ii}]$, a diagonal matrix with elements $d_{ii} = \sum_{j=1}^{m} a_{ij}$. Given the definitions of the Adjacency and Degree matrices, it follows the definition of the Laplacian Matrix:

$$L = \mathcal{D} - \mathcal{A}, \tag{2.2}$$

which is equivalent to $L = [l_{ij}]$ with $l_{ii} = d_{ii} = \sum_{j=1}^{m} a_{ij}$ and $l_{ij} = -a_{ij}$, for $i \neq j$. An

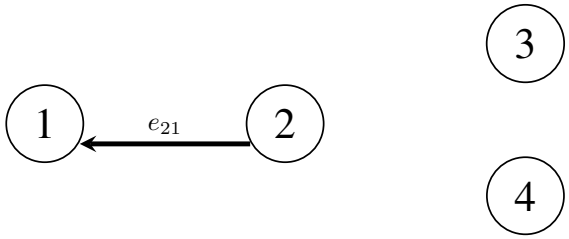

(a) Subgraph $\mathcal{G}_{a,1}$.

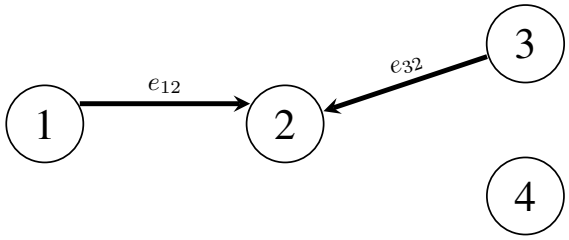

(b) Subgraph $\mathcal{G}_{a,2}$.

(c) Subgraph $\mathcal{G}_{a,3}$.

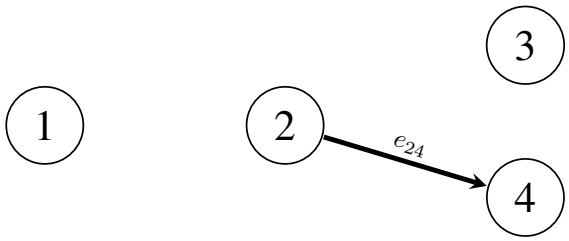

(d) Subgraph $\mathcal{G}_{a,4}$.

Figure 2.2: Example of subgraphs on nodes/agents.

important property of the Laplacian matrix is the following:

$$L1_m = 0_m. \tag{2.3}$$

Subgraphs on nodes/agents

A subgraph of $\mathcal{G}$ is a graph with a subset of vertices from $\mathcal{V}$ and a subset of edges from $\mathcal{E}$. A subgraph on node —or agent— i, $\mathcal{G}_{a,i}$ of $\mathcal{G}$, is defined as the graph with vertices $\mathcal{V}_{a,i} = \mathcal{V}$ but only the edges $e_{ji} \in \mathcal{E}$ having i as the child node. For illustration, the subgraphs on nodes originated from the graph in Figure 2.1b are shown in Figure 2.2. These subgraphs have great importance in the study of input delays.

Directed spanning trees

A directed tree (Bullo et al., 2009) is a type of directed graph in which there is a node called root without parent nodes, i.e. there is no edge pointing towards it. Besides, all the other nodes in the directed tree have exactly one parent. Also, there is a path, a directed sequence of edges, connecting the root to any other node in the tree. Another interesting property is the absence of cycles. A directed graph $\mathcal{G}$ is said to have a directed spanning tree $\mathcal{G}_{span}$ if from the removal of some of the edges in $\mathcal{G}$ a directed tree with the same set of vertices of $\mathcal{G}$ can be formed. This graph is called a spanning tree $\mathcal{G}_{span}$ and is a subgraph of $\mathcal{G}$. Besides, $\mathcal{G}$ can have several spanning trees.

A graph $\mathcal{G}$ is said to be weakly connected if $\mathcal{G}$ has at least one spanning tree. Let $\mathcal{G}_{span,i}$ represent a directed spanning tree with v_i as the root node. Then, $\mathcal{G}$ is called strongly connected if a $\mathcal{G}_{span,i}$ can be formed for all $v_i \in \mathcal{V}$.

Several examples of directed spanning trees that can be formed from $\mathcal{G}$ in Figure 2.1b are shown in Figure 2.3, where the gray dashed lines represent the removed edges in order to form each directed spanning tree. Furthermore, from this example it can be noticed that $\mathcal{G}$ in Figure 2.1b is a strongly connected graph, since there is a directed spanning trees $\mathcal{G}_{span,i}$ for each v_i, as shown in Figures 2.3a, 2.3b, 2.3c, and 2.3d for the nodes v_1, v_2, v_3, and v_4, respectively.

Next lemma regarding the Laplacian of directed spanning trees plays an important role in the analysis of consensus of multi-agent systems:

Lemma 2.1 *(Ren and Beard (2008) [Cor. 2.5]) Given a directed graph $\mathcal{G}$ with Laplacian Matrix L, L has at least one zero eigenvalue with an associated eigenvector 1_m, and all the nonzero eigenvalues are in the open right half plane. Furthermore, L has exactly one zero eigenvalue if and only if the $\mathcal{G}$ has a directed spanning tree.*

2.1.1 Ordered Index for the Edges

In order to simplify the subscript notation, a new ordered index k is assumed to label each edge, replacing the pair (i, j) for a single k, such that $e_{ij}(t) = e_k(t)$. Letting r represent the total number of directed edges in the Graph $\mathcal{G}$ or equivalently the number of elements in $\mathcal{E}$, it follows that $k = 1, \ldots, r$. The assignment of index k is outlined in Algorithm 2.1 with some other additional variables h_k and $\bar{h}_k$ which will be used next to write the Laplacian matrix in an alternative form.

To illustrate the result of Algorithm 2.1, consider its application on the graph presented in Figure 2.1b, the result for the new indices in edges e_k is presented in Figure 2.4.

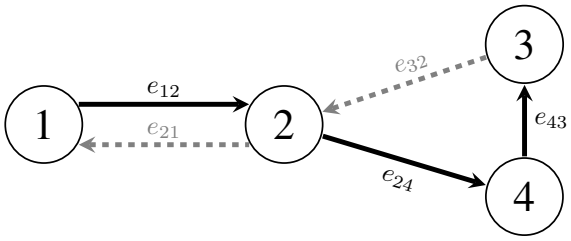

(a) Directed spanning tree $\mathcal{G}_{span,1}$.

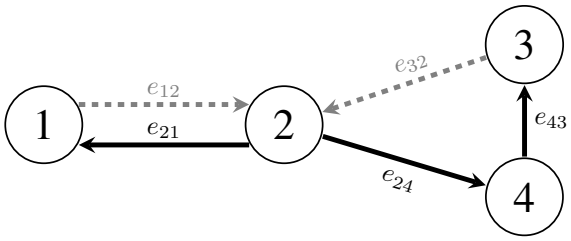

(b) Directed spanning tree $\mathcal{G}_{span,2}$.

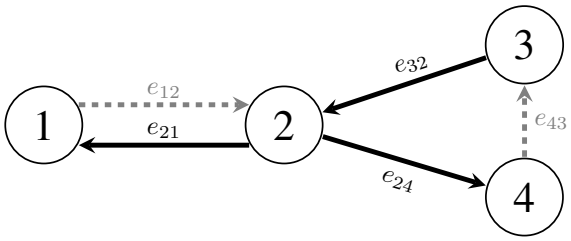

(c) Directed spanning tree $\mathcal{G}_{span,3}$.

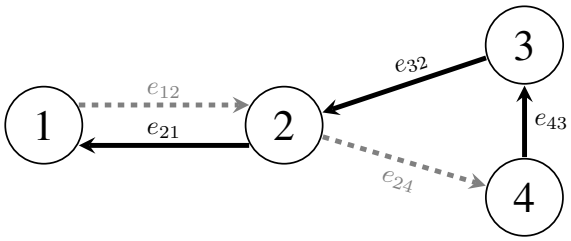

(d) Directed spanning tree $\mathcal{G}_{span,4}$.

Figure 2.3: Example of directed spanning trees $\mathcal{G}_{span}$.

Algorithm 2.1: New indices k

Initialize: $k \leftarrow 0$;
for $i = 1, 2, \ldots, m$ **do**
  for $j = 1, 2, \ldots, m$ **do**
    if $\exists e_{ji} \in \mathcal{E}$ **then**
      $k \leftarrow k + 1$;
      $a_k \leftarrow a_{ij}$;
      $e_k \leftarrow e_{ji}$;
      $h_k \leftarrow$ zero column-vector of size m;
      $\bar{h}_k \leftarrow$ zero column-vector of size m;
      h_k i-th entry $\leftarrow 1$; h_k j-th entry $\leftarrow -1$;
      $\bar{h}_k$ i-th entry $\leftarrow 1$;

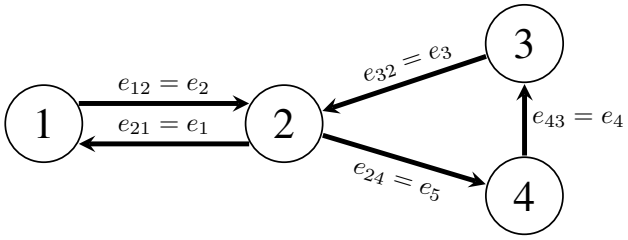

Figure 2.4: New indices k for the edges in a graph.

Subgraphs on edges

For each edge e_k on the graph with the new indices k as in Figure 2.4, it can be defined the subgraph on edge k, $\mathcal{G}_{e,k}$. A subgraph $\mathcal{G}_{e,k}$ of $\mathcal{G}$ has the same set of vertices $\mathcal{V}_{e,k} = \mathcal{V}$ but exactly one edge e_k in set of edges $\mathcal{E}_{e,k} \subset \mathcal{E}$, with $e_k = e_{ji}$ from Algorithm 2.1. Since r is the number of edges in $\mathcal{E}$, a graph $\mathcal{G}$ has r subgraphs $\mathcal{G}_{e,k}$. For illustration purpose, the five subgraphs originated from the graph in Figure 2.4 are shown in Figure 2.5.

2.1.2 Alternative Representation of the Laplacian Matrix

From Algorithm 2.1, the Laplacian Matrix L associated with graph $\mathcal{G}$ is defined in an alternative form, inspired by Godsil and Royle (2003), where the weights a_{ij} of the edges in $\mathcal{E}$ can be conveniently displayed in the diagonal of a Weight Matrix W. This matrix plays an important role in the design methods, later discussed in this work.

Consider the index of each directed edge $e_{ij} \in \mathcal{E}$ rewritten according to Algorithm 2.1, such that the edges are ordered as $e_k = e_{ji}$, with associated weights a_k, and vectors h_k and $\bar{h}_k$. Also $k = 1, \ldots, r$ where r is the number of edges in the Graph $\mathcal{G}$. Thus, the Incidence Matrix of a directed graph $\mathcal{G}$ is defined as

$$H = [h_1 \ \ldots \ h_r], \tag{2.4}$$

and the associated Heading Matrix is defined as

$$\bar{H} = [\bar{h}_1 \ \ldots \ \bar{h}_r], \tag{2.5}$$

both matrices of dimension $m \times r$. Additionally, writing the ordered coupling strengths $a_k = a_{ij}$ according to Algorithm 2.1 in the ascending order of k in the diagonal of a matrix, it is defined the Weight Matrix $\mathcal{W} \in \mathbb{R}^{r \times r}$.

Finally, the Laplacian Matrix can be alternatively written according to the following Lemma.

Lemma 2.2 *From Algorithm 2.1, let H be the $m \times r$ Incidence Matrix as in* (2.4)*, $\bar{H}$ be the $m \times r$ associated Heading Matrix as in* (2.5)*, and $\mathcal{W}$ be the $r \times r$ diagonal Weight*

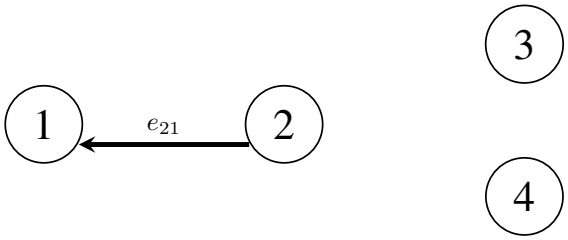

(a) Subgraph $\mathcal{G}_{e,1}$.

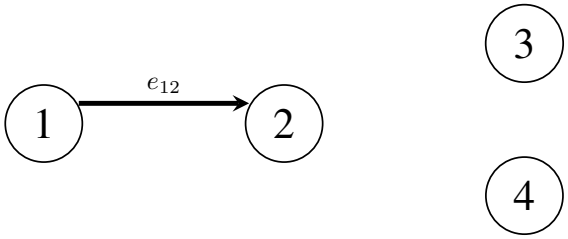

(b) Subgraph $\mathcal{G}_{e,2}$.

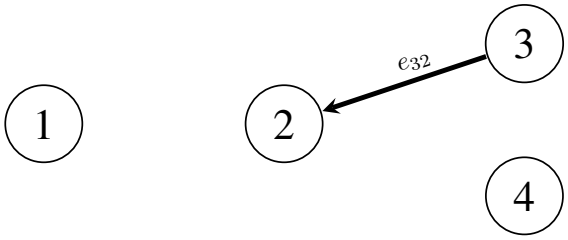

(c) Subgraph $\mathcal{G}_{e,3}$.

(d) Subgraph $\mathcal{G}_{e,4}$.

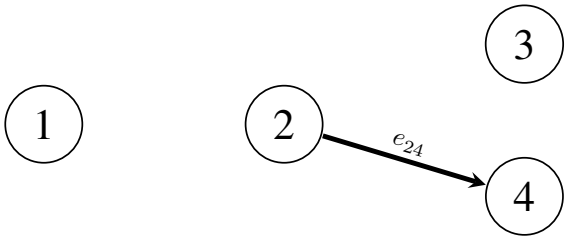

(e) Subgraph $\mathcal{G}_{e,5}$.

Figure 2.5: Example of subgraphs on edges.

Matrix associated with a directed graph $\mathcal{G}$. Thus, the Laplacian Matrix L of $\mathcal{G}$ can be written as

$$L = \bar{H}\mathcal{W}H^T. \tag{2.6}$$

Proof Equation (2.6) can be expanded as

$$\bar{H}\mathcal{W}H^T = \sum_{k=1}^{r} a_k \bar{h}_k h_k^T.$$

Since, from Algorithm 2.1, $\bar{h}_k$ is a column-vector of size m with some i-th entry equal 1 and 0 elsewhere, where i is associated with the head v_i of the edge $e_k = e_{ji}$, the product $a_k\bar{h}_k h_k^T$ gives an $m \times m$ matrix with h_k^T weighted by a_k in the i-th row and 0 elsewhere. This is the Laplacian Matrix of a subgraph on edge $\mathcal{G}_{e,k}$ containing only edge e_k, i.e. $a_k\bar{h}_k h_k^T = L_k$, thus

$$\sum_{k=1}^{r} a_k \bar{h}_k h_k^T = \sum_{k=1}^{r} L_k = L.$$

This completes the proof. □

The following remarks summarize some additional results:

Remark 2.1 *As noted in the proof of Lemma 2.2, Algorithm 2.1 simplifies writing the Laplacians L_k related to the subgraphs $\mathcal{G}_{e,k}$ of each edge e_k, with*

$$L_k = a_k \bar{h}_k h_k^T.$$

Remark 2.2 *The weights $a_k = a_{ij}$ are given in the main diagonal of W, i.e.*

$$W = \text{diag}\{a_1, a_2, \ldots, a_r\}.$$

2.2 Consensus Problem Formulation

In this section, the consensus problem is defined for agents with linear dynamics. Single-order dynamics and high-order integrator dynamics are special cases of this one. Next, the transformation of consensus problem into a stability one is presented for systems with communication delay, systems with input delays, and finally for systems without delays, which is a special case of the previous two.

First, the definition of consensus is formalized:

Definition 2.1 *A multi-agent system composed of m agents with state variables $x_i(t) \in \mathbb{R}^n$, where $i \in \{1, \ldots, m\}$ is the agent index, asymptotically reaches consensus if, for all $i \neq j$,*

$$\lim_{t\to\infty}(x_i(t) - x_j(t)) = 0 \tag{2.7}$$

hold for any initial state condition.

The conditions presented in the next chapters for the analysis of consensus rely on Definition 2.1.

In order to obtain a compact representation of the multi-agent system, a unique stacked state vector is given to comprise all the agent states $x_i(t)$ as

$$x(t) = \begin{bmatrix} x_1(t) \\ x_2(t) \\ \vdots \\ x_m(t) \end{bmatrix}. \tag{2.8}$$

2.2.1 Tree-type Transformation

Consensus can be translated into a stability problem by means of a transformation denominated as tree-type transformation by Sun and Wang (2009). This is done by introducing new variables $z_i(t)$ representing the disagreement on the state variables, given by

$$z_i(t) = x_1(t) - x_{i+1}(t), \tag{2.9}$$

for $i = 1, 2, \ldots, m-1$. The disagreement variables can be stacked in a vector $z(t)$ similarly to $x(t)$ by doing

$$z(t) = \begin{bmatrix} z_1(t) \\ z_2(t) \\ \vdots \\ z_{m-1}(t) \end{bmatrix}, \tag{2.10}$$

or equivalently

$$z(t) = (U \otimes I_n)x(t), \tag{2.11}$$

where

$$U = [1_{m-1} \quad -I_{m-1}], \tag{2.12}$$

which represents the tree-type transformation, with inverse transformation given by

$$x(t) = 1_m \otimes x_1(t) + (W \otimes I_n)z(t), \tag{2.13}$$

where

$$W = \begin{bmatrix} 0_{m-1}^T \\ -I_{m-1} \end{bmatrix}. \tag{2.14}$$

Then, the following proposition establishes the relation between consensus and the stability analysis of the transformed system:

Proposition 2.1 *The multi-agent system with stacked state variables $x(t)$ in (2.8) is in consensus if and only if the stacked disagreement vector $z(t)$ in (2.10) is null.*

Proof It is clear from (2.9) that if the agents reach consensus then $z(t)$ is null. Now, consider that $z(t)$ reaches the origin, thus, from (2.13)

$$x(t) = 1_m \otimes x_1(t) + \cancelto{0}{(W \otimes I_n)z(t)}, \tag{2.15}$$

such that all the agents reach the same state of $x_1(t)$, which means consensus, completing the proof. □

The above proposition essentially establishes that consensus can be assessed by studying stability of the transformed system $z(t)$. Thus, with Proposition 2.1, Definition 2.1 is translated into:

Corollary 2.1 *A multi-agent system composed of m agents with state variables $x_i(t) \in \mathbb{R}^n$, where $i \in \{1, \ldots, m\}$ is the agent index, asymptotically reaches consensus according to Definition 2.1 if and only if the stacked disagreement vector asymptotically reaches the origin, i.e*

$$\lim_{t \to \infty} z(t) = 0 \tag{2.16}$$

holds for any initial state conditions.

Next sections describe the transformation of multi-agent systems with communication delays, input delays, and free of delays.

2.2.2 Consensus Problem with Communication Delay

A multiagent system is modeled by a graph $\mathcal{G}$ where each node represents an agent, and the edges represent communication channels. Consider a system with m agents with linear dynamics:

$$\dot{x}_i(t) = Ax_i(t) + Bu_i(t), \quad i = 1, 2, \ldots, m, \tag{2.17}$$

where $x_i \in \mathbb{R}^n$ are the state variables of the i-th agent, with $n \in \mathbb{N}$ determining the order of the agent dynamics, $u_i \in \mathbb{R}^p$ is the control input of the i-th agent, for $p \in \mathbb{N}$ representing the order of the input, $A \in \mathbb{R}^{n\times n}$, and $B \in \mathbb{R}^{n\times p}$.

The analysis is based on the following consensus protocol with communication delays

$$u_i(t) = -\sum_{j\neq i, j=1}^{m} a_{ij} K\big(x_i(t) - x_j(t-\tau_{ij}(t))\big), \tag{2.18}$$

where $K \in \mathbb{R}^{p\times n}$ is a constant Gain Matrix and $\tau_{ij}(t)$ is the time-varying communication delay from agent j to agent i. The topology of $\mathcal{G}$ is taken into account through $a_{ij} \in \mathcal{A}$, e.g. $a_{ij} = 0$ if node i gets no information from j. The control input $u_i(t)$ is based on the information from neighbors of agent i since $a_{ij} = 0$ if i and j are not neighbors. Initial conditions for the agents' states are denoted by:

$$x_i(\iota) = \phi_i(\iota), \quad \forall \iota \in [-\tau^{\max}, 0], \tag{2.19}$$

where the functions ϕ_i are arbitrary and correspond to the sets of initial conditions considered over the interval $[-\tau^{\max}, 0]$, where $\tau^{\max}$ correspond to the maximum time-delay value. In addition $\tau_{ij}(t) \in [\tau^{\min}, \tau^{\max}]$.

A compact representation of the multi-agent system is given by

$$\dot{x}(t) = (I_m \otimes A)x(t) + (I_m \otimes B)u(t), \tag{2.20}$$

where $x(t)$ is a stacked state vector as in (2.8) and $u(t)$ is a stacked input vector given by

$$u(t) = \begin{bmatrix} u_1(t) \\ u_2(t) \\ \vdots \\ u_m(t) \end{bmatrix} = \sum_{i=1}^{m} \bar{u}_i(t) = \underbrace{\begin{bmatrix} u_1(t) \\ 0_n \\ \vdots \\ 0_n \end{bmatrix}}_{\bar{u}_1(t)} + \underbrace{\begin{bmatrix} 0_n \\ u_2(t) \\ \vdots \\ 0_n \end{bmatrix}}_{\bar{u}_2(t)} + \ldots + \underbrace{\begin{bmatrix} 0_n \\ 0_n \\ \vdots \\ u_m(t) \end{bmatrix}}_{\bar{u}_m(t)}, \tag{2.21}$$

with $\bar{u}_i(t) \in \mathbb{R}^{mn}$ the input vector for the i-th agent only, arranged in the form $\bar{u}_i(t) = \vartheta_i \otimes u_i(t)$, with ϑ_i an m-dimensional column vector with the i-th entry being one and zeros elsewhere. Thus, $u(t)$ can be given as

$$u(t) = \sum_{i=1}^{m} \vartheta_i \otimes u_i(t), \tag{2.22}$$

and replacing the consensus protocol (2.18), gives

$$u(t) = -\sum_{i=1}^{m} \vartheta_i \otimes \sum_{j\neq i, j=1}^{m} a_{ij} K\big(x_i(t) - x_j(t-\tau_{ij}(t))\big), \tag{2.23}$$

$$= \left(\sum_{i=1}^{m} \vartheta_i \otimes K \sum_{j\neq i, j=1}^{m} a_{ij} x_j(t-\tau_{ij}(t))\right) - \left(\sum_{i=1}^{m} \vartheta_i \otimes K \sum_{j\neq i, j=1}^{m} a_{ij} x_i(t).\right) \tag{2.24}$$

It can be shown after some computation that

$$\sum_{j\neq i,j=1}^{m} a_{ij}x_j(t-\tau_{ij}(t)) = \sum_{k=1}^{r}(\vartheta_i^T\mathcal{A}_{e,k}\otimes I_n)x(t-\tau_k(t)), \tag{2.25}$$

and

$$\sum_{j\neq i,j=1}^{m} a_{ij}x_i(t) = d_{ii}x_i(t) = (\vartheta_i^T\mathcal{D}\otimes I_n)x(t), \tag{2.26}$$

where $\mathcal{A}_{e,k}$ is the Adjacency Matrix of the subgraph $\mathcal{G}_{e,k}$, containing edge $e_{ji} = e_k$ with corresponding delay $\tau_{ij}(t) = \tau_k(t)$ according to Algorithm 2.1, and $\mathcal{D}$ is the Degree Matrix of the network graph $\mathcal{G}$.

Replacing (2.26) and (2.25) into (2.24) yields

$$u(t) = \underbrace{\left(\sum_{i=1}^{m}\vartheta_i\otimes K\sum_{k=1}^{r}(\vartheta_i^T\mathcal{A}_{e,k}\otimes I_n)x(t-\tau_k(t))\right)}_{T_I} - \underbrace{\left(\sum_{i=1}^{m}\vartheta_i\otimes K(\vartheta_i^T\mathcal{D}\otimes I_n)x(t)\right)}_{T_{II}}. \tag{2.27}$$

With some properties of the Kronecker product as associativity and the mixed-product $(A\otimes B)(C\otimes D) = (AC)\otimes(BD)$, for A, B, C and D matrices with appropriate dimensions, and considering $x(t-\tau_k(t))$ similarly to (2.22) as $x(t-\tau_k(t)) = \sum_{i=1}^{m}\vartheta_i\otimes x_i(t-\tau_k(t))$, the first term T_I on the right side of (2.27) can be written as

$$T_I = \sum_{i=1}^{m}\vartheta_i\otimes(1\otimes K)\sum_{k=1}^{r}(\vartheta_i^T\otimes I_n)(\mathcal{A}_{e,k}\otimes I_n)\sum_{l=1}^{m}(\vartheta_l\otimes x_l(t-\tau_k(t))), \tag{2.28}$$

$$= \sum_{i=1}^{m}\sum_{k=1}^{r}\sum_{l=1}^{m}(\vartheta_i 1)\otimes\vartheta_i^T\mathcal{A}_{e,k}\vartheta_l\otimes Kx_l(t-\tau_k(t)), \tag{2.29}$$

$$= \sum_{i=1}^{m}\sum_{k=1}^{r}\sum_{l=1}^{m}(\vartheta_i\otimes\vartheta_i^T)(\mathcal{A}_{e,k}\vartheta_l)\otimes Kx_l(t-\tau_k(t)). \tag{2.30}$$

Noticing that

$$\sum_{i=1}^{m}(\vartheta_i\otimes\vartheta_i^T) = I_m, \tag{2.31}$$

yields

$$T_I = \sum_{k=1}^{r}\sum_{l=1}^{m}\mathcal{A}_{e,k}\vartheta_l\otimes Kx_l(t-\tau_k(t)), \tag{2.32}$$

$$= \sum_{k=1}^{r}(\mathcal{A}_{e,k}\otimes K)\sum_{l=1}^{m}(\vartheta_l\otimes x_l(t-\tau_k(t))), \tag{2.33}$$

$$= \sum_{k=1}^{r}(\mathcal{A}_{e,k}\otimes K)x(t-\tau_k(t)). \tag{2.34}$$

Similarly, the second term T_{II} on the right side of (2.27), analogously considering $x(t) = \sum_{i=1}^{m} \vartheta_i \otimes x_i(t)$, can be written as

$$T_{II} = \sum_{i=1}^{m}\sum_{l=1}^{m} \vartheta_i \otimes (1 \otimes K)(\vartheta_i^T \mathcal{D} \otimes I_n)(\vartheta_l \otimes x_l(t)), \tag{2.35}$$

$$= \sum_{i=1}^{m}\sum_{l=1}^{m} (\vartheta_i 1) \otimes \vartheta_i^T \mathcal{D} \vartheta_l \otimes K x_l(t), \tag{2.36}$$

$$= \sum_{i=1}^{m}\sum_{l=1}^{m} (\vartheta_i \otimes \vartheta_i^T)(\mathcal{D}\vartheta_l) \otimes K x_l(t), \tag{2.37}$$

$$= \sum_{l=1}^{m} \mathcal{D}\vartheta_l \otimes K x_l(t), \tag{2.38}$$

$$= (\mathcal{D} \otimes K) \sum_{l=1}^{m} (\vartheta_l \otimes x_l(t)), \tag{2.39}$$

$$= (\mathcal{D} \otimes K) x(t). \tag{2.40}$$

Replacing (2.34) and (2.40) into (2.27), yields the stacked control input of the multi-agent system

$$u(t) = \sum_{k=1}^{r} (\mathcal{A}_{e,k} \otimes K) x(t - \tau_k(t)) - (\mathcal{D} \otimes K) x(t). \tag{2.41}$$

Replacing (2.41) into (2.20), the closed-loop dynamics is given by

$$\dot{x}(t) = (I_m \otimes A)x(t) + (I_m \otimes B)\left(\sum_{k=1}^{r} (\mathcal{A}_{e,k} \otimes K) x(t - \tau_k(t)) - (\mathcal{D} \otimes K) x(t) \right), \tag{2.42}$$

$$= (I_m \otimes A)x(t) - (I_m \otimes B)(\mathcal{D} \otimes K)x(t) + \sum_{k=1}^{r} (I_m \otimes B)(\mathcal{A}_{e,k} \otimes K) x(t - \tau_k(t)), \tag{2.43}$$

$$= \left((I_m \otimes A) - (\mathcal{D} \otimes BK)\right) x(t) + \sum_{k=1}^{r} (\mathcal{A}_{e,k} \otimes BK) x(t - \tau_k(t)). \tag{2.44}$$

From the definition of the Laplacian Matrix in (2.2), $\mathcal{A}_{e,k} = \mathcal{D}_{e,k} - L_{e,k}$ is replaced into (2.44) to rewrite the closed-loop dynamics as

$$\dot{x}(t) = (I_m \otimes A - \mathcal{D} \otimes BK)x(t) + \sum_{k=1}^{r} (\mathcal{D}_{e,k} \otimes BK - L_{e,k} \otimes BK) x(t - \tau_k(t)). \tag{2.45}$$

Transformed System

The analysis of the transformed system $z(t)$ is done by taking the time-derivative of equation (2.11) and considering the system dynamics in (2.45), yielding

$$\dot{z}(t) = (U \otimes I_n)\left((I_m \otimes A - \mathcal{D} \otimes BK)x(t) + \sum_{k=1}^{r}(\mathcal{D}_{e,k} \otimes BK - L_{e,k} \otimes BK)x(t-\tau_k(t))\right). \tag{2.46}$$

Replacing $x(t)$ from (2.13) into the previous equation (2.46):

$$\begin{aligned}
\dot{z}(t) =&(U \otimes I_n)(I_m \otimes A)(1_m \otimes x_1(t)) - (U \otimes I_n)(\mathcal{D} \otimes BK)(1_m \otimes x_1(t)) \\
&+ (U \otimes I_n)(I_m \otimes A)(W \otimes I_n)z(t) - (U \otimes I_n)(\mathcal{D} \otimes BK)(W \otimes I_n)z(t) \\
&+ \sum_{k=1}^{r}(U \otimes I_n)(\mathcal{D}_{e,k} \otimes BK)\big(1_m \otimes x_1(t-\tau_k(t))\big) \\
&- \sum_{k=1}^{r}(U \otimes I_n)(L_{e,k} \otimes BK)\big(1_m \otimes x_1(t-\tau_k(t))\big) \\
&+ \sum_{k=1}^{r}(U \otimes I_n)(\mathcal{D}_{e,k} \otimes BK)(W \otimes I_n)z(t-\tau_k(t)) \\
&- \sum_{k=1}^{r}(U \otimes I_n)(L_{e,k} \otimes BK)(W \otimes I_n)z(t-\tau_k(t)), \\
=&U1_m \otimes I_n A x_1(t) - U\mathcal{D}1_m \otimes BKx_1(t) + (UW \otimes A)z(t) - (U\mathcal{D}W \otimes BK)z(t) \\
&+ \sum_{k=1}^{r} U\mathcal{D}_{e,k}1_m \otimes I_n BKx_1(t-\tau_k(t)) - \sum_{k=1}^{r}(UL_{e,k}1_m \otimes I_n BKx_1(t-\tau_k(t))) \\
&+ \sum_{k=1}^{r}(U\mathcal{D}_{e,k}W \otimes BK)z(t-\tau_k(t)) - \sum_{k=1}^{m}(UL_{e,k}W \otimes BK)z(t-\tau_k(t)).
\end{aligned} \tag{2.47}$$

The following assumptions are considered to allow the summation of $\mathcal{D}_{e,k}$ to become an identity matrix such that the product $U1_m$ can vanish with the terms x_1:

Assumption 2.1 *The multiagent system with communication delay is subject to the same delay in all the communication links, such that $\tau_k(t) = \tau(t)$ for all $k = 1, \ldots, r$.*

Assumption 2.2 *The network topology $\mathcal{G}$ of a multiagent system with communication delay is considered to be a special case of regular graph with $\mathcal{D} = I_m$.*

With assumptions 2.1 and 2.2, equation (2.47) simplifies to

$$\begin{aligned}\dot{z}(t) =& U1_m \otimes I_n A x_1(t) - U1_m \otimes BK x_1(t) + (UW \otimes A)z(t) - (UW \otimes BK)z(t) \\ &+ U1_m \otimes I_n BK x_1(t-\tau(t)) - (UL1_m \otimes I_n BK x_1(t-\tau(t))) \\ &+ (UW \otimes BK)z(t-\tau(t)) - (ULW \otimes BK)z(t-\tau(t)). \end{aligned} \tag{2.48}$$

Then, from the facts that $U1_m = 0_{m-1}$ and $L1_m = 0_m$, which eliminate the terms with $x_1(t)$, and noticing that $UW = I_{m-1}$, the following disagreement system is obtained:

$$\dot{z}(t) = (I_{m-1} \otimes (A - BK))z(t) + ((I_{m-1} - \bar{L}) \otimes BK)z(t-\tau(t)). \tag{2.49}$$

with

$$\bar{L} = ULW \in \mathbb{R}^{(m-1)\times(m-1)}. \tag{2.50}$$

Based on the disagreement of the state variables, consensus for a multiagent system with a network topology described by a regular graph as in Assumption 2.2, for agents with dynamics (2.17) with uniform communication delays, and consensus protocol given similarly to (2.18) with $\tau_k(t) = \tau(t)$, as

$$u_i(t) = -\sum_{j\neq i, j=1}^{m} a_{ij} K\big(x_i(t) - x_j(t-\tau(t))\big), \tag{2.51}$$

can be assessed by establishing stability of the disagreement system in (2.49) according to Corollary (2.1). In this context, Corollary (2.1) can be rewritten as follows:

Proposition 2.2 *The multi-agent system with agent dynamics* (2.17) *and consensus protocol* (2.51)*, asymptotically reaches consensus if and only if the transformed system* (2.49) *with assumptions 2.1 and 2.2 is asymptotically stable, i.e.:*

$$\lim_{t\to\infty} z(t) = 0 \tag{2.52}$$

holds for any initial state condition.

2.2.3 Consensus Problem with Input Delay

Consider a system with m agents with delayed linear dynamics:

$$\dot{x}_i(t) = Ax_i(t) + Bu_i(t-\tau_i(t)), \quad i = 1, 2, \ldots, m, \tag{2.53}$$

where $x_i \in \mathbb{R}^n$ is the state-vector of variables of the i-th agent, n is the order of the agent dynamics, $u_i \in \mathbb{R}^p$ is the control input of the i-th agent, $A \in \mathbb{R}^{n\times n}$, and $B \in \mathbb{R}^{n\times p}$, with p representing the order of the input. The variable $\tau_i(t)$ is a time-varying input delay affecting the control input of the i-th agent.

The analysis is based on the following consensus protocol without communication delays:

$$u_i(t) = -\sum_{j\neq i, j=1}^{m} a_{ij} K\big(x_i(t) - x_j(t)\big), \tag{2.54}$$

where $K \in \mathbb{R}^{p\times n}$ is a constant Gain Matrix, the topology arrangement is taken into account through a_{ij}, and $u_i(t)$ indicates the control input based on the neighbors of agent i. Initial conditions for the agents' states are denoted like (2.19).

A unique augmented dynamics is given to comprise all the agents modeled by (2.53) and consensus protocol (2.54), similarly to (2.20) with (2.22):

$$\dot{x}(t) \quad = (I_m \otimes A)x(t) + (I_m \otimes B)\sum_{i=1}^{m} \vartheta_i \otimes u_i(t - \tau_i(t)) \tag{2.55}$$

where $x(t)$ is the complete stacked state vector as in (2.8).

From (2.54), the control input $\vartheta_i \otimes u_i(t - \tau_i(t))$ becomes

$$\vartheta_i \otimes u_i(t - \tau_i(t)) = -\vartheta_i \otimes \sum_{j\neq i, j=1}^{m} a_{ij} K\big(x_i(t) - x_j(t - \tau_i(t))\big), \tag{2.56}$$

$$= \left(\vartheta_i \otimes K \sum_{j\neq i, j=1}^{m} a_{ij} x_j(t - \tau_i(t))\right) - \left(\vartheta_i \otimes K \sum_{j\neq i, j=1}^{m} a_{ij} x_i(t - \tau_i(t))\right). \tag{2.57}$$

As in (2.25) and (2.26), it is possible to write

$$\sum_{j\neq i, j=1}^{m} a_{ij} x_j(t - \tau_i(t)) = (\vartheta_i^T \mathcal{A}_{a,i} \otimes I_n)x(t - \tau_i(t)), \tag{2.58}$$

and

$$\sum_{j\neq i, j=1}^{m} a_{ij} x_i(t - \tau_i(t)) = d_{ii} x_i(t - \tau_i(t)) = (\vartheta_i^T \mathcal{D}_{a,i} \otimes I_n)x(t - \tau_i(t)), \tag{2.59}$$

where $\mathcal{A}_{a,i}$ and $\mathcal{D}_{a,i}$ are the Adjacency and Degree matrices of the subgraph on node $\mathcal{G}_{a,i}$, respectively, containing edges e_{ji} pointing toward v_i.

Replacing (2.58) and (2.59) into (2.57) yields

$$\vartheta_i \otimes u_i(t - \tau_i(t)) = \vartheta_i \otimes K\big(\vartheta_i^T(\mathcal{A}_{a,i} - \mathcal{D}_{a,i}) \otimes I_n\big)x(t - \tau_i(t)) \tag{2.60}$$

$$= -\vartheta_i \otimes K\big(\vartheta_i^T L_{a,i} \otimes I_n\big)x(t - \tau_i(t)), \tag{2.61}$$

where $L_{a,i}$ is the Laplacian Matrix of $\mathcal{G}_{a,i}$, satisfying $L_{a,i} = \mathcal{D}_{a,i} - \mathcal{A}_{a,i}$ from (2.2). Following the properties of Kronecker product and writing term $x(t-\tau_i(t))$ similarly to (2.22), i.e. $x(t-\tau_i(t)) = \sum_{i=1}^{m} \vartheta_i \otimes x_i(t-\tau_i(t))$, gives

$$\vartheta_i \otimes u_i(t-\tau_i(t)) = -\vartheta_i \otimes (1 \otimes K)\big(\vartheta_i^T L_{a,i} \otimes I_n\big) \sum_{l=1}^{m} (\vartheta_l \otimes x_l(t-\tau_i(t))), \tag{2.62}$$

$$= -\sum_{l=1}^{m} (\vartheta_i 1) \otimes \vartheta_i^T L_{a,i} \vartheta_l \otimes K x_l(t-\tau_i(t)), \tag{2.63}$$

$$= -\sum_{l=1}^{m} (\vartheta_i \otimes \vartheta_i^T)(L_{a,i}\vartheta_l) \otimes K x_l(t-\tau_i(t)). \tag{2.64}$$

Noticing that

$$\sum_{i=1}^{m} (\vartheta_i \otimes \vartheta_i^T) L_{a,i} = L_{a,i}, \tag{2.65}$$

then

$$\vartheta_i \otimes u_i(t-\tau_i(t)) = -\sum_{l=1}^{m} (L_{a,i}\vartheta_l) \otimes K x_l(t-\tau_i(t)), \tag{2.66}$$

$$= -\sum_{l=1}^{m} (L_{a,i} \otimes K)(\vartheta_l \otimes x_l(t-\tau_i(t))), \tag{2.67}$$

$$= -(L_{a,i} \otimes K) x(t-\tau_i(t)). \tag{2.68}$$

Finally, replacing (2.68) into (2.55), the closed-loop dynamics is given by

$$\dot{x}(t) \quad = (I_m \otimes A)x(t) - \sum_{i=1}^{m} (L_{a,i} \otimes BK) x(t-\tau_i(t)). \tag{2.69}$$

Transformed System

As in previous section, the tree-type transformation is used to translate the consensus problem into a stability problem using the disagreement variables $z_i(t)$ in (2.9) with transformation (2.11).

Taking the time-derivative of equation (2.11) and considering the system dynamics in (2.69), yields

$$\dot{z}(t) = (U \otimes I_n) \left((I_m \otimes A)x(t) - \sum_{i=1}^{m} (L_{a,i} \otimes BK) x(t-\tau_i(t)) \right). \tag{2.70}$$

Now, replacing $x(t)$ from the inverse transformation in (2.13) into the previous equation (2.70):

$$\begin{aligned}\dot{z}(t) =&(U \otimes I_n)(I_m \otimes A)(1_m \otimes x_1(t)) + (U \otimes I_n)(I_m \otimes A)(W \otimes I_n)z(t)\\ &- \sum_{i=1}^{m}(U \otimes I_n)(L_{a,i} \otimes BK)\big(1_m \otimes x_1(t-\tau_i(t))\big)\\ &- \sum_{i=1}^{m}(U \otimes I_n)(L_{a,i} \otimes BK)(I_n \otimes W)z(t-\tau_i(t)),\\ =&\,(U1_m) \otimes (Ax_1(t)) + (UW) \otimes (A)\, z(t)\\ &- \sum_{i=1}^{m}(UL_{a,i}1_m) \otimes (BKx_1(t-\tau_i(t))) - \sum_{i=1}^{m}(UL_{a,i}W) \otimes (BK)\, z(t-\tau_i(t)). \quad (2.71)\end{aligned}$$

Then, using the properties $U1_m = 0_{m-1}$ and $L_{a,i}1_m = 0_m$, which eliminate the terms with $x_1(t)$, and noticing that $UW = I_{m-1}$, the following disagreement system is obtained:

$$\dot{z}(t) = (I_{m-1} \otimes A)z(t) - \sum_{i=1}^{m}(\bar{L}_{a,i} \otimes (BK))z(t-\tau_i(t)), \quad (2.72)$$

with

$$\bar{L}_{a,i} = UL_{a,i}W \in \mathbb{R}^{(m-1)\times(m-1)}. \quad (2.73)$$

Based on the disagreement of the state variables, consensus of a directed network of agents with delayed input dynamics (2.53) and consensus protocol given in (2.54) can be assessed by establishing stability of the disagreement system in (2.72) according to Corollary (2.1). In this context, Corollary (2.1) can be rewritten as follows:

Proposition 2.3 *The multi-agent system composed of agents with delayed input dynamics* (2.53) *and consensus protocol* (2.54)*, asymptotically reaches consensus if and only if the transformed system* (2.72) *is asymptotically stable, i.e.:*

$$\lim_{t\to\infty} z(t) = 0 \quad (2.74)$$

holds for any initial state condition.

2.2.4 Consensus free of Time-Delays

A group of m agents free of delays in the control inputs or in the communication links is described according to the agents dynamics in (2.17) and consensus protocol as in (2.54).

The closed-loop stacked dynamics for the multi-agent system can be obtained either from (2.45) or (2.69), just by considering the time-delays null, giving

$$\dot{x}(t) = (I_m \otimes A - L \otimes BK)x(t). \quad (2.75)$$

Equation (2.75) can also be written in the form

$$\dot{x}(t) = \Gamma x(t), \tag{2.76}$$

with $\Gamma = I_m \otimes A - L \otimes BK$.

Likewise, the transformed system can be given by (2.49) or (2.72), also considering null time-delays, as

$$\dot{z}(t) = (I_{m-1} \otimes A)z(t) - (\bar{L} \otimes (BK))z(t). \tag{2.77}$$

Finally consensus can be assessed according to:

Proposition 2.4 *The multi-agent system composed of agents with input dynamics* (2.17) *and consensus protocol* (2.54)*, asymptotically reaches consensus if and only if system* (2.77) *is asymptotically stable, i.e.:*

$$\lim_{t\to\infty} z(t) = 0 \tag{2.78}$$

holds for any initial state condition.

The following lemmas are useful:

Lemma 2.3 *(Ren et al. (2006)) The matrix* Γ *in* (2.76) *has at least n zero eigenvalues. It has exactly n zero eigenvalues if and only if the Laplacian L has a simple zero eigenvalue, i.e. the zero eigenvalue has multiplicity one. Moreover, if L has a simple zero eigenvalue, the zero eigenvalue of* Γ *has only one linearly independent eigenvector associated with the eigenvalue zero.*

Lemma 2.4 *(Ren et al. (2006)) The system in* (2.76) *achieves consensus asymptotically if and only if matrix* Γ *has exactly n zero eigenvalues and all the other eigenvalues have negative real parts.*

Note that, combining Lemmas 2.1, 2.3, and 2.4, consensus in directed networks of multi-agents with dynamics (2.17) and protocol (2.54), free of delays, is achieved if and only if the related graph $\mathcal{G}$ has a directed spanning tree and the nonzero eigenvalues of Γ, in (2.76), lie in the open left half-plane.

Also, regarding the eigenvalues of L and the tree-type transformation, the following proposition is useful for the next results.

Proposition 2.5 *Consider the Laplacian matrix L of a graph that has a directed spanning tree. Then, the eigenvalues of the transformed matrix $\bar{L}$ as in* (2.50) *are the nonzero eigenvalues of L, which are all in the open right half plane.*

Proof Assuming that the graph has a directed spanning tree, and applying Lemma 2.1, it yields that L has exactly one zero eigenvalue and all the other eigenvalues are in the open right half plane.

Now consider the invertible matrix:

$$T = \begin{bmatrix} 1 & 0_{m-1}^T \\ 1_{m-1} & -I_{m-1} \end{bmatrix} = \begin{bmatrix} \nu^T \\ U \end{bmatrix} = T^{-1} = \begin{bmatrix} 1_m & W \end{bmatrix}, \tag{2.79}$$

with $\nu^T = [1 \;\; 0_{m-1}^T]$.

Then the following similarity transformation

$$TLT^{-1} = \begin{bmatrix} \nu^T L 1_m & \nu^T L W \\ U L 1_m & U L W \end{bmatrix} = \begin{bmatrix} 0 & \nu^T L W \\ 0_{m-1} & \bar{L} \end{bmatrix} \tag{2.80}$$

reveals that the matrix $\bar{L}$ has all the nonzero eigenvalues of L. This concludes the proof. □

2.3 Additional Lemmas

The lemmas and definitions summarized next are used to prove the results in the next chapters.

Lemma 2.5 *(Sun et al., 2009) For any constant matrix $M = M^T > 0$ and scalars $t > t - \tau \geq 0$ such that the following integrations are well defined, then*

$$\int_{-\tau}^{0} \int_{t+\zeta}^{t} z^T(\xi) M z(\xi) d\xi d\zeta \geq \frac{2}{\tau^2} \int_{-\tau}^{0} \int_{t+\zeta}^{t} z^T(\xi) d\xi d\zeta M \int_{-\tau}^{0} \int_{t+\zeta}^{t} z(\xi) d\xi d\zeta. \tag{2.81}$$

Lemma 2.6 (Wirtinger inequality) *(Seuret and Gouaisbaut, 2013) For any constant matrix $M = M^T > 0$ and scalars $t > t - \tau \geq 0$ such that the following integrations are well defined, then*

$$\int_{t-\tau}^{t} \dot{z}^T(\xi) M \dot{z}(\xi) d\xi \geq \frac{1}{\tau} \int_{t-\tau}^{t} \dot{z}^T(\xi) d\xi M \int_{t-\tau}^{t} \dot{z}(\xi) d\xi + \frac{3}{\tau} \Omega^T M \Omega, \tag{2.82}$$

with

$$\Omega = z(t-\tau) + z(t) - \frac{2}{\tau} \int_{t-\tau}^{t} z(\xi) d\xi. \tag{2.83}$$

Lemma 2.7 *(Xiong and Lam, 2009) Let a real number $\gamma \in \mathbb{R}$, a square matrix $M \in \mathbb{R}^{n\times n}$, and a symmetric positive definite matrix $N \in \mathbb{R}^{n\times n}$ be given. The following inequality is true:*

$$\gamma(M + M^T) \leq \gamma^2 N + MN^{-1}M^T. \tag{2.84}$$

Lemma 2.8 *(Ren and Beard, 2005) If a nonnegative matrix $\mathcal{A}$ has the same positive constant row sums given by $\mu > 0$, then μ is an eigenvalue of $\mathcal{A}$ with an associated eigenvector 1 and $\rho(\mathcal{A}) = \mu$, where $\rho(\cdot)$ denotes the spectral radius. In addition, the eigenvalue μ of $\mathcal{A}$ has algebraic multiplicity equal one, if and only if the graph associated with $\mathcal{A}$ has a spanning tree. Furthermore, if the graph associated with $\mathcal{A}$ has a spanning tree and $a_{ii} > 0$, then μ is the unique eigenvalue of maximum modulus.*

Definition 2.2 *(Fei et al., 2009) Let a stochastic process be defined by $\theta_t, t \in [0, +\infty]$, the infinitesimal generator applied to an arbitrary function $f(\theta_t)$ is given by*

$$\mathcal{L}f(\theta_t) = \lim_{\Delta\to 0} \mathbb{E}\left[\frac{f(\theta_{t+\Delta}) - f(\theta_t)}{\Delta}\right], \tag{2.85}$$

where $\mathcal{L}$ represents the infinitesimal generator operator and $\mathbb{E}$ the expectancy.

Definition 2.3 (Dynkin's Formula) *(Dynkin (1965)) A stochastic extension of the second fundamental theorem of calculus is given by*

$$\mathbb{E}[f(X(\theta_t))] = f(0) + \mathbb{E}\left[\int_0^t \mathcal{L}f(X(\theta_\xi))d\xi\right]$$

where $f(X(\theta_t))$ is a function on a stochastic variable $X(\theta_t)$.

Chapter 3

Consensus with Constant Time-Delays: Exact Conditions

If a multiagent system is able to achieve consensus, it is said that this system is consensable. The property of being consensable is called consensability. In this chapter, a method to analyze the margins of time-delays in which a multiagent system is consensable is developed based on the Direct Method by Walton and Marshall (1987) for stability analysis. The results show that consensability is given on intervals of communication delays in Theorem 3.1, or input delays in Theorem 3.2. It is also shown that communication and input delays have different impacts in the system dynamics. For example, it is shown that communication delays do not avoid consensus for agents described by single-integrators, but the input delay does, see Corollaries 3.1 and 3.3, respectively. It is also shown that the system can also be independent of communication delays for second-order dynamics when the gains in the consensus protocol are properly adjusted according to Corollary 3.2. For input delays, there is always a delay margins for first- and second-order integrator dynamics in which the system can achieve consensus, see Corollaries 3.3 and 3.4. For higher-order, consensability switches may occur.

Many examples are given to illustrate these results. It is shown an example for a system that can achieve consensus independent of the communication delay. Additionally, it is also presented an example of a system consensable in two different intervals of communication delays, i.e. achieves consensus if the communication delay belongs to the interval $[0, 2.2958)$, is not consensable in $[2.2958, 6.3358]$, and regain the ability to achieve consensus if the delay increases to $(6.3358, 7.2585)$. For input delays, the first examples are given for first- and second-order integrator agents, showing the delay margins of input delays. For third-order agents, an example is shown in which the system is not consensable when free of delay, but if the delay is properly increased to the interval $(0.1332, 0.4349)$ the system is then able to achieve consensus. These examples serve as counterexamples

for the usual acceptance that the time-delay only degrades the system's performance.

Following these results, agents described by a chain of integrators are studied, i.e. high-order integrator dynamics. This class of systems is chosen in order to explicitly present the influence of the order of the chain of integrators and the gains in the consensus protocol. For the analysis of intervals only, other methods like the one presented by de Oliveira et al. (2008) for general linear dynamics could be applied. Ren et al. (2006) showed that consensus in a delay-free network of agents with high-order integrator dynamics depends on the gains in the consensus protocol, even if the topology has a directed spanning tree. Afterwards, Wieland et al. (2008) presented a linear matrix inequality solution to design these gains such that the delay-free system could achieve consensus. Sipahi and Qiao (2011) showed exact results for the input time-delay margin in first-order integrator agents in undirected networks and its relation to the Laplacian eigenvalues. It was extended to second-order dynamics with input delays and communication delays by Cepeda-Gomez and Olgac (2011a,b). More recently, Yang (2013) investigated consensability switches in the time-delay domain, considering high-order consensus but limited to undirected networks.

In this chapter, consensus is studied by checking the stability of the associated transformed system constructed by means of the tree-type transformation, whose characteristic equation is directly related to the Laplacian matrix. This result extends the results for consensability switches by Yang (2013) to the case of directed networks of multi-agent systems with input and communication delays. Furthermore, particular results are presented for networks of agents with first- and second-order dynamics, for both communication and input delays.

The result for consensus on intervals of input delays has been presented by the author in Savino et al. (2015), at the 12th IFAC Workshop on Time Delay Systems. In this chapter, the result is also presented for communication delays.

3.1 Dynamics free of Delay

Consider a multiagent system composed of m agents with state variables

$$x_i(t) = \begin{bmatrix} x_{i,1}(t) \\ x_{i,2}(t) \\ \vdots \\ x_{i,n}(t) \end{bmatrix}, \quad i = 1, 2, \ldots, m, \tag{3.1}$$

with $x_{i,1}(t), x_{i,2}(t), \ldots, x_{i,n}(t) \in \mathbb{R}$ such that $x_i(t) \in \mathbb{R}^n$, and let the dynamics be given by a chain of integrators

$$\begin{aligned} \dot{x}_{i,1}(t) &= x_{i,2}(t), \\ \dot{x}_{i,2}(t) &= x_{i,3}(t), \\ &\vdots \\ \dot{x}_{i,n-1}(t) &= x_{i,n}(t), \\ \dot{x}_{i,n}(t) &= u_i(t), \end{aligned} \tag{3.2}$$

where $u_i(t) \in \mathbb{R}$ is the control input acting only in state $x_{i,n}(t)$. The agent dynamics can be represented as

$$\frac{\mathrm{d}}{\mathrm{d}t}\begin{bmatrix} x_{i,1}(t) \\ x_{i,2}(t) \\ \vdots \\ x_{i,n-1}(t) \\ x_{i,n}(t) \end{bmatrix} = \begin{bmatrix} 0 & 1 & 0 & \ldots & 0 \\ 0 & 0 & 1 & \ldots & 0 \\ \vdots & \vdots & \vdots & \ddots & \vdots \\ 0 & 0 & 0 & \ddots & 1 \\ 0 & 0 & 0 & \ldots & 0 \end{bmatrix} \begin{bmatrix} x_{i,1}(t) \\ x_{i,2}(t) \\ \vdots \\ x_{i,n-1}(t) \\ x_{i,n}(t) \end{bmatrix} + \begin{bmatrix} 0 \\ 0 \\ \vdots \\ 0 \\ 1 \end{bmatrix} u_i(t), \tag{3.3}$$

or generally by

$$\dot{x}_i(t) = \begin{bmatrix} 0_{n-1} & I_{n-1} \\ 0 & 0_{n-1}^T \end{bmatrix} x_i(t) + \begin{bmatrix} 0_{n-1} \\ 1 \end{bmatrix} u_i(t). \tag{3.4}$$

Equation (3.4) can be written similarly to the general form of a linear system in (2.17) as

$$\dot{x}_i(t) = A_{ho} x_i(t) + B_{ho} u_i(t), \tag{3.5}$$

with

$$A_{ho} = \begin{bmatrix} 0_{n-1} & I_{n-1} \\ 0 & 0_{n-1}^T \end{bmatrix}, \tag{3.6}$$

$$B_{ho} = \begin{bmatrix} 0_{n-1} \\ 1 \end{bmatrix}, \tag{3.7}$$

which are equivalent to A and B in (2.17), respectively.

The considered delay-free consensus protocol is given by

$$\begin{aligned} u_i(t) = -\sum_{j \neq i, j=1}^{m} a_{ij} \Big[&\alpha_1 \Big(x_{i,1}(t) - x_{j,1}(t) \Big) + \alpha_2 \Big(x_{i,2}(t) - x_{j,2}(t) \Big) \\ &+ \ldots + \alpha_n \Big(x_{i,n}(t) - x_{j,n}(t) \Big) \Big], \end{aligned} \tag{3.8}$$

where $\alpha_1, \alpha_2, \ldots, \alpha_n > 0$ are arbitrary real constants and a_{ij} are given by the Adjacency Matrix of the graph $\mathcal{G}$ describing the network topology. The consensus protocol (3.8) can also be represented by

$$u_i(t) = -\sum_{j\neq i, j=1}^{m} a_{ij} K_{ho}\big(x_i(t) - x_j(t)\big), \tag{3.9}$$

with

$$K_{ho} = \begin{bmatrix} \alpha_1 & \alpha_2 & \ldots & \alpha_n \end{bmatrix} \tag{3.10}$$

equivalent to K in (2.54).

Considering the agents dynamics (3.5) with consensus protocol (3.9), the system dynamics can be written similarly to (2.75) or with $\Gamma_{ho} = I_m \otimes A_{ho} - L \otimes B_{ho}K_{ho}$ equivalent to Γ in (2.76). Thus, the transformed system is given according to (2.77) by

$$\dot{z}(t) = (I_{m-1} \otimes A_{ho})z(t) - (\bar{L} \otimes (B_{ho}K_{ho}))z(t), \tag{3.11}$$

such that consensus for (3.5) with protocol (3.9) can be assessed by the stability of (3.11).

3.2 Dynamics with Communication Delay

It was shown that the high-order integrator dynamics (3.5) is a particular case of the linear system (2.17) with A, B, and K given by A_{ho}, B_{ho}, and K_{ho}, respectively.

For the analysis carried out with communication delay, the protocol (3.9) is given by

$$u_i(t) = -\sum_{j\neq i, j=1}^{m} a_{ij} K_{ho}\big(x_i(t) - x_j(t-\tau)\big), \tag{3.12}$$

which is similar to (2.18) subject to uniform and constant delay, i.e. $\tau_{ij}(t) = \tau$.

Thus, in order to show consensus according to Proposition 2.2, considering regular graphs by Assumption 2.2, the transformed system to be analyzed is given according to (2.49), considering the dynamics given by A_{ho}, B_{ho}, and K_{ho}, with $\tau(t) = \tau$:

$$\dot{z}(t) = (I_{m-1} \otimes (A_{ho} - B_{ho}K_{ho}))z(t) + ((I_{m-1} - \bar{L}) \otimes B_{ho}K_{ho})z(t-\tau). \tag{3.13}$$

3.2.1 Analysis

Consensus for agents with high-order integrator dynamics (3.5) and communication delay in protocol (3.12), can be assessed by studying the stability of the reduced-dimension

transformed system in (3.13). The stability of (3.13) is dictated by the location of the roots of the transcendental function

$$\Delta_\tau(s) = \det(sI_{n(m-1)} - \bar{A}_{com} - \bar{B}_{com}e^{-s\tau}), \tag{3.14}$$

with $\bar{A}_{com} = (I_{m-1} \otimes (A_{ho} - B_{ho}K_{ho}))$ and $\bar{B}_{com} = ((I_{m-1} - \bar{L}) \otimes B_{ho}K_{ho})$.

Next lemma establishes that the location of the roots of $\Delta_\tau(s)$ in (3.14) in the stability region is equivalent to the location of the roots of a simple set of quasi-polynomials in the stability region. This is a central result for the further analysis.

Lemma 3.1 *Consider the multiagent system in* (3.5) *with protocol* (3.12)*. Assume a directed network topology containing a directed spanning tree with Laplacian Matrix L. Then, the multiagent system is consensable when subject to time-delay τ if and only if all roots of*

$$p_i(s) = s^n + \big(1 + (\lambda_i\{L\} - 1)e^{-s\tau}\big)\sum_{p=1}^{n} s^{p-1}\alpha_p, \tag{3.15}$$

where $\lambda_i\{\cdot\}$ refers to the eigenvalues of a matrix, and α_p given in (3.10) *have negative real part, for $i = 1, 2, \ldots, m-1$.*

Proof Based on Proposition 2.2, the multiagent system in (3.5) with protocol (3.9) asymptotically achieves consensus if and only if (3.13) is asymptotically stable. This happens if and only if all roots of $\Delta_\tau(s)$ in (3.14) have negative real parts.

Note that $\Delta_\tau(s)$ in (3.14) can be rewritten using the Laplace expansion for computing the determinant as

$$\Delta_\tau(s) = \det\left(s^n I_{m-1} + \sum_{p=1}^{n} s^{p-1}\alpha_p\big(I_{m-1} - (I_{m-1} - \bar{L})e^{-s\tau}\big)\right), \tag{3.16}$$

$$= \prod_{i=1}^{m-1}\left(s^n + \lambda_i\Big\{\sum_{p=1}^{n} s^{p-1}\alpha_p\big(I_{m-1} - (I_{m-1} - \bar{L})e^{-s\tau}\big)\Big\}\right). \tag{3.17}$$

It follows

$$\Delta_\tau(s) = \prod_{i=1}^{m-1}\left(s^n + \lambda_i\Big\{\big(I_{m-1} - (I_{m-1} - \bar{L})e^{-s\tau}\big)\Big\}\sum_{p=1}^{n} s^{p-1}\alpha_p\right), \tag{3.18}$$

$$= \prod_{i=1}^{m-1}\Big(s^n + \big(1 - (1 - \lambda_i\{\bar{L}\})e^{-s\tau}\big)\sum_{p=1}^{n} s^{p-1}\alpha_p\Big). \tag{3.19}$$

Based on Proposition 2.5, the eigenvalues of $\bar{L}$ in (3.19) can be directly related to the non-zero eigenvalues of L. Then,

$$\Delta_\tau(s) = \prod_{i=1}^{m-1} \Big(s^n + \big(1 + (\lambda_i\{L\} - 1)e^{-s\tau}\big) \sum_{p=1}^{n} s^{p-1}\alpha_p \Big), \tag{3.20}$$

assuming the eigenvalues of L ordered such that the m-th eigenvalue of L is zero, i.e., $\lambda_m\{L\} = 0$.

Equation (3.20) shows that, for each nonzero eigenvalue of L there are n eigenvalues for the whole system dynamics, given by the roots of the polynomials in (3.15). This completes the proof. □

In short, Lemma 3.1 allows to write the characteristic equation (3.14) as the polynomials in (3.15), whose roots dictate consensability of the multi-agent system due to Proposition 2.2. It is important to note that the polynomials in (3.15) do not require any transformation of the system due to Proposition 2.5.

3.2.2 Consensus on Time-Delay Intervals

The next result is based on the stability analysis of the quasi-polynomials in (3.15), given by Lemma 3.1, which is mainly centered on their roots location. When one varies the constant value of the time-delay, these roots move and eventually can change from the open-right half plane to the open-left half plane, or vice-versa, which may cause consensability switches. This fact is analyzed based on the Direct Method for the stability analysis by Walton and Marshall (1987). This method relies on finding a finite number of zero-crossing frequencies ω_{ij}, at which the roots of $\Delta_\tau(s)$ are over the imaginary axis, *i.e.* $s = j\omega_{ij}$. Furthermore, it is know that if a zero-crossing happens at some τ_{ij}, other pairs of roots $(\omega_{ij}, \tau_{ij}^\ell)$ of $\Delta_\tau(s)$ also cross the imaginary axis at the same $s = j\omega_{ij}$ an infinite number of times for every

$$\tau_{ij}^\ell = \tau_{ij} + 2\ell\omega_{ij}^{-1}\pi, \quad \ell = 0, \pm1, \pm2, \ldots \tag{3.21}$$

Next it is presented a method that shows how to completely characterize the time-delay intervals of consensability in directed networks of multiagent systems with high-order integrator dynamics and communication delays. This result is stated in the next theorem.

Theorem 3.1 *Consider the multi-agent system in* (3.5) *with protocol* (3.12)*. Assume a regular directed network topology according to Assumption 2.2 containing a directed spanning tree with Laplacian L. Let the nonzero eigenvalues of L, subtracted by* 1*, be written in the exponential form:* $\lambda_i\{L\} - 1 = \mu_i e^{j\phi_i}$.
Compute:

i) $N_U(\tau)$ *for* $\tau = 0$*, that is the number of unstable roots of* $\Delta_\tau(s)$ *with* $\tau = 0$*. Note that* $N_U(0)$ *can be determined by the nonzero eigenvalues of* $\Gamma_{ho} = I_m \otimes A_{ho} - L \otimes B_{ho}K_{ho}$ *equivalent to* Γ *in* (2.76)*.*

ii) The triplets $\Psi_{ij} = (\omega_{ij}, \tau_{ij}, \Phi_{ij})$*, for* $i = 1, 2, \ldots, m-1$ *and* $j = 1, 2, \ldots, r_i$*, with* r_i *the number of positive roots of* (3.22) *below, for a given* i*. Moreover,* ω_{ij} *for each* μ_i *are the positive roots of*

$$\rho_i(\omega) = \left|(j\omega)^n + \sum_{p=1}^{n}(j\omega)^{p-1}\alpha_p\right|^2 - \mu_i^2\left|\sum_{p=1}^{n}(j\omega)^{p-1}\alpha_p\right|^2, \tag{3.22}$$

each τ_{ij} *is any value of* τ *for a given* ω_{ij} *that satisfies the system of equations*

$$\begin{cases} \sin(\omega_{ij}\tau - \phi_i) = \dfrac{-a_{0R}a_{iI} + a_{0I}a_{iR}}{|a_i|^2}, \\ \cos(\omega_{ij}\tau - \phi_i) = \dfrac{-a_{0R}a_{iR} - a_{0I}a_{iI}}{|a_i|^2}, \end{cases} \tag{3.23}$$

where $a_{0R}(\omega)$ *and* $a_{0I}(\omega)$ *are the real and imaginary parts of* $a_0(\omega) \equiv (j\omega)^n + \sum_{p=1}^{n}(j\omega)^{p-1}\alpha_p$*, respectively, and similarly* $a_{iR}(\omega)$ *and* $a_{iI}(\omega)$ *are the real and imaginary parts of* $a_i(\omega) \equiv \mu_i \sum_{p=1}^{n}(j\omega)^{p-1}\alpha_p$*, respectively. Finally,* Φ_{ij} *is calculated for each* ω_{ij} *as the sign of*

$$\frac{\mathrm{d}}{\mathrm{d}\omega}\rho_i(\omega)\bigg|_{\omega=\omega_{ij}}. \tag{3.24}$$

Now, define the set

$$\Psi := \{(\Psi_{ij}) : \ i = 1, 2, \ldots, m-1 \text{ and } j = 1, 2, \ldots, r_i\}.$$

Then, depending on the set Ψ *consisting of all obtained triplets* Ψ_{ij}*, there are two possible cases:*

Case 1: *If* $\Psi = \emptyset$*, no consensability switches occur. Therefore, if* $N_U(0) = 0$*, the system achieves consensus for* $\tau = 0$ *and is still consensable for any* $\tau > 0$*, alternatively, if* $N_U(0) > 0$*, the system does not achieve consensus for* $\tau = 0$ *or for any* $\tau > 0$*.*

Case 2: *If* $\Psi \neq \emptyset$*, consensability switches may occur. Then, in order to identify the switches, form a table such that:*

- *The first column entries are* $\tau_{ij}^{\ell} > 0$*, given by* (3.21)*, for all* $\tau_{ij} \in \Psi$*, in the ascending order.*
- *The second column entries are the values of* $\omega_{ij} \in \Psi$ *associated with each* τ_{ij}^{ℓ} *from the first column.*

- *The third column entries are the values of* $\Phi_{ij} \in \Psi$ *associated with each* τ_{ij}^{ℓ} *from the first column.*
- *The fourth column entries are given by the number of unstable roots for a specific value of time-delay* τ*,* $N_U(\tau)$*. Before progressing further, add new lines between each line in the table built so far, the elements in the fourth column will appear only in the new lines added. The first element of this column is* $N_U(0)$*, then the next ones are the number of unstable roots for* $\tau = \tau_{ij}^{\ell} + \epsilon$*,* $0 < \epsilon \ll 1$*. If* $\Phi_{ij} = +1$ *in the line below, then* $N_U(\tau)$ *increases by* 2*, if* $\Phi_{ij} = -1$*, then* $N_U(\tau)$ *decreases by* 2*.*

Finally, the regions in the time-delay domain where the multi-agent system is consensable are those where $N_U(\tau) = 0$*.*

Proof Initially, to identify the time-delay intervals of consensability, the zero-crossing frequencies ω_{ij} of quasi-polynomials (3.15) are found using the Direct Method from Walton and Marshall (1987) in the following procedure.

Considering the conjugate symmetry of (3.15), for some $s = j\omega$, the following holds

$$\left|(j\omega)^n + \sum_{p=1}^{n}(j\omega)^{p-1}\alpha_p\right|^2 - \left|(\lambda_i\{L\} - 1)e^{-j\omega\tau}\sum_{p=1}^{n}(j\omega)^{p-1}\alpha_p\right|^2 = 0. \tag{3.25}$$

Writing the nonzero eigenvalues of L, subtracted by 1, in the exponential form $\lambda_i\{L\} - 1 = \mu_i e^{j\phi_i}$ gives (3.22).

If there is no solution for (3.22), then the roots of the quasi-polynomials in (3.15) never cross the imaginary axis. Therefore, no consensability switches occur, which concludes the proof for Case 1.

On the other hand, if (3.22) has real solutions $\omega_{ij} > 0$, the associated values of the delay τ_{ij} can be found. A similar procedure used by Yang (2013) is followed by separating the terms of (3.15), with $s = j\omega$, in real and imaginary parts, as:

$$p_i(j\omega) = \Big(a_{0R}(\omega) + ja_{0I}(\omega)\Big) + \Big(a_{iR}(\omega) + ja_{iI}(\omega)\Big)e^{-j(\omega\tau - \phi_i)}, \tag{3.26}$$

where $a_{0R}(\omega)$ and $a_{0I}(\omega)$ are the real and imaginary parts of

$$a_0(\omega) \equiv (j\omega)^n + \sum_{p=1}^{n}(j\omega)^{p-1}\alpha_p, \tag{3.27}$$

respectively, and similarly $a_{iR}(\omega)$ and $a_{iI}(\omega)$ are the real and imaginary parts of

$$a_i(\omega) \equiv \mu_i \sum_{p=1}^{n}(j\omega)^{p-1}\alpha_p, \tag{3.28}$$

respectively.

Expanding the exponential term by Euler's form, a value for τ_{ij} for each ω_{ij} can be found solving the following system of equations:

$$\begin{cases} a_{iR}\cos(\omega\tau-\phi_i)+a_{iI}\sin(\omega\tau-\phi_i) &= -a_{0R}, \\ a_{iI}\cos(\omega\tau-\phi_i)-a_{iR}\sin(\omega\tau-\phi_i) &= -a_{0I}, \end{cases} \tag{3.29}$$

which is equivalent to the system of equations (3.23).

Note that an infinite number of values for τ that satisfies the system of equations (3.23) can be found, which is expected due to the periodic property of the transcendental function in (3.14). For each root on the imaginary axis $j\omega_{ij}$ there are associated many periodically spaced delays τ_{ij}^{ℓ} given by (3.21). Therefore, (3.23) can be used to identify only one time-delay and the others can the obtained by (3.21).

Next, the tendency of the roots of (3.15) is analyzed. This allows to investigate consensability switches as the value of the time-delay increases. Then define the quantity

$$\Phi_{ij}=\operatorname{sign}\left(\operatorname{Re}\left(\frac{\mathrm{d}s}{\mathrm{d}\tau}\Big|_{s=j\omega_{ij}}\right)\right) \tag{3.30}$$

which is an indicator of the crossing direction of the imaginary root $j\omega_{ij}$. If $\Phi_{ij}=+1$, a pair of roots of (3.15) cross the imaginary axis at $j\omega_{ij}$ from left to right; conversely, if $\Phi_i=-1$, a pair of roots of (3.15) cross the imaginary axis at $j\omega_{ij}$ from right to left. From Walton and Marshall (1987), this is given by the sign of (3.24).

Finally, it remains to determine the number of roots, if any, in the right half plane, when $\tau=0$. Which can be assessed from the nonzero eigenvalues of $\Gamma_{ho}=I_m\otimes A_{ho}-L\otimes B_{ho}K_{ho}$ equivalent to Γ in (2.76). Note that, for infinitesimally small τ, there will be also infinitely new roots of (3.15) at the infinity of the left half-plane, since the degree of the polynomial $a_0(\omega)$ is strictly greater than the degree of $a_i(\omega)$ (Walton and Marshall (1987)).

Then, organizing this data in the ascending order of time-delay, and considering the increase, or decrease, in the number $N_U(\tau)$ of roots in the open-right half plane, consensability is given whenever this $N_U(\tau)=0$. This concludes Case 2. □

The previous theorem brings out a structured methodology for identifying time-delay intervals where consensus in directed networks of multi-agent systems with high-order integrator dynamics is achieved. However, it can be further simplified when particular cases are considered.

In the following, particular results are obtained for networks of agents with first- and second-order integrator dynamics.

Corollary 3.1 *Agents with first-order dynamic, i.e.* $n = 1$ *in* (3.5) *and in consensus protocol* (3.9)*, with a regular directed network according to Assumption 2.2 containing a directed spanning tree, achieve consensus independently of the communication delay.*

Proof For $n = 1$, matrix $\Gamma_{ho} = I_m \otimes A_{ho} - L \otimes B_{ho}K_{ho}$ becomes $-\alpha_1 L$, and Lemma 2.4 is satisfied according to Lemma 2.1 since the graph has a directed spanning tree. Thus, the system achieves consensus for $\tau = 0$, i.e. $N_U(0) = 0$ in Theorem 3.1. Additionally, equation (3.22) becomes

$$\omega^2 + \alpha_1^2 - \mu_i^2\alpha_1^2 = 0, \tag{3.31}$$

$$\omega^2 = \alpha_1^2(\mu_i^2 - 1). \tag{3.32}$$

Note that the eigenvalues of L are related to $\lambda_i\{L\} = \lambda_i\{\mathcal{D} - \mathcal{A}\}$, and from Assumption 2.2 of regular graphs for networks with communication delays, assuming $\mathcal{D} = I_m$, yields $\lambda_i\{L\} = \lambda_i\{I_m - \mathcal{A}\}$, such that

$$\lambda_i\{L\} - 1 = -\lambda_i\{\mathcal{A}\}. \tag{3.33}$$

Thus, the spectral radius of $\lambda_i\{L\} - 1$ gives $\mu_i^2 \leq 1$ from Lemma 2.8, which yields no solutions for $\omega > 0$ in (3.32). Therefore, this is case 1 in Theorem 3.1 and no crossings occur, meaning that consensus is never lost due to uniform constant communication delays. □

Corollary 3.2 *Agents with second-order integrator dynamics, i.e.* $n = 2$ *in* (3.5) *and in consensus protocol* (3.9)*, with a regular directed network containing a directed spanning tree is delay-independent if all* $\mu_i = 1$ *or*

$$\alpha_1 \leq \min_i \frac{\bar{\mu}_{i,\alpha_2}\left(1 + \left|\sqrt{(1-\mu_i^2)}\right|\right)}{\mu_i^2}, \tag{3.34}$$

with

$$\bar{\mu}_{i,\alpha_2} = \alpha_2^2\frac{(1-\mu_i^2)}{2}. \tag{3.35}$$

If not, crossings occur, and can happen in both directions. Thus, consensability switches may occur.

Proof The proof follows from Theorem 3.1. For second-order integrator, Equation (3.22) becomes

$$| - \omega^2 + j\omega\alpha_2 + \alpha_1|^2 - \mu_i^2|j\omega\alpha_2 + \alpha_1|^2 = 0, \tag{3.36}$$

$$\omega^4 + \omega^2(\alpha_2^2(1-\mu_i^2) - 2\alpha_1) + \alpha_1^2(1-\mu_i^2) = 0, \tag{3.37}$$

yielding

$$\omega_i = \left(\frac{2\alpha_1 - \alpha_2^2(1-\mu_i^2) \pm \sqrt{(\alpha_2^2(1-\mu_i^2) - 2\alpha_1)^2 - 4\alpha_1^2(1-\mu_i^2)}}{2} \right)^{\frac{1}{2}}, \tag{3.38}$$

which can be rewritten as

$$\omega_i = \left(\alpha_1 - \bar{\mu}_{i,\alpha_2} \pm \sqrt{(\bar{\mu}_{i,\alpha_2} - \alpha_1)^2 - 2\left(\frac{\alpha_1}{\alpha_2}\right)^2 \bar{\mu}_{i,\alpha_2}} \right)^{\frac{1}{2}}, \tag{3.39}$$

with $\bar{\mu}_{i,\alpha_2}$ in (3.35).

First, in order to exist real $\omega_i > 0$, the term in the square-root in (3.39) has to be greater or equal to zero, i.e

$$(\bar{\mu}_{i,\alpha_1} - \alpha_1)^2 - 2\left(\frac{\alpha_1}{\alpha_2}\right)^2 \bar{\mu}_{i,\alpha_2} \geq 0, \tag{3.40}$$

$$(\bar{\mu}_{i,\alpha_1} - \alpha_1)^2 - \alpha_1^2(1-\mu_i^2) \geq 0, \tag{3.41}$$

$$(\bar{\mu}_{i,\alpha_2})^2 - 2\bar{\mu}_{i,\alpha_2}\alpha_1 + \alpha_1^2\mu_i^2 \geq 0. \tag{3.42}$$

Thus, the roots α_1 for inequality (3.42) are:

$$\alpha_1' = \frac{\bar{\mu}_{i,\alpha_2}\left(1 - \left|\sqrt{(1-\mu_i^2)}\right|\right)}{\mu_i^2}, \tag{3.43}$$

$$\alpha_1'' = \frac{\bar{\mu}_{i,\alpha_2}\left(1 + \left|\sqrt{(1-\mu_i^2)}\right|\right)}{\mu_i^2}. \tag{3.44}$$

Next, it is considered different cases depending on the location of α_1 in terms of α_1' and α_1''.

Case 1 *For $\alpha_1' < \alpha_1 < \alpha_1''$, implies $\nexists \omega_i > 0$, $\omega_i \in \mathbb{R}$.*

Since $\mu_i^2 > 0$ in (3.42), if $\alpha_1' < \alpha_1 < \alpha_1''$ there is no solution for $\omega_i > 0$, $\omega_i \in \mathbb{R}$, and thus no crossings occur.

Next condition for the existence of $\omega_i > 0$, $\omega_i \in \mathbb{R}$, in (3.39), is that

$$\alpha_1 - \bar{\mu}_{i,\alpha_2} \pm \left| \sqrt{(\bar{\mu}_{i,\alpha_2} - \alpha_1)^2 - \alpha_1^2(1-\mu_i^2)} \right| > 0, \tag{3.45}$$

thus, consider the following two cases.

Case 2 *For $\alpha_1 < \alpha_1'$, implies $\nexists \omega_i > 0$, $\omega_i \in \mathbb{R}$,*

For an arbitrary $\check{\alpha}_1'$ in the interval $0 < \check{\alpha}_1' < \alpha_1'$, it can be shown that $\check{\alpha}_1' < \bar{\mu}_{i,\alpha_2}$. Thus, for $\alpha_1 = \check{\alpha}_1'$ it is sufficient to show

$$\check{\alpha}_1' - \bar{\mu}_{i,\alpha_2} + \left| \sqrt{(\bar{\mu}_{i,\alpha_2} - \check{\alpha}_1')^2 - \check{\alpha}_1'^2(1-\mu_i^2)} \right| > 0, \tag{3.46}$$

$$\left| \sqrt{(\bar{\mu}_{i,\alpha_2} - \check{\alpha}_1')^2 - \check{\alpha}_1'^2(1-\mu_i^2)} \right| > \bar{\mu}_{i,\alpha_2} - \check{\alpha}_1'. \tag{3.47}$$

Since $\bar{\mu}_{i,\alpha_2} - \check{\alpha}_1' > 0$,

$$(\bar{\mu}_{i,\alpha_2} - \check{\alpha}_1')^2 - \check{\alpha}_1'^2(1-\mu_i^2) > (\bar{\mu}_{i,\alpha_2} - \check{\alpha}_1')^2, \tag{3.48}$$

$$\check{\alpha}_1'^2(1-\mu_i^2) < 0. \tag{3.49}$$

Condition (3.49) is a contradiction, thus (3.45) has no solution for $\omega_i > 0$, $\omega_i \in \mathbb{R}$, and thus no crossings occur.

Case 3 *For $\alpha_1 > \alpha_1''$, implies $\exists \omega_i > 0$, $\omega_i \in \mathbb{R}$, if and only if $\mu_i < 1$.*

For an arbitrary $\hat{\alpha}_1''$ in the interval $\hat{\alpha}_1'' > \alpha_1''$, it can be shown that $\hat{\alpha}_1'' > \bar{\mu}_{i,\alpha_2}$. Thus, for $\alpha_1 = \hat{\alpha}_1''$ it is sufficient to show

$$\hat{\alpha}_1'' - \bar{\mu}_{i,\alpha_2} + \left| \sqrt{(\bar{\mu}_{i,\alpha_2} - \hat{\alpha}_1'')^2 - \hat{\alpha}_1''^2(1-\mu_i^2)} \right| > 0, \tag{3.50}$$

$$\left| \sqrt{(\bar{\mu}_{i,\alpha_2} - \hat{\alpha}_1'')^2 - \hat{\alpha}_1''^2(1-\mu_i^2)} \right| > \bar{\mu}_{i,\alpha_2} - \hat{\alpha}_1''. \tag{3.51}$$

Since $\bar{\mu}_{i,\alpha_2} - \hat{\alpha}_1'' < 0$,

$$(\bar{\mu}_{i,\alpha_2} - \hat{\alpha}_1'')^2 - \hat{\alpha}_1''^2(1-\mu_i^2) < (\bar{\mu}_{i,\alpha_2} - \hat{\alpha}_1'')^2, \tag{3.52}$$

$$\hat{\alpha}_1''^2(1-\mu_i^2) > 0. \tag{3.53}$$

Condition (3.53) is feasible if and only if $\mu_i < 1$, yielding solutions $\omega_i > 0$, $\omega_i \in \mathbb{R}$, in (3.45). Therefore crossings occur.

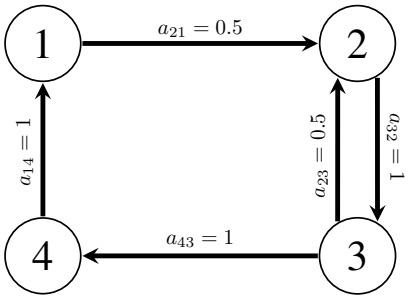

Figure 3.1: Regular directed network with four agents.

If crossings occur, they occur in both directions, thus consensability switches may occur. For the direction in which the crossing occurs, equation (3.24) becomes:

$$\Phi_{ij} = \text{sign}\left(\omega_{ij}^2 + \bar{\mu}_{i,\alpha_2} - \alpha_1\right). \tag{3.54}$$

Replacing (3.39) into equation above gives

$$\Phi_{ij} = \text{sign}\left(\pm\left|\sqrt{\left(\bar{\mu}_{i,\alpha_2} - \alpha_1\right)^2 - 2\left(\frac{\alpha_1}{\alpha_2}\right)^2 \bar{\mu}_{i,\alpha_2}}\right|\right), \tag{3.55}$$

which yields both positive and negative results.

From the combination of cases 1, 2, and 3, crossings occur only when $\alpha_1 > \alpha_1''$ and $\mu_i < 1$. Therefore, there are no zero-crossing roots if

$$\alpha_1 \leq \min_i \frac{\bar{\mu}_{i,\alpha_2}\left(1 + \left|\sqrt{(1-\mu_i^2)}\right|\right)}{\mu_i^2}, \tag{3.56}$$

which turns the system into a delay-independent system. □

3.2.3 Numerical Examples

Consider the multi-agent system represented by the directed network topology depicted in Figure 3.1, with corresponding Adjacency Matrix

$$\mathcal{A} = \begin{bmatrix} 0 & 0 & 0 & 1 \\ 0.5 & 0 & 0 & 0.5 \\ 0 & 1 & 0 & 0 \\ 0 & 0 & 1 & 0 \end{bmatrix} \tag{3.57}$$

and Laplacian Matrix

$$L = \begin{bmatrix} 1 & 0 & 0 & -1 \\ -0.5 & 1 & 0 & -0.5 \\ 0 & -1 & 1 & 0 \\ 0 & 0 & -1 & 1 \end{bmatrix}. \tag{3.58}$$

The agents are considered to have second-order integrator dynamics, i.e. $n = 2$ in (3.5) and (3.9). The example follows the application of Corollary 3.2. First, the eigenvalues of $\lambda_i\{L\} - 1$ are written in the exponential form $\mu_i e^{j\phi_i}$:

$$\lambda_1\{L\} - 1 = 0.6478 = 0.6478e^{j0}, \tag{3.59}$$

$$\lambda_2\{L\} - 1 = 0.1761 + j0.8607 = 0.8785e^{j1.369}, \tag{3.60}$$

$$\lambda_3\{L\} - 1 = 0.1761 - j0.8607 = 0.8785e^{-j1.369}, \tag{3.61}$$

such that

$$\mu_1 = 0.6478,\ \phi_1 = 0, \tag{3.62}$$

$$\mu_2 = 0.8785,\ \phi_2 = 1.369, \tag{3.63}$$

$$\mu_3 = 0.8785,\ \phi_3 = -1.369. \tag{3.64}$$

Choosing $\alpha_2 = 1$, the maximum value of α_1 such that consensability is delay-independent is checked using (3.34). Thus

$$\alpha_1 \leq \min \frac{\bar{\mu}_{i,\alpha_2}\left(1 + \left|\sqrt{(1-\mu_i^2)}\right|\right)}{\mu_i^2}, \tag{3.65}$$

$$\alpha_1 \leq \min(1.2183,\ 0.2184,\ 0.2184), \tag{3.66}$$

$$\alpha_1 \leq 0.2184. \tag{3.67}$$

It means that if α_1 is chosen $\alpha_1 \leq 0.2184$, no crossings occur and the system becomes delay-independent.

Delay-independet

Consider $\alpha_2 = 0.21$ and, for delay-free dynamics, consensability is checked by the nonzero eigenvalues of $\Gamma_{ho} = I_m \otimes A_{ho} - L \otimes B_{ho}K_{ho}$. For this example

$$\begin{bmatrix} 1 & 0 & 0 & 0 \\ 0 & 1 & 0 & 0 \\ 0 & 0 & 1 & 0 \\ 0 & 0 & 0 & 1 \end{bmatrix} \otimes \begin{bmatrix} 0 & 1 \\ 0 & 0 \end{bmatrix} - \begin{bmatrix} 1 & 0 & 0 & -1 \\ -0.5 & 1 & 0 & -0.5 \\ 0 & -1 & 1 & 0 \\ 0 & 0 & -1 & 1 \end{bmatrix} \otimes \begin{bmatrix} 0 \\ 1 \end{bmatrix} \begin{bmatrix} 0.21 & 1 \end{bmatrix}, \tag{3.68}$$

and the eigenvalues of (3.68) are: 0, 0, $-0.2343 \pm j0.0296$, -0.247, $-0.9418 \pm j0.8903i$, and -1.4008. The two zero eigenvalues are expected since the graph has a directed spanning tree, according to Lemma 2.3, and the system achieves consensus asymptotically since all the nonzero eigenvalues have negative real parts, according to Lemma 2.4.

Since the system free of delay achieves consensus, and the value of α_2 is chosen such that the system is delay-independent, the multi-agent system will always be able to achieve consensus for any value of communication delay τ.

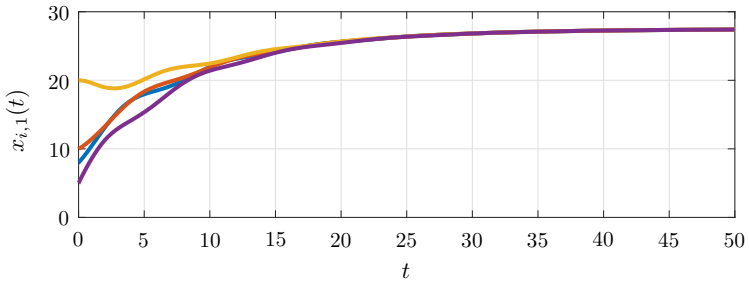

(a) State trajectories for $x_{i,1}(t)$.

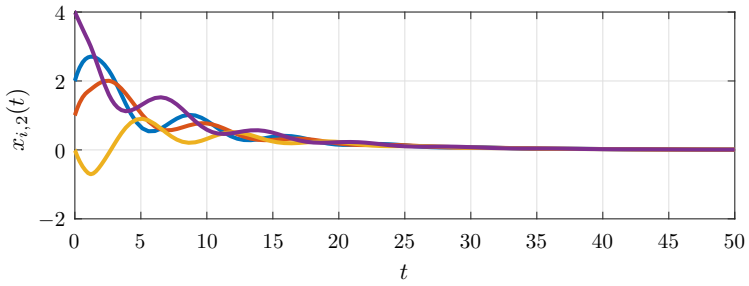

(b) State trajectories for $x_{i,2}(t)$.

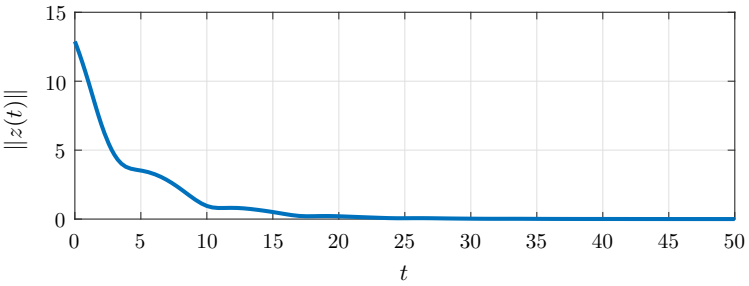

(c) Disagreement $\|z(t)\|$.

Figure 3.2: State trajectories and error for $\tau = 1$s.

Simulations are carried out for $\tau = 1s$, $\tau = 5s$, and $\tau = 10s$, in order to show that the system is consensable for any of these cases. See the system state trajectories in Figures 3.2, 3.3, and 3.4, respectively. Additionally, an error metrics given as the norm of the stacked disagreement vector $\|z(t)\|$ is introduced in Figures 3.2c, 3.3c, and 3.4c to check stability of the transformed system as the error between the agents decreases.

An interesting fact from Figure 3.4 is that the error between the agents' states converges to zero asymptotically in Figure 3.4c, although the states $x_{i,1}(t)$ in Figure 3.2 and $x_{i,2}(t)$ in Figure 3.3 are varying. Note, however, that the states vary similarly.

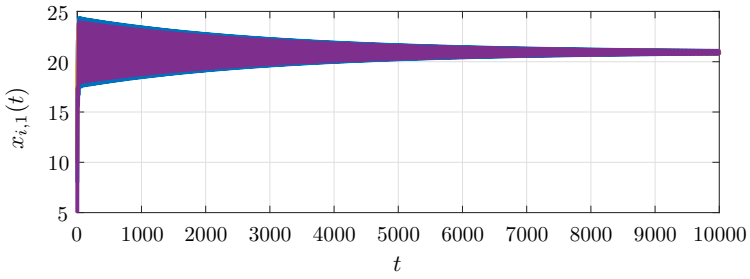

(a) State trajectories for $x_{i,1}(t)$.

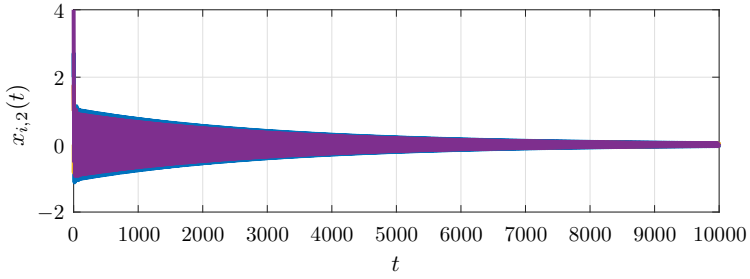

(b) State trajectories for $x_{i,2}(t)$.

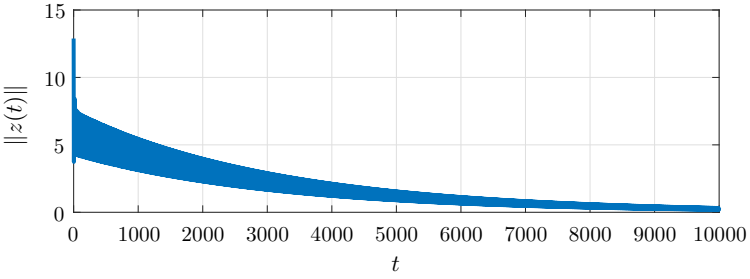

(c) Disagreement $\|z(t)\|$.

Figure 3.3: State trajectories and error for $\tau = 5$s.

Consensus on intervals

Finally, assume $\alpha_2 = 0.30$. For the delay-free dynamics, consensability is checked by the non-zero eigenvalues of $\Gamma_{ho} = I_m \otimes A_{ho} - L \otimes B_{ho}K_{ho}$, where

$$\Gamma_{ho} = \begin{bmatrix} 1 & 0 & 0 & 0 \\ 0 & 1 & 0 & 0 \\ 0 & 0 & 1 & 0 \\ 0 & 0 & 0 & 1 \end{bmatrix} \otimes \begin{bmatrix} 0 & 1 \\ 0 & 0 \end{bmatrix} - \begin{bmatrix} 1 & 0 & 0 & -1 \\ -0.5 & 1 & 0 & -0.5 \\ 0 & -1 & 1 & 0 \\ 0 & 0 & -1 & 1 \end{bmatrix} \otimes \begin{bmatrix} 0 \\ 1 \end{bmatrix} \begin{bmatrix} 0.30 & 1 \end{bmatrix}, \tag{3.69}$$

and its eigenvalues are: $0, 0, -0.3416 \pm j0.0726, -0.3944, -0.8345 \pm j0.9333i$, and -1.2534. The two zero eigenvalues are expected since the graph has a directed spanning tree, according to Lemma 2.3. Since the number of positive nonzero eigenvalues is null, then $N_U(0) = 0$, following the procedure in Theorem 3.1.

Next, the triplets $\Psi_{ij} = (\omega_{ij}, \tau_{ij}, \Phi_{ij})$ are computed and the set Ψ is written. The elements of Ψ are summarized in the Table 3.1. As it is obtained $\Psi \neq \emptyset$, this example is

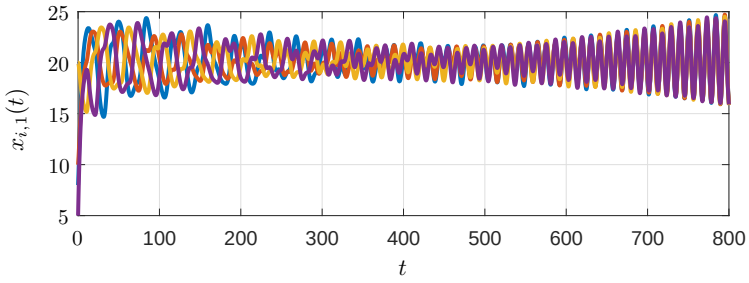

(a) State trajectories for $x_{i,1}(t)$.

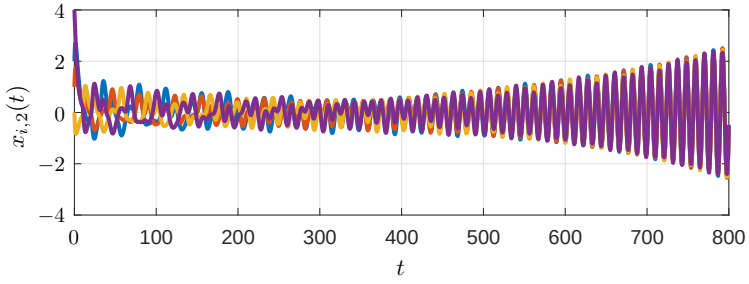

(b) State trajectories for $x_{i,2}(t)$.

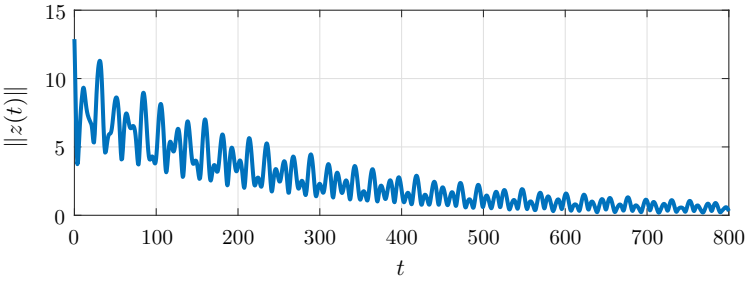

(c) Disagreement $\|z(t)\|$.

Figure 3.4: State trajectories and error for $\tau = 10$s.

Table 3.1: Elements of Ψ

i	j	ω_{ij}	τ_{ij}	Φ_{ij}
2	1	0.2597	16.8773	-1
2	2	0.5517	7.2585	$+1$
3	1	0.2597	6.3358	-1
3	2	0.5517	2.2958	$+1$

the Case 2 in Theorem 3.1.

Then, following the procedure of Theorem 3.1, Case 2, Table 3.2 is built in the ascending order of τ_{ij}^{ℓ}.

By looking at Table 3.2 consensability intervals can be analyzed. Note that the system is consensable in the first time-delay interval $[0, 2.2958)$. As the communication time-delay increases, the system becomes unable to achieve consesus in the interval

Table 3.2: Consensusability switches analysis

τ_{ij}^{ℓ}	ω_{ij}	Φ_{ij}	$N_U(\tau)$
			0
2.2958	0.5517	1	
			2
6.3358	0.2597	-1	
			0
7.2585	0.5517	1	
			2
13.6844	0.5517	1	
			4
16.8773	0.2597	-1	
			2
18.6471	0.5517	1	
			4
25.0730	0.5517	1	
			6
30.0356	0.5517	1	
			8
30.5268	0.2597	-1	
$\vdots$	$\vdots$	$\vdots$	$\vdots$

$\tau \in [2.2958, 6.3358]$. However, if the delay is even greater within $\tau \in (6.3358, 7.2585)$ the system is able to achieve consensus again, loosing consensability after $\tau >= 7.2585$. Thus, the system is consensable only in the intervals $\tau \in [0, 2.2958)$ and $\tau \in (6.3358, 7.2585)$, because after $\tau = 7.2585$ there will be always more roots crossing the imaginary axis from left to right ($\Phi_{ij} = +1$) than from right to left ($\Phi_{ij} = -1$), which prevents the system achieving consensus ever again. In order to illustrate this situation, the system state trajectories are presented for $\tau = 2$, $\tau = 4$, $\tau = 7$, and $\tau = 8$, in Figures 3.5, 3.6, 3.7, and 3.8, respectively. This last scenario serves as a counterexample for the usual claim that the time-delay only degrades the system's performance.

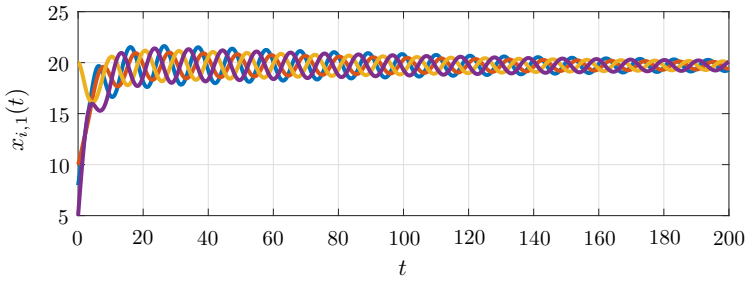

(a) State trajectories for $x_{i,1}(t)$.

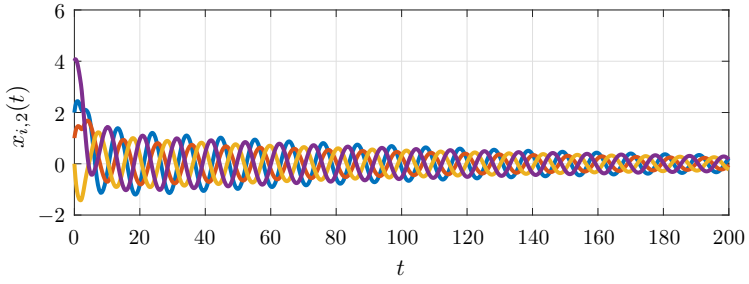

(b) State trajectories for $x_{i,2}(t)$.

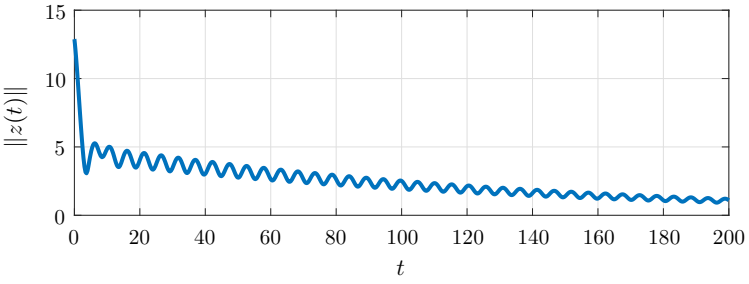

(c) Disagreement $\|z(t)\|$.

Figure 3.5: State trajectories and error for $\tau = 2$s.

3.3 Dynamics with Input Delay

In the presence of input delay, the agent dynamics in (3.2) is considered with the control input in (3.8) subject to uniform and constant delays, i.e. $\tau(t) = \tau$, such that

$$\begin{aligned} \dot{x}_{i,1}(t) &= x_{i,2}(t) \\ \dot{x}_{i,2}(t) &= x_{i,3}(t) \\ &\vdots \\ \dot{x}_{i,n-1}(t) &= x_{i,n}(t) \\ \dot{x}_{i,n}(t) &= u_i(t-\tau), \end{aligned} \tag{3.70}$$

which can be simplified to

$$\dot{x}_i(t) = A_{ho}x_i(t) + B_{ho}u_i(t-\tau), \tag{3.71}$$

with A_{ho} and B_{ho} in (3.6) and (3.7), respectively.

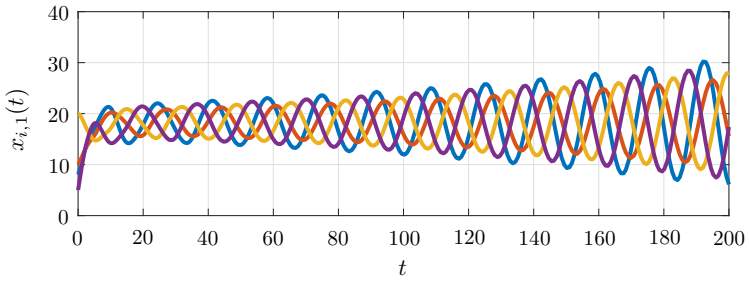

(a) State trajectories for $x_{i,1}(t)$.

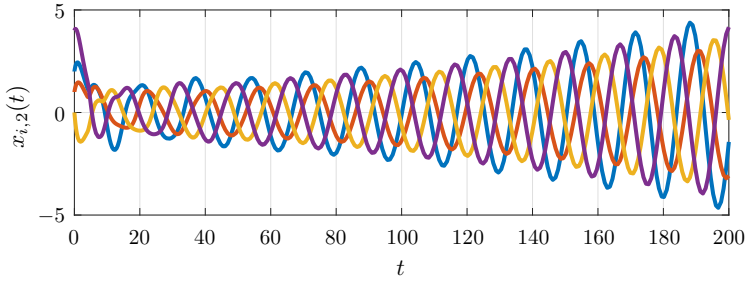

(b) State trajectories for $x_{i,2}(t)$.

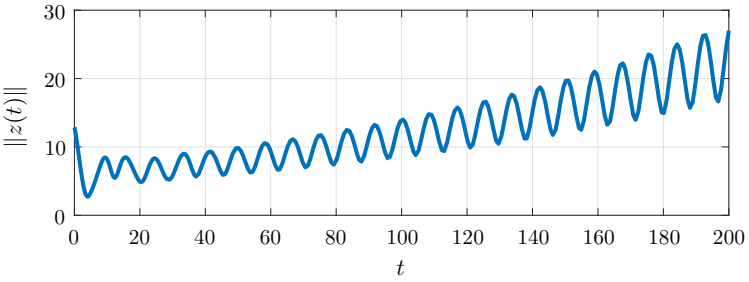

(c) Disagreement $\|z(t)\|$.

Figure 3.6: State trajectories and error for $\tau = 4$s.

The consensus protocol is given by (3.8), or simplified as (3.9) with K_{ho} in (3.10).

In the presence of input delay, the system can be described by a closed-loop dynamics as presented in (2.69), with $\tau(t) = \tau$. The dynamics of the system can be described by the same matrices A_{ho}, B_{ho}, and K_{ho}, analogous to A, B, and K, respectively. Therefore, the system to be analyzed can be written as

$$\dot{x}(t) \quad = (I_m \otimes A_{ho})x(t) - (L \otimes B_{ho}K_{ho})x(t-\tau). \tag{3.72}$$

Proposition 2.3 can be used in order to show consensus for (3.72) through the analysis of a transformed system as shown for (2.72), given by

$$\dot{z}(t) = (I_{m-1} \otimes A_{ho})z(t) - (\bar{L} \otimes (B_{ho}K_{ho}))z(t-\tau_i(t)). \tag{3.73}$$

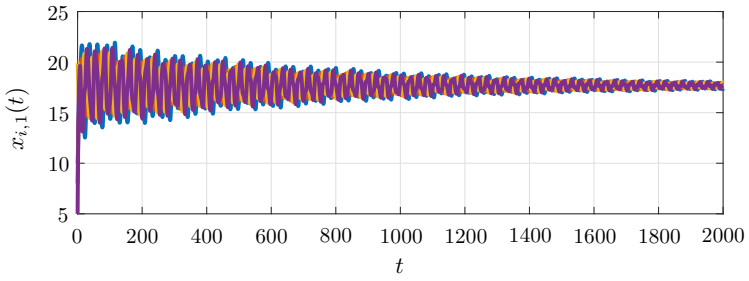

(a) State trajectories for $x_{i,1}(t)$.

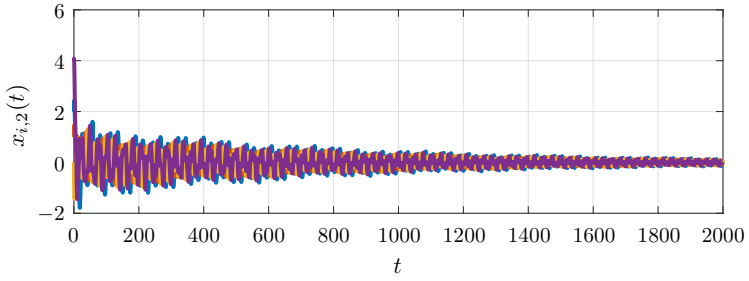

(b) State trajectories for $x_{i,2}(t)$.

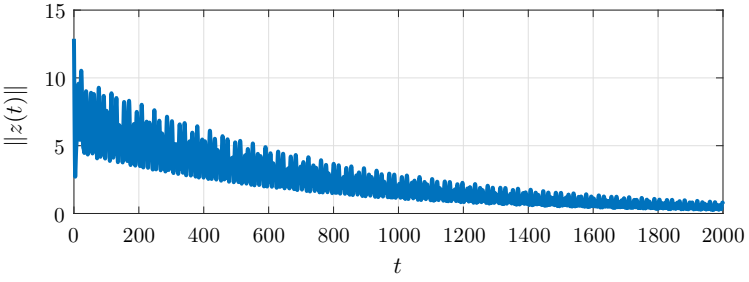

(c) Disagreement $\|z(t)\|$.

Figure 3.7: State trajectories and error for $\tau = 7$s.

3.3.1 Analysis

Consensus for agents with high-order integrator dynamics and input time-delay as in (3.71), subject to protocol (3.8), can be assessed by studying stability of the reduced-dimension transformed system in (3.73), dictated by the location of the roots of the transcendental function

$$\Delta_\tau(s) = \det(sI_{n(m-1)} - \bar{A}_{in} + \bar{B}_{in}e^{-s\tau}), \tag{3.74}$$

with $\bar{A}_{in} = (I_{m-1} \otimes A_{ho})$ and $\bar{B}_{in} = (\bar{L} \otimes (B_{ho}K_{ho}))$.

Similar to Lemma 3.1, next lemma is presented to establish the stability of the roots of $\Delta_\tau(s)$ in (3.74) equivalently to the stability of the roots of a set of quasi-polynomials.

Lemma 3.2 *Consider the multiagent system in* (3.71) *with protocol* (3.8). *Assume a directed network topology containing a directed spanning tree with Laplacian Matrix* L.

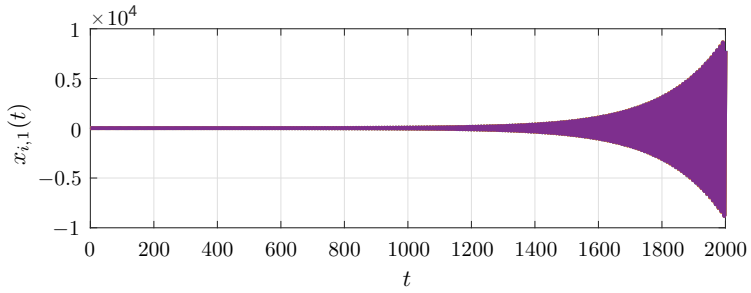

(a) State trajectories for $x_{i,1}(t)$.

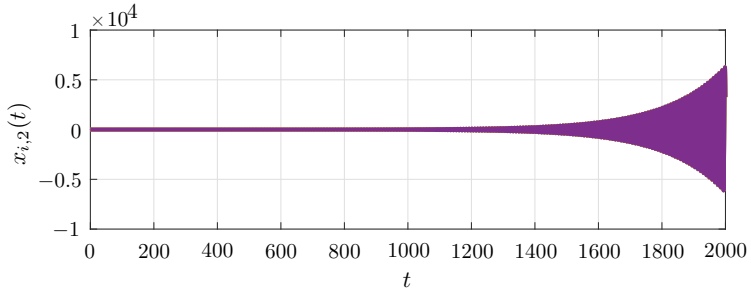

(b) State trajectories for $x_{i,2}(t)$.

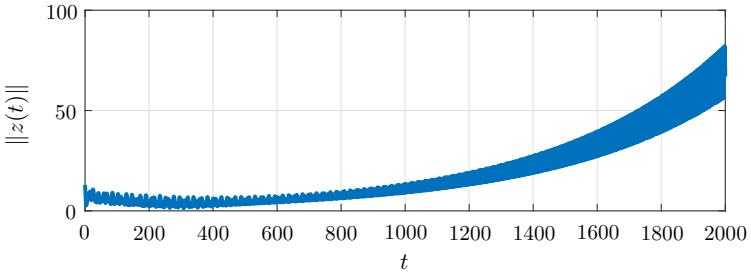

(c) Disagreement $\|z(t)\|$.

Figure 3.8: State trajectories and error for $\tau = 8$s.

Then, the multiagent system is consensable when subject to input time-delay τ if and only if all roots of

$$p_i(s) = s^n + \lambda_i\{L\}e^{-s\tau}\sum_{p=1}^{n} s^{p-1}\alpha_p \tag{3.75}$$

have negative real part, for $i = 1, 2, \ldots, m-1$.

Proof Based on Proposition 2.3, the multiagent system in (3.71) with protocol (3.8) asymptotically achieves consensus if and only if all roots of $\Delta_\tau(s)$ in (3.74) have negative real part.

Note that $\Delta_\tau(s)$ in (3.74) can be rewritten after some computation as

$$\Delta_\tau(s) = \det\left(s^n I_{m-1} + \left(\sum_{p=1}^{n} s^{p-1}\alpha_p\right) e^{-s\tau}\bar{L}\right) \tag{3.76}$$

$$= \prod_{i=1}^{m-1}\left(s^n + \lambda_i\left\{\left(\sum_{p=1}^{n} s^{p-1}\alpha_p\right) e^{-s\tau}\bar{L}\right\}\right) \tag{3.77}$$

$$= \prod_{i=1}^{m-1}\left(s^n + \lambda_i\{\bar{L}\}e^{-s\tau}\sum_{p=1}^{n} s^{p-1}\alpha_p\right). \tag{3.78}$$

Based on Proposition 2.5, the eigenvalues of $\bar{L}$ in (3.78) can be directly related to the nonzero eigenvalues of L, assuming $\lambda_m\{L\} = 0$. Then,

$$\Delta_\tau(s) = \prod_{i=1}^{m-1}\left(s^n + \lambda_i\{L\}e^{-s\tau}\sum_{p=1}^{n} s^{p-1}\alpha_p\right). \tag{3.79}$$

Equation (3.79) shows that, for each nonzero eigenvalue of L there are n eigenvalues for the whole system dynamics, given by the roots of the quasi-polynomials in (3.75). This completes the proof. □

3.3.2 Consensus on Time-Delay Intervals

Next result is based on the stability analysis of the quasi-polynomials in (3.75), given by Lemma 3.2, following the same procedure in previous section for communication delays. The result is stated in the next theorem.

Theorem 3.2 *Consider the multiagent system in* (3.71) *with protocol* (3.8)*. Assume a directed network topology containing a directed spanning tree with Laplacian Matrix L. Let the nonzero eigenvalues of L be written in the exponential form: $\lambda_i\{L\} = \mu_i e^{j\phi_i}$. Compute:*

i) $N_U(\tau)$ for $\tau = 0$, that is the number of unstable roots of $\Delta_\tau(s)$ with $\tau = 0$. Note that $N_U(0)$ can be determined by the nonzero eigenvalues of $\Gamma_{ho} = I_m \otimes A_{ho} - L \otimes B_{ho}K_{ho}$.

ii) The triplets $\Psi_{ij} = (\omega_{ij}, \tau_{ij}, \Phi_{ij})$, for $i = 1, 2, \ldots, m-1$ and $j = 1, 2, \ldots, r_i$, with r_i the number of positive roots of (3.80) *below for a given i. Moreover, ω_{ij} for each μ_i are the positive roots of*

$$\rho_i(\omega) = \omega^{2n} - \mu_i^2\left|\sum_{p=1}^{n}(j\omega)^{p-1}\alpha_p\right|^2, \tag{3.80}$$

each τ_{ij} is any value of τ for a given ω_{ij} that satisfies the system of equations

$$\begin{cases} \sin(\omega_{ij}\tau - \phi_i) = \dfrac{-a_{0R}a_{iI} + a_{0I}a_{iR}}{\omega_{ij}^{2n}}, \\ \cos(\omega_{ij}\tau - \phi_i) = \dfrac{-a_{0R}a_{iR} - a_{0I}a_{iI}}{\omega_{ij}^{2n}}, \end{cases} \tag{3.81}$$

where a_{0R} and a_{0I} are the real and imaginary parts of $a_0(\omega) \equiv (j\omega_{ij})^n$, respectively, and a_{iR} and a_{iI} are the real and imaginary parts of $a_i(\omega) \equiv \mu_i \sum_{p=1}^{n}(j\omega_{ij})^{p-1}\alpha_p$, respectively. Finally, Φ_{ij} is calculated for each ω_{ij} as the sign of

$$\frac{\mathrm{d}}{\mathrm{d}\omega}\rho_i(\omega)\bigg|_{\omega=\omega_{ij}}. \tag{3.82}$$

Now, define the set

$$\Psi := \{(\Psi_{ij}) : \ i = 1, 2, \ldots, m-1 \text{ and } j = 1, 2, \ldots, r_i\}.$$

Then, depending on the set Ψ consisting of all obtained triplets Ψ_{ij}, there are two possible cases:

Case 1: *If $\Psi = \emptyset$, no consensability switches occur. Therefore, if $N_U(0) = 0$, then the system achieves consensus for $\tau = 0$ and is still consensable for any $\tau > 0$, alternatively, if $N_U(0) > 0$, the system does not achieve consensus for $\tau = 0$ or for any $\tau > 0$.*

Case 2: *If $\Psi \neq \emptyset$, consensability switches may occur. Then, in order to identify the switches, form a table whose:*

- *The first column entries are $\tau_{ij}^{\ell} > 0$, given by (3.21), for all $\tau_{ij} \in \Psi$, in the ascending order.*
- *The second column entries are the values of $\omega_{ij} \in \Psi$ associated with each τ_{ij}^{ℓ} from the first column.*
- *The third column entries are the values of $\Phi_{ij} \in \Psi$ associated with each τ_{ij}^{ℓ} from the first column.*
- *The fourth column entries are given by the number of unstable roots for a specific value of time-delay τ, $N_U(\tau)$. Before progressing further, add new lines between each line in the table built so far, the elements in the fourth column will appear only in the new lines added. The first element of this column is $N_U(0)$, then the next ones are the number of unstable roots for $\tau = \tau_{ij}^{\ell} + \epsilon$, $0 < \epsilon \ll 1$. If the $\Phi_{ij} = +1$ in line below, then $N_U(\tau)$ increases by 2, if $\Phi_{ij} = -1$, then $N_U(\tau)$ decreases by 2.*

Finally, the regions in the time-delay domain where the multi-agent system is consensable are those where $N_U(\tau) = 0$.

Proof The proof is similar to the proof of Theorem 3.1. From the conjugate symmetry of (3.75), for some $s = j\omega$, the following holds

$$|(j\omega)^n|^2 - |\lambda_i\{L\}e^{-j\omega\tau}\sum_{p=1}^{n}(j\omega)^{p-1}\alpha_p|^2 = 0, \tag{3.83}$$

and writing the eigenvalues of L in the exponential form $\lambda_i\{L\} = \mu_i e^{j\phi_i}$, equation (3.80) is achieved in order to find the zero-crossing frequencies.

If there is no solution for (3.80), then the roots of the quasi-polynomials in (3.75) never cross the imaginary axis. Therefore, no consensability switches occur. Which concludes the proof of Case 1.

If (3.80) has solutions $\omega_{ij} > 0$, a procedure similar to the one used by Yang (2013) is followed. Therefore, separate the terms of (3.75), with $s = j\omega$, in real and imaginary parts, as:

$$p_i(j\omega) = \Big(a_{0R}(\omega) + ja_{0I}(\omega)\Big) + \Big(a_{iR}(\omega) + ja_{iI}(\omega)\Big)e^{-j(\omega\tau-\phi_i)}, \tag{3.84}$$

where $a_{0R}(\omega)$ and $a_{0I}(\omega)$ are the real and imaginary parts of $a_0(\omega) \equiv (j\omega)^n$, respectively, and similarly $a_{iR}(\omega)$ and $a_{iI}(\omega)$ are the real and imaginary parts of $a_i(\omega) \equiv \mu_i\sum_{p=1}^{n}(j\omega)^{p-1}\alpha_p$, respectively.

Expanding the exponential term by Euler's form, a value for τ_{ij}, for each ω_{ij}, can be found solving the system of equations in (3.29) repeated for convenience in (3.81), which is equivalent to the system of equations (3.23).

For each root on the imaginary axis $j\omega_{ij}$, the periodically spaced delays τ_{ij}^{ℓ} are given by (3.21). Therefore, (3.81) can be used to identify one of these time-delay, and the others can the obtained by (3.21).

Next, the tendency of the roots in (3.75) is shown by Φ_{ij} as defined in (3.30), which indicates the direction on which the imaginary root $j\omega_{ij}$ crosses the imaginary axis. For $\Phi_{ij} = +1$, a pair of roots crosses the imaginary axis from left to right; conversely, for $\Phi_i = -1$, the pair crosses from right to left.

Finally, the number of roots in the right half plane is determined when $\tau = 0$. This can be assessed from the eigenvalues of $\Gamma_{ho} = I_m \otimes A_{ho} - L \otimes B_{ho}K_{ho}$.

Organizing this data in the ascending order of time-delay, and considering the increase, or decrease, in the number $N_U(\tau)$ of roots in the right open half-plane, consensability is given whenever this $N_U(\tau) = 0$. This proves the procedure of Case 2. □

In the following, particular results are obtained for networks of agents with first- and second-order integrator dynamics. Equivalent results are shown by Xi et al. (2013) and Yu et al. (2010), respectively. These results show that if the multiagent system is consensable, it achieves consensus for any time-delay in the interval $\tau \in [0, \tau^*)$ with a unique $0 < \tau^* \leq \infty$.

Corollary 3.3 *Agents with first-order dynamics in* (3.71) *under protocol* (3.8)*, with a network containing a directed spanning tree, achieve consensus if and only if* $\tau \in [0, \tau^*)$ *with*

$$\tau^* = \min_{1 \leq i \leq m-1} \left(\frac{\pi/2 + \phi_i}{\mu_i \alpha_1} \right), \tag{3.85}$$

where $\lambda_i\{L\} = \mu_i e^{j\phi_i}$.

Proof For this case $\Gamma_{ho} = I_m \otimes A_{ho} - L \otimes B_{ho}K_{ho}$ is given by $-\alpha_1 L$, and Lemma 2.4 is satisfied according to Lemma 2.1 since the graph has a directed spanning tree. Thus, the system achieves consensus for $\tau = 0$, i.e. $N_U(0) = 0$ in Theorem 3.2.

From Theorem 3.2, for first-order dynamics, equation (3.80) becomes

$$\omega^2 - \mu_i^2 \alpha_1^2 = 0,$$

which yields only one solution $\omega_{i1} = \mu_i \alpha_1$. Then, the crossing direction given by equation (3.82) becomes $\Phi_{i1} = \text{sign}\,(2\omega_{i1})$, which is always positive and the roots cross the imaginary axis at $j\omega_{i1}$ only from left to right. Then, the first crossing in the imaginary axis indicates that the consensability is lost. The value of the delay associated with this crossing is obtained solving (3.81), yielding (3.85). □

Corollary 3.4 *Agents with second-order integrator dynamics in* (3.71) *under protocol* (3.8)*, with a network containing a directed spanning tree, achieve consensus if and only if matrix* $\Gamma_{ho} = I_m \otimes A_{ho} - L \otimes B_{ho}K_{ho}$ *has exactly two zero eigenvalues and all the other eigenvalues have negative real parts, and* $\tau \in [0, \tau^*)$ *with*

$$\tau^* = \min_{1 \leq i \leq m-1} \left(\frac{\arctan(\omega_{i1}\alpha_2/\alpha_1) + \phi_i}{\omega_{i1}} \right), \tag{3.86}$$

with

$$\omega_{i1} = \sqrt{\frac{\mu_i^2 \alpha_2^2 + \sqrt{\mu_i^4 \alpha_2^4 + 4\mu_i^2 \alpha_1^2}}{2}}. \tag{3.87}$$

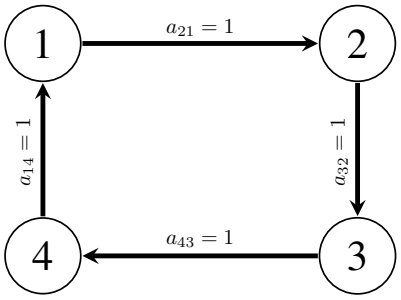

Figure 3.9: Directed network with four agents.

Proof From Theorem 3.2 for second-order dynamics, equation (3.80) becomes

$$\omega^4 - \mu_i^2\alpha_2^2\omega^2 - \mu_i^2\alpha_1^2 = 0,$$

which yields only one positive frequency given in (3.87). Equation (3.82) becomes

$$\Phi_{ij} = \text{sign}\left(2\omega_{ij}^2 - \mu_i^2\alpha_2^2\right), \tag{3.88}$$

and replacing (3.87), yields

$$\Phi_{i1} = \text{sign}\left(\sqrt{\mu_i^4\alpha_2^4 + 4\mu_i^2\alpha_1^2}\right), \tag{3.89}$$

which is always positive. This indicates that the roots only move from the left to the right half plane.

Finally, the delay-free stability is analyzed by matrix $\Gamma_{ho} = I_m \otimes A_{ho} - L \otimes B_{ho}K_{ho}$ according to Lemma 2.4, and the first zero-crossing is calculated solving (3.81), yielding (3.86). □

3.3.3 Numerical Examples

Consider the multi-agent system represented by the directed network topology depicted in Figure 3.9.

For this graph, the Laplacian Matrix is given by

$$L = \begin{bmatrix} 1 & 0 & 0 & -1 \\ -1 & 1 & 0 & 0 \\ 0 & -1 & 1 & 0 \\ 0 & 0 & -1 & 1 \end{bmatrix}, \tag{3.90}$$

with eigenvalues: $\lambda_1\{L\} = 1.4142e^{j0.7854}$, $\lambda_2\{L\} = 1.4142e^{-j0.7854}$, $\lambda_3\{L\} = 2$, and $\lambda_4\{L\} = 0$.

In the following, three scenarios are studied, given the agents with first-, second-, and third-order integrator dynamics.

First-order integrator agents

Initially, it is assumed that all agents have a first-order integrator dynamics with gain $\alpha_1 = 1$ in the consensus protocol. Thus, applying Corollary 3.3, it is given that the system achieves consensus if and only if $\tau \in [0, 0.5554)$.

Second-order integrator agents

Next, it is assumed a second-order integrator dynamics with $\alpha_2 = 1$ and $\alpha_1 = 0.25$ in the consensus protocol. Applying Corollary 3.4, it is given that the system achieves consensus when free of delay, since

$$\Gamma_{ho} = I_4 \otimes \begin{bmatrix} 0 & 1 \\ 0 & 0 \end{bmatrix} - L \otimes \begin{bmatrix} 0 \\ 1 \end{bmatrix} \begin{bmatrix} 0.25 & 1 \end{bmatrix} \tag{3.91}$$

has exactly two zero eigenvalues and all the others with negative real parts. The zero crossing frequencies are given by $w_{1,1} = 1.4355$, $w_{2,1} = 1.4355$, and $w_{3,1} = 2.0153$. Therefore, τ^* is given by $\min(1.5213, 0.4270, 0.7182)$. Thus, the system achieves consensus if and only if $\tau \in [0, 0.427)$.

Third-order integrator agents

Finally, assume third-order integrator dynamics with gains $\alpha_3 = 1$, $\alpha_2 = 0.25$, and $\alpha_1 = 0.33$ in the consensus protocol. Following the procedure in Theorem 3.1, it is given $N_U(0) = 2$, since

$$\Gamma_{ho} = I_4 \otimes \begin{bmatrix} 0 & 1 & 0 \\ 0 & 0 & 1 \\ 0 & 0 & 0 \end{bmatrix} - L \otimes \begin{bmatrix} 0 \\ 0 \\ 1 \end{bmatrix} \begin{bmatrix} 0.33 & 0.25 & 1 \end{bmatrix} \tag{3.92}$$

has a pair of conjugate eigenvalues with positive real parts, *i.e.* $0.0049 \pm j0.7135$.

Next, the triplets $\Psi_{ij} = (\omega_{ij}, \tau_{ij}, \Phi_{ij})$ are computed and the set Ψ is obtained as summarized in Table 3.3. Since $\Psi \neq \emptyset$, this example is the Case 2 in Theorem 3.1. Then, following the procedure of Theorem 3.1, Case 2, Table 3.4 is built in the ascending order of τ_{ij}^{ℓ}.

From Table 3.4 consensability intervals can be analyzed. Note that the system is not consensable when free of delay, or in the first time-delay interval $[0, 0.1332)$. However, if the control input is properly delayed with $\tau \in (0.1332, 0.4349)$ the system achieves consensus. The system is consensable only on the interval $\tau \in (0.1332, 0.4349)$, because after $\tau = 0.4349$ there will be always more roots crossing the imaginary axis from left to right ($\Phi_{ij} = +1$) than from right to left ($\Phi_{ij} = -1$). This is illustrated by the simulations shown in figures 3.10, 3.11, and 3.12, with the state trajectories and error for $\tau = 0.07$,

Table 3.3: Elements of Ψ

i	j	ω_{ij}	τ_{ij}	Φ_{ij}
1	1	1.0396	1.9459	$+1$
1	2	0.7471	2.2356	-1
1	3	0.6008	1.6460	$+1$
2	1	1.0396	0.4349	$+1$
2	2	0.7471	0.1332	-1
2	3	0.6008	-0.9684	$+1$
3	1	1.8220	0.7792	$+1$

Table 3.4: Consensability switches

τ_{ij}^{ℓ}	ω_{ij}	Φ_{ij}	$N_U(\tau)$
			2
0.1332	0.7471	-1	
			0
0.4349	1.0396	1	
			2
0.7792	1.822	1	
			4
1.646	0.6008	1	
			6
1.9459	1.0396	1	
			8
2.2356	0.7471	-1	
			6
4.2277	1.822	1	
			8
6.4787	1.0396	1	
			10
7.6762	1.822	1	
$\vdots$	$\vdots$	$\vdots$	$\vdots$

$\tau = 0.35$, and $\tau = 0.44$, respectively. Once more, this is a counterexample for the usual acceptance that the time-delay only degrades the system's performance.

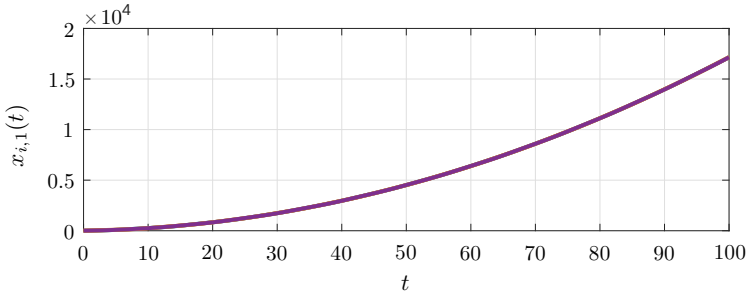

(a) State trajectories for $x_{i,1}(t)$.

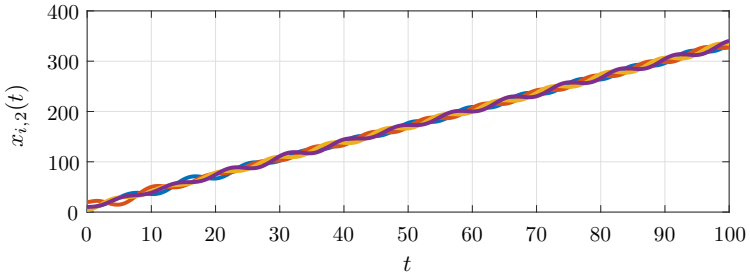

(b) State trajectories for $x_{i,2}(t)$.

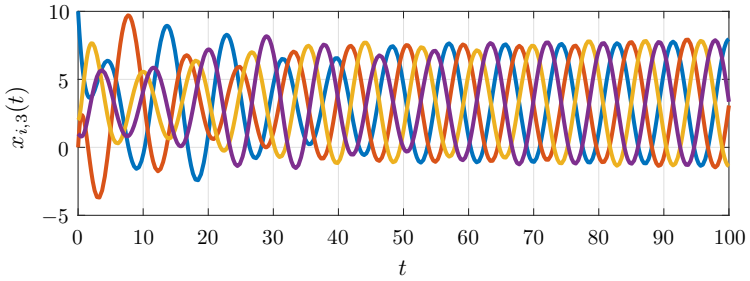

(c) State trajectories for $x_{i,3}(t)$.

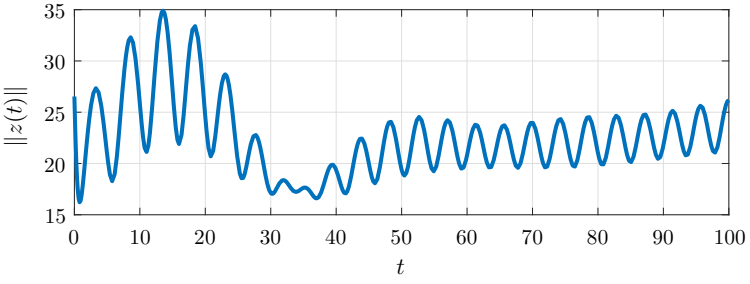

(d) Disagreement $\|z(t)\|$.

Figure 3.10: State trajectories and error for $\tau = 0.07$s.

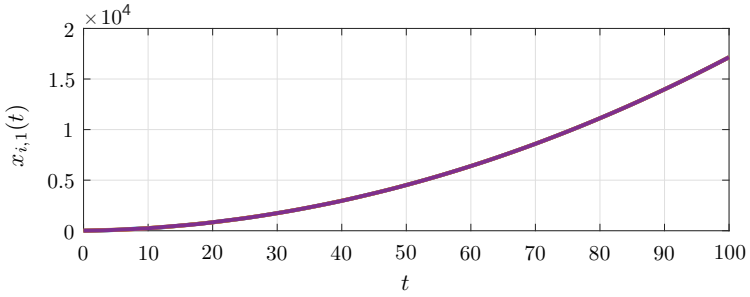

(a) State trajectories for $x_{i,1}(t)$.

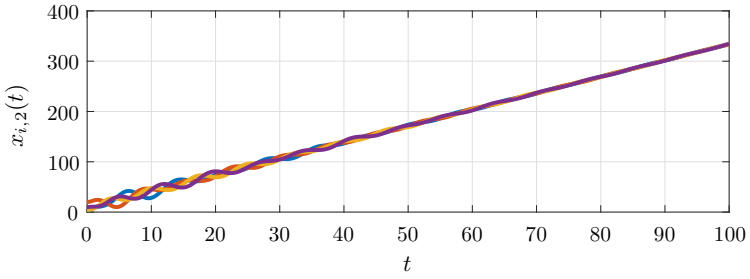

(b) State trajectories for $x_{i,2}(t)$.

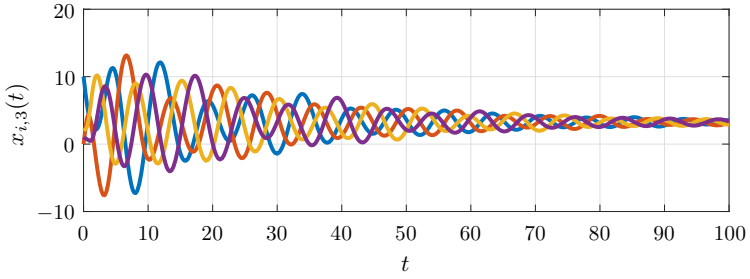

(c) State trajectories for $x_{i,3}(t)$.

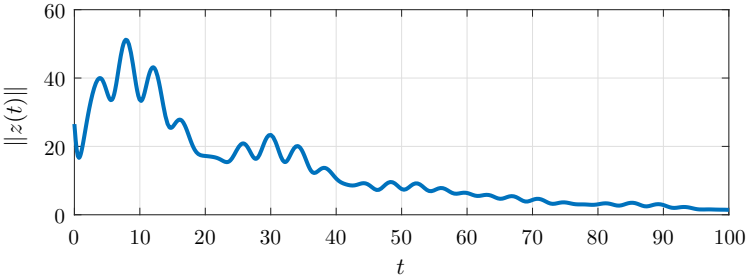

(d) Disagreement $\|z(t)\|$.

Figure 3.11: State trajectories and error for $\tau = 0.35$s.

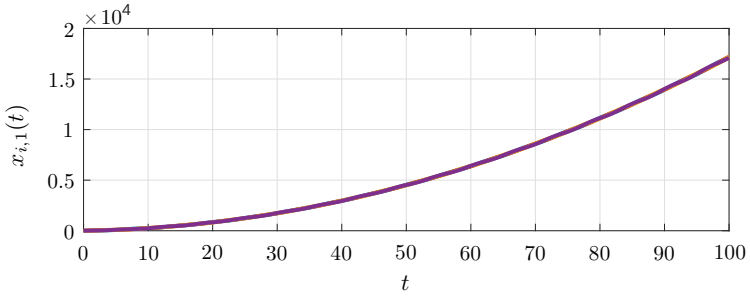

(a) State trajectories for $x_{i,1}(t)$.

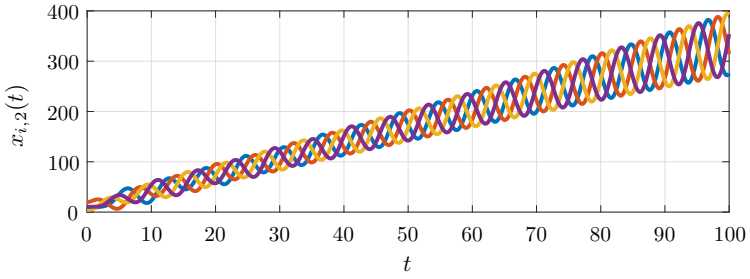

(b) State trajectories for $x_{i,2}(t)$.

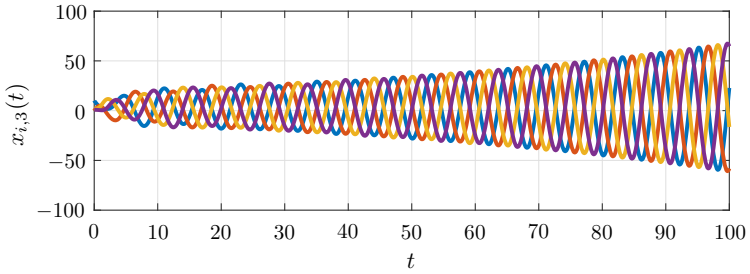

(c) State trajectories for $x_{i,3}(t)$.

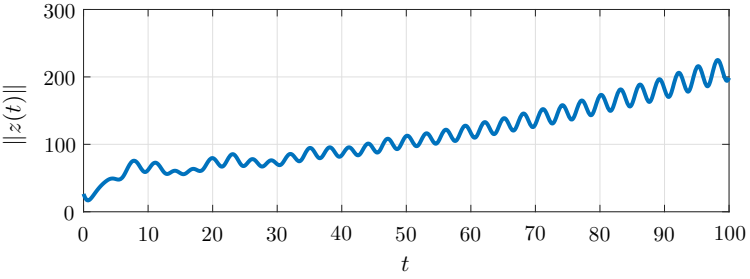

(d) Disagreement $\|z(t)\|$.

Figure 3.12: State trajectories and error for $\tau = 0.44$s.

Chapter 4

Consensus with Time-Varying Delays: Sufficient Conditions

Time-varying delays have been considered by Sun and Wang (2009) and Xi et al. (2013) for consensus on directed communication networks. The authors considered the possibility of nonuniform and non-differentiable time-varying delays, i.e. different values for the delays in each communication link and unknown or fast-varying delays without any constraints on the delay derivative (Fridman and Niculescu, 2008), satisfying $0 \leq \tau_{ij}(t) \leq \tau_{ij}^{\max}$, where $\tau_{ij}(t)$ refers to the time-delay between any agents i and j, and $\tau_{ij}^{\max} > 0$ are constants indicating the maximum values for the delays. These results however can only guarantee consensus in the first interval of time-delay, i.e. from zero to $\tau_{ij}^{\max}$. However, as shown in the previous chapter the system can also achieve consensus in other intervals of time-delays.

In Chapter 3, it was shown that the multiagent system can achieve consensus in different intervals of time-delays. More specifically, there was an example in which the system is consensable only in an interval $(0.1332, 0.4349)$ for input delays. It was also shown an example in which the agents achieve consensus in the first interval of communication delays $[0, 2.2958)$, but also in $(6.3358, 7.2585)$. Therefore, better than analyzing the delays varying in $0 \leq \tau_{ij}(t) \leq \tau_{ij}^{\max}$, which covers only the first interval, is to consider a lower bound for this interval, possibly greater than zero. Considering this, it is possible to verify consensus in different regions in the domain of time-delay as shown in the previous chapter.

This chapter shows sufficient conditions for the analysis of consensus in the presence of time-varying delays considering a lower bound for the time delay that can be different from zero. The network is considered to be directed, and the agent dynamics are described by any linear system as in (2.17) with communication delays in the consensus protocol,

or (2.53) with input delays. It generalizes the results published by the author in Savino et al. (2013), Savino et al. (2014a), Savino et al. (2014b), and Savino et al. (2016b).

The time-delays are considered to be nonuniform, time-varying and non-differentiable. Furthermore, it is assumed that all of them vary in an interval defined as $[\tau-\mu,\ \tau+\mu]$, *i.e.* $\tau_{ij}(t) \in [\tau-\mu,\ \tau+\mu]$, for $\tau_{ij}(t) > 0$, where τ and μ are given constants. The presented results are shown to be less conservative than previously published conditions in the numerical examples run with both single-order integrator (Xi et al., 2013) and second-order integrator dynamics (Liu et al., 2012). Furthermore, it extends the literature to high-order dynamics and analyzes convergence rate by means of a guaranteed exponential decay under non-differentiable time-varying delays.

The analysis is carried out for the transformed system in Section 2.2.2, using the Lyapunov-Krasovskii theory (Gu et al., 2003; Fridman, 2014) taking advantage of the Wirtinger-based improved integral inequality in Lemma 2.6 (Seuret and Gouaisbaut, 2013) and LMIs. The choice of Lyapunov-Krasovskii theory and LMIs to derive these results is made since it can adequately deal with systems subject to uncertain time-delays.

4.1 Consensus analysis

For convenience the agent dynamics with input delays is repeated here:

$$\dot{x}_i(t) = Ax_i(t) + Bu_i(t-\tau_i(t)), \quad i = 1, 2, \ldots, m, \tag{4.1}$$

$$u_i(t) = -\sum_{j\neq i, j=1}^{m} a_{ij} K\big(x_i(t) - x_j(t)\big), \tag{4.2}$$

given in (2.53) and (2.54), respectively, and for uniform communication delays:

$$\dot{x}_i(t) = Ax_i(t) + Bu_i(t), \quad i = 1, 2, \ldots, m, \tag{4.3}$$

$$u_i(t) = -\sum_{j\neq i, j=1}^{m} a_{ij} K\big(x_i(t) - x_j(t-\tau(t))\big), \tag{4.4}$$

given in (2.17) and (2.51), respectively. It is important to note that A, B, and K are the same in (4.1)–(4.4), no matter the type of delay being analyzed.

Following the procedure presented in Chapter 2 the closed-loop dynamics for a multi-agent system is transformed into a stability problem in the form

$$\dot{z}(t) = \bar{A}_{\square} z(t) + \sum_{k=1}^{k_{max}} \bar{B}_{k,\square} z(t-\tau_k(t)), \tag{4.5}$$

where the square index, it is referred to the possibility of replacing $\square$ by the index *in* for input delays, and *comm* for communication delays. For k, it can be replaced by the index i from 1 to $k_{\max} = m$ in the case of input delays, and for communication delays k refers to the edges and $k_{\max} = r$, the number of edges in the graph. Due to the Assumption 2.1, all the communication delays are considered equal such that $\tau_k(t) = \tau(t)$ and $\sum_{k=1}^{r} \bar{B}_{k,comm} = \bar{B}_{comm}$, which eliminates the summation in (4.5).

For input delays, replacing $\square$ by *in* and k by i, from 1 to $k_{\max} = m$, the matrices $\bar{A}_{in}$ and $\bar{B}_{i,in}$ are given according to the transformed system in (2.72), such that

$$\bar{A}_{in} = I_{m-1} \otimes A, \tag{4.6}$$

$$\bar{B}_{i,in} = -\bar{L}_i \otimes (BK), \tag{4.7}$$

$$\sum_{i=1}^{m} \bar{B}_{i,in} = \bar{B}_{in} = -\bar{L} \otimes (BK), \tag{4.8}$$

where A and B are given by the agent dynamics, K is the gain in the consensus protocol, and $\bar{L}_i = UL_iW \in \mathbb{R}^{(m-1)\times(m-1)}$ is the transformed Laplacian Matrix in (2.73), with U and W given in (2.12) and (2.14), respectively. The Laplacian Matrix L_i is associated to the subgraph on node $\mathcal{G}_{a,i}$ on the i-th agent.

For communication delays, since uniform delays are considered, the matrices in (4.5) are written as $\bar{A}_{comm}$ and $\bar{B}_{comm}$, given, according to the transformed system in (2.49), by:

$$\bar{A}_{comm} = I_{m-1} \otimes (A - BK), \tag{4.9}$$

$$\sum_{k=1}^{r} \bar{B}_{k,comm} = \bar{B}_{comm} = (I_{m-1} - \bar{L}) \otimes BK. \tag{4.10}$$

Finally, it is defined the exponential convergence rate as follows.

Definition 4.1 *The transformed multiagent system in* (4.5) *achieves consensus with guaranteed exponential convergence rate δ if*

$$||z(t)|| \ \leq \ \kappa e^{-\delta t}, \quad \forall t \geq 0,$$

where κ is an appropriate scalar.

The main result of this chapter is stated in the next theorem. It gives new sufficient conditions to verify consensus of a multiagent system with linear dynamics and nonuniform time-varying delays which vary within a given domain.

Theorem 4.1 *Let be given $\tau > 0$, $\tau \geq \mu_m \geq 0$, and $\delta > 0$. Then, the transformed multi-agent system in (4.5) with all $\tau_k(t) \in [\tau - \mu_m,\ \tau + \mu_m]$, $k = 1, 2, \ldots, k_{max}$, achieves consensus with guaranteed exponential convergence rate δ, if there exist real matrices: F, G, $P_1 = P_1^T$, P_2, $P_3 = P_3^T$, $Q = Q^T > 0$, $R = R^T > 0$, $S = S^T > 0$ and $Z = Z^T > 0$, with dimensions $n(m-1) \times n(m-1)$, such that the following LMIs hold:*

$$\begin{bmatrix} P_1 & P_2 \\ * & P_3 \end{bmatrix} > 0, \tag{4.11}$$

and

$$\begin{bmatrix} \Phi & \mu_m \Gamma \\ * & \frac{-\mu_m}{e_2} Z \end{bmatrix} < 0\ , \tag{4.12}$$

with $e_1 = e^{-2\delta\tau}$, $e_2 = e^{-2\delta(\mu_m + \tau)}$,

$$\Phi = \Phi_P + \Phi_Z + \Phi_R + \Phi_{QS} + \Phi_{FG}, \tag{4.13}$$

and

$$\Gamma = \begin{bmatrix} F\bar{B}_\square \\ G\bar{B}_\square \\ 0 \\ 0 \end{bmatrix}, \tag{4.14}$$

with

$$\Phi_P = \begin{bmatrix} 2\delta P_1 + P_2 + P_2^T & P_1 & -P_2 & 2\delta P_2 + P_3 \\ * & 0 & 0 & P_2 \\ * & * & 0 & -P_3 \\ * & * & * & 2\delta P_3 \end{bmatrix}, \tag{4.15}$$

$$\Phi_Z = \begin{bmatrix} 0 & 0 & 0 & 0 \\ * & 2\mu_m Z & 0 & 0 \\ * & * & 0 & 0 \\ * & * & * & 0 \end{bmatrix}, \quad \Phi_R = \begin{bmatrix} -\frac{4e_1}{\tau} R & 0 & -\frac{2e_1}{\tau} R & \frac{6e_1}{\tau^2} R \\ * & \tau R & 0 & 0 \\ * & * & -\frac{4e_1}{\tau} R & \frac{6e_1}{\tau^2} R \\ * & * & * & -\frac{12e_1}{\tau^3} R \end{bmatrix}, \tag{4.16}$$

$$\Phi_{QS} = \begin{bmatrix} Q - 2e_1 S & 0 & 0 & \frac{2e_1}{\tau} S \\ * & \frac{\tau^2}{2} S & 0 & 0 \\ * & * & -e_1 Q & 0 \\ * & * & * & -\frac{2e_1}{\tau^2} S \end{bmatrix}, \tag{4.17}$$

and

$$\Phi_{FG} = \begin{bmatrix} -e_2 F\bar{A}_\square - e_2 \bar{A}_\square^T F^T & e_2 F - e_2 \bar{A}_\square^T G^T & -e_2 F\bar{B}_\square & 0 \\ * & e_2 G + e_2 G^T & -e_2 G\bar{B}_\square & 0 \\ * & * & 0 & 0 \\ * & * & * & 0 \end{bmatrix}. \tag{4.18}$$

Proof This proof is concerned with the conditions for stability of the system in (4.5), which may represent (2.49) or (2.72), and showing consensus with communication or input delays according to Propositions 2.2 or 2.3, respectively.

Consider the following Lyapunov-Krasovskii functional (LKF) candidate:

$$\begin{aligned} V(z_t) =& \chi^T(t)P\chi(t) + \int_{t-\tau}^{t} e^{2\delta\xi} z^T(\xi)Qz(\xi)d\xi + \int_{-\tau}^{0}\int_{t+s}^{t} e^{2\delta\xi}\dot{z}^T(\xi)R\dot{z}(\xi)d\xi ds \\ &+ \int_{-\tau}^{0}\int_{\theta}^{0}\int_{t+s}^{t} e^{2\delta\xi}\dot{z}^T(\xi)S\dot{z}(\xi)d\xi ds d\theta + \int_{-\mu_m}^{\mu_m}\int_{t+s-\tau}^{t} e^{2\delta\xi}\dot{z}^T(\xi)Z\dot{z}(\xi)d\xi ds, \end{aligned} \tag{4.19}$$

where $\chi^T(t) = \left[e^{\delta t}z^T(t) \quad e^{\delta t}\int_{t-\tau}^{t} z^T(\xi)d\xi\right]$,

$$P = \begin{bmatrix} P_1 & P_2 \\ * & P_3 \end{bmatrix}, \tag{4.20}$$

and there exist some real matrices $P_1 = P_1^T$, P_2, $P_3 = P_3^T$, $Q = Q^T$, $R = R^T$, $S = S^T$, and $Z = Z^T$.

Initially, the condition $V(z_t) > 0$ has to satisfied, where z_t corresponds to the value of $z(\sigma)$ with $\sigma \in [t-\tau-\mu_m,\ t]$. Thus, each matrix variable in each term of (4.19) is assumed to be positive definite: $P > 0$ in (4.11), $Q > 0$, $R > 0$, $S > 0$, and $Z > 0$. If these conditions are satisfied, then $V(z_t) > 0$.

Now, it is shown the condition for the functional in (4.19) to satisfy the derivative condition $\dot{V}(z_t) < 0$. Initially, consider the following null term (Mozelli et al., 2010; Souza et al., 2008), derived from the system's equation (4.5):

$$0 = 2\Lambda(t)\left[\dot{z}(t) - \bar{A}_{\square}z(t) - \sum_{k=1}^{k_{max}}\bar{B}_{k,\square}z(t-\tau_k(t))\right]e^{\delta(t-\tau-\mu_m)} \tag{4.21}$$

$$= 2\Lambda(t)\left[\dot{z}(t) - \bar{A}_{\square}z(t) - \sum_{k=1}^{k_{max}}\bar{B}_{k,\square}\left(z(t-\tau) - \int_{-\tau_k(t)}^{-\tau}\dot{z}(t+\xi)d\xi\right)\right]e^{\delta(t-\tau-\mu_m)} \tag{4.22}$$

$$= 2\Lambda(t)\left[\dot{z}(t) - \bar{A}_{\square}z(t) - \bar{B}_{\square}z(t-\tau)\right]e^{\delta(t-\tau-\mu_m)} + v(t), \tag{4.23}$$

with

$$v(t) = \sum_{k=1}^{k_{max}}\int_{-\tau_k(t)}^{-\tau} 2\Lambda(t)\bar{B}_{k,\square}\dot{z}(t+\xi)e^{\delta(t-\tau-\mu_m)}d\xi, \tag{4.24}$$

$$\Lambda(t) = e^{\delta(t-\tau-\mu_m)}\left[z^T(t)F \quad \dot{z}^T(t)G\right], \tag{4.25}$$

and F and G matrices with $n(m-1)$ square dimensions.

Then, applying the inequality $2a^Tb \leq a^TXa + b^TX^{-1}b$ in (4.24), where a^T and b are the vectors $\Lambda(t)\bar{B}_{k,\square}$ and $\dot{z}(t+\xi)e^{\delta(t-\tau-\mu_m)}$, respectively, and X is a positive-definite matrix

chosen to be $\frac{Z}{k_{max}}$, yields

$$\begin{aligned} v(t) \leq & \sum_{k=1}^{k_{max}} \int_{-\tau_k(t)}^{-\tau} (\Lambda(t)\bar{B}_{k,\square}) k_{max} Z^{-1} (\Lambda(t)\bar{B}_{k,\square})^T d\xi \\ & + \sum_{k=1}^{k_{max}} \int_{-\tau_k(t)}^{-\tau} e^{2\delta(t-\tau-\mu_m)} \dot{z}^T(t+\xi) \frac{Z}{k_{max}} \dot{z}(t+\xi) d\xi. \end{aligned} \tag{4.26}$$

Considering appropriate upper bounds for the integral terms, it gives

$$v(t) \leq \sum_{k=1}^{k_{max}} \mu_m (\Lambda(t)\bar{B}_{k,\square}) k_{max} Z^{-1} (\Lambda(t)\bar{B}_{k,\square})^T + e^{2\delta(t-\tau-\mu_m)} \int_{t-\tau-\mu_m}^{t-\tau+\mu_m} \dot{z}^T(\xi) Z \dot{z}(\xi) d\xi. \tag{4.27}$$

Replace (4.27) in (4.23) and define $e_2 = e^{-2\delta(\tau+\mu_m)}$ to obtain

$$\begin{aligned} 0 \leq & 2e^{2\delta t} z^T(t) e_2 F \dot{z}(t) + 2e^{2\delta t} \dot{z}^T(t) e_2 G \dot{z}(t) - 2e^{2\delta t} z^T(t) e_2 F \bar{A}_\square z(t) \\ & - 2e^{2\delta t} \dot{z}^T(t) e_2 G \bar{A}_\square z(t) - 2e^{2\delta t} z^T(t) e_2 F \bar{B}_\square z(t-\tau) - 2e^{2\delta t} \dot{z}^T(t) e_2 G \bar{B}_\square z(t-\tau) \\ & + \sum_{k=1}^{k_{max}} \mu_m (\Lambda(t)\bar{B}_{k,\square}) k_{max} Z^{-1} (\Lambda(t)\bar{B}_{k,\square})^T + e^{2\delta(t-\tau-\mu_m)} \int_{t-\tau-\mu_m}^{t-\tau+\mu_m} \dot{z}^T(\xi) Z \dot{z}(\xi) d\xi. \end{aligned} \tag{4.28}$$

Moreover, the time-derivative of the functional $V(z_t)$ in (4.19) is

$$\begin{aligned} \dot{V}(z_t) = & \chi^T(t) P \dot{\chi}(t) + \dot{\chi}^T(t) P \chi(t) \\ & + e^{2\delta t} z^T(t) Q z(t) - e^{2\delta(t-\tau)} z^T(t-\tau) Q z(t-\tau) \\ & + \tau e^{2\delta t} \dot{z}^T(t) R \dot{z}(t) - \int_{t-\tau}^{t} e^{2\delta\xi} \dot{z}^T(\xi) R \dot{z}(\xi) d\xi \\ & + \frac{\tau^2}{2} e^{2\delta t} \dot{z}^T(t) S \dot{z}(t) - \int_{-\tau}^{0} \int_{t+s}^{t} e^{2\delta\xi} \dot{z}^T(\xi) S \dot{z}(\xi) d\xi ds \\ & + 2\mu_m e^{2\delta t} \dot{z}^T(t) Z \dot{z}(t) - \int_{t-\tau-\mu_m}^{t-\tau+\mu_m} e^{2\delta\xi} \dot{z}^T(\xi) Z \dot{z}(\xi) d\xi. \end{aligned}$$

Then, the integrals with terms R and S may be bounded as in Lemma 2.6 and

Lemma 2.5, respectively, such that

$$\begin{aligned}\dot{V}(z_t) \leq & \chi^T(t)P\dot{\chi}(t) + \dot{\chi}^T(t)P\chi(t) \\ & + e^{2\delta t}z^T(t)Qz(t) - e_1e^{2\delta t}z^T(t-\tau)Qz(t-\tau) \\ & + \tau e^{2\delta t}\dot{z}^T(t)R\dot{z}(t) - \frac{e_1e^{2\delta t}}{\tau}\int_{t-\tau}^{t}\dot{z}^T(\xi)d\xi R\int_{t-\tau}^{t}\dot{z}(\xi)d\xi - \frac{3e_1e^{2\delta t}}{\tau}\tilde{\Omega}^T R\tilde{\Omega} \\ & + \frac{\tau^2}{2}\dot{z}^T(t)S\dot{z}(t) - 2e_1e^{2\delta t}z^T(t)Sz(t) \\ & + \frac{4e_1e^{2\delta t}}{\tau}z^T(t)S\int_{t-\tau}^{t}z(\xi)d\xi - \frac{2e_1e^{2\delta t}}{\tau^2}\int_{t-\tau}^{t}z^T(\xi)d\xi\ S\int_{t-\tau}^{t}z(\xi)d\xi \\ & + 2\mu_m e^{2\delta t}\dot{z}^T(t)Z\dot{z}(t) - e^{2\delta(t-\tau-\mu_m)}\int_{t-\tau-\mu_m}^{t-\tau+\mu_m}\dot{z}^T(\xi)Z\dot{z}(\xi)d\xi. \end{aligned} \tag{4.29}$$

with $\tilde{\Omega}$ given as Ω in (2.83) replacing a by $t-\tau$ and b by t.

Adding the null term (4.28) to $\dot{V}(z_t)$ in (4.29), gives:

$$\begin{aligned}\dot{V}(z_t) \leq & \chi^T(t)P\dot{\chi}(t) + \dot{\chi}^T(t)P\chi(t) \\ & + e^{2\delta t}z^T(t)Qz(t) - e_1e^{2\delta t}z^T(t-\tau)Qz(t-\tau) \\ & + \tau e^{2\delta t}\dot{z}^T(t)R\dot{z}(t) - \frac{e_1e^{2\delta t}}{\tau}\int_{t-\tau}^{t}\dot{z}^T(\xi)d\xi R\int_{t-\tau}^{t}\dot{z}(\xi)d\xi - \frac{3e_1e^{2\delta t}}{\tau}\tilde{\Omega}^T R\tilde{\Omega} \\ & + \frac{\tau^2}{2}\dot{z}^T(t)S\dot{z}(t) - 2e_1e^{2\delta t}z^T(t)Sz(t) \\ & + \frac{4e_1e^{2\delta t}}{\tau}z^T(t)S\int_{t-\tau}^{t}z(\xi)d\xi - \frac{2e_1e^{2\delta t}}{\tau^2}\int_{t-\tau}^{t}z^T(\xi)d\xi\ S\int_{t-\tau}^{t}z(\xi)d\xi \\ & + 2\mu_m e^{2\delta t}\dot{z}^T(t)Z\dot{z}(t) - \cancel{e^{2\delta(t-\tau-\mu_m)}\int_{t-\tau-\mu_m}^{t-\tau+\mu_m}\dot{z}^T(\xi)Z\dot{z}(\xi)d\xi} \\ & + 2e^{2\delta t}z^T(t)e_2F\dot{z}(t) + 2e^{2\delta t}\dot{z}^T(t)e_2G\dot{z}(t) \\ & - 2e^{2\delta t}z^T(t)e_2F\bar{A}_{\square}z(t) - 2e^{2\delta t}\dot{z}^T(t)e_2G\bar{A}_{\square}z(t) \\ & - 2e^{2\delta t}z^T(t)e_2F\bar{B}_{\square}z(t-\tau) - 2e^{2\delta t}\dot{z}^T(t)e_2G\bar{B}_{\square}z(t-\tau) \\ & + \sum_{k=1}^{k_{max}}\mu_m(\Lambda(t)\bar{B}_{k,\square})k_{max}Z^{-1}(\Lambda(t)\bar{B}_{k,\square})^T + \cancel{e^{2\delta(t-\tau-\mu_m)}\int_{t-\tau-\mu_m}^{t-\tau+\mu_m}\dot{z}^T(\xi)Z\dot{z}(\xi)d\xi}. \end{aligned} \tag{4.30}$$

Making

$$\Gamma_k = \begin{bmatrix} F\bar{B}_{k,\square} \\ G\bar{B}_{k,\square} \\ 0 \\ 0 \end{bmatrix} \tag{4.31}$$

and $\Upsilon^T(t) = [e^{\delta t}z^T(t) \quad e^{\delta t}\dot{z}^T(t) \quad e^{\delta t}z^T(t-\tau) \quad e^{\delta t}\int_{t-\tau}^{t} z^T(\xi)d\xi]$, it can be written the product $\Lambda(t)\bar{B}_{k,\square} = e^{-\delta(\tau+\mu_m)}\Upsilon^T(t)\Gamma_k$. Additionally, given Φ in (4.13), the derivative of the LKF can be written as

$$\dot{V}(z_t) \leq \Upsilon^T(t)\Phi\Upsilon(t) + \sum_{k=1}^{r} \mu_m e_2 \Upsilon^T(t)\Gamma_k k_{max} Z^{-1}\Gamma_k^T \Upsilon(t), \tag{4.32}$$

$$= \Upsilon^T(t)\left(\sum_{k=1}^{k_{max}}\left(\frac{1}{k_{max}}\Phi + \mu_m e_2 \Gamma_k k_{max} Z^{-1}\Gamma_k^T\right)\right)\Upsilon(t). \tag{4.33}$$

In order to guarantee $\dot{V}(z_t) < 0$ for any $\zeta \neq 0$, the term between the larger parentheses in (4.33) must be negative definite. Thus, applying Schur's complement, it is obtained:

$$\sum_{k=1}^{k_{max}} \begin{bmatrix} \frac{1}{k_{max}}\Phi & \mu_m\Gamma_k \\ * & \frac{-\mu_m}{e_2 k_{max}}Z \end{bmatrix} = \begin{bmatrix} \Phi & \mu_m\Gamma \\ * & \frac{-\mu_m}{e_2}Z \end{bmatrix} < 0,$$

where $\Gamma = \sum_{k=1}^{k_{max}} \Gamma_k$, leading to the LMI condition in (4.12). Then, if the LMI in (4.12) holds, the LKF time-derivative condition $\dot{V}(z_t) < 0$) is satisfied.

Next, it is shown that if the LMIs conditions presented in the theorem are satisfied, then the transformed system in (4.5) achieves consensus with exponential convergence rate δ. Thereby, assuming that the LMIs are satisfied then $\dot{V}(z_t) < 0$ and $V(z_t) > 0$, yielding

$$0 \leq V(z_t) \leq \bar{V}(z_t) \leq \bar{V}(z_t)|_{t=0}, \tag{4.34}$$

with

$$\begin{aligned}\bar{V}(z_t) =& \lambda_{\max}\{P\}||\chi(t)||^2 + \lambda_{\max}\{Q\}\int_{t-\tau}^{t} e^{2\delta\xi}||z(\xi)||^2 d\xi \\ &+ \left(\tau\lambda_{\max}\{R\} + \tau^2\lambda_{\max}\{S\}\right)\int_{t-\tau}^{t} e^{2\delta\xi}||\dot{z}(\xi)||^2 d\xi + \lambda_{\max}\{Z\}\int_{t-\tau-\mu_m}^{t} e^{2\delta\xi}||\dot{z}(\xi)||^2 d\xi,\end{aligned} \tag{4.35}$$

where $\lambda_{\max}\{\cdot\}$ is the maximum eigenvalue of a matrix, and,

$$\begin{aligned}\bar{V}(z_t)|_{t=0} \leq& \left(\lambda_{\max}\{P\}\right)\sup_{-\tau\leq\theta\leq 0}\{||\chi(\theta)||\} + \left(\lambda_{\max}\{Q\}\int_{-\tau}^{0} e^{2\delta\xi}d\xi\right)\sup_{-\tau\leq\theta\leq 0}\{||z(\theta)||\} \\ &+ \Bigg(\left(\tau\lambda_{\max}\{R\} + \tau^2\lambda_{\max}\{S\}\right)\int_{-\tau}^{0} e^{2\delta\xi}d\xi \\ &+ (\tau+\mu_m)\sum_{k=1}^{r}\lambda_{\max}\{Z_k\}\int_{-\tau-\mu_m}^{0} e^{2\delta\xi}d\xi\Bigg)\sup_{-(\tau+\mu_m)\leq\theta\leq 0}\{||\dot{z}(\theta)||\} = \rho(\delta).\end{aligned} \tag{4.36}$$

Therefore, it can be noticed from (4.34) and (4.36), that

$$e^{2\delta t}\lambda_{\min}\{P_1\}||z(t)||^2 \leq \bar{V}(z_t) \leq \rho(\delta),$$

where $\lambda_{\min}\{P_1\}$ is the minimum eigenvalue of the matrix P_1, then

$$||z(t)|| \leq \sqrt{\frac{\rho(\delta)}{\lambda_{\min}\{P_1\}}}\, e^{-\delta t} \triangleq \kappa e^{-\delta t}.$$

Therefore, the transformed multiagent system in (4.5) achieves consensus with exponential convergence rate δ according to Definition 4.1. This completes the proof. □

It is worth to mention that some steps in this proof regarding the bounds of the time-delays are inspired in the work by Fridman (2006) and Fridman and Niculescu (2008), where it is also assumed similar description for the time-delay adopted here.

When the time-delays are considered to be constant, i.e $\mu_m = 0$ the following corollary can be derived from Theorem 4.1.

Corollary 4.1 *Let be given $\tau > 0$ and $\delta > 0$. Then, the transformed multiagent system in* (4.5) *with all $\tau_k(t) = \tau$, $k = 1, 2, \ldots, k_{max}$, achieves consensus with guaranteed exponential convergence rate δ, if there exist real matrices: F, G, $P_1 = P_1^T$, P_2, $P_3 = P_3^T$, $Q = Q^T > 0$, $R = R^T > 0$, and $S = S^T > 0$, of dimensions $n(m-1) \times n(m-1)$, such that the LMI* (4.11) *and $\bar{\Phi} < 0$ hold, where $\bar{\Phi} = \Phi_P + \Phi_R + \Phi_{QS} + \Phi_{FG}$ given as in* (4.13).

Proof The proof follows from Theorem 4.1 by making $\mu_m = 0$ such that, in (4.33), $\Phi < 0$ is sufficient to guarantee $\dot{V}(z_t) < 0$. Additionally, since $\mu_m = 0$ the term with Z vanishes, which gives $\bar{\Phi} = \Phi - \Phi_Z < 0$, or $\bar{\Phi} = \Phi_P + \Phi_R + \Phi_{QS} + \Phi_{FG}$. This completes the proof. □

Remark 4.1 *In the proposed method the choice of the LKF plays a major role in the method conservativeness. One efficient strategy to reduce the conservativeness in this context is the delay discretization technique; see for example Gu et al. (2003), however in this case the complexity of LMIs computations is increased as a result of an increase in the number of discretizations. Thus the conservativeness of the proposed method can be reduced by applying discretization techniques, at the cost of higher computational complexity.*

4.2 Numerical Examples

In this section, the proposed method is applied in different examples. For comparison purpose, the same directed network with 4 agents in the work of Yu et al. (2010) is

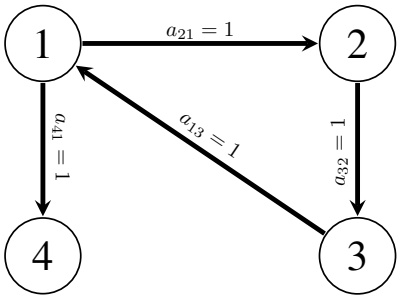

Figure 4.1: Directed network with four agents.

considered. This topology is shown in Figure 4.1 with an associated Laplacian Matrix given by

$$L = \begin{bmatrix} 1 & 0 & -1 & 0 \\ -1 & 1 & 0 & 0 \\ 0 & -1 & 1 & 0 \\ -1 & 0 & 0 & 1 \end{bmatrix}. \tag{4.37}$$

Note that this graph satisfies Assumption 2.2 for the analysis of consensus with communication delays.

Initially, it is considered the case of uniform and constant time delay, *i.e.*, $\tau_k(t) = \tau$. For comparison purpose, consider the agents with dynamics described as a chain of integrators, with first-, second-, third- and fourth-order dynamics as in (3.2). With $\mu = 0$ and $\delta \approx 0$, a search is made for the highest value of τ such that the LMI conditions in Corollary 4.1 hold. For illustration purposes, the gains in matrix K, for the consensus protocol in (3.9), are considered to be [1], [1 1], [0.3 1 1], and [0.2 0.3 1 1] for fist-, second-, third-, and fourth-order integrator dynamics, respectively.

4.2.1 Constant Delays

The obtained results are compared with some related methods for consensus with input delay using LMIs, such as Xi et al. (2013) and Liu et al. (2012), for first- and second-order integrator dynamics. Besides, the first interval of delay can be assessed by the analytical results presented in Theorem 3.1 for communication delays, and Theorem 3.2 for input delays. The results for input delays are summarized in Table 4.1, and for communication delays in Table 4.2.

Table 4.1 and Table 4.2 show that Corollary 4.1 presents results that are very close to the analytical result provided by Theorem 3.2 and Theorem 3.1, respectively, confirming the validity of the method. Moreover, differently from Xi et al. (2013) and Liu et al.

Table 4.1: Maximum allowed constant input delay $\tau_i(t) = \tau$ obtained for multiagent system in Figure 4.1.

	Method	1-integr.,	2-integr.	3-integr.	4-integr.
Sufficient	Xi et al. (2013)	0.5773	-	-	-
	Liu et al. (2012)	-	0.2870	-	-
	Corollary 4.1	0.6043	0.2941	0.2768	0.2918
Analytical	Theorem 3.2	0.6046	0.2942	0.2769	0.2919

Table 4.2: Maximum allowed constant communication delay $\tau(t) = \tau$ obtained for multiagent system in Figure 4.1.

	Method	2-integrators	3-integrators	4-integrators
Sufficient	Corollary 4.1	0.6104	0.4996	0.5576
Analytical	Theorem 3.1	0.6105	0.4997	0.5577

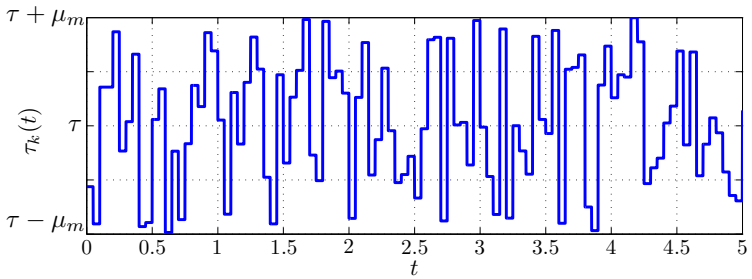

Figure 4.2: Time-varying delay $\tau_k(t)$ with random amplitude.

(2012), the proposed method can handle consensus problems with dynamical systems with any number of integrators and can also deal with communication delays.

4.2.2 Time-varying Delays

Another advantage of the proposed method is its ability to handle any linear dynamics and non-differentiable time-varying delay, i.e. time-delays without knowledge of the time derivative of $\tau_k(t)$. The delays are considered to belong to the interval given by $\tau_k(t) \in [\tau - \mu_m,\ \tau + \mu_m], 0 \leq \mu \leq \tau$. An example of the random form of the time-delay for further analysis is depicted in Figure 4.2.

A multiagent system composed of vehicles with the dynamics given in (1.35) is considered for the analysis. Thus, the agent dynamics is described by the state variables

$\begin{bmatrix} s_i(t) & v_i(t) & a_i(t) \end{bmatrix}^T$ and the matrices

$$A = \begin{bmatrix} 0 & 1 & 0 \\ 0 & 0 & 1 \\ 0 & 0 & \frac{-1}{\iota_i} \end{bmatrix} \tag{4.38}$$

and

$$B = \begin{bmatrix} 0 \\ 0 \\ \frac{1}{\iota_i} \end{bmatrix}. \tag{4.39}$$

For the consensus protocol consider the gain matrix $K = [0.3 \quad 1 \quad 1]$. Also, consider the inertial delay $\iota_i = 0.5$.

It is illustrated the efficiency given by the proposed method by showing that the system achieves consensus with guaranteed convergence rate δ with the considered time-varying delay. The test is the one of finding the largest value of δ for given pairs of τ and μ, such that the LMI conditions are feasible. The obtained results for input delays and communication delays are shown in Table 4.3 and Table 4.4, respectively.

Table 4.3: Largest δ obtained for input delays with given pair (τ, μ)

(τ, μ)	$(0.10, 0.05)$	$(0.15, 0.05)$	$(0.10, 0.10)$	$(0.15, 0.10)$
δ	0.26	0.26	0.25	0.12

Table 4.4: Largest δ obtained for communication delays with given pair (τ, μ)

(τ, μ)	$(0.30, 0.10)$	$(0.30, 0.20)$	$(0.50, 0.20)$	$(0.60, 0.20)$
δ	0.26	0.26	0.24	0.19

Figure 4.3 shows the state trajectories for the system during simulation for the case of communication delay varying in the interval $\tau(t) \in [0.10, 0.50]$, i.e. $\tau = 0.30$, $\mu = 0.20$. The three state variables are represented in three graphics showing that the multiagent system achieves consensus in all of them. It is also shown the norm of the transformed variables $||z(t)||$, representing the disagreement as it goes to zero. The latter also shows the convergence curve with $\delta = 0.26$, represented by the dashed line of an exponential function that converges similarly to the system and can adequately describe the time needed to achieve consensus.

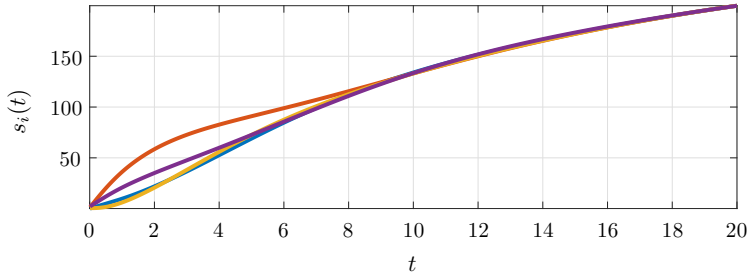

(a) State trajectories for $s_i(t)$.

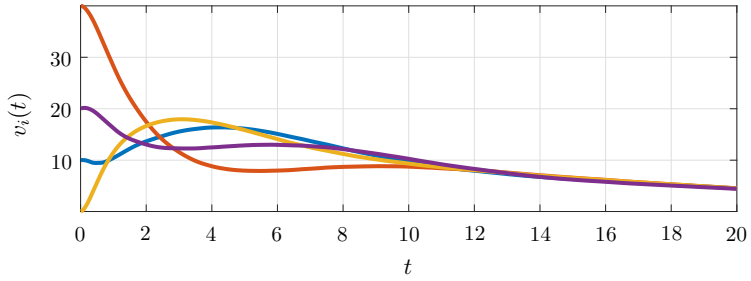

(b) State trajectories for $v_i(t)$.

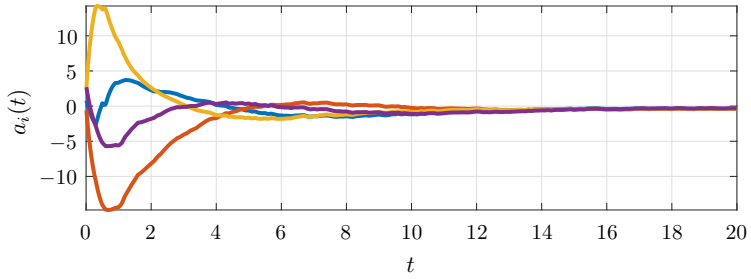

(c) State trajectories for $a_i(t)$.

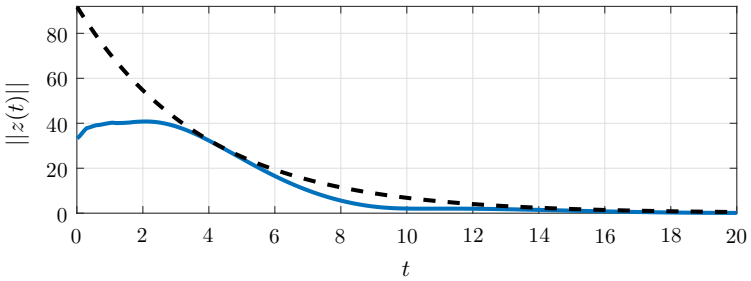

(d) Disagreement $\|z(t)\|$ with dashed exponential convergence curve with $\delta = 0.26$.

Figure 4.3: State trajectories and error with communication delay given by $\tau = 0.30$ and $\mu_m = 0.20$.

Chapter 5

Consensus Analysis with Switching Topologies

This chapter proposes a sufficient method for the analysis of consensus on multiagent systems subject to time-varying delays and switching topology. The switches in the network topology are of great interest and can model failures in the communication channels, obstructions, and packages dropout. The main contribution is given in Theorem 5.1. It shows a sufficient condition for consensus on a multiagent system based on linear matrix inequalities that takes into account the joint effect of time-varying delays and switching network topology.

The case of multiagent systems subject to switching topology has been addressed in the literature using several methodologies. For example, Zhao et al. (2011) uses Markov processes to formulate a mean-square consensus problem for second-order multiagent systems with time-delays and unknown transition probabilities; in the work by Qin et al. (2014) communication constraints and linear system dynamics are considered; and by Ren et al. (2007) the switching topology is considered non-stochastic. In this scenario, many practical applications in which the network topology may vary can be analyzed using consensus-based approaches with switching topologies, for example, flight formation of quadrotors as presented by Michael et al. (2010); Schwager et al. (2011).

The following result is a reprint of the result published by the author in Savino et al. (2016a), which also generalizes dos Santos Junior et al. (2014) and dos Santos Junior et al. (2015). Additionally, the result is also extended to the case of multiagent systems subject to communication delays.

It is assumed that the topology switch behaves as a continuous time Markov chain with uncertain transition rates, which can be related to systems where the stochastic model

is not exactly known. Thus the multi-agent system is transformed into a Markov jump linear system (MJLS) and the consensus analysis is carried out by providing sufficient conditions written as Linear Matrix Inequalities (LMIs) to guarantee the stability of the transformed system. The treatment given to the uncertain transition rates is inspired on the ideas presented by Xiong et al. (2005), Xiong and Lam (2009), Zhang et al. (2008), and Zhang and Boukas (2009).

An extension of the formulation of the problem is presented next, in order to describe the multiple possible topologies.

5.1 Problem Formulation with Switching Topologies

Let θ_t be the representation of the topology of the multi-agent system at the instant of time t, and $\mathcal{S} = 1, 2, \ldots, s$ the image of θ_t, where s is the total number of topologies. Each topology is associated with a weighted directed graph $\mathcal{G}(\ell) = (\mathcal{V}, \mathcal{E}(\ell), \mathcal{A}(\ell), \mathcal{W})$, for all $\ell \in \mathcal{S}$, with same set of vertices $\mathcal{V}$ and Weight Matrix $\mathcal{W}$, but different sets of edges $\mathcal{E}(\ell)$, such that the Adjacency Matrix $\mathcal{A}(\ell) = [a_{ij}(\ell)]$ with elements $a_{ij}(\ell)$ is given by:

$$a_{ij}(\ell) = \begin{cases} 0, & \text{if } i = j \text{ or } \nexists\ e_{ji} \in \mathcal{E}(\ell), \\ w_{ij}, & \text{if and only if } \exists\ e_{ji} \in \mathcal{E}(\ell), \end{cases} \tag{5.1}$$

where $w_{ij} > 0$.

Remark 5.1 *Same edges e_{ji} in different graphs $\mathcal{G}(\ell)$ are associated to the same weights w_{ij}. An element w_{ij} exists in $\mathcal{W}$ even if e_{ji} does not exist in $\mathcal{E}(\ell)$.*

Consider the set $\bar{\mathcal{E}} = \bigcup_{\ell=1}^{s} \mathcal{E}(\ell)$ the union of all the edges in each graph $\mathcal{G}(\ell)$, for all $\ell = 1, 2, \ldots, s$. Thus, it is defined the Joint Graph $\bar{\mathcal{G}}$:

Definition 5.1 *The Joint Graph $\bar{\mathcal{G}} = (\mathcal{V}, \bar{\mathcal{E}}, \bar{\mathcal{A}}, \mathcal{W})$ is the graph composed of the union of the edges in the subgraphs $\mathcal{G}(\ell)$, for all $\ell = 1, 2, \ldots, s$. The vertices $\mathcal{V}$ and weights $\mathcal{W}$ are the same for all $\mathcal{G}(\ell)$ and $\bar{\mathcal{G}}$, and the joint Adjacency Matrix $\bar{\mathcal{A}} = [\bar{a}_{ij}]$ is given by:*

$$\bar{a}_{ij}(\ell) = \begin{cases} 0, & \textit{if } \ i = j \textit{ or } \nexists\ e_{ji} \in \bar{\mathcal{E}}, \\ w_{ij}, & \textit{if and only if } \exists\ e_{ji} \in \bar{\mathcal{E}}. \end{cases} \tag{5.2}$$

Similarly to (2.2) it can be defined the Laplacian matrices $L(\ell)$ for each $\mathcal{G}(\ell)$,

$$L(\ell) = \mathcal{D}(\ell) - \mathcal{A}(\ell), \tag{5.3}$$

where $\mathcal{D}(\ell)$ is the degree matrix associated to the adjacency matrix $\mathcal{A}(\ell)$ of graph $\mathcal{G}(\ell)$.

Consider a multiagent system with m agents in a directed network. The following pairs of equations describe the dynamics of the agents with input delays or communication delays. With input delays, the dynamics is given by

$$\dot{x}_i(t) = Ax_i(t) + Bu_i(\theta_t, t - \tau_i(t)), \quad i = 1, 2, \ldots, m, \tag{5.4}$$

and the following protocol is considered

$$u_i(\theta_t, t) = -\sum_{j\neq i, j=1}^{m} a_{ij}(\theta_t)K\big(x_i(t) - x_j(t)\big). \tag{5.5}$$

Under communication delays, the dynamics is given by

$$\dot{x}_i(t) = Ax_i(t) + Bu_i(\theta_t, t), \quad i = 1, 2, \ldots, m, \tag{5.6}$$

and protocol

$$u_i(\theta_t, t) = -\sum_{j\neq i, j=1}^{m} a_{ij}(\theta_t)K\big(x_i(t) - x_j(t - \tau(t))\big). \tag{5.7}$$

The time-varying variable θ_t represents the current topology of the multi-agent system at each instant of time t, and $u_i(\theta_t, t)$ indicates the control input based on the current connected neighbors of agent i.

The dynamics of the parameter θ_t is given by a continuous time Markov chain (Wentzell et al. (1981)) with discrete states given by a set $\mathcal{S} = 1, 2, ..., s$, with s the number of different topologies, and a probability transition matrix $\Psi = [\psi_{pq}]$ defined by:

$$\psi_{pq}{=}\mathbb{P}\{\theta_{t+\Delta}{=}q|\theta_t{=}p\}{=}\begin{cases}(\pi_{pq} + \epsilon_{pq})\Delta + o(\Delta), & p \neq q,\\ 1 + (\pi_{pp} + \epsilon_{pp})\Delta + o(\Delta), & p = q,\end{cases} \tag{5.8}$$

in which ψ_{pq} represents the probability of switching from topology p to q in an interval $\Delta > 0$ at given time t, for $p, q \in \mathcal{S}$, and where $\lim_{\Delta\to 0}\frac{o(\Delta)}{\Delta} = 0$, and $(\pi_{pq} + \epsilon_{pq})$ are elements of the uncertain transition rate matrix

$$\Pi = \begin{bmatrix} \pi_{11} + \epsilon_{11} & \pi_{12} + \epsilon_{12} & \cdots & \pi_{1s} + \epsilon_{1s} \\ \pi_{21} + \epsilon_{21} & \pi_{22} + \epsilon_{22} & \cdots & \pi_{2s} + \epsilon_{2s} \\ \vdots & \vdots & \ddots & \vdots \\ \pi_{s1} + \epsilon_{s1} & \pi_{s2} + \epsilon_{s2} & \cdots & \pi_{ss} + \epsilon_{ss} \end{bmatrix}. \tag{5.9}$$

The value π_{pq} is an estimate of the transition rate from state p to state q, and ϵ_{pq} represents the error (uncertainty) of this estimate. It is assumed that ϵ_{pq} is an unknown constant scalar taking values within a known interval $\epsilon_{pq} \in [-\delta_{pq},\ \delta_{pq}]$, $\delta_{pq} > 0$, $\delta_{pq} < \pi_{pq}$. Note that

$\pi_{pq} + \delta_{pq} > 0$, $\pi_{pp} = -\sum_{q=1,q\neq p}^{s} \pi_{pq}$, $\epsilon_{pp} = -\sum_{q=1,q\neq p}^{s} \epsilon_{pq}$, and consequently $\sum_{q=1}^{s}(\pi_{pq} + \epsilon_{pq}) = 0$. Finally, denote $\nu = (\nu_1, \ldots, \nu_s)$ the initial distribution of the Markov chain, related to the probability of the initial topology and first switches.

In order to obtain a compact representation of the multi-agent system, the augmented system dynamics comprising all the agents with input delays, given by the closed-loop of (5.4) with protocol (5.5), is

$$\dot{x}(t) \quad = (I_m \otimes A)x(t) - \sum_{i=1}^{m}(L_{a,i}(\theta_t) \otimes BK)x(t - \tau_i(t)) \tag{5.10}$$

and for communication delays, the closed-loop of (5.6) with protocol (5.7) is

$$\dot{x}(t) = (I_m \otimes A - \mathcal{D} \otimes BK)x(t) + \sum_{k=1}^{r}(\mathcal{D}(\theta_t) \otimes BK - L(\theta_t) \otimes BK)x(t - \tau(t)), \tag{5.11}$$

where (5.10) and (5.11) are obtained similarly to (2.69) and (2.45), respectively.

Consider the closed-loop dynamics for a multiagent system written as

$$\dot{x}(t) = A_{\square}x(t) + \sum_{k=1}^{k_{max}} B_{k,\square}(\theta_t)x(t - \tau_k(t)), \tag{5.12}$$

with the square index $\square$ referring to the index *in* for input delays, and *comm* for communication delays. As presented previously in Section 4.1, k can be replaced by the index i from 1 to $k_{max} = m$ in the case of input delays, and for communication delays k refers to the edges and $k_{max} = r$, which due to Assumption 2.1, all $\tau_k(t) = \tau(t)$ making $\sum_{k=1}^{r} B_{k,comm} = B_{comm}$. Thus, for input delays, it yields

$$A_{in} = I_m \otimes A, \tag{5.13}$$

$$B_{i,in}(\theta_t) = -L_{a,i}(\theta_t) \otimes (BK), \tag{5.14}$$

$$\sum_{i=1}^{m} B_{i,in}(\theta_t) = B_{in}(\theta_t) = -L(\theta_t) \otimes (BK), \tag{5.15}$$

and for communication delays

$$A_{comm} = I_m \otimes (A - BK), \tag{5.16}$$

$$\sum_{k=1}^{r} B_{k,comm}(\theta_t) = B_{comm}(\ell) = (I_m - L(\theta_t)) \otimes BK. \tag{5.17}$$

With these definitions, it is formalized the definition of consensus under stochastic topologies:

Definition 5.2 *(Miao et al. (2014)) Under stochastic switching topology, the closed-loop multiagent system* (5.12)*, reaches mean-square consensus if, for all* $i \neq j$*, the limits* $\lim_{t\to\infty} \mathbb{E}||x_i(t) - x_j(t)||^2 = 0$ *hold in the mean-square sense for any initial distribution* $\nu = (\nu_1, \ldots, \nu_s)$ *for* θ_t*,* $t = 0$*, and any initial state conditions.*

Next, conditions are proposed to verify whether the multiagent system in (5.12) achieves consensus according to Definition 5.2.

The tree-type transformation can be applied in (5.10) and (5.11) as in Chapter 2, in order to obtain the transformed disagreement systems analogous to (2.72) and (2.49), respectively, taking into account the variable θ_t, yielding

$$\dot{z}(t) = \bar{A}_{\square} z(t) + \sum_{k=1}^{k_{max}} \bar{B}_{k,\square}(\theta_t) z(t - \tau_k(t)). \tag{5.18}$$

The square index can be filled with index *in* in order to make

$$\bar{A}_{in} = I_{m-1} \otimes A, \tag{5.19}$$

$$\bar{B}_{i,in}(\theta_t) = -\bar{L}_{a,i}(\theta_t) \otimes (BK), \tag{5.20}$$

$$\sum_{i=1}^{m} \bar{B}_{i,in}(\theta_t) = \bar{B}_{in}(\theta_t) = -\bar{L}(\theta_t) \otimes (BK), \tag{5.21}$$

for input delays, or with index *comm* giving

$$\bar{A}_{comm} = I_{m-1} \otimes (A - BK), \tag{5.22}$$

$$\sum_{k=1}^{r} \bar{B}_{k,comm}(\theta_t) = \bar{B}_{comm}(\theta_t) = (I_{m-1} - \bar{L}(\theta_t)) \otimes BK, \tag{5.23}$$

for communication delays, where (5.19)–(5.23) are analogous to (4.6)–(4.10), with the introduction of term θ_t.

Remark 5.2 *For the analysis with communication delays, all the possible graphs that the multiagent system can assume must satisfy Assumption 2.2, and the time-varying delays have to be considered uniform, i.e.* $\tau_k(t) = \tau(t)$ *(Assumption 2.1), in order to the tree-type transformation to be satisfied.*

Based on the disagreement of the state variables, consensus on system (5.12) is assessed by establishing stability of the transformed system in (5.18). In this context, Definition 5.2 can be rewritten as follows:

Definition 5.3 *Under stochastic switching topology, the closed-loop multiagent system in* (5.12)*, reaches mean-square consensus if the transformed system* (5.18) *is stochastically stable in the mean-square sense, i.e.:*

$$\lim_{t\to\infty} \mathbb{E}[z^T(t)z(t)] = 0 \tag{5.24}$$

holds in mean square sense for any initial distribution of the Markov chain and initial state conditions.

Remark 5.3 *For simplicity in the notation of the stochastic variables, the dependency on the argument θ_t will be denoted by the subscript index ℓ, when no confusion can arise. For example, a matrix $M(\theta_t)$ will be denoted simply by M_ℓ.*

5.2 Consensus analysis

The main result of this chapter is stated in the next theorem. This theorem gives new sufficient conditions to verify consensus of a specified multiagent system with linear dynamics and, possibly, switching topology and time-varying delays. The only restriction about the topologies is that they switch accordingly as a specified Markov chain switches from one state to another. The time-delays can be regarded as communication or input delays.

Theorem 5.1 *Consider the closed-loop multiagent system in* (5.12) *with $\tau > 0$, $\tau \geq \mu_m \geq 0$, and Π defined as in* (5.9)*, whose $\epsilon_{pq} \in [-\delta_{pq},\ \delta_{pq}]$ with $\delta_{pq} > 0\ \forall\ p, q \in \mathcal{S}$, and multiple time-delays $\tau_k(t) \in [\tau - \mu_m, \tau + \mu_m]$, for $k = 1, 2, ..., m$. For communication delay it is considered $\tau_k(t) = \tau(t)$ and all the topologies to be regular. Then, the multiagent system* (5.12) *achieves consensus in the mean-square sense if there exist $n(m-1)\times n(m-1)$ matrices F_ℓ, G_ℓ, $P_{1\ell} = P_{1\ell}^T$, $P_{2\ell}$, $P_{3\ell} = P_{3\ell}^T$, $Q = Q^T > 0$, $R = R^T > 0$, $S = S^T > 0$, and $Z = Z^T > 0$, such that the following LMIs hold $\forall \ell = 1, 2, ..., s$:*

$$\begin{bmatrix} P_{1\ell} & P_{2\ell} \\ * & P_{3\ell} \end{bmatrix} > 0, \tag{5.25}$$

and

$$\begin{bmatrix} \Phi_\ell & \mu_m\Gamma_\ell \\ * & -\mu_m Z \end{bmatrix} < 0, \tag{5.26}$$

where

$$\Phi_\ell = \Phi_{P\ell} + \Phi_Z + \Phi_R + \Phi_{QS} + \Phi_{FG\ell}, \tag{5.27}$$

and

$$\Gamma_\ell = \begin{bmatrix} F_\ell \bar{B}_\square(\ell) \\ G_\ell \bar{B}_\square(\ell) \\ 0 \\ 0 \end{bmatrix}, \tag{5.28}$$

with

$$\Phi_{P\ell} = \begin{bmatrix} P_{2\ell} + P_{2\ell}^T + \Sigma_{\pi\delta}(P_{1q}) & P_{1\ell} & -P_{2\ell} & P_{3\ell} + \Sigma_{\pi\delta}(P_{2q}) \\ * & 0 & 0 & P_{2\ell} \\ * & * & 0 & -P_{3\ell} \\ * & * & * & \Sigma_{\pi\delta}(P_{3q}) \end{bmatrix}, \tag{5.29}$$

where $\Sigma_{\pi\delta}(\cdot)$ is a matrix function such that, for any matrix M_q, $\Sigma_{\pi\delta}(M_q) = \sum_{q=1}^{s} \pi_{\ell q} M_q + \sum_{q=1}^{s} \frac{5\delta_{\ell q}}{4} M_q$,

$$\Phi_Z = \begin{bmatrix} 0 & 0 & 0 & 0 \\ * & 2\mu_m Z & 0 & 0 \\ * & * & 0 & 0 \\ * & * & * & 0 \end{bmatrix}, \quad \Phi_R = \begin{bmatrix} -\frac{4}{\tau} R & 0 & -\frac{2}{\tau} R & \frac{6}{\tau^2} R \\ * & \tau R & 0 & 0 \\ * & * & -\frac{4}{\tau} R & \frac{6}{\tau^2} R \\ * & * & * & -\frac{12}{\tau^3} R \end{bmatrix}, \tag{5.30}$$

$$\Phi_{QS} = \begin{bmatrix} Q - 2S & 0 & 0 & \frac{2}{\tau} S \\ * & \frac{\tau^2}{2} S & 0 & 0 \\ * & * & -Q & 0 \\ * & * & * & -\frac{2}{\tau^2} S \end{bmatrix}, \tag{5.31}$$

and

$$\Phi_{FG\ell} = \begin{bmatrix} -F_\ell \bar{A}_\square - \bar{A}_\square^T F_\ell^T & F_\ell - \bar{A}_\square^T G_\ell^T & -F_\ell \bar{B}_\square(\ell) & 0 \\ * & G_\ell + G_\ell^T & -G_\ell \bar{B}_\square(\ell) & 0 \\ * & * & 0 & 0 \\ * & * & * & 0 \end{bmatrix}. \tag{5.32}$$

Proof First, it is shown that if the proposed LMIs hold, then the inequalities $V(z_t, \ell) > 0$ and $\mathcal{L}V(z_t, \ell) < 0$ are satisfied, where $\mathcal{L}$ is the infinitesimal generator operator given in Definition 2.2, and $V(z_t, \ell)$ is the following Lyapunov–Krasovskii stochastic functional:

$$V(z_t, \ell) = V_1(z_t, \ell) + V_2(z_t) + V_3(z_t) + V_4(z_t) + V_5(z_t), \tag{5.33}$$

where z_t corresponds to the state vector $z(\sigma)$ values for σ within the interval $[t-\tau-\mu_m, t]$,

$$V_1(z_t, \ell) = \chi^T(t) P_\ell \chi(t), \tag{5.34}$$

$$V_2(z_t) = \int_{t-\tau}^{t} z^T(\xi) Q z(\xi) d\xi, \tag{5.35}$$

$$V_3(z_t) = \int_{-\tau}^{0} \int_{t+\zeta}^{t} \dot{z}^T(\xi) R \dot{z}(\xi) d\xi d\zeta, \tag{5.36}$$

$$V_4(z_t) = \int_{-\tau}^{0} \int_{\theta}^{0} \int_{t+\zeta}^{t} \dot{z}^T(\xi) S \dot{z}(\xi) d\xi d\zeta d\theta, \tag{5.37}$$

$$V_5(z_t) = \int_{-\mu_m}^{\mu_m} \int_{t-\tau+\zeta}^{t} \dot{z}^T(\xi) Z \dot{z}(\xi) d\xi d\zeta, \tag{5.38}$$

with $\chi^T(t) = [z^T(t) \quad \int_{t-\tau}^{t} z^T(\xi) d\xi]$, and there exist some real matrices

$$P_\ell = \begin{bmatrix} P_{1\ell} & P_{2\ell} \\ * & P_{3\ell} \end{bmatrix} = P_\ell^T,$$

$Q = Q^T$, $R = R^T$, $S = S^T$, and $Z = Z^T$.

To satisfy the condition $V(z_t, \ell) > 0$, assume each matrix variable in each term of (5.33) to be positive definite: $P_\ell > 0$, as in LMI (5.25); $Q > 0$; $R > 0$; $S > 0$; and $Z > 0$. If these conditions are satisfied, then $V(z_t, \ell) > 0$.

Next, it is shown the LMI condition to guarantee $\mathcal{L}V(z_t, \ell) < 0$. Initially, consider the following null term (Mozelli et al., 2010; Souza et al., 2008), with procedure similar to the one presented in Chapter 4, derived from the system's equation (5.18):

$$0 = 2\Lambda_\ell(t) \left[\dot{z} - \bar{A}_\square z(t) - \sum_{k=1}^{m} \bar{B}_{k\square}(\ell) z(t - \tau_k(t)) \right] \tag{5.39}$$

$$= 2\Lambda_\ell(t) \left[\dot{z} - \bar{A}_\square z(t) - \sum_{k=1}^{m} \bar{B}_{k\square}(\ell) \left(z(t-\tau) - \int_{-\tau_k(t)}^{-\tau} \dot{z}(t+\xi) d\xi \right) \right] \tag{5.40}$$

$$= 2\Lambda_\ell(t) \left[\dot{z}(t) - \bar{A}_\square z(t) - \sum_{k=1}^{m} \bar{B}_{k\square}(\ell) z(t-\tau) \right] + v_\ell(t), \tag{5.41}$$

with

$$v_\ell(t) = \sum_{k=1}^{m} \int_{-\tau_k(t)}^{-\tau} 2\Lambda_\ell(t) \bar{B}_{k\square}(\ell) \dot{z}(t+\xi) d\xi, \tag{5.42}$$

$\Lambda_\ell(t) = [z^T(t) F_\ell + \dot{z}^T(t) G_\ell]$, and F_ℓ and G_ℓ with appropriate dimensions.

Then, applying the inequality $2a^T b \leq a^T X a + b^T X^{-1} b$ in (5.42), where a^T and b are the vectors $\Lambda_\ell(t)\bar{B}_{k\square}(\ell)$ and $\dot{z}(t+\xi)$, respectively, and X is a positive definite matrix

chosen $\frac{Z}{m}$, it gives

$$\begin{aligned} v_\ell(t) \leq & \sum_{k=1}^{m} \int_{-\tau_k(t)}^{-\tau} (\Lambda_\ell(t)\bar{B}_{k\square}(\ell)) m Z^{-1} (\Lambda_\ell(t)\bar{B}_{k\square}(\ell))^T d\xi \\ & + \sum_{k=1}^{m} \int_{-\tau_k(t)}^{-\tau} \dot{z}^T(t+\xi)\frac{Z}{m}\dot{z}(t+\xi)d\xi \\ & \leq \sum_{k=1}^{m} (\Lambda_\ell(t)\bar{B}_{k\square}(\ell))\mu_m m Z^{-1} (\Lambda_\ell(t)\bar{B}_{k\square}(\ell))^T + \int_{t-\tau-\mu_m}^{t-\tau+\mu_m} \dot{z}^T(\xi) Z \dot{z}(\xi) d\xi. \end{aligned} \tag{5.43}$$

Replace (5.43) in (5.39) to obtain

$$\begin{aligned} 0 \leq & -2z^T(t)F_\ell \dot{z}(t) + 2z^T(t)F_\ell \bar{A}_{\square} z(t) - 2\dot{z}^T(t)G_\ell \dot{z}(t) + 2\dot{z}^T(t)G_\ell \bar{A}_{\square} z(t) \\ & - 2z^T(t)F_\ell \sum_{k=1}^{m} \bar{B}_{k\square}(\ell) z(t-\tau) - 2\dot{z}^T(t)G_\ell \sum_{k=1}^{m} \bar{B}_{k\square}(\ell) z(t-\tau) \\ & + \sum_{k=1}^{m} \mu_m (\Lambda_\ell(t)\bar{B}_{k\square}(\ell)) m Z^{-1} (\Lambda_\ell(t)\bar{B}_{k\square}(\ell))^T + \int_{t-\tau-\mu_m}^{t-\tau+\mu_m} \dot{z}^T(\xi) Z \dot{z}(\xi) d\xi. \end{aligned} \tag{5.44}$$

Moreover, invoking the operator $\mathcal{L}$ of infinitesimal generator in the functional in (5.33), yields

$$\mathcal{L}V(z_t, \ell) = \mathcal{L}V_1(z_t, \ell) + \mathcal{L}V_2(z_t) + \mathcal{L}V_3(z_t) + \mathcal{L}V_4(z_t) + \mathcal{L}V_5(z_t). \tag{5.45}$$

The term $\mathcal{L}V_1(z_t, \ell)$ is given by:

$$\begin{aligned} \mathcal{L}V_1(z_t, \ell) &= 2\dot{\chi}^T(t)P_\ell \chi(t) + \chi^T(t)\left[\sum_{q=1}^{s} (\pi_{\ell q} + \epsilon_{\ell q})P_q\right]\chi(t), \\ &= 2\dot{\chi}^T(t)P_\ell \chi(t) + \chi^T(t)\left(\sum_{q=1}^{s} \pi_{\ell q} P_q\right)\chi(t) + \chi^T(t)\left(\sum_{q=1}^{s} \epsilon_{\ell q} P_q\right)\chi(t). \end{aligned} \tag{5.46}$$

By Lemma 2.7, it is given that:

$$\begin{aligned} \chi^T(t)\left(\sum_{q=1}^{s} \epsilon_{\ell q} P_q\right)\chi(t) &= \chi^T(t)\left[\sum_{q=1}^{s} \frac{1}{2}\epsilon_{\ell q}(P_q + P_q)\right]\chi(t), \\ &\leq \chi^T(t)\sum_{q=1}^{s}\left[\left(\frac{\epsilon_{\ell q}}{2}\right)^2 N + P_q N^{-1} P_q\right]\chi(t). \end{aligned} \tag{5.47}$$

Since $\epsilon_{\ell q} \in [-\delta_{\ell q},\ \delta_{\ell q}]$, thus $\epsilon_{\ell q}^2 \leq \delta_{\ell q}^2$, such that

$$\chi^T(t)\left(\sum_{q=1}^{s} \epsilon_{\ell q} P_q\right)\chi(t) \leq \chi^T(t)\sum_{q=1}^{s}\left(\frac{\delta_{\ell q}^2}{4} N + P_q N^{-1} P_q\right)\chi(t). \tag{5.48}$$

Choosing $N = \frac{1}{\delta_{\ell q}} P_q$, since P_q is assumed to be positive-definite $\forall q = 1, ..., s$, it gives

$$\begin{aligned}\chi^T(t)\left(\sum_{q=1}^{s}\epsilon_{\ell q}P_q\right)\chi(t) &\leq \chi^T(t)\sum_{q=1}^{s}\left[\frac{\delta_{\ell q}}{4}P_q + \delta_{\ell q}P_q\right]\chi(t)\\ &\leq \chi^T(t)\left(\sum_{q=1}^{s}\frac{5\delta_{\ell q}}{4}P_q\right)\chi(t). \end{aligned} \tag{5.49}$$

Then, $\mathcal{L}V_1(z(t), \ell)$ can be written as

$$\mathcal{L}V_1(z_t, \ell) \leq 2\dot{\chi}^T(t)P_\ell\chi(t) + \chi^T(t)\left(\sum_{q=1}^{s}\pi_{\ell q}P_q\right)\chi(t) + \chi^T(t)\left(\sum_{q=1}^{s}\frac{5\delta_{\ell q}}{4}P_q\right)\chi(t). \tag{5.50}$$

The next terms are given by

$$\mathcal{L}V_2(z_t) = z^T(t)Qz(t) - z^T(t-\tau)Qz(t-\tau), \tag{5.51}$$

$$\mathcal{L}V_3(z_t) = \tau\dot{z}^T(t)R\dot{z}(t) - \int_{t-\tau}^{t}\dot{z}^T(\xi)R\dot{z}(\xi)d\xi, \tag{5.52}$$

and with $R > 0$ Lemma 2.6 can be applied to yield

$$\mathcal{L}V_3(z_t) \leq \tau\dot{z}^T(t)R\dot{z}(t) - \frac{1}{\tau}\int_{t-\tau}^{t}\dot{z}^T(\xi)d\xi R\int_{t-\tau}^{t}\dot{z}(\xi)d\xi - \frac{3}{\tau}\tilde{\Omega}^T R\tilde{\Omega}, \tag{5.53}$$

with $\tilde{\Omega}$ given as Ω in (2.83) replacing a by $t-\tau$ and b by t.

For $\mathcal{L}V_4(z_t)$:

$$\mathcal{L}V_4(z_t) = \frac{\tau^2}{2}\dot{z}^T(t)S\dot{z}(t) - \int_{-\tau}^{0}\int_{t+\zeta}^{t}\dot{z}^T(\xi)S\dot{z}(\xi)d\xi d\zeta, \tag{5.54}$$

and with $S > 0$ Lemma 2.5 can be applied, giving

$$\begin{aligned}\mathcal{L}V_4(z_t) \leq &\frac{\tau^2}{2}\dot{z}^T(t)S\dot{z}(t) - 2z^T(t)Sz(t)\\ &+ \frac{4}{\tau}z^T(t)S\int_{t-\tau}^{t}z(\xi)d\xi - \frac{2}{\tau^2}\int_{t-\tau}^{t}z^T(\xi)d\xi S\int_{t-\tau}^{t}z(\xi)d\xi. \end{aligned} \tag{5.55}$$

Finally, for $\mathcal{L}V_5(z_t)$:

$$\mathcal{L}V_5(z_t) = 2\mu_m\dot{z}^T(t)Z\dot{z}(t) - \int_{t-\tau-\mu_m}^{t-\tau+\mu_m}\dot{z}^T(\xi)Z\dot{z}(\xi)d\xi. \tag{5.56}$$

Adding the null-term in (5.44) to the $\mathcal{L}$-infinitesimal of the functional in (5.45), and replacing $\mathcal{L}V_1(z_t)$, $\mathcal{L}V_3(z_t)$, and $\mathcal{L}V_4(z_t)$ by the upper bounds (5.50), (5.53), and (5.55), respectively, gives

$$\mathcal{L}V(z_t, \ell) \leq \Upsilon^T\Phi_\ell\Upsilon + \sum_{k=1}^{m}\mu_m(\Lambda_\ell(t)\bar{B}_{k\square}(\ell))mZ^{-1}(\Lambda_\ell(t)\bar{B}_{k\square}(\ell))^T, \tag{5.57}$$

where $\Upsilon^T = \begin{bmatrix} z^T(t) & \dot{z}^T(t) & z(t-\tau) & \int_{t-\tau}^{t} z(\xi)d\xi \end{bmatrix}$ and Φ_ℓ as defined in (5.27).

Note that $\Lambda_\ell(t)\bar{B}_{k,\square}(\ell) = \Upsilon^T(t)\Gamma_{k\ell}$ with

$$\Gamma_{k\ell} = \begin{bmatrix} F_\ell \bar{B}_{k,\square}(\ell) \\ G_\ell \bar{B}_{k,\square}(\ell) \\ 0 \\ 0 \end{bmatrix}. \tag{5.58}$$

Thus, (5.57) can be written as

$$\begin{aligned} \mathcal{L}V(z_t,\ell) &\leq \Upsilon^T \Phi_\ell \Upsilon + \sum_{k=1}^{m} \mu_m \Upsilon^T \Gamma_{k\ell} m Z^{-1} \Gamma_{k\ell}^T \Upsilon, \\ &\leq \Upsilon^T \left(\sum_{k=1}^{m} \left(\frac{1}{m}\Phi_\ell + \mu_m \Gamma_{k\ell} m Z^{-1} \Gamma_{k\ell}^T \right) \right) \Upsilon. \end{aligned} \tag{5.59}$$

In order to guarantee $\mathcal{L}V(z_t,\ell) < 0$ for any $\Upsilon \neq 0$, the matrix between the larger parentheses in (5.59) must be imposed negative. Thus, applying Schur's complement, it gives

$$\sum_{k=1}^{m} \begin{bmatrix} \frac{1}{m}\Phi_\ell & \mu_m \Gamma_{k\ell} \\ * & -\frac{\mu_m}{m} Z \end{bmatrix} = \begin{bmatrix} \Phi_\ell & \mu_m \Gamma_\ell \\ * & -\mu_m Z \end{bmatrix} < 0 \tag{5.60}$$

where $\Gamma_\ell = \sum_{k=1}^{m} \Gamma_{k\ell}$, leading to the inequality in (5.26). If $R > 0$, $S > 0$, and the LMI in (5.26) holds, then the $\mathcal{L}$-infinitesimal condition $\mathcal{L}V(z_t,\ell) < 0$ is satisfied.

Finally, assume that the LMIs (5.25) and (5.26) hold, then $V(z_t,\ell) > 0$ and

$$\mathcal{L}V(z_t,\ell) \leq -\rho z^T(t) z(t), \tag{5.61}$$

for some sufficiently small $\rho > 0$. Applying the expectancy, it is obtained: $\mathbb{E}[V(z_t,\ell)] > 0$ and

$$\mathbb{E}[\mathcal{L}V(z_t,\ell)] \leq -\rho \mathbb{E}[z^T(t) z(t)]. \tag{5.62}$$

Then, applying the Dynkin's formula (Definition 2.3), which can be seen as an stochastic extension of the second fundamental theorem of calculus, it yields

$$\begin{aligned} \mathbb{E}\left[V(z_t,\ell)\right] - V(z(0),\ell_0) &= \int_0^t \mathbb{E}\left[\mathcal{L}V(z(\xi),\ell)\right] d\xi, \\ &\leq -\rho \int_0^t \mathbb{E}\left[z^T(\xi) z(\xi)\right] d\xi, \end{aligned} \tag{5.63}$$

where ℓ_0 is the arbitrary initial topology at $t = 0$. Thus,

$$\rho \int_0^t \mathbb{E}\left[z^T(\xi)z(\xi)\right] d\xi < V(z(0), \ell_0) - \mathbb{E}\left[V(z_t, \ell)\right]$$
$$\int_0^t \mathbb{E}\left[z^T(\xi)z(\xi)\right] d\xi < \frac{1}{\sigma} V(z(0), \ell_0). \tag{5.64}$$

which implies $\lim_{t\to\infty} \mathbb{E}[z^T(t)z(t)] \to 0$, meaning that (5.18) is stochastic asymptotically stable in the mean-square sense. Consequently, system (5.12) achieves consensus according to Definition 5.3. This completes the proof. □

When the time-delays are considered to be constant, i.e $\mu_m = 0$ like in Corollary 4.1 for static topology, the following corollary can be derived from Theorem 5.1.

Corollary 5.1 *Consider the closed-loop multiagent system in* (5.12) *with* $\tau > 0$ *and* Π *defined as in* (5.9)*, whose* $\epsilon_{pq} \in [-\delta_{pq},\ \delta_{pq}]$ *with* $\delta_{pq} > 0\ \forall\ p, q \in \mathcal{S}$*, and all* $\tau_k(t) = \tau$*, for* $k = 1, 2, ..., m$*. Then, the multiagent system* (5.12) *achieves consensus in the mean-square sense if there exist* $n(m-1) \times n(m-1)$ *matrices* F_ℓ*,* G_ℓ*,* $P_{1\ell} = P_{1\ell}^T$*,* $P_{2\ell}$*,* $P_{3\ell} = P_{3\ell}^T$*,* $Q = Q^T > 0$*,* $R = R^T > 0$*, and* $S = S^T > 0$*, such that the LMIs* (5.25) *and* $\bar{\Phi} < 0$ *hold* $\forall \ell = 1, 2, ..., s$*, where* $\bar{\Phi}_\ell = \Phi_{P\ell} + \Phi_R + \Phi_{QS} + \Phi_{FG\ell}$ *given as in* (5.27)*.*

Proof The proof follows from Theorem 5.1 making $\mu_m = 0$ such that, in (5.59), $\Phi_\ell < 0$ is sufficient to guarantee $\mathcal{L}V(z_t, \ell) < 0$. Additionally, since $\mu_m = 0$ the term with Z vanishes, which gives $\bar{\Phi}_\ell = \Phi_\ell - \Phi_Z < 0$, or $\bar{\Phi}_\ell = \Phi_{P\ell} + \Phi_R + \Phi_{QS} + \Phi_{FG\ell}$. This completes the proof. □

5.3 Numerical Example

A numerical example is presented to illustrate the applicability of Theorem 5.1 and Corollary 5.1. In order to show that the method can indeed provide interesting results in practical problems, consider the following scenario: a team of three networked quadrotors coordinating themselves with the objective of reaching formation on one of its coordinate axis, in relation to a given inertial frame assuming intermittent communication caused by links that drop unexpectedly.

Initially, assume the dynamics free of delays. The quadrotors are assumed with the same second order model described by Michael et al. (2010); Schwager et al. (2011), but also considering switching topology:

$$\ddot{p}_i(t) + b\dot{p}_i(t) + cp_i(t) = \bar{u}_i(\theta_t), \tag{5.65}$$

where $p_i(t)$ is the position of the quadrotor along the axis in which formation is desired, and b and c are the damping and spring constants, respectively. Equation (5.65) can be compactly written in state space as

$$\begin{bmatrix}\dot{p}_i(t)\\ \ddot{p}_i(t)\end{bmatrix} = \begin{bmatrix}0 & 1\\ -c & -b\end{bmatrix}\begin{bmatrix}p_i(t)\\ \dot{p}_i(t)\end{bmatrix} + \begin{bmatrix}0\\ 1\end{bmatrix}\bar{u}_i(\theta_t). \tag{5.66}$$

In order to analyze this problem by the proposed methodology, the formation problem is rewritten as a consensus one using the distributed control law

$$\bar{u}_i(\theta_t, t) = c\alpha_i - \sum_{j\neq i, j=1}^{m} a_{ij}(\theta_t)k_q\big(p_i(t) - \alpha_i - p_j(t) + \alpha_j\big), \tag{5.67}$$

where α_i and α_j are used to compute the desired constant distance between the j-th and i-th agents as $\alpha_{j,i} = \alpha_j - \alpha_i$, and k is the control gain. Replacing (5.67) into (5.66), the system can be reformulated as

$$\begin{bmatrix}\dot{p}_i(t)\\ \ddot{p}_i(t)\end{bmatrix} = \begin{bmatrix}0 & 1\\ -c & -b\end{bmatrix}\begin{bmatrix}p_i(t) - \alpha_i\\ \dot{p}_i(t)\end{bmatrix} + \begin{bmatrix}0\\ 1\end{bmatrix}u_i(\theta_t) \tag{5.68}$$

with

$$u_i(\theta_t, t) = -\sum_{j\neq i, j=1}^{m} a_{ij}(\theta_t)\begin{bmatrix}k_q & 0\end{bmatrix}\left(\begin{bmatrix}p_i(t) - \alpha_i\\ \dot{p}_i(t)\end{bmatrix} - \begin{bmatrix}p_j(t) - \alpha_j\\ \dot{p}_j(t)\end{bmatrix}\right). \tag{5.69}$$

The previous two equations are in the same format of (5.4) and (5.5), respectively, by making

$$x_i(t) = \begin{bmatrix}p_i(t) - \alpha_i\\ \dot{p}_i(t)\end{bmatrix}, \tag{5.70}$$

such that A, B, and K matrices in (5.4) are equivalent to $\begin{bmatrix}0 & 1\\ -c & -b\end{bmatrix}$, $\begin{bmatrix}0\\ 1\end{bmatrix}$, and $\begin{bmatrix}k_q & 0\end{bmatrix}$, respectively. For input and communication delays, matrices A, B and K in (5.6) can be obtained similarly to the procedure above.

With the definitions of A, B and K, the transformed system, with both input or communication delays, can be written according to (5.18). Thus, Theorem 5.1 and Corollary (5.1) can be applied. In the following example, it is considered $b = 1$, $c = 0$, and $k_q = 1$.

Intermittent communication is modeled with a directed network topology switching between two topologies: $\mathcal{G}_1$ and $\mathcal{G}_2$. These topologies are illustrated in Figure 5.1 for input-delays, where the arrows indicate the existing communication channels in each case and $\tau_i(t)$ is the value of the associated time delay, and in Figure 5.2, with regular graphs

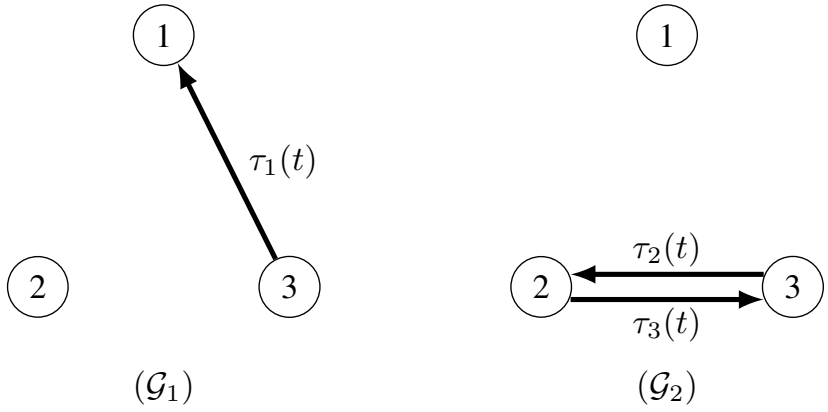

Figure 5.1: Multi-agent system subject to input delays $\tau_i(t)$, composed of three agents with switching topologies $\mathcal{G}_1$ and $\mathcal{G}_2$.

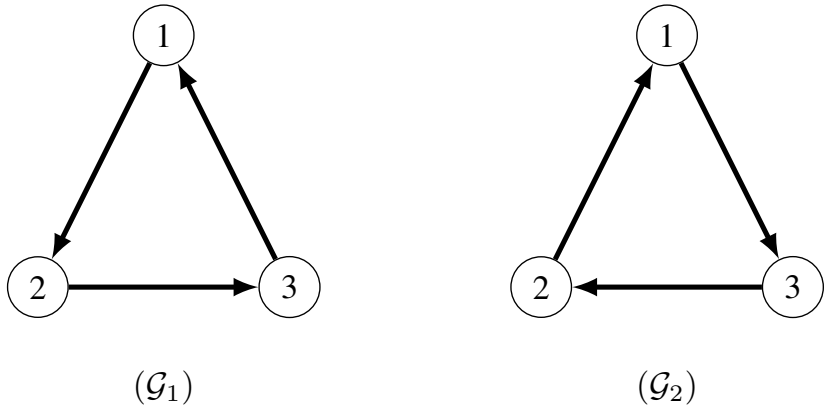

Figure 5.2: Multi-agent system subject to communication delays $\tau(t)$, composed of three agents with switching topologies $\mathcal{G}_1$ and $\mathcal{G}_2$.

according to Assumption 2.2 and uniform communication delays $\tau(t)$ from Assumption 2.1. The Laplacians for $\mathcal{G}_1$ and $\mathcal{G}_2$ in Figure 5.1 with unitary weights are:

$$L_1 = \begin{bmatrix} 1 & 0 & -1 \\ 0 & 0 & 0 \\ 0 & 0 & 0 \end{bmatrix} \quad \text{and} \quad L_2 = \begin{bmatrix} 0 & 0 & 0 \\ 0 & 1 & -1 \\ 0 & -1 & 1 \end{bmatrix}. \tag{5.71}$$

Similarly, the Laplacians for $\mathcal{G}_1$ and $\mathcal{G}_2$ in Figure 5.2 are:

$$L_1 = \begin{bmatrix} 1 & 0 & -1 \\ -1 & 1 & 0 \\ 0 & -1 & 1 \end{bmatrix} \quad \text{and} \quad L_2 = \begin{bmatrix} 1 & -1 & 0 \\ 0 & 1 & -1 \\ -1 & 0 & 1 \end{bmatrix}. \tag{5.72}$$

Notice the important fact that this system would never be able to achieve consensus if the topology were fixed at either $\mathcal{G}_1$ or $\mathcal{G}_2$ in Figure 5.1, for input-delays, since none of

these graphs contains a spanning tree. However, the joint graph of the stochastic switch between the two topologies makes consensus possible.

Suppose the transition rates not precisely known but modeled by $\pi_{pq} = 1$, $\forall(p \neq s)$, $p, q \in \mathcal{S}$ and uncertainty $\epsilon_{pq} = \pm 0.25$, $\forall\ p, q \in \mathcal{S}$, such that

$$\Pi = \begin{bmatrix} -1 \pm 0.25 & 1 \pm 0.25 \\ 1 \pm 0.25 & -1 \pm 0.25 \end{bmatrix}. \tag{5.73}$$

In the remainder, the application of the results in this chapter is illustrated in various scenarios.

First consider the case of constant and uniform time-delays, i.e, $\mu_m = 0$. In order to find the upper bound for the delay, a search for the highest value of τ guaranteeing the feasibility of LMIs in Corollary 5.1 is made, both for input and communication delays. The maximum value on which the LMIs hold for input delays is $\tau = 0.274$, and for communication delays is $\tau = 0.731$.

Next, it is considered the case with input time-varying delays. For given values of τ, a search is made for the highest value of μ_m satisfying Theorem 5.1. Results are summarized in Table 5.1. Notice that $--$ stands for unfeasibility.

Table 5.1: Largest μ_m obtained for given τ

	τ	0.100	0.200	0.300	0.400	0.500	0.600
Input delay (Fig. 5.1)	μ_m	0.100	0.059	$--$	$--$	$--$	$--$
Comm. delay (Fig. 5.2)	μ_m	0.100	0.200	0.207	0.158	0.111	0.063

Finally, the values of τ and μ_m are chosen for different pairs, with transition rates $\pi_{pq} = \bar{\pi}$ $(\forall\ p, q \in \mathcal{S})$, in order to search for common largest interval bound, $\delta_{pq} = \bar{\delta}$ $(\forall\ p, q \in \mathcal{S})$, for the uncertain transition rates in (5.9) that satisfy Theorem 5.1. This search is performed for various triplets $(\tau, \mu_m, \bar{\pi})$ and the results are summarized in Table 5.2.

Table 5.2: Largest $\bar{\delta}$ obtained for given $(\tau, \mu_m, \bar{\pi})$

$(\tau, \mu_m, \bar{\pi})$	$(0.15, 0.10, 0.5)$	$(0.15, 0.10, 1)$	$(0.15, 0.10, 2)$
Input delay (Fig. 5.1)	0.14	0.25	0.47
Comm. delay (Fig. 5.2)	0.50	0.81	1.27

For illustration, a simulation of the state trajectories for $p_i(t)$ and $\dot{p}_i(t)$, for all the agents, is shown in Figure 5.3 for the multiagent system with input-delays switching

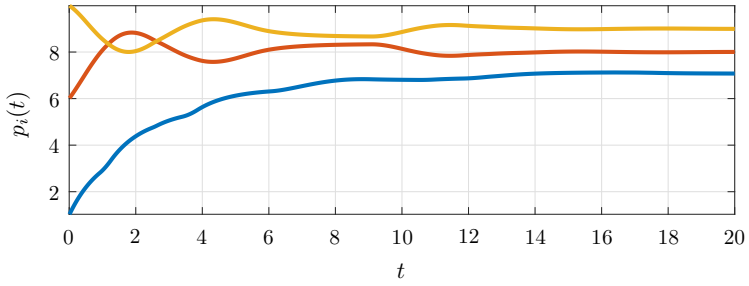

(a) State trajectories for $p_i(t)$.

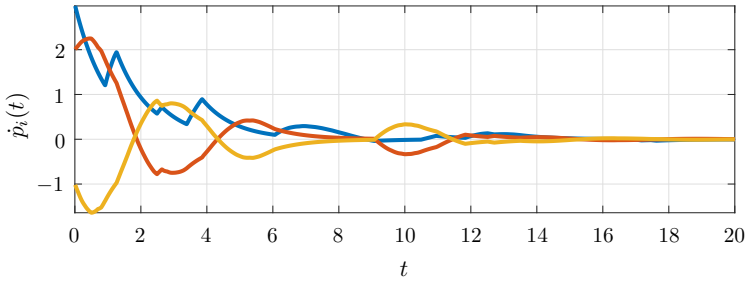

(b) State trajectories for $\dot{p}_i(t)$.

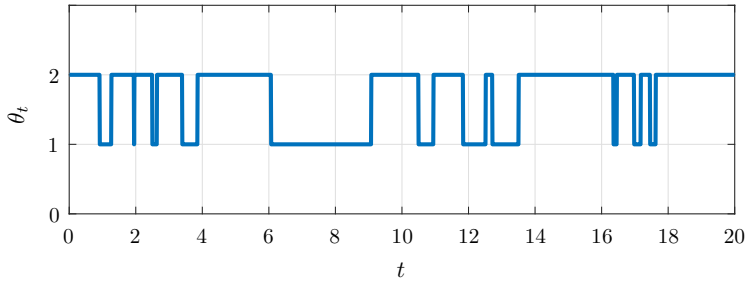

(c) State of the switching topology θ_t, $\mathcal{G}_1$ and $\mathcal{G}_2$, for $\theta_t = 1$ and $\theta_t = 2$, respectively.

Figure 5.3: Simulation with time-varying delay and switching topologies with $\tau = 0.15$ and $\mu_m = 0.10$.

between $\mathcal{G}_1$ and $\mathcal{G}_2$ in Figure 5.1. It is considered the desired displacements between the agents defined by $\alpha_1 = 1$, $\alpha_2 = 2$, and $\alpha_3 = 3$, i.e., $\alpha_{2,1} = 1$, $\alpha_{3,1} = 2$ and $\alpha_{3,2} = 1$. The initial conditions are $p_1(0) = 0$, $p_2(0) = 4$, and $p_3(0) = 7$ for the position, and $\dot{p}_1(0) = 3$, $\dot{p}_2(0) = 2$, and $\dot{p}_3(0) = -1$ for the velocity. The bottom plot in Figure 5.3 shows the switching behavior of θ_t which governs the switch between the topologies $\mathcal{G}_1$ and $\mathcal{G}_2$ (see Figure 5.1). The topology $\mathcal{G}_1$ is active when $\theta_t = 1$ and the topology $\mathcal{G}_2$ is active when $\theta_t = 2$. The simulation is performed with input-delays given by the parameters $\tau = 0.15$ and $\mu_m = 0.10$, such that all $\tau_k \in [0.05, 0.25]$. Π is chosen as in (5.73).

This example illustrates that the proposed method can be applied in the verification of consensus of time-delayed systems with linear dynamics also considering an upper and a lower bound for the delay variation. Furthermore, the simulation illustrates how the system converges even when switching from two topologies that have no spanning trees,

as indicated by the analysis. Finally, since the transition rates are only estimates, this method can analyze consensus while considering uncertainties in the transition rates, which allows a more flexible, while still guaranteed, analysis for consensus.

Chapter 6

Design of the Coupling Strengths for Agents with First-Order Integrator Dynamics

This chapter proposes a method that allows the design of the coupling strengths between agents in an arbitrary directed network. The design of the coupling gains helps achieving consensus and also meeting a guaranteed convergence rate. Numerical simulations are provided to demonstrate the effectiveness of the proposed results compared to previous results in the literature. The results presented in this Chapter are part of a book chapter to be published on the series of Advances in Delays and Dynamics, Springer (Savino et al., 2016c).

The design of the weights of the coupling strengths associated to the network communication links, i.e. the choice of a_{ij} related to gain attributed to each agent interaction as in the graph shown in Figure 6.1, has been considered in order to enable consensus or improve overall performance reducing the settling time of the system. In the works of Xiao and Boyd (2004) and Jakovetic et al. (2010) the authors used optimization to adjust these values and improve the convergence rate. An analytical study and design of the coupling strengths considering time-delays is shown by Qiao and Sipahi (2013) for fully connected networks, with a concept based on the placement of the rightmost eigenvalue of the Laplacian. An adaptive approach, based on the availability of the instantaneous value of time-delay, is used by Qiao and Sipahi (2014) to deal with time-varying delays.

This chapter presents a new LMI-based method to solve the problem of designing the coupling strengths in networks of agents with first-order dynamics. A guaranteed exponential convergence rate is considered in order to enable performance improvement. It is considered multiple time-delays in the control inputs, which are assumed to be non-

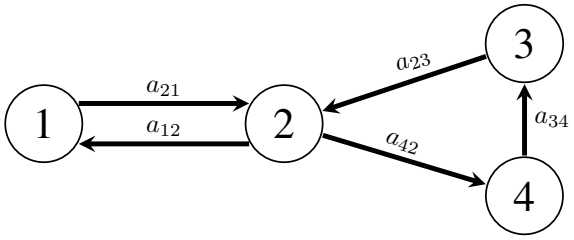

Figure 6.1: Coupling strengths a_{ij} to be designed.

differentiable and nonuniform. Differently from Qiao and Sipahi (2013, 2014) this method does not require fully connected topologies, on the contrary, it can deal with arbitrary directed networks.

Although single-integrator dynamics is considered for each agent in the multiagent system, its applications are vast in the context of mechanical systems described by kinematic models. See examples by Gonçalves et al. (2010), Pimenta et al. (2013), and the models for the mobile manipulators considered in Chapter 7. Numerical examples are given to show the applicability of the proposed method. Besides, the examples show comparable or better results in terms of settling time when compared to related works.

The design of the coupling strengths emerges from the adoption of special cases for matrices F and G presented in Theorems 4.1 and 5.1 for single-order integrator dynamics. It is considered the alternative representation of the Laplacian Matrices written in the alternative form presented as in Lemma 2.2, in order to obtain the designed weights in a diagonal matrix.

6.1 Fixed Topology

For convenience, the model of single-order integrator dynamics with input delays is repeated here:

$$\dot{x}_i(t) = u_i(t - \tau_i(t)), \quad i = 1, 2, \ldots, m, \tag{6.1}$$

$$u_i(t) = -\sum_{j \neq i, j=1}^{m} a_{ij}\big(x_i(t) - x_j(t)\big), \tag{6.2}$$

given in (2.53) and (2.54), respectively, with $x_i \in \mathbb{R}$, $u_i \in \mathbb{R}$, $A = 0$, $B = 1$, and $K = 1$.

Consider the closed-loop dynamics for a fixed topology multi-agent system transformed into a stability problem as in (2.72) in the form

$$\dot{z}(t) = \sum_{i=1}^{m} \bar{L}_{a,i} z(t - \tau_i(t)), \tag{6.3}$$

where $\bar{L}_{a,i} = UL_{a,i}W$ as in (2.73), with $L_{a,i}$ the Laplacian matrix of the subgraph on the i-th agent, as described in Section 2.1, and U and W defined in (2.12) and (2.14), respectively.

Thus, with the following Theorem one is able to design the coupling strengths also considering a convergence rate as a performance requirement to be satisfied.

Theorem 6.1 *Let be given $\tau > 0$, $\tau \geq \mu_m \geq 0$, $\delta > 0$, and g a tuning scalar parameter. Then, the transformed multiagent system in (6.3) with all $\tau_i(t) \in [\tau - \mu_m,\ \tau + \mu_m]$, $i = 1, 2, \ldots, m$, achieves consensus with guaranteed exponential convergence rate δ, if there exist a scalar f and real matrices: $P_1 = P_1^T$, P_2, $P_3 = P_3^T$, $Q = Q^T > 0$, $R = R^T > 0$, $S = S^T > 0$ and $Z = Z^T > 0$, of dimensions $(m-1) \times (m-1)$, such that the following LMIs hold:*

$$\begin{bmatrix} P_1 & P_2 \\ * & P_3 \end{bmatrix} > 0, \tag{6.4}$$

and

$$\begin{bmatrix} \Phi & \mu_m \Gamma \\ * & \frac{-\mu_m}{e_2} Z \end{bmatrix} < 0\ , \tag{6.5}$$

given $e_1 = e^{-2\delta\tau}$, $e_2 = e^{-2\delta(\mu_m+\tau)}$,

$$\Phi = \Phi_P + \Phi_Z + \Phi_R + \Phi_{QS} + \Phi_{FG}, \tag{6.6}$$

and

$$\Gamma = \begin{bmatrix} U\bar{H}\mathcal{W}_d H^T W \\ gU\bar{H}\mathcal{W}_d H^T W \\ 0 \\ 0 \end{bmatrix}, \tag{6.7}$$

with

$$\Phi_P = \begin{bmatrix} 2\delta P_1 + P_2 + P_2^T & P_1 & -P_2 & 2\delta P_2 + P_3 \\ * & 0 & 0 & P_2 \\ * & * & 0 & -P_3 \\ * & * & * & 2\delta P_3 \end{bmatrix}, \tag{6.8}$$

$$\Phi_Z = \begin{bmatrix} 0 & 0 & 0 & 0 \\ * & 2\mu_m Z & 0 & 0 \\ * & * & 0 & 0 \\ * & * & * & 0 \end{bmatrix}, \quad \Phi_R = \begin{bmatrix} -\frac{4e_1}{\tau}R & 0 & -\frac{2e_1}{\tau}R & \frac{6e_1}{\tau^2}R \\ * & \tau R & 0 & 0 \\ * & * & -\frac{4e_1}{\tau}R & \frac{6e_1}{\tau^2}R \\ * & * & * & -\frac{12e_1}{\tau^3}R \end{bmatrix}, \tag{6.9}$$

$$\Phi_{QS} = \begin{bmatrix} Q - 2e_1 S & 0 & 0 & \frac{2e_1}{\tau}S \\ * & \frac{\tau^2}{2}S & 0 & 0 \\ * & * & -e_1 Q & 0 \\ * & * & * & -\frac{2e_1}{\tau^2}S \end{bmatrix}, \tag{6.10}$$

and

$$\Phi_{FG} = \begin{bmatrix} 0 & e_2 f I & -e_2 U\bar{H}\mathcal{W}_d H^T W & 0 \\ * & 2e_2 g f I & -e_2 g U\bar{H}\mathcal{W}_d H^T W & 0 \\ * & * & 0 & 0 \\ * & * & * & 0 \end{bmatrix}. \tag{6.11}$$

Thus, the designed weights a_k of the coupling strengths are given in the diagonal of $\mathcal{W} = \frac{1}{f}\mathcal{W}_d$ and the Laplacian is given by $L = \bar{H}\frac{1}{f}\mathcal{W}_d H^T$ according to Lemma 2.2, where the indices k are given according to Algorithm 2.1.

Proof The proof follows from the results in Theorem 4.1. However, the system is assumed to be of single-order dynamics. In order to keep the problem as an LMI, differently from Theorem 4.1, matrices F and G are chosen to be the scalars f and gf, respectively, with g an arbitrary tuning scalar.

Besides, the Laplacian matrix is written in an alternative form given by Lemma 2.2. Thus, all terms with $F\bar{B}$ and $G\bar{B}$ in Theorem 4.1 become, respectively, $fU\bar{H}\mathcal{W}H^T W$ and $gfU\bar{H}\mathcal{W}H^T W$. Finally, the design procedure is obtained by making the product $f\mathcal{W}$ a single matrix variable $\mathcal{W}_d$. The designed weights of the coupling strengths are thus obtained by making $\mathcal{W} = \frac{1}{f}\mathcal{W}_d$. □

The applicability of Theorem 6.1 is dependent on the prior knowledge of the global topology when the gains are being designed, which is a limitation of the method. However, despite the necessity of global information for design, only local information is used at the execution of the consensus protocols at running time. Moreover, the following remarks discuss some conservatism and complexity related issues of the presented method.

Remark 6.1 *It is known that the introduction of slack variables in LMI conditions can reduce the conservatism of delay dependent conditions, see e.g. Xu and Lam (2005). Therefore, the consideration of f and g as scalars, instead of full matrices, can be seen as a source of conservativeness, imposed in order to keep Theorem 6.1 formulated via LMI conditions. Therefore, a possible strategy to reduce the conservatism of the proposed method is to replace the scalars f and g by full matrices, however such changes lead to bilinear matrix inequality (BMI) conditions. Thus BMI methods as used by Kanev et al. (2004) can be studied in order to relax this source of conservativeness. This method is intended to be studied in a future research.*

6.2 Switching Topology

Consider a multiagent system composed of m single-order agents arranged in a switching directed network. Consider also the dynamics of each agent as in (5.4), with $A = 0$, and $B = 1$, given by

$$\dot{x}_i(t) = u_i(\theta_t, t - \tau_i(t)), \quad i = 1, 2, ..., m, \tag{6.12}$$

where θ_t represents the topology of the multi-agent system at the instant of time t. The considered consensus protocol is given as in (5.5) with $K = 1$, i.e.

$$u_i(\theta_t, t) = -\sum_{j=1}^{n} a_{ij}(\theta_t)\big(x_i(t) - x_j(t)\big). \tag{6.13}$$

Let θ_t be modeled as a continuous time Markov chain as in Section 5.1, where each topology $\ell = 1, 2, \ldots s$ (with s the number of different topologies), is associated with a weighted directed graph $\mathcal{G}(\ell) = (\mathcal{V}, \mathcal{E}(\ell), \mathcal{W})$.

In order to simplify the subscript notation, it is assumed the ordered index k related to each edge, instead of the pair (i, j), such that $e_k(t) = e_{ji}(t)$, letting r represent the total number of directed edges in the Joint Graph $\bar{\mathcal{G}}$, such that $k = 1, \ldots, r$. The assignment of index k is an extension of Algorithm 2.1, outlined in Algorithm 6.1 below with some other useful additional variables.

From Algorithm 6.1, it is defined the Laplacian matrices $L(\ell)$ for each $\mathcal{G}(\ell)$ in which the weights of the edges can be conveniently displayed in the main diagonal of a matrix. This form plays an important role in the design method for switching topologies. Consider the index of each directed edge $e_{ij} \in \bar{\mathcal{E}}$ rewritten according to Algorithm 6.1, such that the edges are ordered as $e_k = e_{ji}$, with associated weights w_k, and vectors $h_k(\ell)$ and $\bar{h}_k(\ell)$ for each $\mathcal{G}(\ell)$. Also $k = 1, \ldots, r$ where r is the number of edges in the Joint Graph $\bar{\mathcal{G}}$. Thus, it is defined the Incidence matrix of each graph $\mathcal{G}(\ell)$ as $H(\ell) = [h_1(\ell) \ \ldots \ h_r(\ell)]$, and

Algorithm 6.1: New indices k

```
Initialize: k ← 0;
forall the i = 1, 2, ..., m do
    forall the j = 1, 2, ..., m do
        if ∃e_ji ∈ Ē, for Ē ∈ Ḡ then
            k ← k + 1;
            w_k ← a_ij;
            e_k ← e_ji;
            forall the ℓ = 1, 2, ..., s do
                h_k(ℓ) ← zero column-vector of size m;
                h̄_k(ℓ) ← zero column-vector of size m;
                if ∃e_ji ∈ E(ℓ) for E ∈ G then
                    h_k(ℓ) i-th entry ← 1;   h_k(ℓ) j-th entry ← −1;
                    h̄_k(ℓ) i-th entry ← 1;
```

also the associated Heading matrix $\bar{H}(\ell) = [\bar{h}_1(\ell) \ \ldots \ \bar{h}_r(\ell)]$, both matrices of dimension $m \times r$. Additionally, the coupling strengths, related to the weights $w_k = w_{ij}$ according to Algorithm 6.1, in a weight diagonal matrix $W \in \Re^{r\times r}$ are written in the ascending order of k. Then, the Laplacian matrix of each graph $\mathcal{G}(\ell)$ can be written according to the following Lemma.

Lemma 6.1 *Let $H(\ell) = [h_1(\ell) \ \ldots \ h_r(\ell)]$ be the $m \times r$ Incidence matrix. Similarly, let $\bar{H}(\ell) = [\bar{h}_1(\ell) \ \ldots \ \bar{h}_r(\ell)]$ be the $m \times r$ associated Heading matrix, and W be the $r \times r$ Weight diagonal matrix associated with a weighted directed graph $\mathcal{G}(\ell)$. Thus, the Laplacian matrix $L(\ell)$ can be written as*

$$L(\ell) = \bar{H}(\ell)\, W H^T(\ell). \tag{6.14}$$

Remark 6.2 *The weights $w_k = w_{ij}$ are given in the main diagonal of W, i.e.*

$$W = \text{diag}\{w_1, w_2, \ldots, w_r\}.$$

Finally, similarly to (5.12), the closed loop dynamics is given by

$$\dot{x}(t) = -\sum_{i=1}^{m} L_{a,i}(\theta_t) x(t - \tau_i(t)), \tag{6.15}$$

with $A_{in} = 0$ and $B_{i,in} = L_{a,i}$ in (5.12), with $L_{a,i}$ the Laplacian matrix of the subgraph on the i-th agent, and θ_t is the stochastic variable indicating the state ℓ of the Markov chain at the instant of time t.

The main result of this chapter is stated in the next theorem. This theorem presents conditions based on linear matrix inequalities. The feasibility of the LMI conditions allows for design of proper coupling strengths to enable consensus.

Theorem 6.2 *Let be given $\tau \geq \mu_m \geq 0$, Π defined as in (5.9), whose $\epsilon_{pq} \in [-\delta_{pq},\ \delta_{pq}]$ with $\delta_{pq} > 0\ \forall\ p, q \in \mathcal{S}$, and g a tuning scalar parameter. Then, the closed-loop multiagent system in (6.15) with multiple input time-delays $\tau_i(t) \in [\tau - \mu_m, \tau + \mu_m]$, for $i = 1, 2, ..., m$, achieves consensus in the mean-square sense with the designed coupling strengths w_k given as in Remark 6.2, if there exist: $(m-1) \times (m-1)$ matrices $P_{1\ell} = P_{1\ell}^T$, $P_{2\ell}$, $P_{3\ell} = P_{3\ell}^T$, $Q = Q^T > 0$, $R = R^T > 0$, $S = S^T > 0$, and $Z = Z^T > 0$; a $r \times r$ diagonal matrix W_d; and a scalar f; such that the following LMIs hold $\forall \ell = 1, 2, ..., s$:*

$$\begin{bmatrix} P_{1\ell} & P_{2\ell} \\ * & P_{3\ell} \end{bmatrix} > 0, \tag{6.16}$$

and

$$\begin{bmatrix} \Phi_\ell & \mu_m \Gamma_\ell \\ * & -\mu_m Z \end{bmatrix} < 0, \tag{6.17}$$

where

$$\Phi_\ell = \Phi_{P\ell} + \Phi_Z + \Phi_R + \Phi_{QS} + \Phi_{FG\ell}, \tag{6.18}$$

and

$$\Gamma_\ell = \begin{bmatrix} fU\bar{H}(\ell)\mathcal{W}H^T(\ell) \\ gfU\bar{H}(\ell)\mathcal{W}H^T(\ell) \\ 0 \\ 0 \end{bmatrix}, \tag{6.19}$$

with

$$\Phi_{P\ell} = \begin{bmatrix} P_{2\ell} + P_{2\ell}^T + \Sigma_{\pi\delta}(P_{1q}) & P_{1\ell} & -P_{2\ell} & P_{3\ell} + \Sigma_{\pi\delta}(P_{2q}) \\ * & 0 & 0 & P_{2\ell} \\ * & * & 0 & -P_{3\ell} \\ * & * & * & \Sigma_{\pi\delta}(P_{3q}) \end{bmatrix}, \tag{6.20}$$

where $\Sigma_{\pi\delta}(\cdot)$ *is a matrix function such that, for any matrix* M_q, $\Sigma_{\pi\delta}(M_q) = \sum_{q=1}^{s} \pi_{\ell q} M_q + \sum_{q=1}^{s} \frac{5\delta_{\ell q}}{4} M_q$,

$$\Phi_Z = \begin{bmatrix} 0 & 0 & 0 & 0 \\ * & 2\mu_m Z & 0 & 0 \\ * & * & 0 & 0 \\ * & * & * & 0 \end{bmatrix}, \quad \Phi_R = \begin{bmatrix} -\frac{4}{\tau}R & 0 & -\frac{2}{\tau}R & \frac{6}{\tau^2}R \\ * & \tau R & 0 & 0 \\ * & * & -\frac{4}{\tau}R & \frac{6}{\tau^2}R \\ * & * & * & -\frac{12}{\tau^3}R \end{bmatrix}, \tag{6.21}$$

$$\Phi_{QS} = \begin{bmatrix} Q - 2S & 0 & 0 & \frac{2}{\tau}S \\ * & \frac{\tau^2}{2}S & 0 & 0 \\ * & * & -Q & 0 \\ * & * & * & -\frac{2}{\tau^2}S \end{bmatrix}, \tag{6.22}$$

and

$$\Phi_{FG\ell} = \begin{bmatrix} 0 & fI & -fU\bar{H}(\ell)\mathcal{W}H^T(\ell) & 0 \\ * & 2gf & -gfU\bar{H}(\ell)\mathcal{W}H^T(\ell) & 0 \\ * & * & 0 & 0 \\ * & * & * & 0 \end{bmatrix}. \tag{6.23}$$

Thus, the designed weights w_k *of the coupling strengths are given in the diagonal of* $\mathcal{W} = \frac{1}{f}\mathcal{W}_d$ *and the Laplacian matrices are given by* $L(\ell) = \bar{H}(\ell)\frac{1}{f}\mathcal{W}_d H^T(\ell)$ *according to Lemma 6.1, where the indices* k *are given according to Algorithm 6.1.*

Proof The proof follows from Theorem 5.1, for single-order dynamics. As in the previous result, in order to keep the conditions formulated by LMIs, matrices F_ℓ and G_ℓ are chosen to be f and gf, respectively, with g an arbitrary tuning scalar.

Besides, the Laplacian matrices $L(\ell)$ are written in the alternative form given by Lemma 6.1. Thus, all terms with $F_\ell \bar{B}_\ell$ and $G_\ell \bar{B}_\ell$ in Theorem 5.1 can be rewritten as $fU\bar{H}(\ell)\mathcal{W}H^T(\ell)W$ and $gfU\bar{H}(\ell)\mathcal{W}H^T(\ell)W$, respectively. Finally, the design procedure is obtained by making the product $f\mathcal{W}$ a single matrix variable $\mathcal{W}_d$. The designed weights of the coupling strengths are thus obtained by making $\mathcal{W} = \frac{1}{f}\mathcal{W}_d$. □

6.3 Numerical Examples for fixed topology

In the following, some examples are given in order to show the applicability of Theorem 6.1 for fixed topology. Besides, it is shown that Theorem 6.1, differently from the other

design methods in the literature, can be applied to directed networks. Furthermore, by restricting the problem to undirected networks, Theorem 6.1 is compared to some results in the literature. Therefore, throughout this section it is shown that the proposed method is more general and performs better or comparable to similar ones in the literature.

Consider the network topology given in Figure 6.2 with seven agents, i.e. $m = 7$. The edges e_{ij} and weights a_{ij} are represented in Figure 6.2(a). After the application of Algorithm 2.1, the indices are changed according to Figure 6.2(b), with $r = 8$. Resulting from the application of Algorithm 2.1, it is also obtained the vectors h_k and $\bar{h}_k$ and the Incidence and Heading matrices are written according to Lemma 2.2, containing each of the h_k and $\bar{h}_k$ in its columns, respectively,

$$H = \begin{bmatrix} 1 & -1 & 0 & 0 & 0 & 0 & 0 & 0 \\ 0 & 1 & -1 & 0 & 0 & 0 & 0 & 0 \\ 0 & 0 & 1 & 1 & 0 & 0 & 0 & 0 \\ 0 & 0 & 0 & -1 & 1 & -1 & 0 & 0 \\ 0 & 0 & 0 & 0 & 0 & 1 & -1 & 0 \\ 0 & 0 & 0 & 0 & 0 & 0 & 1 & -1 \\ -1 & 0 & 0 & 0 & -1 & 0 & 0 & 1 \end{bmatrix} \text{ and } \bar{H} = \begin{bmatrix} 1 & 0 & 0 & 0 & 0 & 0 & 0 & 0 \\ 0 & 1 & 0 & 0 & 0 & 0 & 0 & 0 \\ 0 & 0 & 1 & 1 & 0 & 0 & 0 & 0 \\ 0 & 0 & 0 & 0 & 1 & 0 & 0 & 0 \\ 0 & 0 & 0 & 0 & 0 & 1 & 0 & 0 \\ 0 & 0 & 0 & 0 & 0 & 0 & 1 & 0 \\ 0 & 0 & 0 & 0 & 0 & 0 & 0 & 1 \end{bmatrix}. \tag{6.24}$$

Note that in order to apply Theorem 6.1, it is required the Laplacian given by the alternative form in Lemma 2.2, using H and $\bar{H}$ in (6.24). Before applying Theorem 6.1 it is worth to mention that this multiagent system with unitary coupling strengths $a_k = 1$ and subject to constant time-delay, i.e. $\tau_k(t) = \tau$, achieves consensus if and only if $\tau \in [0,\ 0.5554)$ Bliman and Ferrari-Trecate (2008).

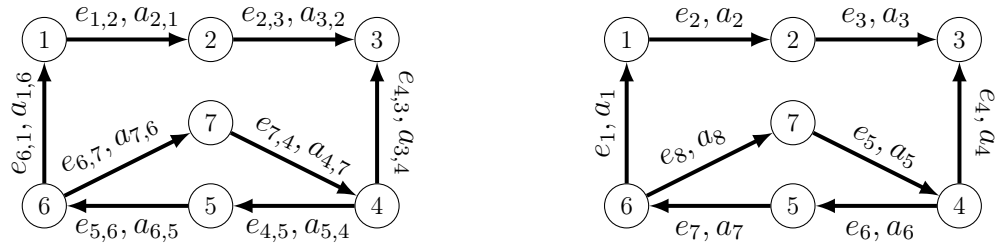

(a) Graph with indices i, j. (b) Graph with indices k.

Figure 6.2: Directed graph of the network topology with indices i, j in (a), and k in (b) after the application of Algorithm 2.1.

For illustration purpose, the multiagent system in the network given in Figure 6.2 is simulated, with dynamics in (6.1) under protocol (6.2) with unitary coupling strengths $a_k = 1$ and time-varying delays $\tau_i(t) \in [0.55,\ 0.65]$. The state trajectories for this simulation are shown in Figure 6.3 which as expected do not achieve consensus.

Now, Theorem 6.1 is applied in order to enable the system to achieve consensus when it is subject to time-varying delays out of the range $[0,\ 0.5554)$. Thus, it is used H and

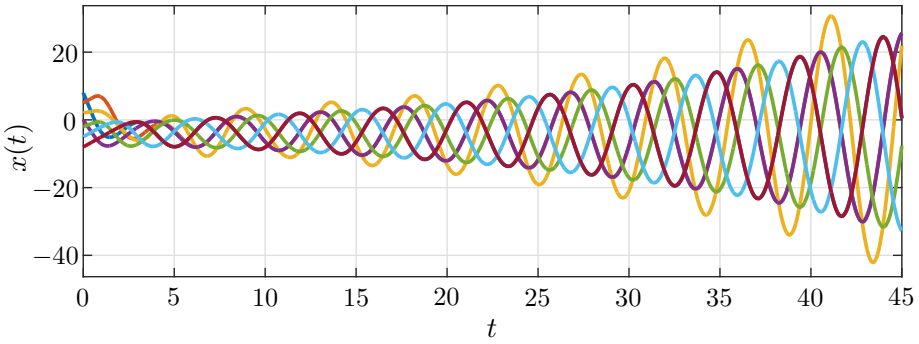

Figure 6.3: The state trajectories for the multi-agent system in Fig. 6.2, with unitary coupling strengths, subject to multiple time-varying delays $\tau_i(t) \in [0.55,\ 0.65]$, and initial states $p(0) = [8\ 5\ 2\ 0\ \ -2\ \ -5\ \ -8]^T$.

$\bar{H}$ in (6.24), $m = 7$ the number of agents, $r = 8$ the number of delays, and $\tau = 0.60$ and $\mu_m = 0.05$, such that $\tau_i(t) \in [0.55,\ 0.65]$. Moreover, initially, it is set a approximately zero convergence rate $\delta > 0$ ($\delta = 10^{-15}$) since there is no performance requirement, and choose $g = 1$ for simplicity. With this data, the LMI constraints in Theorem 6.1 are feasible and return the matrix $\mathcal{W} = \text{diag}\{0.1111,\ 0.3511,\ 0.1755,\ 0.1684,\ 0.3002,\ 0.2476,\ 0.2072,\ 0.1834\}$, containing the designed weights in its main diagonal, and thus the Laplacian for the network in Figure 6.2 with the designed weights is given by

$$L = \begin{bmatrix} 0.1111 & 0 & 0 & 0 & 0 & 0 & -0.1111 \\ -0.3511 & 0.3511 & 0 & 0 & 0 & 0 & 0 \\ 0 & -0.1755 & 0.3439 & -0.1684 & 0 & 0 & 0 \\ 0 & 0 & 0 & 0.3002 & 0 & 0 & -0.3002 \\ 0 & 0 & 0 & -0.2476 & 0.2476 & 0 & 0 \\ 0 & 0 & 0 & 0 & -0.2072 & 0.2072 & 0 \\ 0 & 0 & 0 & 0 & 0 & -0.1834 & 0.1834 \end{bmatrix}. \tag{6.25}$$

The simulation for the multiagent system achieving consensus with the designed weights is shown in Figure 6.4a.

Finally, Theorem 6.1 is applied in order to design the weights of the coupling strengths leading to better performance. For that, a search for the highest δ is carried out in a given set of discrete values for g such that the LMI conditions are feasible. Figure 6.5 illustrates the feasibility of Theorem 6.1 for various pairs (g, δ), with g ranging from 0 to 4 with a step size of 0.1, where one can check that the highest δ found is $\delta = 0.19$. Thus, for the pair with $g = 0.8$ and $\delta = 0.19$, the corresponding designed weights are given by $\mathcal{W} = \text{diag}\{0.1907,\ 1.0271,\ 0.4175,\ 0.1387,\ 0.6219,\ 0.5745,\ 0.3133,\ 0.2156\}$. The designed

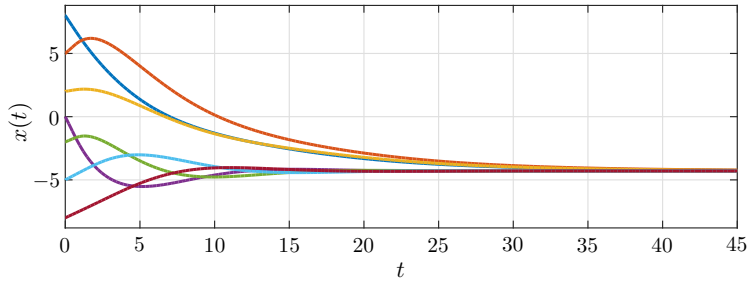

(a) Design for enabling consensus.

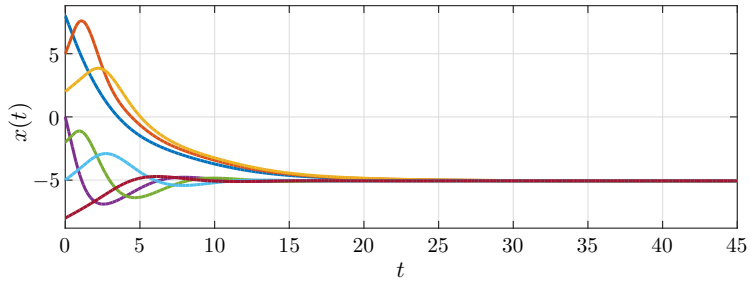

(b) Design for consensus with the highest convergence rate found.

Figure 6.4: The state trajectories for the multi-agent system in Fig. 6.2 subject to multiple time-varying delays $\tau_i(t) \in [0.55,\ 0.65]$, with initial states $p(0) = [8\ 5\ 2\ 0\ \ -2\ \ -5\ \ -8]^T$ and designed coupling strengths by Theorem 6.1 for: (a) very small $\delta > 0$ and $g = 1$; (b) $\delta = 0.19$ and $g = 0.8$.

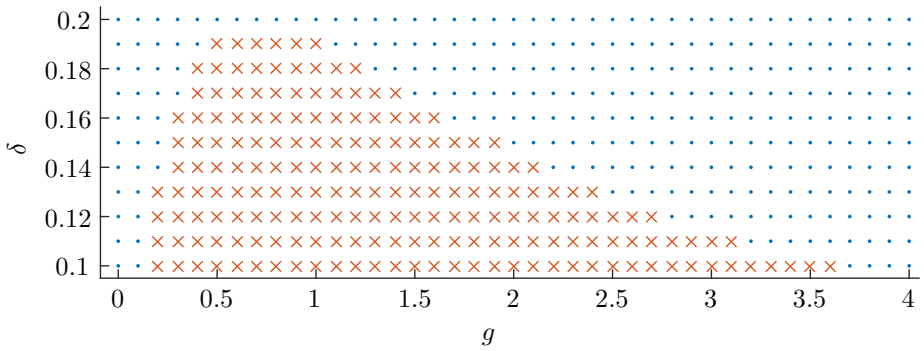

Figure 6.5: Feasibility of Theorem 6.1 for various pairs (g, δ), with g ranging from 0 to 4 with a step size of 0.1 and δ ranging from 0.1 to 0.2 with a step size of 0.01. A feasible pair is represented by cross, and an unfeasible one by dot.

Laplacian matrix is

$$L = \begin{bmatrix} 0.1907 & 0 & 0 & 0 & 0 & 0 & -0.1907 \\ -1.0271 & 1.0271 & 0 & 0 & 0 & 0 & 0 \\ 0 & -0.4175 & 0.5562 & -0.1387 & 0 & 0 & 0 \\ 0 & 0 & 0 & 0.6219 & 0 & 0 & -0.6219 \\ 0 & 0 & 0 & -0.5745 & 0.5745 & 0 & 0 \\ 0 & 0 & 0 & 0 & -0.3133 & 0.3133 & 0 \\ 0 & 0 & 0 & 0 & 0 & -0.2156 & 0.2156 \end{bmatrix}. \tag{6.26}$$

The simulation considering the designed weights is presented in Figure 6.4b. The improvement in the performance for the design with higher convergence rate is noted regarding the time needed to achieve consensus compared to Figure 6.4a.

6.3.1 Fully connected network with constant time-delay

Next, this method is compared to the example by Qiao and Sipahi (2013). This example consists of a fully connected network with seven agents, subject to a constant time-delay $\tau = 0.027$. In the work by Qiao and Sipahi (2013), a controller design procedure is shown to improve this system's performance by placing the rightmost eigenvalue further to the left of the imaginary axis. Figure 6.6 shows the simulation result using the method by Qiao and Sipahi (2013) with initial conditions $x(0) = [0\ 5\ 1\ 3\ 0\ 1\ 2]^T$, whose settling time is about 0.22 sec.

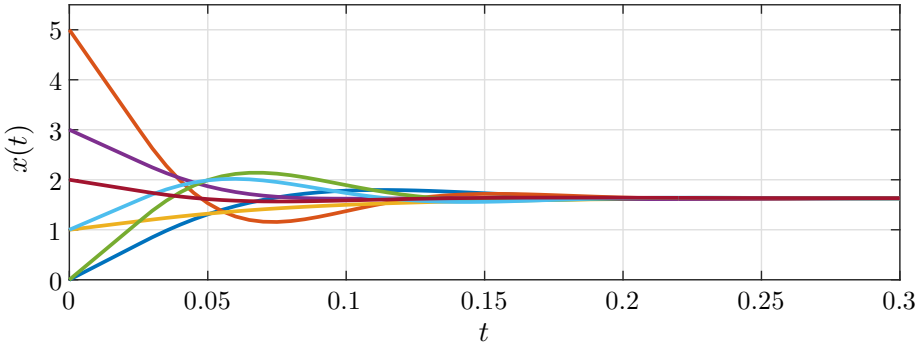

Figure 6.6: Simulation for fully connected network with coupling strengths designed by Qiao and Sipahi (2013) and constant time-delay $\tau = 0.027$.

Next, Theorem 6.1 is used to design the weights of the coupling strengths for the same example. For this fully connected topology with seven agents, $m = 7$, there are $r = 42$ directed edges, which is the maximum number of directed links in the network, i.e. $m(m-1)$. Matrices H and $\bar{H}$ are given according to Algorithm 2.1. Also, the Weight matrix W is a diagonal matrix $\text{diag}\{a_1, a_2, \ldots, a_{42}\}$.

In order to design the coupling strengths, a search for the pair (g, δ) with highest δ is carried out, with g ranging from 0 to 1 with a step size of 0.01. The highest δ found is $\delta = 23$, with $g = 0.03$. The coupling strengths are thus designed such that the Laplacian matrix is given by

$$L = \begin{bmatrix} 13.4096 & -2.2350 & -2.2349 & -2.2349 & -2.2349 & -2.2349 & -2.2350 \\ -2.2348 & 13.4092 & -2.2350 & -2.2348 & -2.2348 & -2.2349 & -2.2350 \\ -2.2350 & -2.2350 & 13.4097 & -2.2349 & -2.2348 & -2.2349 & -2.2350 \\ -2.2351 & -2.2348 & -2.2349 & 13.4096 & -2.2348 & -2.2349 & -2.2350 \\ -2.2350 & -2.2349 & -2.2349 & -2.2349 & 13.4096 & -2.2349 & -2.2351 \\ -2.2352 & -2.2350 & -2.2350 & -2.2349 & -2.2349 & 13.4099 & -2.2350 \\ -2.2347 & -2.2350 & -2.2349 & -2.2349 & -2.2349 & -2.2349 & 13.4093 \end{bmatrix}.$$

The aspect of symmetry noted in the Laplacian matrix above is expected due to the symmetry of the fully connected network topology. Note that no restrictions related to symmetry have been imposed.

Figure 6.7 shows the simulation results with the same initial conditions and the Laplacian matrix designed by the proposed method, with settling time reduced to about 0.12 sec. In this comparison, it is shown that the method is able to achieve performance better than the one presented by Qiao and Sipahi (2013). Moreover, unlike the method by Qiao and Sipahi (2013), the proposed method is able to deal with multiagent systems subject to time-varying delays, as considered next.

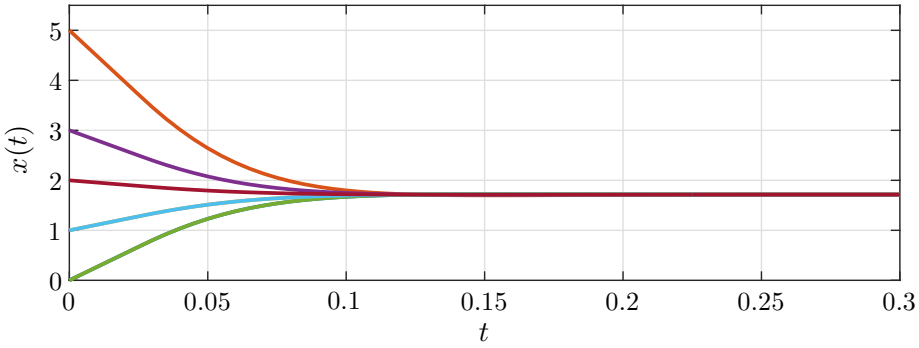

Figure 6.7: Simulation for fully connected network with coupling strengths designed by Theorem 6.1 and constant time-delay $\tau = 0.027$.

6.3.2 Fully connected network with non-differentiable time-varying delay

Now it is considered an example by Qiao and Sipahi (2014), where the authors design adaptive coupling strengths while considering a non-differentiable time-varying delay in the range $[1, 2.2]$. The multi-agent system consists of a fully connected network of five agents, $(m = 5)$, which was previously unable to achieve consensus if the time-delay is higher than 0.5166. Figure 6.8 shows the simulation considering the adaptive controller by Qiao and Sipahi (2014) with initial conditions $x(0) = [0\ 5\ 3\ 1\ 2]^T$ and settling time of about 25 sec.

For this fully connected topology with five agents there are $r = 20$ directed edges. Matrices H and $\bar{H}$ are given according to Algorithm 2.1. The Weight matrix $\mathcal{W}$ is now a diagonal matrix $\text{diag}\{a_1, a_2, \ldots, a_{20}\}$. Using Theorem 6.1, given $\tau = 1.6$ and $\mu = 0.6$ such that $\tau_i(t) \in [1,\ 2.2]$, the highest feasible δ achieved with g ranging from 0 to 2.5 with a step size of 0.01 was $\delta = 0.24$ for $g = 2.07$. The associated Laplacian matrix with the

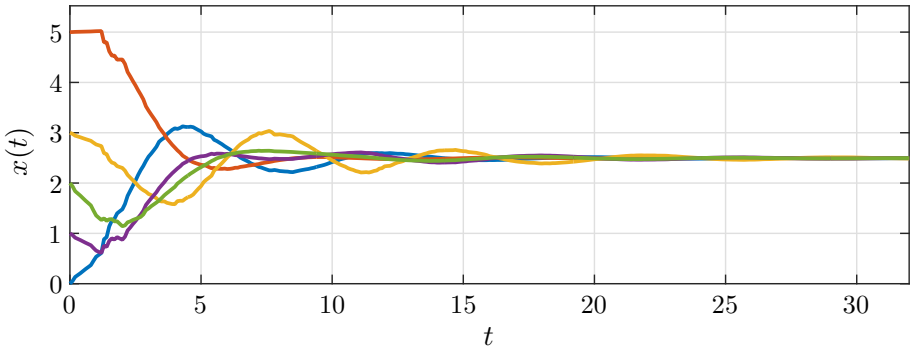

Figure 6.8: Simulation for fully connected network with adaptive controller designed by Qiao and Sipahi (2014) with non-differentiable time-varying delay in the range $[1, 2.2]$.

designed coupling strength is given by

$$L = \begin{bmatrix} 0.1894 & -0.0473 & -0.0473 & -0.0473 & -0.0473 \\ -0.0473 & 0.1894 & -0.0473 & -0.0473 & -0.0473 \\ -0.0473 & -0.0473 & 0.1894 & -0.0473 & -0.0473 \\ -0.0473 & -0.0473 & -0.0473 & 0.1894 & -0.0473 \\ -0.0473 & -0.0473 & -0.0473 & -0.0473 & 0.1894 \end{bmatrix}.$$

Figure 6.9 shows the simulation results using the proposed method for this example, with settling time reduced to about 12 sec.

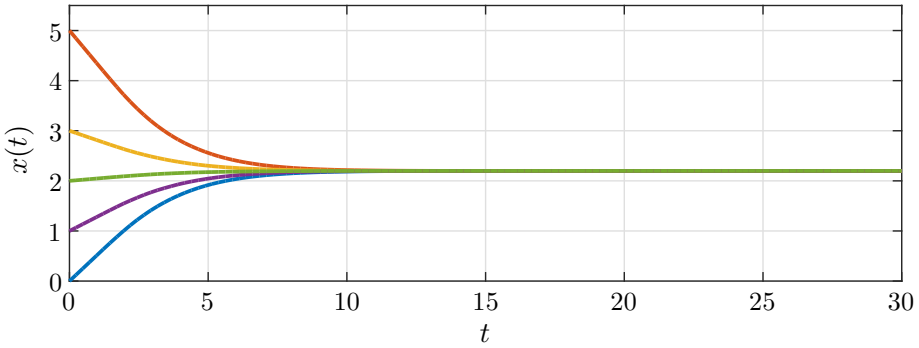

Figure 6.9: Simulation for fully connected network with coupling strengths designed by Theorem 6.1 with non-differentiable time-varying delay in the range $[1, 2.2]$.

6.4 Numerical Example for Switching Topologies

In order to illustrate the applicability of Theorem 6.2 it is considered a team of four agents that must achieve consensus on a given variable x_i, for $i = 1, \ldots, 4$, assuming time-varying delayed control inputs and intermittent communication.

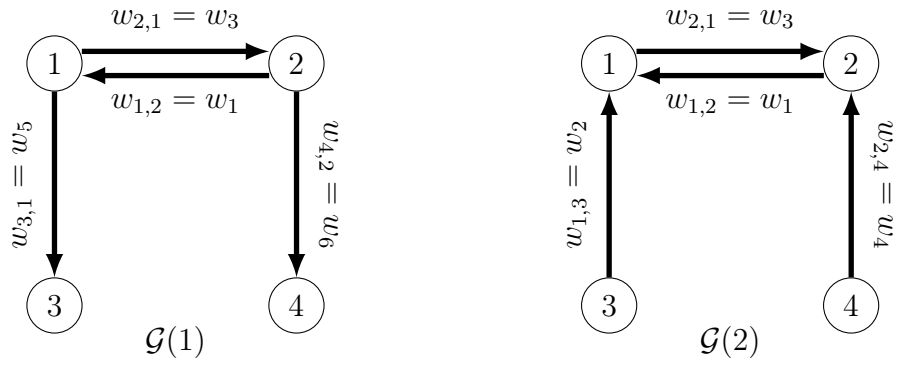

Figure 6.10: Graphs $\mathcal{G}(1)$ and $\mathcal{G}(2)$ representing the two possible topologies of the multi-agent system.

The intermittent communication is modeled as a network topology switching between the graphs $\mathcal{G}(1)$ and $\mathcal{G}(2)$. These two topologies are illustrated in Figure 6.10, also showing the representation of the coupling-strengths $w_{ij} = w_k$, for $k = 1, \ldots, 6$ the edge index according to Algorithm 6.1.

In this example, it is worth noticing that when the system is on the topology $\mathcal{G}(2)$ agents 3 and 4 do not receive information from the other agents, therefore if the system never leaves this topology it will never reach consensus, unless agents 3 and 4 are in consensus occasionally.

Initially, to represent the multi-agent system as in (6.15) it is given $r = 6$ the total number of links in the Joint graph $\bar{\mathcal{G}}$. Also, the subgraphs $\mathcal{G}(\ell)$ are associated with the following Incidence matrix $H(\ell)$ and Heading matrix $\bar{H}(\ell)$ given by Algorithm 6.1:

$$H(1) = \begin{bmatrix} 1 & 0 & -1 & 0 & -1 & 0 \\ -1 & 0 & 1 & 0 & 0 & -1 \\ 0 & 0 & 0 & 0 & 1 & 0 \\ 0 & 0 & 0 & 0 & 0 & 1 \end{bmatrix}, \quad \bar{H}(1) = \begin{bmatrix} 1 & 0 & 0 & 0 & 0 & 0 \\ 0 & 0 & 1 & 0 & 0 & 0 \\ 0 & 0 & 0 & 0 & 1 & 0 \\ 0 & 0 & 0 & 0 & 0 & 1 \end{bmatrix}, \tag{6.27}$$

and

$$H(2) = \begin{bmatrix} 1 & 1 & -1 & 0 & 0 & 0 \\ -1 & 0 & 1 & 1 & 0 & 0 \\ 0 & -1 & 0 & 0 & 0 & 0 \\ 0 & 0 & 0 & -1 & 0 & 0 \end{bmatrix}, \quad \bar{H}(2) = \begin{bmatrix} 1 & 1 & 0 & 0 & 0 & 0 \\ 0 & 0 & 1 & 1 & 0 & 0 \\ 0 & 0 & 0 & 0 & 0 & 0 \\ 0 & 0 & 0 & 0 & 0 & 0 \end{bmatrix}, \tag{6.28}$$

where indices $\ell = 1$ and $\ell = 2$ are associated to the topologies $\mathcal{G}(1)$ and $\mathcal{G}(2)$. Thus, the number of topologies is $s = 2$ and $m = 4$ is the number of agents.

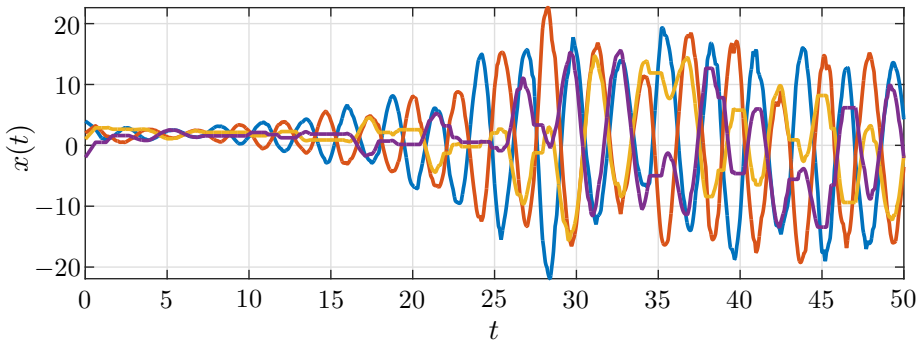

Figure 6.11: State trajectories of the multi-agent system in the numerical example without any design of the coupling strengths. The initial states are $x(0) = [4 \quad 2 \quad 1 \quad -2]^T$.

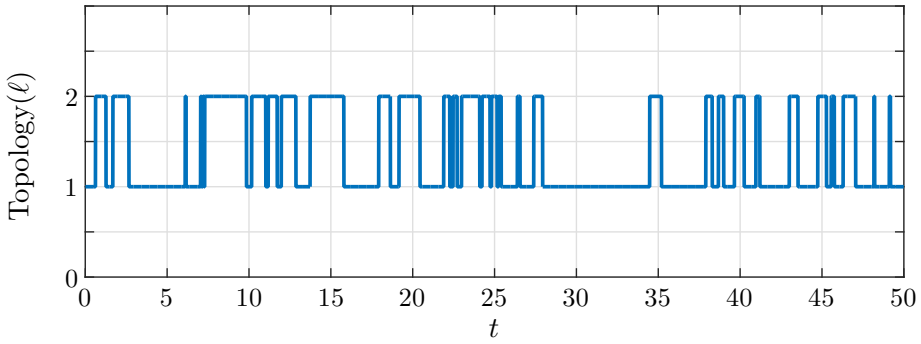

Figure 6.12: Switches of the topology for one simulation, where $l = 1, 2$ are the Markov chain states.

Moreover, assume that the switching topology dynamics is described by a continuous time Markov chain with transition rate matrix

$$\Pi = \begin{bmatrix} -1 & 1 \\ 1 & -1 \end{bmatrix}. \tag{6.29}$$

Besides, consider that the system is subject to non-differentiable and nonuniform time-varying delays $\tau_i(t) \in [\tau - \mu_m, \tau + \mu_m]$.

A numerical simulation is run considering the introduced multiagent system with $\tau = 0.7$ and $\mu_m = 0.3$, such that the time-delays can vary in the interval $\tau_i(t) \in [0.40, 1.00]$, for all i. Initially, it was considered the system without any design for the coupling strengths, i.e. all the weights of the coupling strengths $w_k = 1$ and simulated the system for 50 seconds. During this simulation, consensus is not achieved. Figure 6.11 shows the state trajectories of the multiagent system and the disagreement of the agents. The switches of topology are shown in Figure 6.12.

Next, Theorem 6.2 is used to design proper weights. So, for $\tau = 0.7$, $\mu_m = 0.3$, Π in (6.29), and the topologies described by $H(1)$, $\bar{H}(1)$ in (6.27), and $H(2)$, $\bar{H}(2)$ in

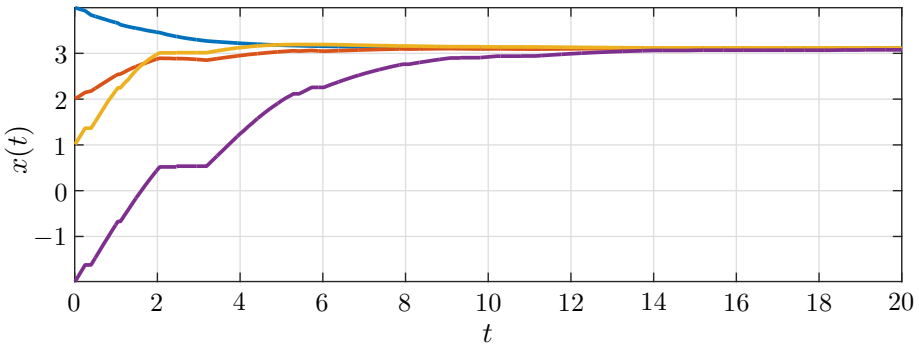

Figure 6.13: State trajectories of the multi-agent system in the numerical example with the designed coupling strengths.

(6.28), an LMI solver is applied to obtain a feasible solution. Since $\mathcal{W} = \frac{1}{f}\mathcal{W}_d$, where f and $\mathcal{W}_d$ are variables with solutions returned by the LMI solver, it results in $\mathcal{W} = \text{diag}\{0.1392,\ 0.1244,\ 0.2880,\ 0.0900,\ 0.4825,\ 0.3751\}$ such that w_k are given in its main diagonal, from w_1 to w_6.

With the designed coupling strengths, the system is simulated for 20 seconds to show that consensus is achieved, as illustrated in Figure 6.13.

Chapter 7

Dual Quaternion Pose-Consensus and Robotics

This chapter shows the extension of consensus to the algebra of dual quaternions. It enables the application of general results of consensus onto rigid-bodies pose-consensus and formation for multiple mobile manipulators. In addition, future extensions can consider this problem with the results presented for time-delays, switching topologies, and design of the coupling strengths. Examples are shown for the formation control of scalable systems with rigid-bodies and applications in cooperative robotics. It summarizes the results obtained during the exchange program at the Interactive Robotics Group in the Massachusetts Institute of Technology, in collaboration with Prof. Bruno Vilhena Adorno (UFMG) and Julie Shah (MIT). Part of the results have also been published in the work by Brito et al. (2015).

Some studies in consensus have considered multiagent systems described as rigid-bodies, with the objective of achieving a common attitude or pose (position and orientation). Some recent results are summarized next. Hatanaka et al. (2015) use homogeneous representations to describe the complete pose and make use of passivity in rigid motion to show consensus in strongly connected networks. Mayhew et al. (2012) show consensus in the attitude for undirected networks by applying a hybrid controller and a representation based on quaternions. Aldana et al. (2015) expressed the pose by means of vectors for the position and quaternions for the orientation, showing consensus in undirected networks also supporting a leader-following problem. Wang et al. (2012) considered dual quaternions for the pose in order to show consensus for networks limited to rooted-tree topologies (a tree type graph in which one of the nodes is designated as a root) and applied a control law based on the logarithm of the dual quaternions.

A unit quaternion is a singularity-free representation used to describe rigid-body ori-

entation. The logarithm of a quaternion was defined by Kim et al. (1996), which served as base for the logarithmic controller by Wang et al. (2012). Of major interest in the work of Kim et al. (1996) is the differential formula for an exponential map and is highly related to the proposed control law presented in this chapter. Additionally, as pointed by Adorno and Fraisse (2016), dual quaternions are of great interest in the representation of complete rigid motions, twists, wrenches, and several geometrical primitives—e.g. Plucker lines and planes—due to its many benefits such as: the more compact representation than, for example, Homogeneous Transformation Matrices (HTM); the ease to extract geometric parameters from a given unit dual quaternion (translation, axis of rotation and angle of rotation); the low computational cost for the multiplications of dual quaternions compared to HTM; the absence of representational singularities (although this feature is also present in HTM); and dual quaternions are easily mapped into a vector structure, which can be particularly convenient when controlling a robot, as there is no need to extract parameters from the dual quaternion to perform such task. Additionally, complex systems can be easily modeled with dual quaternions using a whole-body approach (Adorno, 2011).

The contributions of this chapter are the following: (*i*) first, the differentiable logarithmic mapping by Kim et al. (1996) is extended to dual quaternions; (*ii*) second, differently from the literature, a standard consensus-based approach is used to show consensus in the pose by means of an output given by the logarithmic mapping of the dual quaternion describing the pose of each agent, this is of great interest since making consensus in unit dual quaternions is much more complicated because unit dual quaternions lie in a non-Euclidean topological space ($\mathrm{Spin}(3) \ltimes \mathbb{R}^3$); (*iii*) this result enables the application of general results of consensus in Euclidean spaces with time-delays, switching topologies, and design of the coupling strengths onto rigid-bodies pose-consensus; (*iv*) whole-body control and consensus are used to propose a strategy that allows decentralized formation control in the 3D space for the end-effectors of mobile manipulators with kinematics models given by the algebra of dual quaternions; (*v*) finally, the proposed strategy is verified in a real world cooperative manipulation task.

7.1 Dual quaternions

A quaternion $\boldsymbol{h}$ is a number composed of one real element and three complex elements associated to the quaternionic imaginary units $\hat{\imath}$, $\hat{\jmath}$, and $\hat{k}$, such that $\boldsymbol{h} = h_1 + h_2\hat{\imath} + h_3\hat{\jmath} + h_4\hat{k}$, where $h_1, \ldots, h_4 \in \mathbb{R}$, and $\hat{\imath}^2 = \hat{\jmath}^2 = \hat{k}^2 = \hat{\imath}\hat{\jmath}\hat{k} = -1$ (Selig, 2005). The notation $\mathbb{H}$ is used to represent this set. A unit quaternion $\boldsymbol{h}$ is defined as a quaternion with unit norm $\|\boldsymbol{h}\| = 1$, with the norm of $\boldsymbol{h}$ given by $\|\boldsymbol{h}\| = \sqrt{\boldsymbol{h}^*\boldsymbol{h}}$, where $\boldsymbol{h}^* = h_1 - h_2\hat{\imath} - h_3\hat{\jmath} - h_4\hat{k}$ is the conjugate of $\boldsymbol{h}$. Unit quaternions represent the group of rotations $\mathrm{Spin}(3)$, which double

covers the 3D rotation group, often denoted as the special orthogonal group $SO(3)$. A rotation from an inertial frame $\mathcal{F}_0$ to frame $\mathcal{F}_i$ can always be represented by

$$\boldsymbol{r}_i = \cos\left(\frac{\phi_i}{2}\right) + \sin\left(\frac{\phi_i}{2}\right)\boldsymbol{n}_i, \tag{7.1}$$

where $0 \leq \phi_i < 2\pi$ is the angle of the rotation around the rotation axis $\boldsymbol{n}_i = n_{ix}\hat{\imath} + n_{iy}\hat{\jmath} + n_{iz}\hat{k}$, $\|\boldsymbol{n}_i\| = 1$. Quaternions defined as $\boldsymbol{n}_i$, whose real parts are zero, are called pure quaternions and are isomorphic to $\mathbb{R}^3$ under the addition operation, and thus can be used to represent translations (Selig, 2005).

Dual quaternions, represented by the set $\mathcal{H}$, extend the algebra of quaternions with the addition of Clifford's dual unit ε, where $\varepsilon^2 \triangleq 0$, but $\varepsilon \neq 0$ (Selig, 2005). They are composed of two quaternions as $\underline{\boldsymbol{h}} = \boldsymbol{h}_p + \varepsilon\boldsymbol{h}_d$, with $\underline{\boldsymbol{h}} \in \mathcal{H}$ the dual quaternion, and $\boldsymbol{h_p}, \boldsymbol{h}_d \in \mathbb{H}$ the primary and dual parts. More specifically, the dual quaternion can be written as $\underline{\boldsymbol{h}} = h_1 + h_2\hat{\imath} + h_3\hat{\jmath} + h_4\hat{k} + \varepsilon\left(h_5 + h_6\hat{\imath} + h_7\hat{\jmath} + h_8\hat{k}\right)$, where $h_1, \ldots, h_8 \in \mathbb{R}$. Unit dual quaternions, i.e. $\underline{\boldsymbol{x}}_i \in \mathcal{H}$ with unit norm $\sqrt{\underline{\boldsymbol{x}}_i^*\underline{\boldsymbol{x}}_i} = 1$, represent the group of rigid motions $\mathrm{Spin}(3) \ltimes \mathbb{R}^3$, which double covers $SE(3)$. Thus, a rigid motion from an inertial frame $\mathcal{F}_0$ to frame $\mathcal{F}_i$, given by a translation followed by a rotation, can always be represented by (Selig, 2005)

$$\underline{\boldsymbol{x}}_i \;=\; \boldsymbol{r}_i + \varepsilon\frac{1}{2}\boldsymbol{p}_i\boldsymbol{r}_i, \tag{7.2}$$

where $\boldsymbol{p}_i$ is a pure quaternion representing the translation from $\mathcal{F}_0$ to $\mathcal{F}_i$ and $\boldsymbol{r}_i$ is a unit quaternion representing the rotation from $\mathcal{F}_0$ to $\mathcal{F}_i$ as in (7.1).

Since $\mathrm{Spin}(3)$ and $\mathrm{Spin}(3) \ltimes \mathbb{R}^3$ are non-commutative groups, analogous to $SO(3)$ and $SE(3)$, quaternions and dual quaternions are also non-commutative under multiplications. However, some operators, called Hamilton operators, are matrices defined by Adorno (2011) for both quaternions and dual quaternions in order to commute these terms in algebraic expressions, such that, for $\boldsymbol{h}_1, \boldsymbol{h}_2 \in \mathbb{H}$ and $\underline{\boldsymbol{h}}_1, \underline{\boldsymbol{h}}_2 \in \mathcal{H}$,

$$\mathrm{vec}_4(\boldsymbol{h}_1\boldsymbol{h}_2) = \overset{+}{\mathrm{H}}_4(\boldsymbol{h}_1)\mathrm{vec}_4\boldsymbol{h}_2 = \overset{-}{\mathrm{H}}_4(\boldsymbol{h}_2)\mathrm{vec}_4\boldsymbol{h}_1, \tag{7.3}$$

$$\mathrm{vec}_8(\underline{\boldsymbol{h}}_1\underline{\boldsymbol{h}}_2) = \overset{+}{\mathrm{H}}_8(\underline{\boldsymbol{h}}_1)\mathrm{vec}_8\underline{\boldsymbol{h}}_2 = \overset{-}{\mathrm{H}}_8(\underline{\boldsymbol{h}}_2)\mathrm{vec}_8\underline{\boldsymbol{h}}_1, \tag{7.4}$$

where $\mathrm{vec}_4\boldsymbol{h} = [h_1 \ \ldots \ h_4]^T$ and $\mathrm{vec}_8\underline{\boldsymbol{h}} = [h_1 \ \ldots \ h_8]^T$ is a bijective mapping of quaternions into $\mathbb{R}^4$ and dual quaternions into $\mathbb{R}^8$, respectively, i.e. $\mathrm{vec}_4 : \mathbb{H} \to \mathbb{R}^4$ and $\mathrm{vec}_8 : \mathcal{H} \to \mathbb{R}^8$. Also,

$$\overset{+}{\mathrm{H}}_4(\boldsymbol{h}) = \begin{bmatrix} h_1 & -h_2 & -h_3 & -h_4 \\ h_2 & h_1 & -h_4 & h_3 \\ h_3 & h_4 & h_1 & -h_2 \\ h_4 & -h_3 & h_2 & h_1 \end{bmatrix}, \quad \overset{-}{\mathrm{H}}_4(\boldsymbol{h}) = \begin{bmatrix} h_1 & -h_2 & -h_3 & -h_4 \\ h_2 & h_1 & h_4 & -h_3 \\ h_3 & -h_4 & h_1 & h_2 \\ h_4 & h_3 & -h_2 & h_1 \end{bmatrix}, \tag{7.5}$$

$$\overset{+}{\mathrm{H}}_8(\underline{\boldsymbol{h}}) = \begin{bmatrix} \overset{+}{\mathrm{H}}_4(\boldsymbol{h}_p) & 0 \\ \overset{+}{\mathrm{H}}_4(\boldsymbol{h}_d) & \overset{+}{\mathrm{H}}_4(\boldsymbol{h}_p) \end{bmatrix}, \quad \overset{-}{\mathrm{H}}_8(\underline{\boldsymbol{h}}) = \begin{bmatrix} \overset{-}{\mathrm{H}}_4(\boldsymbol{h}_p) & 0 \\ \overset{-}{\mathrm{H}}_4(\boldsymbol{h}_d) & \overset{-}{\mathrm{H}}_4(\boldsymbol{h}_p) \end{bmatrix}, \tag{7.6}$$

where $\underline{\boldsymbol{h}} = \boldsymbol{h}_p + \varepsilon \boldsymbol{h}_d$, and $\overset{+}{\mathrm{H}}_4(\cdot)$, $\overset{-}{\mathrm{H}}_4(\cdot)$, $\overset{+}{\mathrm{H}}_8(\cdot)$, and $\overset{-}{\mathrm{H}}_8(\cdot)$ are the Hamilton operators defined by Adorno (2011).

The logarithm of a unit quaternion as in (7.1) is defined as (Kim et al., 1996)

$$\log \boldsymbol{r}_i = \frac{\phi_i}{2} \boldsymbol{n}_i. \tag{7.7}$$

Similarly, the logarithm of a unit dual quaternion as in (7.2) is defined as (Han et al., 2008)

$$\log \underline{\boldsymbol{x}}_i = \frac{1}{2}(\phi_i \boldsymbol{n}_i + \varepsilon \boldsymbol{p}_i). \tag{7.8}$$

Remark 7.1 *Unit dual quaternions double cover $SE(3)$, with $\underline{\boldsymbol{x}}_i$ representing the same rigid-motion as $-\underline{\boldsymbol{x}}_i$. There are cases when $\log \underline{\boldsymbol{x}}_i = \log(-\underline{\boldsymbol{x}}_i)$, although representing the same pose.*

The following Theorem, adapted from the differential formula of the exponential map by Kim et al. (1996) is of major importance for the next results.

Theorem 7.1 *Given a unit quaternion $\boldsymbol{r}_i = r_{i1} + r_{i2}\hat{\imath} + r_{i3}\hat{\jmath} + r_{i4}\hat{k}$, $\boldsymbol{r}_i = \cos(\phi_i/2) + \sin(\phi_i/2)\,\boldsymbol{n}_i$, $0 \leq \phi_i < 2\pi$, $\boldsymbol{n}_i = n_{ix}\hat{\imath} + n_{iy}\hat{\jmath} + n_{iz}\hat{k}$, $\|\boldsymbol{n}_i\| = 1$, and its logarithm given by the pure quaternion $\boldsymbol{y}_i = \log \boldsymbol{r}_i$ defined as in (7.7), $\boldsymbol{y}_i = y_{i1}\hat{\imath} + y_{i2}\hat{\jmath} + y_{i3}\hat{k}$, the logarithmic mapping is continuously differentiable and*

$$vec_4\, \dot{\boldsymbol{r}}_i = Q_4(\boldsymbol{r}_i)\, vec_4\, \dot{\boldsymbol{y}}_i, \tag{7.9}$$

where

$$Q_4(\boldsymbol{r}_i) = \begin{bmatrix} -vec_4 \boldsymbol{r}_i & \dfrac{\partial\, vec_4 \boldsymbol{r}_i}{\partial(y_{i1}, y_{i2}, y_{i3})} \end{bmatrix}, \tag{7.10}$$

$$\frac{\partial\, vec_4 \boldsymbol{r}_i}{\partial(y_{i1}, y_{i2}, y_{i3})} = \begin{bmatrix} -r_{i2} & -r_{i3} & -r_{i4} \\ \Gamma n_{ix}^2 + \Theta & \Gamma n_{ix} n_{iy} & \Gamma n_{ix} n_{iz} \\ \Gamma n_{iy} n_{ix} & \Gamma n_{iy}^2 + \Theta & \Gamma n_{iy} n_{iz} \\ \Gamma n_{iz} n_{ix} & \Gamma n_{iz} n_{iy} & \Gamma n_{iz}^2 + \Theta \end{bmatrix}, \tag{7.11}$$

with $\Gamma = r_{i1} - \Theta$, and

$$\Theta = \begin{cases} 1, & \text{if } \phi_i = 0, \\ \dfrac{\sin(\phi_i/2)}{(\phi_i/2)}, & \text{otherwise.} \end{cases} \tag{7.12}$$

Furthermore, $\text{vec}_4\,\dot{\boldsymbol{r}}_i = 0_4$ if and only if $\text{vec}_4\,\dot{\boldsymbol{y}}_i = 0_4$.

Proof The proof follows from Kim et al. (1996) noticing that $\boldsymbol{r}_i = \exp(\boldsymbol{y}_i)$. Differently from Kim et al. (1996), (7.11) is written in an alternative form and the definition of $Q_4(\boldsymbol{r}_i)$ includes the vector $-\text{vec}_4\boldsymbol{r}_i$ yielding a 4×4 dimensional matrix. This allows to use $\text{vec}_4\,\dot{\boldsymbol{y}}_i$ instead of the 3-dimensional vector of the pure quaternion $\dot{\boldsymbol{y}}_i$ in the work of Kim et al. (1996). This is done to simplify notation.

Furthermore, computing the determinant of $Q_4(\boldsymbol{r}_i)$ gives

$$\det Q_4(\boldsymbol{r}_i) = -r_{i1}[\Gamma\Theta^2(n_{ix}^2 + n_{iy}^2 + n_{iz}^2) + \Theta^3] - r_{i2}^2\Theta^2 - r_{i3}^2\Theta^2 - r_{i4}^2\Theta^2. \tag{7.13}$$

Since $\|\boldsymbol{n}_i\| = \sqrt{n_{ix}^2 + n_{iy}^2 + n_{iz}^2} = 1$, and $\Gamma = r_{i1} - \Theta$ then

$$\begin{aligned}
\det Q_4(\boldsymbol{r}_i) &= -r_{i1}^2\Theta^2 - r_{i2}^2\Theta^2 - r_{i3}^2\Theta^2 - r_{i4}^2\Theta^2, &(7.14)\\
&= -[\cos^2(\phi_i/2) + (n_{ix}^2 + n_{iy}^2 + n_{iz}^2)\sin^2(\phi_i/2)]\Theta^2, &(7.15)\\
&= -[\cos^2(\phi_i/2) + \sin^2(\phi_i/2)]\Theta^2 = -\Theta^2, &(7.16)
\end{aligned}$$

which is different from zero for $0 \leq \phi_i < 2\pi$. Thus, $Q_4(\boldsymbol{r}_i)$ is nonsingular, then $\text{vec}_4\,\dot{\boldsymbol{r}}_i = 0_4$ if and only if $\text{vec}_4\,\dot{\boldsymbol{y}}_i = 0_4$. □

Remark 7.2 *Any column-vector can be chosen for the first column of $Q_4(\boldsymbol{r}_i)$ in (7.10), yielding the same mapping for $vec_4\dot{\boldsymbol{r}}_i$. This is true since the first element of $vec_4\dot{\boldsymbol{y}}_i$ is always zero. The choice of $-vec_4\boldsymbol{r}_i$ as this column-vector in Theorem 7.1 is made in order to provide a non-singular matrix for the interval of $\phi_i \in [0, 2\pi)$.*

Next, this result is extended to the relation between the time-derivative of a unit dual quaternion and the logarithm of a unit dual quaternion.

Theorem 7.2 *Given a unit dual quaternion $\underline{\boldsymbol{x}}_i$ defined as in (7.2), and its logarithm given by the pure dual quaternion $\underline{\boldsymbol{y}}_i = \log\underline{\boldsymbol{x}}_i$ defined as in (7.8), thus*

$$vec_8\dot{\underline{\boldsymbol{x}}}_i = Q_8(\underline{\boldsymbol{x}}_i)vec_8\dot{\underline{\boldsymbol{y}}}_i, \tag{7.17}$$

with

$$Q_8(\underline{\boldsymbol{x}}_i) = \begin{bmatrix} Q_4(\boldsymbol{r}_i) & 0 \\ \frac{1}{2}\overset{+}{\mathrm{H}}_4(\boldsymbol{p}_i)Q_4(\boldsymbol{r}_i) & \overset{-}{\mathrm{H}}_4(\boldsymbol{r}_i) \end{bmatrix}, \tag{7.18}$$

where 0 is a zero matrix 4×4 and $Q_4(\boldsymbol{r}_i)$ is given in Theorem 7.1. Furthermore, $\text{vec}_8\,\dot{\underline{\boldsymbol{x}}}_i = 0_8$ if and only if $\text{vec}_8\,\dot{\underline{\boldsymbol{y}}}_i = 0_8$.

Proof Taking the time derivative of $\underline{\boldsymbol{x}}_i$ in (7.2) yields

$$\dot{\underline{\boldsymbol{x}}}_i = \dot{\boldsymbol{r}}_i + \varepsilon\frac{1}{2}(\dot{\boldsymbol{p}}_i\boldsymbol{r}_i + \boldsymbol{p}_i\dot{\boldsymbol{r}}_i). \tag{7.19}$$

Applying the operator vec_8, and the Hamilton operators $\overset{+}{\mathrm{H}}_4(\cdot)$ and $\overset{-}{\mathrm{H}}_4(\cdot)$, it gives

$$\mathrm{vec}_8\dot{\underline{\boldsymbol{x}}}_i = \begin{bmatrix} \mathrm{vec}_4\,\dot{\boldsymbol{r}}_i \\ \frac{1}{2}\overset{-}{\mathrm{H}}_4(\boldsymbol{r}_i)\mathrm{vec}_4\,\dot{\boldsymbol{p}}_i + \frac{1}{2}\overset{+}{\mathrm{H}}_4(\boldsymbol{p}_i)\mathrm{vec}_4\,\dot{\boldsymbol{r}}_i \end{bmatrix} \tag{7.20}$$

From the definition of the logarithm, $\underline{\boldsymbol{y}}_i = \boldsymbol{y}_i + \varepsilon\frac{1}{2}\boldsymbol{p}_i$, with $\boldsymbol{y}_i = \log\boldsymbol{r}_i$. Then, taking the time-derivative of $\underline{\boldsymbol{y}}_i$ and applying the vec_8 operator yields

$$\mathrm{vec}_8\dot{\underline{\boldsymbol{y}}}_i = \begin{bmatrix} \mathrm{vec}_4\,\dot{\boldsymbol{y}}_i \\ \frac{1}{2}\mathrm{vec}_4\,\dot{\boldsymbol{p}}_i, \end{bmatrix} \tag{7.21}$$

Since, from Theorem 7.1, $\mathrm{vec}_4\,\dot{\boldsymbol{r}}_i = Q_4(\boldsymbol{r}_i)\mathrm{vec}_4\,\dot{\boldsymbol{y}}_i$, considering (7.20) and (7.21) gives (7.17).

Finally, since $Q_4(\boldsymbol{r}_i)$ and $\overset{-}{\mathrm{H}}_4(\boldsymbol{r}_i)$ are nonsingular for $0 \leq \phi_i < 2\pi$, then $Q_8(\boldsymbol{r}_i)$ is nonsingular, and $\mathrm{vec}_8\,\dot{\underline{\boldsymbol{x}}}_i = 0_8$ if and only if $\mathrm{vec}_8\,\dot{\underline{\boldsymbol{y}}}_i = 0_8$. This completes the proof. □

7.2 Dual Quaternion Consensus

Consider a multiagent system with m agents, in which each agent has an output state related to a given variable of interest defined as a dual quaternion. Define the dual quaternion $\underline{\boldsymbol{y}}_i$ as the output of the i-th agent, for $i = 1, \ldots, m$. The topology of the information exchange in the network is described by a directed graph as defined in Chapter 2. The output consensus problem is to make the multiagent system reach an agreement on the output variable of interest considering only the information provided by neighboring agents. Then it is defined output consensus with dual quaternions:

Definition 7.1 *The multiagent system with output variables $\underline{\boldsymbol{y}}_i(t) \in \mathcal{H}, \forall i$, is said to asymptotically achieve output consensus on the dual quaternion variable of interest if and only if*

$$\lim_{t\to\infty}\left(\underline{\boldsymbol{y}}_i(t) - \underline{\boldsymbol{y}}_j(t)\right) = 0,\ \forall i, j = 1, \ldots, m. \tag{7.22}$$

Given the definition of output consensus, the following theorem shows a consensus protocol that enables the multi-agent system to achieve output consensus.

Theorem 7.3 *The multi-agent system composed of m agents with dynamics given by*

$$\dot{\underline{\boldsymbol{y}}}_i = \underline{\boldsymbol{u}}_i, \tag{7.23}$$

for all $i = 1, \ldots, m$, with the consensus protocol given by

$$\underline{\boldsymbol{u}}_i = -\sum_{j=1}^{m} a_{ij} \left(\underline{\boldsymbol{y}}_i - \underline{\boldsymbol{y}}_j \right), \tag{7.24}$$

where a_{ij} are the elements of the adjacency matrix of a directed graph $\mathcal{G}$ describing the network topology, achieves output consensus according to Definition 7.1 if and only if $\mathcal{G}$ has a directed spanning tree.

Proof The consensus problem in the dual quaternion variables $\underline{\boldsymbol{y}}_i$, $\forall i$ can be transformed into a stability problem with an extension to the dual quaternions of the tree-type transformation shown in Section 2.2.1. Thus, for a multi-agent system with m agents, it is defined $m-1$ dual quaternions as error variables given by

$$\underline{\boldsymbol{z}}_i = \underline{\boldsymbol{y}}_1 - \underline{\boldsymbol{y}}_{(i+1)}, \qquad i = 1, \ldots, m-1. \tag{7.25}$$

Stacking these error variables $\underline{\boldsymbol{z}}_i$ in a vector of dual quaternions $z \in \mathcal{H}^{m-1}$, where $z = [\underline{\boldsymbol{z}}_1 \ \underline{\boldsymbol{z}}_2 \ \ldots \ \underline{\boldsymbol{z}}_{(m-1)}]^T$, output consensus is asymptotically achieved if and only if z goes to zero as shown in Section 2.2.1, Proposition 2.1. Therefore, similarly to (2.11),

$$z = \underbrace{\begin{bmatrix} 1 & -1 & 0 & \cdots & 0 \\ 1 & 0 & -1 & & 0 \\ \vdots & & & \ddots & \vdots \\ 1 & 0 & 0 & \cdots & -1 \end{bmatrix}}_{U} \underbrace{\begin{bmatrix} \underline{\boldsymbol{y}}_1 \\ \underline{\boldsymbol{y}}_2 \\ \vdots \\ \underline{\boldsymbol{y}}_m \end{bmatrix}}_{y}, \tag{7.26}$$

where $U \in \mathbb{Z}^{(m-1)\times m}$ and $y = [\underline{\boldsymbol{y}}_1 \ \underline{\boldsymbol{y}}_2 \ \ldots \ \underline{\boldsymbol{y}}_m]^T$. Considering (7.26), the inverse transformation is given as in (2.13), by

$$y = \underbrace{\begin{bmatrix} 1 \\ 1 \\ \vdots \\ 1 \end{bmatrix}}_{1_m} \underline{\boldsymbol{y}}_1 + \underbrace{\begin{bmatrix} 0 & 0 & \cdots & 0 \\ -1 & 0 & \cdots & 0 \\ 0 & -1 & \cdots & 0 \\ \vdots & \vdots & \ddots & \vdots \\ 0 & 0 & \cdots & -1 \end{bmatrix}}_{W} z. \tag{7.27}$$

Thus, $y = 1_m \underline{\boldsymbol{y}}_1 + Wz$, where $W \in \mathbb{Z}^{m\times(m-1)}$.

The closed-loop dynamics considering (7.24) into (7.23) gives

$$\dot{\underline{\boldsymbol{y}}}_i = -\sum_{j=1}^{m} a_{ij}\left(\underline{\boldsymbol{y}}_i - \underline{\boldsymbol{y}}_j\right), \tag{7.28}$$

which can be written using the Laplacian matrix of the network topology $\mathcal{G}$, considering the whole multiagent system:

$$\dot{y} = -Ly. \tag{7.29}$$

Taking the time-derivative of (7.26), and then considering (7.27) and (7.29), yields

$$\dot{z} = -ULy = -UL(1_m \underline{\boldsymbol{y}}_1 + Wz),$$

and since $L1_m = 0_m$ from (2.3), it follows that

$$\dot{z} = -ULWz. \tag{7.30}$$

The equilibrium point $z = 0_{m-1}$ in (7.30) is asymptotically stable if and only if all the eigenvalues of ULW have positive real parts. As in Proposition 2.5, this happens if and only if $\mathcal{G}$ has a directed spanning tree. This concludes the proof. □

Therefore, Theorem 7.3 indicates that a dynamical system that can be written in the form of (7.28), achieves consensus depending only on the network topology.

7.3 Pose Consensus

Since the dynamical system written in the form of (7.28) relies on linear operations, which can be regarded as the most traditional consensus algorithm, the result in Theorem 7.3 can only correctly perform averaging in Euclidean spaces (Jorstad et al., 2010). For dual quaternions, consensus can not be directly applied to the unit dual quaternions $\underline{\boldsymbol{x}}_i$ in (7.2) since the group of rigid motions $\mathrm{Spin}(3) \ltimes \mathbb{R}^3$ is not Euclidean, and directly averaging unit dual quaternions does not produce meaningful values, generally not yielding a unit dual quaternion.

A workaround to this problem is to choose an output for the system that is not required to be a unit dual quaternion and thus can be averaged without losing its group properties, i.e. the logarithm $\underline{\boldsymbol{y}}_i = \log \underline{\boldsymbol{x}}_i$. From Remark 7.1 and Definition 7.1, dual quaternion pose consensus is defined.

Definition 7.2 *The multiagent system with output variables* $\underline{\boldsymbol{y}}_i = \log \underline{\boldsymbol{x}}_i$, $\forall i$, *asymptotically achieves pose consensus if consensus on the dual quaternions* $\underline{\boldsymbol{y}}_i$ *is asymptotically achieved.*

Next result summarizes the application of dual quaternion pose consensus to multiagent rigid-bodies.

Theorem 7.4 *Consider a group of* m *agents described as rigid-bodies with pose expressed by* $\underline{\boldsymbol{x}}_i$ *in* (7.2). *Let the kinematics for each agent be given as*

$$vec_8 \dot{\underline{\boldsymbol{x}}}_i = vec_8 \underline{\boldsymbol{u}}_i, \ i = 1, \ldots, m, \tag{7.31}$$

with output

$$\underline{\boldsymbol{y}}_i = \log \underline{\boldsymbol{x}}_i, \ i = 1, \ldots, m. \tag{7.32}$$

Under consensus protocol

$$vec_8 \underline{\boldsymbol{u}}_i = -Q_8(\underline{\boldsymbol{x}}_i) \sum_{j=1}^{n} a_{ij} \left(vec_8 \underline{\boldsymbol{y}}_i - vec_8 \underline{\boldsymbol{y}}_j \right), \tag{7.33}$$

where $Q_8(\underline{\boldsymbol{x}}_i)$ *is given in Theorem 7.2, the multiagent system asymptotically achieves consensus in the dual quaternion output* $\underline{\boldsymbol{y}}_i$, *which implies consensus in the pose according to Definition 7.2, if and only if the network topology described by* $\mathcal{G}$ *has a directed spanning tree.*

Proof From Theorem 7.3, a multiagent system described in the form of (7.28) is able to achieve consensus on $\underline{\boldsymbol{y}}_i$ if and only if the $\mathcal{G}$ has a directed spanning tree, which applying the vec_8 operator is equivalent to

$$\mathrm{vec}_8 \dot{\underline{\boldsymbol{y}}}_i = -\sum_{j=1}^{n} a_{ij} \left(\mathrm{vec}_8 \underline{\boldsymbol{y}}_i - \mathrm{vec}_8 \underline{\boldsymbol{y}}_j \right). \tag{7.34}$$

From Theorem 7.2, the relationship between $\dot{\underline{\boldsymbol{x}}}_i$ and $\dot{\underline{\boldsymbol{y}}}_i$ can be applied to give

$$\mathrm{vec}_8 \dot{\underline{\boldsymbol{x}}}_i = \mathrm{vec}_8 \underline{\boldsymbol{u}}_i = Q_8(\underline{\boldsymbol{x}}_i) \mathrm{vec}_8 \dot{\underline{\boldsymbol{y}}}_i. \tag{7.35}$$

Choosing $\mathrm{vec}_8 \underline{\boldsymbol{u}}_i$ as (7.33), implies (7.34) since $Q_8(\underline{\boldsymbol{x}}_i)$ is nonsingular, allowing the system to achieve consensus on the pose according to Definition 7.2. □

Corollary 7.1 *Consider the kinematics of each agent expressed by*

$$\dot{\underline{\boldsymbol{x}}}_i = \frac{1}{2} \underline{\boldsymbol{\xi}}_i \underline{\boldsymbol{x}}_i, \ i = 1, \ldots, m, \tag{7.36}$$

where $\underline{\boldsymbol{x}}_i$ *is given in* (7.2) *and the dual quaternion*

$$\underline{\boldsymbol{\xi}}_i = \boldsymbol{\omega}_i + \varepsilon(\dot{\boldsymbol{p}}_i + \boldsymbol{p}_i \times \boldsymbol{\omega}_i) \tag{7.37}$$

is the twist of agent i *at the inertial frame* $\mathcal{F}_0$*, including the angular velocity* $\boldsymbol{\omega}_i$ *and linear velocity* $\dot{\boldsymbol{p}}_i$*, and the cross-product for pure quaternions is given by*

$$\boldsymbol{p}_i \times \boldsymbol{\omega}_i = \frac{\boldsymbol{p}_i\boldsymbol{\omega}_i - \boldsymbol{\omega}_i\boldsymbol{p}_i}{2}, \tag{7.38}$$

which is equivalent to the vector product in $\mathbb{R}^3$ *given the isomorphism between pure quaternions and* $\mathbb{R}^3$ *relative to additions. If the input control actions are given as*

$$vec_8\underline{\boldsymbol{\xi}}_i = vec_8\underline{\boldsymbol{u}}_i,\ i = 1, \ldots, m, \tag{7.39}$$

consensus on the pose can be achieved by using protocol

$$vec_8\underline{\boldsymbol{u}}_i = -2\bar{\mathrm{H}}_8(\underline{\boldsymbol{x}}_i^*)Q_8(\underline{\boldsymbol{x}}_i)\sum_{j=1}^{n} a_{ij}\left(vec_8\underline{\boldsymbol{y}}_i - vec_8\underline{\boldsymbol{y}}_j\right). \tag{7.40}$$

Proof The proof follows from the application of the Hamilton operators in (7.36) and considering the protocol (7.33) in Theorem 7.4. □

7.4 Consensus-Based Formation

As presented in Section 1.4.1, in formation control problem, the goal is to make a group of agents achieve desired relative poses in relation to neighbor agents and keep this formation anywhere in space. Figure 7.1 illustrates the case of a system composed of four agents in a two-dimensional space for better visualization, and formulates the problem in terms of dual quaternions representing the poses.

The agents in the desired formation are shown in Figure 7.1a, with the coordinate frame (x-axis,y-axis) representing the inertial reference frame, (x_c, y_c) the center of formation relative to the inertial frame, and (x_i, y_i) the local coordinate frames for each agent, for all i-th agent. Each agent's desired relative pose to the center of formation is represented by the rigid motion given by the dual quaternion $\underline{\boldsymbol{\delta}}_i \in \mathcal{H}$. The dual quaternion representing the relation from the inertial frame to the center of formation, i.e. the pose of group formation, is represented by $\underline{\boldsymbol{x}}_c \in \mathcal{H}$.

The pose of each agent can be expressed by $\underline{\boldsymbol{x}}_i \in \mathcal{H}$, and the desired relation $\underline{\boldsymbol{\delta}}_i$ to the center of formation is locally known and constant. Then, each agent has its local opinion regarding the center of formation, which is considered as the agent's state and given by

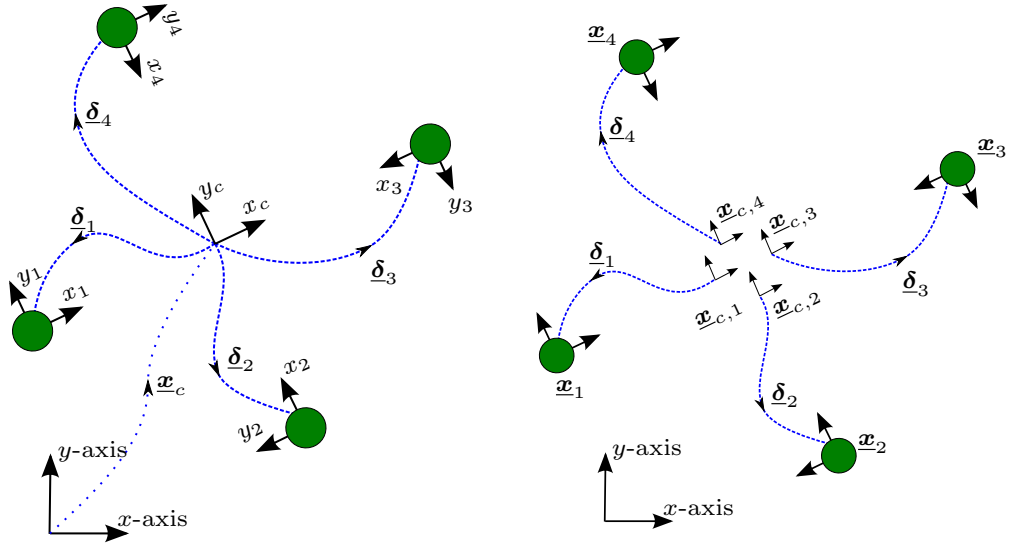

(a) Desired formation. (b) Consensus approach.

Figure 7.1: Each agent has a desired relation with the center of formation. The information exchanged is each agent's opinion on this center.

$\underline{\boldsymbol{x}}_{c,i} = \underline{\boldsymbol{x}}_i \underline{\boldsymbol{\delta}}_i^*$ as shown in Figure 7.1b. A consensus-based approach is used in order to enable all the agents to reach a common center of formation.

The information shared with neighboring agents is given by an output given as the logarithmic mapping of the agent's state, i.e.

$$\underline{\boldsymbol{y}}_{c,i} = \log \underline{\boldsymbol{x}}_{c,i} = \log(\underline{\boldsymbol{x}}_i \underline{\boldsymbol{\delta}}_i^*). \tag{7.41}$$

Finally, since the desired $\underline{\boldsymbol{\delta}}_i \in \mathcal{H}$ is locally defined (i.e. only the i-th agent has the information about its desired constant $\underline{\boldsymbol{\delta}}_i$) and the only variable that $\underline{\boldsymbol{x}}_{c,i}$ depends on is the pose $\underline{\boldsymbol{x}}_i$, the formation control problem can be defined as the problem of reaching output consensus on the $\underline{\boldsymbol{y}}_{c,i}$ variables. Therefore, the consensus protocol that enables the system to achieve formation is presented in the following theorem.

Theorem 7.5 *Consider a multiagent system composed of m agents described as rigid-bodies with pose expressed by $\underline{\boldsymbol{x}}_i$ as given in* (7.2)*. Let the kinematics for each agent be given by*

$$vec_8 \dot{\underline{\boldsymbol{x}}}_i = vec_8 \underline{\boldsymbol{u}}_i, \ i = 1, \ldots, m, \tag{7.42}$$

and each agent's output

$$\underline{\boldsymbol{y}}_{c,i} = \log(\underline{\boldsymbol{x}}_i \underline{\boldsymbol{\delta}}_i^*), \ i = 1, \ldots, m, \tag{7.43}$$

with $\underline{\boldsymbol{\delta}}_i$ the desired pose in relation to the center of formation. By means of the consensus

protocol given by

$$vec_8\underline{\boldsymbol{u}}_i = -\bar{\mathrm{H}}_8(\underline{\boldsymbol{\delta}}_i)Q_8(\underline{\boldsymbol{x}}_{c,i})\sum_{j=1}^{n} a_{ij}\left(vec_8\underline{\boldsymbol{y}}_{c,i} - vec_8\underline{\boldsymbol{y}}_{c,j}\right), \tag{7.44}$$

where a_{ij} are the elements of the adjacency matrix of the directed graph $\mathcal{G}$ describing the network topology, the multiagent system asymptotically achieves formation if and only if $\mathcal{G}$ has a directed spanning tree.

Proof From Theorem 7.2, it is given that

$$\mathrm{vec}_8\dot{\underline{\boldsymbol{x}}}_{c,i} = Q_8(\underline{\boldsymbol{x}}_{c,i})\mathrm{vec}_8\dot{\underline{\boldsymbol{y}}}_{c,i}. \tag{7.45}$$

The time-derivative of the agent's state $\underline{\boldsymbol{x}}_{c,i} = \underline{\boldsymbol{x}}_i\underline{\boldsymbol{\delta}}_i^*$ can also be given by the following, with constant $\underline{\boldsymbol{\delta}}_i$:

$$\dot{\underline{\boldsymbol{x}}}_{c,i} = \dot{\underline{\boldsymbol{x}}}_i\underline{\boldsymbol{\delta}}_i^*, \tag{7.46}$$

$$\dot{\underline{\boldsymbol{x}}}_i = \dot{\underline{\boldsymbol{x}}}_{c,i}\underline{\boldsymbol{\delta}}_i. \tag{7.47}$$

Applying the Hamilton and vec operators in (7.47) and taking $\mathrm{vec}_8\dot{\underline{\boldsymbol{x}}}_{c,i}$ from (7.45), it gives

$$\mathrm{vec}_8\dot{\underline{\boldsymbol{x}}}_i = \mathrm{vec}_8\underline{\boldsymbol{u}}_i = \bar{\mathrm{H}}_8(\underline{\boldsymbol{\delta}}_i)Q_8(\underline{\boldsymbol{x}}_{c,i})\mathrm{vec}_8\dot{\underline{\boldsymbol{y}}}_{c,i}. \tag{7.48}$$

From Theorem 7.3, a system is able to achieve consensus on $\underline{\boldsymbol{y}}_i$ if and only if the $\mathcal{G}$ has a directed spanning tree, and

$$\mathrm{vec}_8\dot{\underline{\boldsymbol{y}}}_{c,i} = -\sum_{j=1}^{n} a_{ij}\left(\mathrm{vec}_8\underline{\boldsymbol{y}}_{c,i} - \mathrm{vec}_8\underline{\boldsymbol{y}}_{c,j}\right) \tag{7.49}$$

Choosing $\underline{\boldsymbol{u}}_i$ as in (7.44), since $\bar{\mathrm{H}}_8(\underline{\boldsymbol{\delta}}_i)Q_8(\underline{\boldsymbol{x}}_{c,i})$ are all nonsingular matrices, then (7.49) is satisfied, and the system achieves consensus according to Theorem (7.3). This completes the proof. □

Corollary 7.2 *If the kinematics of each agent is expressed by* (7.36) *and the input control actions are given by*

$$vec_8\underline{\boldsymbol{\xi}}_i = vec_8\underline{\boldsymbol{u}}_i,\ i = 1,\ldots,m, \tag{7.50}$$

consensus-based formation can be achieved by using the consensus protocol

$$vec_8\underline{\boldsymbol{u}}_i = -2\bar{\mathrm{H}}_8(\underline{\boldsymbol{x}}_i^*)\bar{\mathrm{H}}_8(\underline{\boldsymbol{\delta}}_i)Q_8(\underline{\boldsymbol{x}}_{c,i})\sum_{j=1}^{n} a_{ij}\left(vec_8\underline{\boldsymbol{y}}_{c,i} - vec_8\underline{\boldsymbol{y}}_{c,j}\right). \tag{7.51}$$

Proof The proof follows from Theorem 7.5, by applying the Hamilton operators in (7.36) and considering protocol (7.44).

Remark 7.3 *It can be shown that* $\bar{\mathrm{H}}(\underline{\boldsymbol{x}}_i^*)\bar{\mathrm{H}}(\underline{\boldsymbol{\delta}}_i) = \bar{\mathrm{H}}(\underline{\boldsymbol{x}}_{c,i}^*)$*, which gives an equivalence between* (7.51) *and* (7.40) *when comparing* $\underline{\boldsymbol{x}}_{c,i}$ *and* $\underline{\boldsymbol{x}}_i$*.*

7.5 Examples

It is presented simulation results for a system composed of $m = 5$ agents. In this example, the desired formation is a circle in which $\underline{\boldsymbol{\delta}}_i$ is given such that the agents poses are equally distributed in a complete revolution around the z-axis of the center of formation, and the displacement in relation to this center is $p_y = -0.5$ in the y-axis after rotation. More specifically, for $i = 1, \ldots, 5$, the geometrical parameters are given by

$$\phi_{\delta,i} = \frac{2\pi(i-1)}{m}, \qquad \boldsymbol{p}_{\delta,i} = p_y\hat{\jmath}, \tag{7.52}$$

and

$$\boldsymbol{r}_{\delta,i} = \cos\left(\frac{\phi_{\delta,i}}{2}\right) + \hat{k}\sin\left(\frac{\phi_{\delta,i}}{2}\right), \tag{7.53}$$

$$\underline{\boldsymbol{\delta}}_i \triangleq \boldsymbol{r}_{\delta,i} + \varepsilon\frac{1}{2}\boldsymbol{r}_{\delta,i}\boldsymbol{p}_{\delta,i}. \tag{7.54}$$

For any initial position the system must achieve formation as described by $\underline{\boldsymbol{\delta}}_i$ in (7.54) anywhere in the space. The network topology is depicted in Figure 7.2, as a directed graph with a spanning tree, and does not require to be strongly connected. For simulation, the numerical integration is carried out by the formula

$$\underline{\boldsymbol{x}}_i(t + \Delta t) = \exp\left(\frac{\Delta t}{2}\underline{\boldsymbol{\xi}}_i\right)\underline{\boldsymbol{x}}_i(t), \tag{7.55}$$

where Δt is the time interval of integration, and the exponential map $\exp(\cdot)$ is given by Adorno (2011).

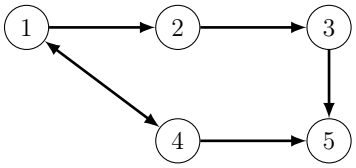

Figure 7.2: Network topology.

The simulation result is shown in Figure 7.3, where the initial and final poses are represented by orthogonal axes, the initial positions of the agents are randomly chosen and

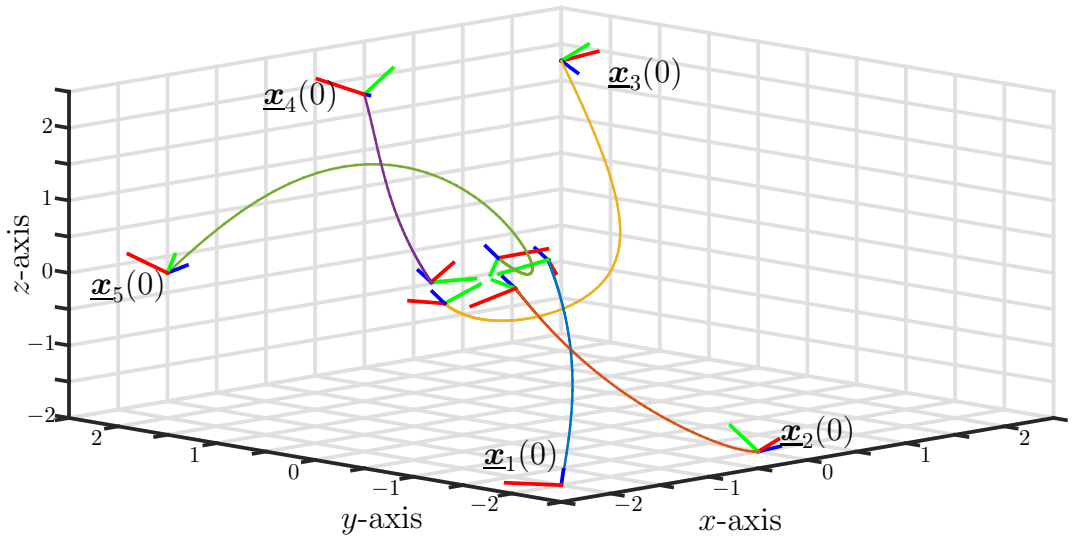

Figure 7.3: Simulation for five agents in a circular formation.

marked by $\underline{\boldsymbol{x}}_i(0)$, for $i = 1, \ldots, 5$, and the trajectories executed by each agent are shown by the continuous lines. The final circular formation is shown at the center of the figure. The state-trajectories for each part of $\underline{\boldsymbol{y}}_{c,i}(t) = y_{2c,i}\hat{\imath}+y_{3c,i}\hat{\jmath}+y_{4c,i}\hat{k}+\varepsilon(y_{6c,i}\hat{\imath}+y_{7c,i}\hat{\jmath}+y_{8c,i}\hat{k})$ are shown in Figure 7.4 as the agents achieve consensus in the dual quaternion output.

Finally, in order to show scalability, a simulation with a random fixed directed network, containing a spanning tree, and random initial poses is carried out with $m = 300$ agents. The objective is to reach a circular formation with $\underline{\boldsymbol{\delta}}_i$ chosen similarly to previous example given by (7.52), (7.53) and (7.54), with radius $p_y = 1$. The simulation is shown in Figure 7.5, where T is a unit of time dependent on the topology. Figure 7.5a shows the random initial poses, Figures 7.5b and 7.5c show snapshots as the time evolves, and Figure 7.5d shows the final achieved formation.

7.6 Whole Body Kinematics Model

Now, the results are applied in mobile manipulators modeled using dual quaternion algebra. A whole-body model is used to describe the pose of the end-effector, and the control inputs are the angular velocities of the manipulator joints and the velocities of the mobile base.

Consider a holonomic mobile base moving in the plane XY and an inertial reference frame $\mathcal{F}_0$ somewhere in the space. The position of the local reference frame $\mathcal{F}_b$ in the center of the mobile base is given by the coordinates (x, y), and the orientation is given by the rotation angle ϕ around axis Z. Thus, the generalized coordinates of the base can be written as $\theta_b = [x\ y\ \phi]^T$ and its pose, relative to $\mathcal{F}_0$, is given by the following dual

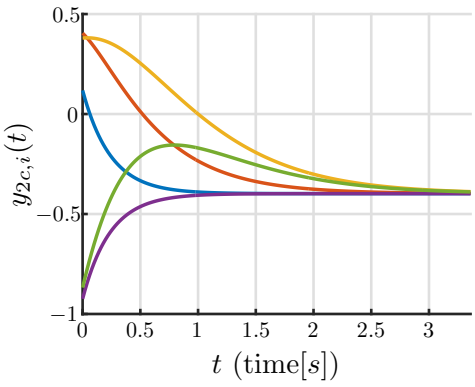

(a) $y_{2c,i}(t)$ for all agents.

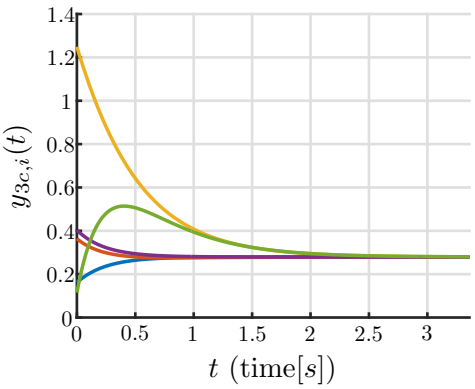

(b) $y_{3c,i}(t)$ for all agents.

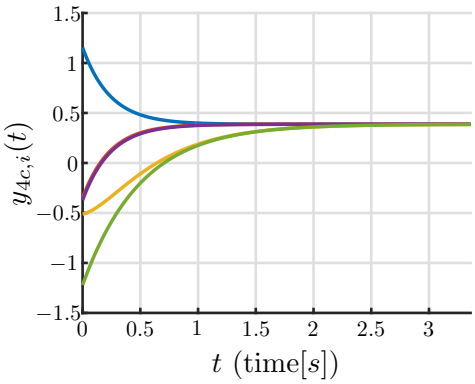

(c) $y_{4c,i}(t)$ for all agents.

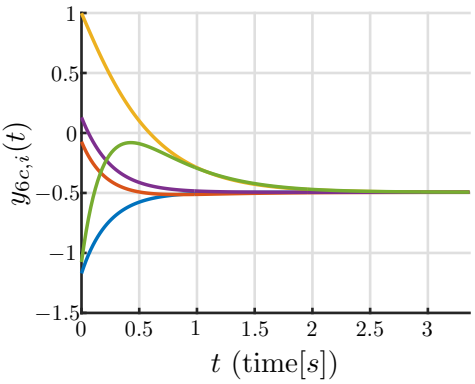

(d) $y_{6c,i}(t)$ for all agents.

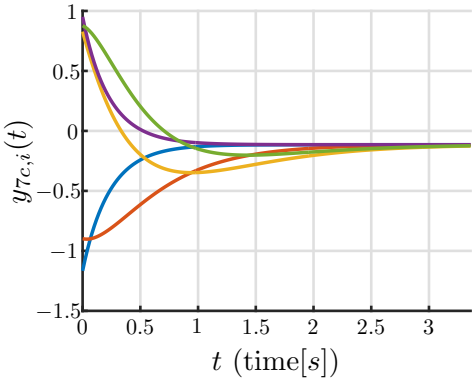

(e) $y_{7c,i}(t)$ for all agents.

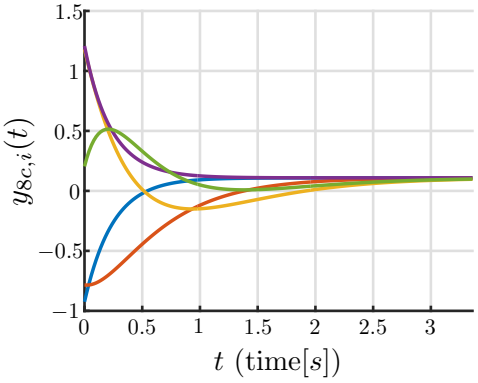

(f) $y_{8c,i}(t)$ for all agents.

Figure 7.4: Time-evolution for each part of the output.

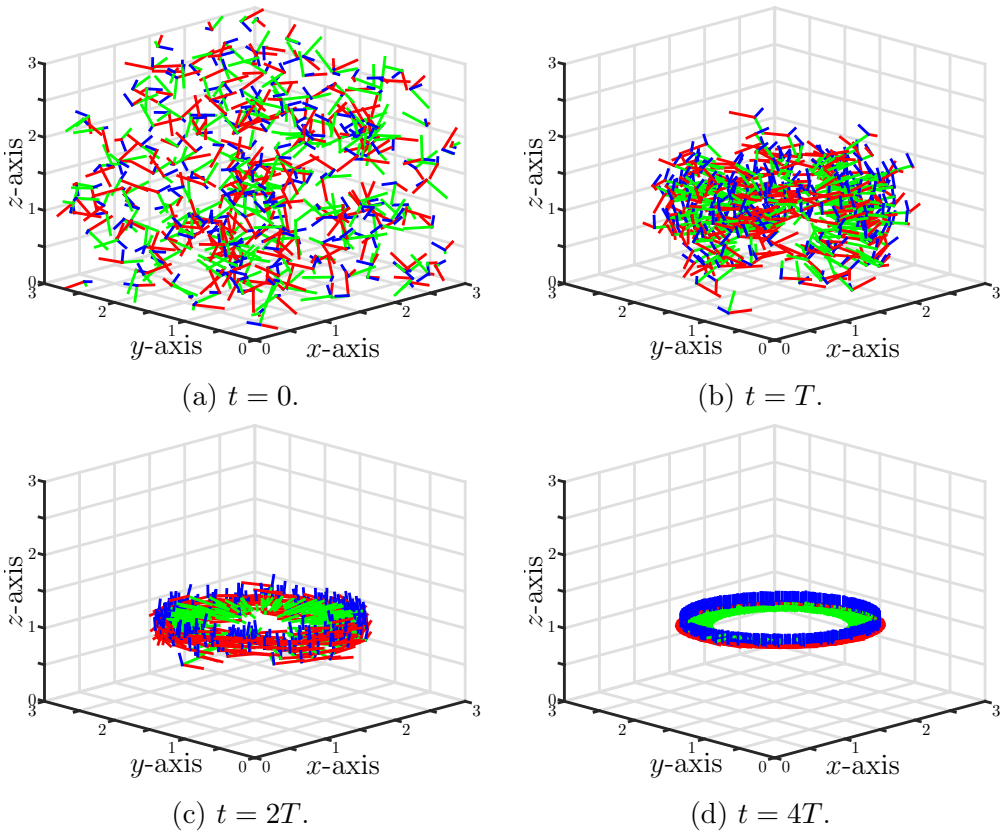

(a) $t = 0$. (b) $t = T$.

(c) $t = 2T$. (d) $t = 4T$.

Figure 7.5: Simulation for 300 agents in a circular formation.

quaternion

$$\underline{\boldsymbol{x}}_b^0 = \boldsymbol{r}_b^0 + \varepsilon \frac{1}{2} \boldsymbol{p}_b^0 \boldsymbol{r}_b^0, \tag{7.56}$$

where $\boldsymbol{r}_b^0 = \cos(\phi/2) + \hat{k}\sin(\phi/2)$ and $\boldsymbol{p}_b^0 = x\hat{\imath} + y\hat{\jmath}$ Adorno (2011).

Thus, taking the first time-derivative of (7.56) and mapping into $\mathbb{R}^8$ with the vec_8 operator, the differential forward kinematics of the holonomic mobile base is given by

$$\text{vec}_8 \dot{\underline{\boldsymbol{x}}}_b^0 = J_b \dot{\theta}_b, \tag{7.57}$$

where $J_b = [b_{ij}] \in \mathbb{R}^{8\times 3}$ with

$$\begin{aligned}
b_{13} &= -b_{62} = b_{71} = -\frac{1}{2}\sin\left(\frac{\phi}{2}\right), \\
b_{43} &= b_{61} = b_{72} = \frac{1}{2}\cos\left(\frac{\phi}{2}\right), \\
b_{63} &= -\frac{x}{4}\sin\left(\frac{\phi}{2}\right) + \frac{y}{4}\cos\left(\frac{\phi}{2}\right), \\
b_{73} &= -\frac{x}{4}\cos\left(\frac{\phi}{2}\right) - \frac{y}{4}\sin\left(\frac{\phi}{2}\right),
\end{aligned}$$

and all other elements equal zero (Adorno, 2011).

Next, consider a manipulator on top of the mobile base. Let the reference frame of the manipulator's base be $\mathcal{F}_m$ and $\underline{\boldsymbol{x}}_m^b$ be a constant dual quaternion representing the rigid-motion from $\mathcal{F}_b$ to $\mathcal{F}_m$. For a serial manipulator with η revolute joints, with θ_k the angle of the k-th joint, for $k = 1, \ldots, \eta$, the forward kinematics that relates the frame $\mathcal{F}_e$ of the end-effector to the base of the manipulator $\mathcal{F}_m$ is a function of all joints, i.e. the pose of the end-effector related to the base of the manipulator is given by the dual quaternion $\underline{\boldsymbol{x}}_e^m = f(\theta_m)$, with $\theta_m = [\theta_1 \ \ldots \ \theta_\eta]^T$ the vector containing all the joint angles.

The differential forward kinematics is given by $\dot{\underline{\boldsymbol{x}}}_e^m = f'(\theta_m)$, where $f' \triangleq df/dt$. Thus, applying the vec_8 operator, the differential forward kinematics of the manipulator is

$$\text{vec}_8 \dot{\underline{\boldsymbol{x}}}_e^m = J_m \dot{\theta}_m, \tag{7.58}$$

where $J_m = \partial f / \partial \theta_m \in \mathbb{R}^{8\times\eta}$ is the analytical Jacobian relating the joint velocities to the dual quaternion derivative. Notice that both forward kinematics and differential forward kinematics are obtained in the algebra of dual quaternions (Adorno, 2011).

Coupling the manipulator to the mobile base, the pose of the end-effector, related to the inertial coordinate frame $\mathcal{F}_0$, is described by the composition of each subsystem, i.e.

$$\underline{\boldsymbol{x}}_e^0 = \underline{\boldsymbol{x}}_b^0 \underline{\boldsymbol{x}}_m^b \underline{\boldsymbol{x}}_e^m. \tag{7.59}$$

In order to obtain the differential forward kinematics for the whole-body mobile manipulator, take the time-derivative of (7.59) (recall that $\underline{\boldsymbol{x}}_m^b$ is constant):

$$\dot{\underline{\boldsymbol{x}}}_e^0 = \dot{\underline{\boldsymbol{x}}}_b^0 \underline{\boldsymbol{x}}_m^b \underline{\boldsymbol{x}}_e^m + \underline{\boldsymbol{x}}_b^0 \underline{\boldsymbol{x}}_m^b \dot{\underline{\boldsymbol{x}}}_e^m. \tag{7.60}$$

Mapping (7.60) into $\mathbb{R}^8$, using the Hamilton operators given in (7.4), and considering the differential forward kinematics for each subsystem (7.57) and (7.58), yields

$$\text{vec}_8 \dot{\underline{\boldsymbol{x}}}_e^0 = \bar{\text{H}}_8(\underline{\boldsymbol{x}}_m^b \underline{\boldsymbol{x}}_e^m) J_b \dot{\theta}_b + \overset{+}{\text{H}}_8(\underline{\boldsymbol{x}}_b^0 \underline{\boldsymbol{x}}_m^b) J_m \dot{\theta}_m,$$

which can be written as

$$\text{vec}_8 \dot{\underline{\boldsymbol{x}}}_e^0 = J_w \dot{\theta}_w, \tag{7.61}$$

with

$$J_w = \begin{bmatrix} \bar{\text{H}}_8(\underline{\boldsymbol{x}}_m^b \underline{\boldsymbol{x}}_e^m) J_b & \overset{+}{\text{H}}_8(\underline{\boldsymbol{x}}_b^0 \underline{\boldsymbol{x}}_m^b) J_m \end{bmatrix} \tag{7.62}$$

and $\dot{\theta}_w = \begin{bmatrix} \dot{\theta}_b \\ \dot{\theta}_m \end{bmatrix}$.

7.6.1 Mobile Manipulators Formation Control

The result presented in Theorem 7.5 can be applied in the context of a multiagent system composed of multiple mobile manipulators. In this case, the objective is to achieve desired formations for the set of mobile manipulator end-effectors. Each end-effector is regarded to one agent in the multiagent system. Thus, in analogy to Theorem 7.5, define

$$\underline{\boldsymbol{x}}_{e,i}^{0} \triangleq \underline{\boldsymbol{x}}_{i}^{0}, \tag{7.63}$$

such that $\underline{\boldsymbol{x}}_{e,i}^{0}$ is the pose of the end-effector of the i-th robot, for $i = 1, \ldots, m$, given as in (7.59), with the addition of the index i relating to the i-th robot. Therefore, a whole-body control strategy is used to move the joints accordingly. Hence, from (7.61) and considering the agents kinematics (7.42) considered in Theorem 7.5, the robot's low level controller can be given by

$$\dot{\theta}_{w,i} = J_{w,i}^{\dagger}\mathrm{vec}_8\dot{\underline{\boldsymbol{x}}}_{e,i}^{0} = J_{w,i}^{\dagger}\mathrm{vec}_8\underline{\boldsymbol{u}}_i, \tag{7.64}$$

where $J_{w,i}^{\dagger}$ is the Moore-Penrose Generalized Pseudoinverse of $J_{w,i}$. Finally, replacing (7.44) into (7.64) yields the control law to achieve formation on the end-effectors of the mobile manipulators, given by

$$\dot{\theta}_{w,i} = -J_{w,i}^{\dagger}\bar{\mathrm{H}}_8(\underline{\boldsymbol{\delta}}_i)Q_8(\underline{\boldsymbol{x}}_{c,i})\sum_{j=1}^{n} a_{ij}\left(\mathrm{vec}_8\underline{\boldsymbol{y}}_{c,i} - \mathrm{vec}_8\underline{\boldsymbol{y}}_{c,j}\right).$$

Remark 7.4 *It is assumed that $vec_8\underline{\boldsymbol{u}}_i$ is in the range space of $J_{w,i}$ in order to guarantee feasible $\dot{\theta}_{w,i}$ to respect the desired $\dot{\underline{\boldsymbol{x}}}_{e,i}^{0}$ in* (7.64)*. In other words, it is assumed that the manipulator is not in a singular configuration or has not reached its joint limits (both in position and velocity).*

7.6.2 Experiment with two real KUKA youBots and a fixed reference

An experiment with actual robots is presented next. It is considered the multiagent system composed of mobile manipulators with holonomic base, namely KUKA youBots (Bischoff et al., 2011). These robots are modeled using the whole-body kinematics modeling as given in Section 7.6. Each robot is equipped with a Mini-ITX board as onboard computer, with a processor Intel AtomTM Dual Core D510 (1M Cache, 2×1.66 GHz), 2GB single-channel DDR2 667MHz memory, 32GB SSD drive, and communicate via a usb connected Vonets Wireless Wifi Vap11g. The experiments were performed at CSAIL, MIT in a laboratory equipped with a Vicon motion capture system providing the local pose for each robot wirelessly at 50Hz. The control algorithm was implemented in ROS[1] using a unit dual quaternion computational open-source library, called DQ_robotics[2].

[1] http://www.ros.org

[2] http://dqrobotics.sourceforge.net/

The formation task is described as follows. The two agents are able to send information to each other. Additionally, there is also a third virtual agent, considered as an additional agent acting as a leader, which provides a constant output reference related to the desired center of formation. This fixed reference is modeled as an agent that provides information without listening to other agents and without executing the consensus protocol to update these variables. This can be modeled by the network topology given in Figure 7.6, where node 3 is the reference and 1 and 2 are the robots.

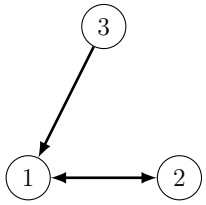

Figure 7.6: Network topology.

In this framework, agent 3 gives the constant reference about the desired center of formation, and is only reachable to agent 1. In the example below, the objective is to achieve formation around a box, whereas the position of the box is informed by the state of agent 3. For this task, the $\underline{\boldsymbol{\delta}}_i$'s are defined such that the end-effectors of agents 1 and 2 should point to the reference at a distance of 0.30m in the x axis in opposite directions, i.e.

$$\underline{\boldsymbol{\delta}}_1 = 1 - \varepsilon 0.15\hat{\imath} \tag{7.65}$$

and

$$\underline{\boldsymbol{\delta}}_2 = 1\hat{k} - \varepsilon 0.15\hat{\jmath}. \tag{7.66}$$

The initial configuration of the experiment is shown in Figure 7.7a, showing the two KUKA YouBots, agents 1 in the left and 2 in the right, and the box, whose pose will be informed by the virtual agent 3. The Laplacian Matrix is thus given by

$$L = \begin{bmatrix} 0.5 & -0.5 & 0 \\ -0.5 & 1 & -0.5 \\ 0 & 0 & 0 \end{bmatrix}, \tag{7.67}$$

where the weights of each link were all chosen 0.5 from several trials of the experiment for better performance.

During the execution of the experiment, as shown in Figures 7.7b, 7.7c, and finally Figure 7.7d, the agents are able to achieve formation around the box with the desired poses

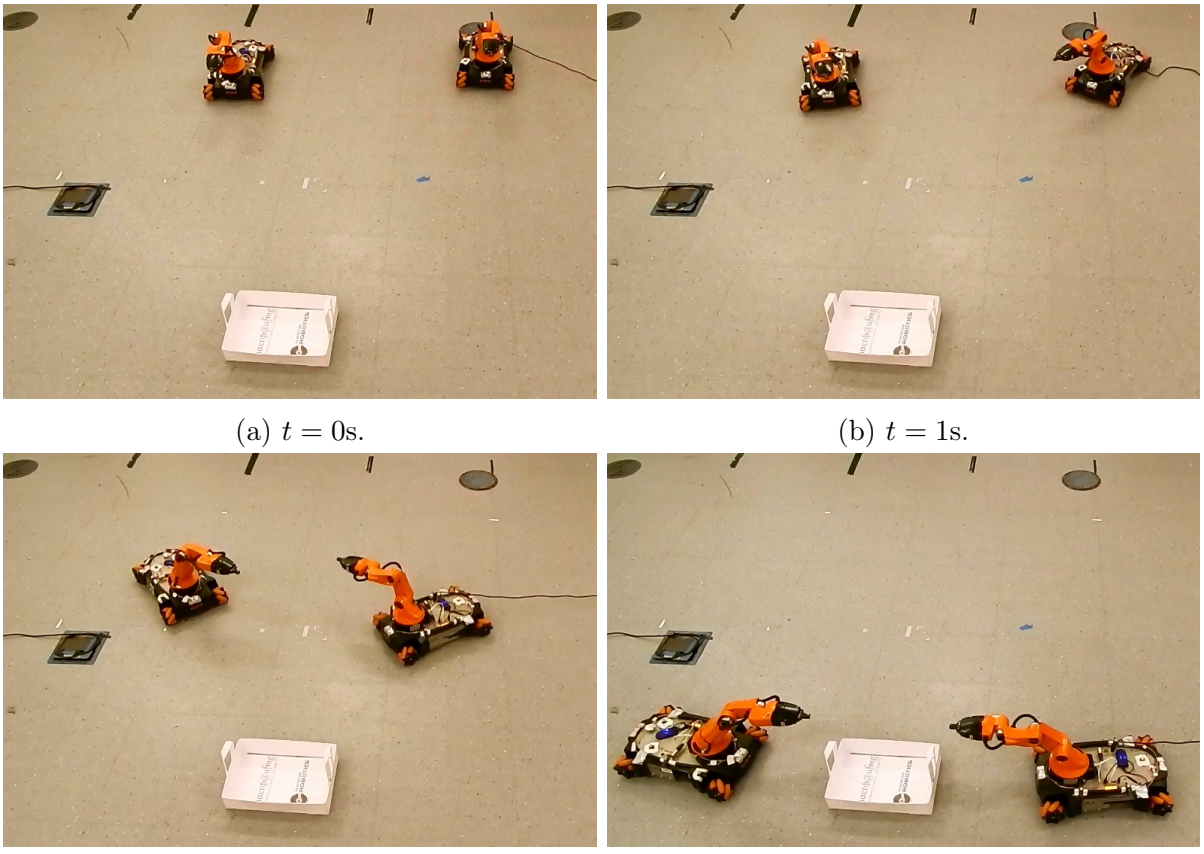

(a) $t = 0$s. (b) $t = 1$s.

(c) $t = 3$s. (d) $t = 14$s.

Figure 7.7: Experiment on formation with KUKA YouBots.

given by $\underline{\boldsymbol{\delta}}_1$ and $\underline{\boldsymbol{\delta}}_2$, relative to the center of formation, around the box. Additional trials have been recorded and are available in https://www.youtube.com/watch?v=zgz1SlpFJ5k and https://www.youtube.com/watch?v=zCD4pMG-Zdc.

The state trajectories of the outputs $\underline{\boldsymbol{y}}_{c,i} = y_{c,i,2}\hat{\imath}+y_{c,i,3}\hat{\jmath}+y_{c,i,4}\hat{k}+\varepsilon(y_{c,i,6}\hat{\imath}+y_{c,i,7}\hat{\jmath}+y_{c,i,8}\hat{k})$ for each agent are shown in Figure 7.8. The constant yellow line represents the leader state, and the blue and orange represent agents 1 and 2, respectively. The continuous lines represents the measurements of the agents outputs, and the thinner dashed lines represent a simulation carried out with the same initial pose configurations. The states mainly follow the expected behavior given by the simulation, although noises, delays, and initial conditions on velocities, which are not considered, may cause the noticed differences.

7.6.3 Application of the main result in cooperative manipulation

Finally, the proposed technique is applied to a cooperative manipulation task. It's considered the same multiagent system and communication network from Section 7.6.2, where the two agents start in arbitrary initial positions in Figure 7.7a. Given a reference about the pose of the object (box), which is passed by agent 3 to agent 1 only, and also consid-

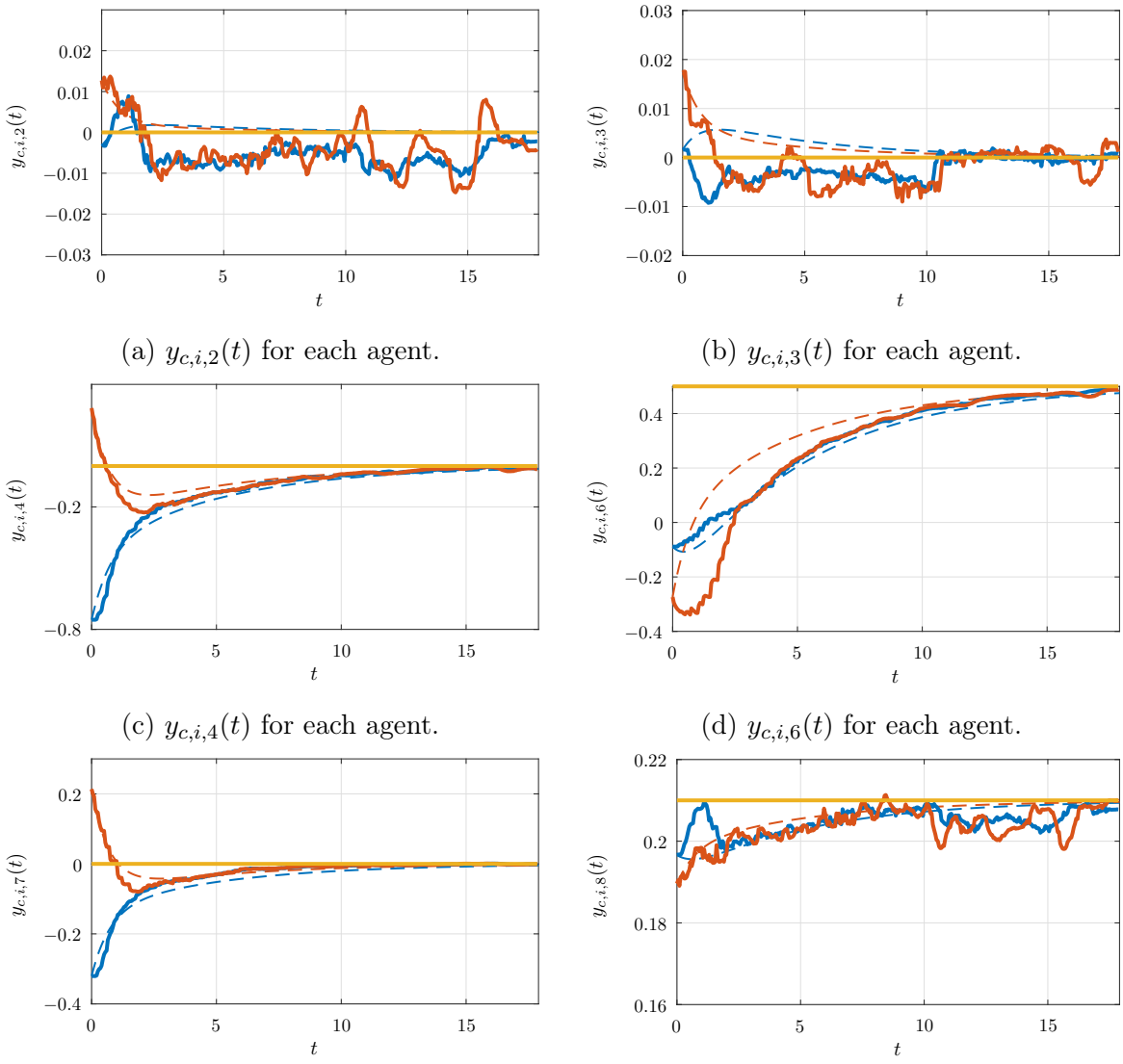

(a) $y_{c,i,2}(t)$ for each agent.

(b) $y_{c,i,3}(t)$ for each agent.

(c) $y_{c,i,4}(t)$ for each agent.

(d) $y_{c,i,6}(t)$ for each agent.

(e) $y_{c,i,7}(t)$ for each agent.

(f) $y_{c,i,8}(t)$ for each agent.

Figure 7.8: Measure and simulation of each part of the output of each agent in the experiment on formation with two KUKA YouBots.

ering the predefined $\underline{\boldsymbol{\delta}}_i$'s in (7.65) and (7.66) assigned to each agent, the agents achieve the desired formation around the box in Figure 7.7b.

Then, the references $\underline{\boldsymbol{\delta}}_i$ are changed to a lower position in the z axis and rotated around the y axis, so that the agents achieve a pre-grasping position (Figure 7.9a). By reducing the distance of each $\underline{\boldsymbol{\delta}}_i$ and returning the reference to a higher position in the z axis, the agents grasp the box by the flexible straps (Figure 7.9b). Next, the reference is changed in order to drive the agents to a pick up zone where the box is loaded (Figure 7.9c). After loading, the reference is changed again and the agents carry the box in the direction of a delivery zone, passing through the position shown in Figure 7.9d, then reaching the delivery zone in Figure 7.9e. Once the agents reach the delivery zone, the $\underline{\boldsymbol{\delta}}_i$'s are changed

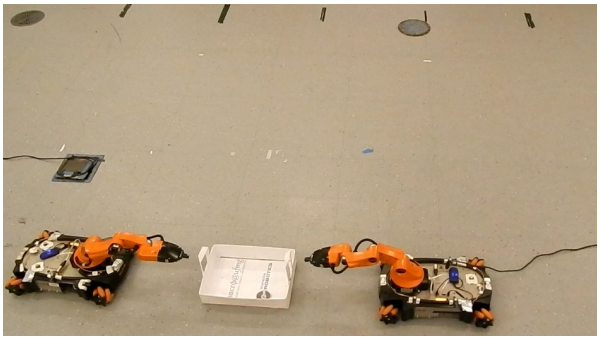

(a) Pre-grasping.

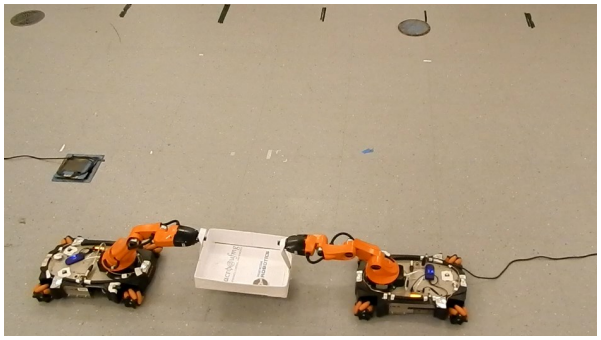

(b) Carrying the box.

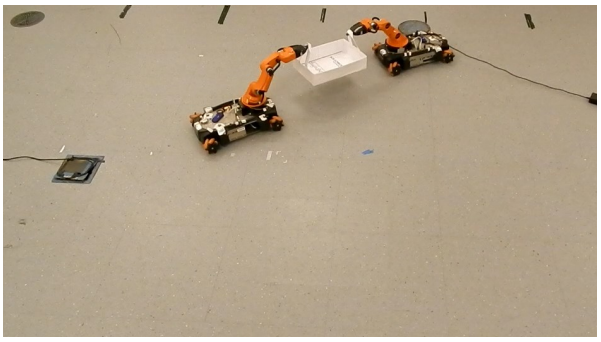

(c) Pick-up zone.

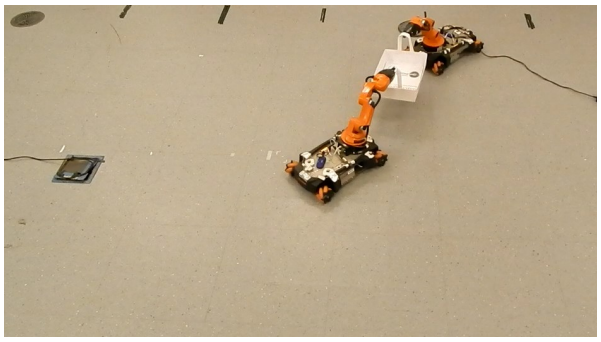

(d) Carrying the box to the delivery zone.

(e) Delivery zone.

(f) Delivering the box.

Figure 7.9: Experiment on cooperative manipulation with KUKA YouBots.

in order to release and deliver the box (Figure 7.9f).

With the interplay between changing the reference of an object, controlled by agent 3, and providing different assignments of $\underline{\boldsymbol{\delta}}_i$'s, many different tasks can be achieved, as depicted in the given example.

Conclusion

The study of consensus problems is of major importance due to the growing availability of networked distributed systems. The exchange in information and the necessity to cooperate in tasks can be appropriately described by consensus-based approaches. Chapter 1 briefly summarizes how some distributed tasks can be written as consensus problems; examples were given in formation control, flocking, and platoon. In this context, the delays in communication and processes are always present and need to be analyzed accordingly. Therefore, the effects of delays in consensus problems form the main focus of this thesis. The rewriting of the consensus problem as a stability analysis one form the basis to develop the results proposed in this thesis. To this end, Chapter 2 provides some preliminary and background results.

In Chapter 3, necessary and sufficient, i.e. exact, results were presented for the analysis of consensus in multiagent systems with agents' dynamics described by a chain of integrators subject to constant communication or input delays. The analysis carried out analytically is motivated to understand the influence of the protocol gains and the order of the chain of integrators in order to analyze the influence of different values of delays. The results have shown that the system can achieve consensus in multiple disjoint intervals of time-delay. To illustrate the theoretical results, some numerical examples were constructed and presented. Also in Chapter 3, it is presented different effects that a multiagent system may suffer when subject to communication or input delays. It was shown in Corollary 3.1 that a multiagent system with agents described as a single integrator can achieve consensus independently of the communication delay. The same is not true for input delays, as shown in Corollary 3.3 the input delay has an upper delay margin to guarantee consensus on first-order agent dynamics. For second-order integrator dynamics, in Corollary 3.2 it is shown that the system can be independent of the communication delay if the gains in the consensus protocol are properly adjusted. However for input delays, there is always an upper delay margin for the value of the delay to guarantee consensus. Therefore, it was shown the importance of studying the time-delays on intervals. It means, there are cases in which the multiagent system cannot achieve consensus when free of delays, but the introduction of the delays can lead the system to consensus, which

goes against the usual acceptance that time-delays only degrade performance. This is the main motivation for the analysis of consensus with time-varying delays with lower bound greater than zero. Different methods for the analysis of the delay margins such as de Oliveira et al. (2008) can be applied when general linear dynamics, other than a chain of integrators, has to be analyzed, however this method cannot present the explicit influence of some of the agents parameters like the order of the dynamics and the gains in the consensus protocol.

With the conclusions about delay margins of Chapter 3 in hand, Chapter 4 is centered on delay-range consensus analysis in multiagent systems subject to multiple non-differentiable time-varying delays. Due to the uncertainties in the time-delays, some sufficient conditions for the consensus analysis are proposed based on techniques usually applied in robust control such as Lyapunov-Krasovskii theory and linear matrix inequalities. An exponential decay rate was considered in the Lyapunov-Krasovskii functional which can be related to the time needed for the system to achieve consensus. These results have significantly improved the analysis of the delay margins for systems subject to multiple time-varying delays. The comparisons with previous results from the literature have shown the improvement of the method's result, which are mainly due to the treatment given to the proposed Lypaunov-Krasovskii functional, the null term, and the improved Wirtinger inequality. The transformation carried out presented limitations on the study of communication delays, in which the network topology had to be considered as a regular graph and thus cannot handle leader-following problems. Different approaches to the analysis may remove this limitation and generalize the study of communication delays. This is regarded as a future work.

In real world applications there are cases in which the multiagent system's network is subject to switches in the topology, for example when communication links fail, some sensors are obstructed, or when congestion in the communication network causes the drop of packages. Chapter 5 addresses such problems and gives some results following the lines of the analysis with Lyapunov-Krasovskii and LMIs in Chapter 4. The switching behavior was modeled as a Markov chain with uncertain transition rates, which is valuable when the model is not exactly known, as is most practical cases. It is shown that a multiagent system with switching topologies can achieve consensus even if the system is not consensable in each possible topology considered individually, this is illustrated in the numerical example of formation control with second-order models of quadrotors in Chapter 5. However, differently from the results in Chapter 4, the analysis for switching topologies has not considered the exponential convergence rate. This can be regarded as a future work and is expected to assist as a performance requirement for the design.

The design of the weights assigned to each link in the network topology, was considered in Chapter 6. The objective of this chapter was to develop a method able to provide the gains for the network couplings such that the system becomes consensable in regions of time-delays where the agents were previously unable to achieve consensus. This method is based on LMIs and is limited to single-order integrator dynamics. However, when compared to similar results in the literature, there is a noticeable improvement in the system's performance, both regarded to the convergence rate and to the delay margins. The limitation of this method is the necessity of the knowledge of the global topology or, in the case of switching topologies, all the possible topologies, and thus can only be applied prior to the execution of the task. Future results can be addressed to extension of this design to general linear dynamics, which is mainly thought by the application of BMI conditions.

As a main concern presented in the introduction of this thesis regarded to the application of consensus problems, Chapter 8 presented the application of consensus in multiagent systems composed of mobile manipulators. The main result in this chapter shows how the results on consensus presented in previous chapters can be extended to the algebra of dual quaternions and then to consensus on the pose of rigid-bodies such as robot manipulators. This is of great interest since general results for consensus on $\mathbb{R}^n$ Euclidean spaces could be extended to consensus on the pose described by the logarithm of unit dual quaternions lying on the topological space $\mathrm{Spin}(3) \ltimes \mathbb{R}^3$. The result was demonstrated in formation problems carried out in both simulations and experiments, and a framework for cooperative manipulation was described. The inherent problem of unwinding, i.e. the behavior that can cause the controller to unnecessarily perform a full rotation instead of a small angle rotation, has not been addressed, and future results can deal with switching controllers to handle this problem. Initial results in human-robot interaction have been addressed by considering the human operator as an extra agent in the system, which can lead to many future results in interactive robotics. The results presented in this final chapter were obtained during the exchange doctoral program in the context of a collaboration project between the universities UFMG (Brazil) and MIT (USA) in cooperative robotics[3].

The contributions are summarized next:

- The analytical analysis of the delay margins for multiagent systems consensus composed of agents with dynamics described by a chain of integrators. It is written the influence of the order and the gains in the consensus protocol in the delay margin

[3]Development of a framework for risk-aware heterogeneous multi-agent cooperative manipulation – CNPq/MIT N^{o} 88/2013, coordinated by Professors Bruno Adorno and Julie Shah.

intervals.

- Sufficient conditions for the analysis of consensus for agents with general linear dynamics subject to time-varying delays with guaranteed convergence rate are presented based on LMI conditions. The results perform better than similar sufficient conditions in the literature.
- It is presented guaranteed conditions for consensus with switching topologies. The topology switch is modeled as a Markov jump linear system and the transition rates are considered to be uncertain. The results are presented based on sufficient LMI conditions.
- The design for the coupling strength between the agents, with single-order integrator dynamics, is presented by means of an LMI synthesis method. This is done in order to improve the delay margins or increase the exponential convergence rate.
- The results are extended to the algebra of dual quaternions and applied on rigid-body pose consensus. The results are then applied into a practical example of formation and cooperative manipulation in system composed of multiple mobile manipulators.

The following topic are addressed as future results:

- To remove the restriction of a regular graph for the analysis of consensus with communication delays. This might be possible with the adoption of a different transformation, other than the tree-type transformation.
- The analysis of multiagent system subject to both communication and input delays.
- The extension of the analysis of switching topologies with the consideration of an exponential convergence rate.
- The extension of the design of the coupling strengths for general linear dynamics. This can possibly be addressed with the use of BMI conditions.
- Analysis of consensus with different policies for adaptive attribution of the coupling strengths or the gains in the consensus protocol. The application of Fuzzy-Logic could lead to improvements in this topic.
- The analysis of the delay margins after the application of the design of the coupling strengths. There is an interest to check if, after the synthesis of the controller for a given delay interval, the system might still be unstable in a first time-delay interval.

- The results presented in this thesis could be extended to many other problems in consensus, as the analysis of consensus with quantized outputs, consensus with heterogeneous agents, switching dynamics, platoon, etc.
- Results in cooperative manipulation, considering the interaction between human operators and multiple robots. Initial results have already been achieved on this topic.
- Analysis of hybrid controllers to deal with the unwinding problem in pose consensus.

List of Publications

During the development of this Doctoral Thesis, the following publications have been published or are in press:

1. Brito, R. P., Savino, H. J., Adorno, B. V., and Pimenta, L. C. A. (2015). Consenso utilizando Álgebra de quatérnios duais em sistemas compostos por manipuladores móveis. In *Simpósio Brasileiro de Automação Inteligente (SBAI)*, pages 1907–1912, Natal, Brazil.
2. dos Santos Junior, C. R. P., Souza, F. O., and Savino, H. J. (2014). Consenso em sistemas multiagentes sujeitos a atrasos na comunicação e topologia variável. In *Congresso Brasileiro de Automática (CBA)*, pages 99–106, Belo Horizonte, Brazil.
3. dos Santos Junior, C. R. P., Souza, F. O., and Savino, H. J. (2015). Consensus analysis in multi-agent systems subject to delays and switching topology. In *12th IFAC Workshop on Time Delay Systems (TDS)*, pages 147–152, Ann Arbor, USA.
4. Savino, H. J., Cota, A. P. L., Souza, F. O., Pimenta, L. C. A., Mendes, E. M. A. M., and Mozelli, L. A. (2013). Consensus of multi-agent systems with nonuniform non-differentiable time-varying delays. In *European Control Conference (ECC)*, pages 1884–1889, Zurich, Switzerland.
5. Savino, H. J., dos Santos, C, R. P., Souza, F. O., Pimenta, L. C. A., de Oliveira, M., and Palhares, R. M. (2016a). Conditions for consensus of multi-agent systems with time-delays and uncertain switching topology. *IEEE Transactions on Industrial Electronics*, 63(2):1258–1267.
6. Savino, H. J., Souza, F. O., and Pimenta, L. C. A. (2014a). Consenso de múltiplos agentes de segunda ordem sujeitos a retardos variantes no tempo. In *Congresso Brasileiro de Automática (CBA)*, pages 3978–3985, Belo Horizonte, Brazil.

7. Savino, H. J., Souza, F. O., and Pimenta, L. C. A. (2014b). Consensus with convergence rate in directed networks with multiple non-differentiable input delays. In *IEEE International Symposium on Intelligent Control (ISIC)*, pages 252–257, Juan-les-Pins, France.

8. Savino, H. J., Souza, F. O., and Pimenta, L. C. A. (2015). Consensus on time-delay intervals in networks of high-order integrator agents. In *12th IFAC Workshop on Time Delay Systems (TDS)*, pages 153–158, Ann Arbor, USA.

9. Savino, H. J., Souza, F. O., and Pimenta, L. C. A. (2016d). Consensus with guaranteed convergence rate of high-order integrator agents in the presence of time-varying delays. *International Journal of Systems Science*, 47(10):2475–2468.

10. Savino, H. J., Souza, F. O., and Pimenta, L. C. A. (2016e). Coupling design for consensus in switching topologies with time-varying delays. *Advances in Delays and Dynamics, in press.*

Bibliography

Adorno, B. V. (2011). *Two-arm Manipulation: From Manipulators to Enhanced Human-Robot Collaboration [Contribution à la manipulation à deux bras : des manipulateurs à la collaboration homme-robot]*. Phd dissertation, Université Montpellier 2.

Adorno, B. V. and Fraisse, P. (2016). The cross-motion invariant group and its application to kinematics. *IMA Journal of Mathematical Control and Information, online*.

Aldana, C. I., Romero, E., Nuño, E., and Basañez, L. (2015). Pose consensus in networks of heterogeneous robots with variable time delays. *International Journal of Robust and Nonlinear Control*, 25(14):2279–2298.

Bai, H. and Wen, J. T. (2010). Cooperative load transport: A formation-control perspective. *IEEE Transactions on Robotics*, 26(4):742–750.

Bischoff, R., Huggenberger, U., and Prassler, E. (2011). KUKA youBot - a mobile manipulator for research and education. In *2011 IEEE International Conference on Robotics and Automation*, pages 1–4. IEEE.

Bliman, P.-A. and Ferrari-Trecate, G. (2008). Average consensus problems in networks of agents with delayed communications. *Automatica*, 44(8):1985–1995.

Brito, R. P., Savino, H. J., Adorno, B. V., and Pimenta, L. C. A. (2015). Consenso utilizando álgebra de quatérnios duais em sistemas compostos por manipuladores móveis. In *Simpósio Brasileiro de Automação Inteligente (SBAI)*, pages 1907–1912, Natal, Brazil.

Bullo, F., Cortes, J., and Martinez, S. (2009). *Distributed control of robotic networks: A mathematical approach to motion coordination algorithms*. Princeton University Press.

Cao, Y., Yu, W., Ren, W., and Chen, G. (2013). An overview of recent progress in the study of distributed multi-agent coordination. *IEEE Transactions on Industrial Informatics*, 9(1):427–438.

Cepeda-Gomez, R. and Olgac, N. (2011a). Exhaustive stability analysis in a consensus system with time delay and irregular topologies. *International Journal of Control*, 84(4):746–757.

Cepeda-Gomez, R. and Olgac, N. (2011b). Responsible eigenvalue concept for the stability of a class of single-delay consensus dynamics with fixed topology. *IEEE Transactions on Automatic Control*, 56(7):1734–1740.

Cheng, L., Hou, Z. G., and Tan, M. (2008). Decentralized adaptive consensus control for multi-manipulator system with uncertain dynamics. In *IEEE International Conference on Systems, Man and Cybernetics*, pages 2712–2717, Singapore.

de Oliveira, M. C., Souza, F. O., and Palhares, R. M. (2008). Assessing stability of time-delay systems using rational systems. In *47th IEEE Conference on Decision and Control (CDC)*, pages 4012–4017, Cancun, Mexico.

DeGroot, M. H. (1974). Reaching a consensus. *Journal of the American Statistical Association*, 69(345):118–121.

dos Santos Junior, C. R. P., Souza, F. O., and Savino, H. J. (2014). Consenso em sistemas multiagentes sujeitos a atrasos na comunicação e topologia variável. In *Congresso Brasileiro de Automática (CBA)*, pages 99–106, Belo Horizonte, Brazil.

dos Santos Junior, C. R. P., Souza, F. O., and Savino, H. J. (2015). Consensus analysis in multi-agent systems subject to delays and switching topology. In *12th IFAC Workshop on Time Delay Systems (TDS)*, pages 147–152, Ann Arbor, USA.

Dynkin, B. O. (1965). *Markov Processes*. Springer-Verlag.

Eisenberg, E. and Gale, D. (1959). Consensus of subjective probabilities: The pari-mutuel method. *The Annals of Mathematical Statistics*, 30(1):165–168.

Fax, J. A. and Murray, R. M. (2002). Graph Laplacians and stabilization of vehicle formations. In *Proceedings of the 15th IFAC World Congress*, pages 283–288, Barcelona, Spain.

Fei, Z., Gao, H., and Shi, P. (2009). New results on stabilization of Markovian jump systems with time delay. *Automatica*, 45(10):2300–2306.

Fridman, E. (2006). A new Lyapunov technique for robust control of systems with uncertain non-small delays. *IMA Journal of Mathematical Control and Information*, 24(2):165–179.

Fridman, E. (2014). *Introduction to time-delay systems: Analysis and control*. Springer.

Fridman, E. and Niculescu, S.-I. (2008). On complete Lyapunov–Krasovskii functional techniques for uncertain systems with fast-varying delays. *International Journal of Robust and Nonlinear Control*, 18(3):364–374.

Ge, Z. and Dongya, Z. (2014). Robust consensus control for multiple robotic manipulators. In *33rd Chinese Control Conference*, pages 2229–2233, Nanjing, China.

Godsil, C. and Royle, G. F. (2003). *Algebraic graph theory*, volume 207. Springer Science & Business Media.

Gonçalves, V. M., Pimenta, L. C. A., Maia, C. A., and Pereira, G. A. S. (2010). Circulation of curves using vector fields: Actual robot experiments in 2D and 3D workspaces. In *Proceedings of the International Conference on Robotics and Automation (ICRA)*, pages 1136–1141, Anchorage, USA.

Greengard, S. (2015). *The Internet of things*. MIT Press.

Gu, K., Kharitonov, V., and Chen, J. (2003). *Stability of time-delay systems*. Birkhuser, Boston, MA.

Han, D., Wei, Q., Li, Z., and Sun, W. (2008). Control of oriented mechanical systems: A method based on dual quaternion. In *Proceedings of the 17th IFAC World Congress, Seoul, Korea*, pages 3836–3841.

Hatanaka, T., Chopra, N., Fujita, M., and Spong, M. (2015). *Passivity-Based Control and Estimation in Networked Robotics*. Springer.

Hou, Z.-G., Cheng, L., and Tan, M. (2009). Decentralized robust adaptive control for the multiagent system consensus problem using neural networks. *IEEE Transactions on Systems, Man, and Cybernetics. Part B, Cybernetics*, 39(3):636–647.

Ishii, H. and Tempo, R. (2014). The pagerank problem, multiagent consensus, and web aggregation. *IEEE Control Systems*, 34(3):34–54.

Jadbabaie, A., Lin, J., and Morse, A. S. (2003). Coordination of groups of mobile autonomous agents using nearest neighbor rules. *IEEE Transactions on Automatic Control*, 48(6):988–1001.

Jakovetic, D., Xavier, J., and Moura, J. M. (2010). Weight optimization for consensus algorithms with correlated switching topology. *IEEE Transactions on Signal Processing*, 58(7):3788–3801.

Jia, D., Lu, K., Wang, J., Zhang, X., and Shen, X. (2016). A survey on platoon-based vehicular cyber-physical systems. *IEEE Communications Surveys & Tutorials*, 18(1):263–284.

Jorstad, A., DeMenthon, D., Wang, I., Burlina, P., et al. (2010). Distributed consensus on camera pose. *IEEE Transactions on Image Processing*, 19(9):2396–2407.

Kanev, S., Scherer, C., Verhaegen, M., and Schutter, B. D. (2004). Robust output-feedback controller design via local BMI optimization. *Automatica*, 40(7):1115–1127.

Kecai, C., Chunxiang, L., Xiang, G., and Yang, H. (2011). Consensus in multi-agent with time-varying delays. In *Proceedings of the IEEE International Conference on Computer Science and Automation Engineering (CSAE)*, volume 4, pages 313–317, Shanghai, China.

Kim, M.-J., Kim, M.-S., and Shin, S. Y. (1996). A compact differential formula for the first derivative of a unit quaternion curve. *Journal of Visualization and Computer Animation*, 7(1):43–57.

Li, S., Li, K., Rajamani, R., and Wang, J. (2011a). Model predictive multi-objective vehicular adaptive cruise control. *IEEE Transactions on Control Systems Technology*, 19(3):556–566.

Li, S. E., Li, K., and Wang, J. (2013). Economy-oriented vehicle adaptive cruise control with coordinating multiple objectives function. *Vehicle System Dynamics*, 51(1):1–17.

Li, S. E., Zheng, Y., Li, K., and Wang, J. (2015). An overview of vehicular platoon control under the four-component framework. In *IEEE Intelligent Vehicles Symposium (IV)*, pages 286–291, Seoul, Korea.

Li, Y., Papachristodoulou, A., Chiang, M., and Calderbank, A. R. (2011b). Congestion control and its stability in networks with delay sensitive traffic. *Computer Networks*, 55(1):20–32.

Lin, P., Jia, Y., Du, J., and Yu, F. (2009). Average consensus for networks of continuous-time agents with delayed information and jointly-connected topologies. In *Proceedings of the American Control Conference (ACC)*, pages 3884–3889, St. Louis, USA.

Lin, P., Jia, Y., and Li, L. (2008). Distributed robust H_∞ consensus control in directed networks of agents with time-delay. *Systems & Control Letters*, 57(8):643–653.

Liu, K., Xie, G., and Wang, L. (2012). Consensus for multi-agent systems under double integrator dynamics with time-varying communication delays. *International Journal of Robust and Nonlinear Control*, 22(17):1881–1898.

Lynch, N. A. (1996). *Distributed Algorithms*. Morgan Kaufmann, San Franciso, CA.

Mayhew, C. G., Sanfelice, R. G., Sheng, J., Arcak, M., and Teel, A. R. (2012). Quaternion-based hybrid feedback for robust global attitude synchronization. *IEEE Transactions on Automatic Control*, 57(8):2122–2127.

Mesbahi, M. (2002). On a dynamic extension of the theory of graphs. In *Proceedings of the American Control Conference (ACC)*, volume 2, pages 1234–1239, Anchorage, USA.

Mesbahi, M. and Hadaegh, F. Y. (1999). Graphs, matrix inequalities, and switching for the formation flying control of multiple spacecraft. In *Proceedings of the American Control Conference (ACC)*, volume 6, pages 4148–4152, San Diego, USA.

Mesbahi, M. and Hadaegh, F. Y. (2001). Formation flying control of multiple spacecraft via graphs, matrix inequalities, and switching. *Journal of Guidance, Control, and Dynamics*, 24(2):369–377.

Miao, G., Xu, S., Zhang, B., and Zou, Y. (2014). Mean square consensus of second-order multi-agent systems under Markov switching topologies. *IMA Journal of Mathematical Control and Information*, 31(2):151–164.

Michael, N., Schwager, M., Kumar, V., and Rus, D. (2010). An experimental study of time scales and stability in networked multi-robot systems. In *Proceedings of the 2010 International Symposium on Experimental Robotics*, pages 1–13, New Delhi, India.

Moreau, L. (2004). Stability of continuous-time distributed consensus algorithms. In *Proceedings of the 43rd IEEE Conference on Decision and Control (CDC)*, volume 4, pages 3998–4003, Bahamas.

Moreau, L. (2005). Stability of multiagent systems with time-dependent communication links. *IEEE Transactions on Automatic Control*, 50(2):169–182.

Mou, S., Morse, A., and Anderson, B. (2014). Toward robust control of minimally rigid undirected formations. In *IEEE 54th Annual Conference on Decision and Control (CDC)*, pages 643–647, Los Angeles, USA.

Mozelli, L. A., Palhares, R. M., and Mendes, E. M. A. M. (2010). Equivalent techniques, extra comparisons, and less conservative control design for TS fuzzy systems. *IET Control Theory & Applications*, 4(12):2813–2822.

Neumann, J. and Burks, A. W. (1966). *Theory of self-reproducing automata*. University of Illinois press.

Norvig, T. (1967). Consensus of subjective probabilities: A convergence theorem. *The Annals of Mathematical Statistics*, 38(1):221–225.

Olfati-Saber, R. and Murray, R. (2003). Consensus protocols for networks of dynamic agents. In *Proceedings of the American Control Conference (ACC)*, volume 2, pages 951–956, Denver, USA.

Olfati-Saber, R. and Murray, R. (2004). Consensus problems in networks of agents with switching topology and time-delays. *IEEE Transactions on Automatic Control*, 49(9):1520–1533.

Pan, H., Nian, X., and Guo, L. (2014). Second-order consensus in multi-agent systems based on second-order neighbours' information. *International Journal of Systems Science*, 45(5):902–914.

Partridge, B. L. (1982). The structure and function of fish schools. *Scientific american*, 246(6):114–123.

Pimenta, L. C. A., Pereira, G. A. S., Gonçalves, M. M., Michael, N., Turpin, M., and Kumar, V. (2013). Decentralized controllers for perimeter surveillance with teams of aerial robots. *Advanced Robotics*, 27(9):697–709.

Qiao, W. and Sipahi, R. (2013). A linear time-invariant consensus dynamics with homogeneous delays: Analytical study and synthesis of rightmost eigenvalues. *SIAM Journal on Control and Optimization*, 51(5):3971–3992.

Qiao, W. and Sipahi, R. (2014). Delay-dependent coupling for a multi-agent LTI consensus system with inter-agent delays. *Physica D: Nonlinear Phenomena*, 267:112–122.

Qin, J., Yu, C., and Gao, H. (2014). Coordination for linear multiagent systems with dynamic interaction topology in the leader-following framework. *IEEE Transactions on Industrial Electronics*, 61(5):2412–2422.

Ren, W. (2007). Consensus strategies for cooperative control of vehicle formations. *IET Control Theory & Applications*, 1(2):505–512.

Ren, W. and Atkins, E. (2007). Distributed multi-vehicle coordinated control via local information exchange. *Int. J. Robust Nonlinear Control*, 17:1002–1033.

Ren, W. and Beard, R. (2008). *Distributed consensus in multi-vehicle cooperative control: theory and applications*. Springer-Verlag, London, U.K.

Ren, W., Beard, R., and Atkins, E. (2007). Information consensus in multivehicle cooperative control. *IEEE Control Systems Magazine*, 27(2):71–82.

Ren, W. and Beard, R. W. (2005). Consensus seeking in multiagent systems under dynamically changing interaction topologies. *IEEE Transactions on Automatic Control*, 50(5):655–661.

Ren, W., Moore, K., and Chen, Y. Q. (2006). High-order consensus algorithms in cooperative vehicle systems. In *IEEE International Conference on Networking, Sensing and Control (ICNSC)*, pages 457–462, Mexico City, Mexico.

Reynolds, C. W. (1987). Flocks, herds and schools: A distributed behavioral model. *ACM SIGGRAPH Computer Graphics*, 21(4):25–34.

Rigatos, G., Siano, P., and Zervos, N. (2014). Sensorless control of distributed power generators with the derivative-free nonlinear Kalman filter. *IEEE Transactions on Industrial Electronics*, 61(11):6369–6382.

Ruparelia, N. B. (2016). *Cloud computing*. MIT Press.

Sakurama, K. and Nakano, K. (2015). Necessary and sufficient condition for average consensus of networked multi-agent systems with heterogeneous time delays. *International Journal of Systems Science*, 46(5):1–13.

Savino, H. J., Cota, A. P. L., Souza, F. O., Pimenta, L. C. A., Mendes, E. M. A. M., and Mozelli, L. A. (2013). Consensus of multi-agent systems with nonuniform non-differentiable time-varying delays. In *European Control Conference (ECC)*, pages 1884–1889, Zurich, Switzerland.

Savino, H. J., dos Santos, C, R. P., Souza, F. O., Pimenta, L. C. A., de Oliveira, M., and Palhares, R. M. (2016a). Conditions for consensus of multi-agent systems with time-delays and uncertain switching topology. *IEEE Transactions on Industrial Electronics*, 63(2):1258–1267.

Savino, H. J., Souza, F. O., and Pimenta, L. C. A. (2014a). Consenso de múltiplos agentes de segunda ordem sujeitos a retardos variantes no tempo. In *Congresso Brasileiro de Automática (CBA)*, pages 3978–3985, Belo Horizonte, Brazil.

Savino, H. J., Souza, F. O., and Pimenta, L. C. A. (2014b). Consensus with convergence rate in directed networks with multiple non-differentiable input delays. In *IEEE International Symposium on Intelligent Control (ISIC)*, pages 252–257, Juan-les-Pins, France.

Savino, H. J., Souza, F. O., and Pimenta, L. C. A. (2015). Consensus on time-delay intervals in networks of high-order integrator agents. In *12th IFAC Workshop on Time Delay Systems (TDS)*, pages 153–158, Ann Arbor, USA.

Savino, H. J., Souza, F. O., and Pimenta, L. C. A. (2016b). Consensus with guaranteed convergence rate of high-order integrator agents in the presence of time-varying delays. *International Journal of Systems Science*, 47(10):2475–2468.

Savino, H. J., Souza, F. O., and Pimenta, L. C. A. (2016c). Coupling design for consensus in switching topologies with time-varying delays. *Advances in Delays and Dynamics, in press*.

Schaffer, A. (2016). 10 breakthrough technologies for 2016: Robots that teach each other. *MIT Technology Review*, 119(2).

Schwager, M., Michael, N., Kumar, V., and Rus, D. (2011). Time scales and stability in networked multi-robot systems. In *2011 IEEE International Conference on Robotics and Automation (ICRA)*, pages 3855–3862, Shanghai, China.

Selig, J. M. (2005). *Geometric fundamentals of robotics*. Springer-Verlag New York Inc., 2nd edition.

Seuret, A. and Gouaisbaut, F. (2013). Wirtinger-based integral inequality: Application to time-delay systems. *Automatica*, 49(9):2860–2866.

Sipahi, R. and Qiao, W. (2011). Responsible eigenvalue concept for the stability of a class of single-delay consensus dynamics with fixed topology. *IET Control Theory & Applications*, 5(4):622–629.

Souza, F. O., Palhares, R. M., and Barbosa, K. A. (2008). New improved delay-dependent H_∞ filter design for uncertain neutral systems. *IET Control Theory & Applications*, 2(12):1033–1043.

Stone, M. (1961). The opinion pool. *The Annals of Mathematical Statistics*, 32(4):1339–1342.

Sugihara, K. and Suzuki, I. (1990). Distributed motion coordination of multiple mobile robots. In *Proceedings of the 5th IEEE International Symposium on Intelligent Control (ISIC)*, pages 138–143, Philadelphia, USA.

Sun, J., Liu, G. P., and Chen, J. (2009). Delay-dependent stability and stabilization of neutral time-delay systems. *Int. J. Robust Nonlinear Control*, 19(12):1364–1375.

Sun, Y. G. and Wang, L. (2009). Consensus of multi-agent systems in directed networks with nonuniform time-varying delays. *IEEE Transactions on Automatic Control*, 54(7):1607–1613.

Sun, Z., Helmke, U., and Anderson, B. D. (2015). Rigid formation shape control in general dimensions: An invariance principle and open problems. In *IEEE 54th Annual Conference on Decision and Control (CDC)*, pages 6095–6100, Osaka, Japan.

Suzuki, I. and Yamashita, M. (1999). Distributed anonymous mobile robots: Formation of geometric patterns. *SIAM Journal on Computing*, 28(4):1347–1363.

Swaroop, D., Hedrick, J. K., Chien, C. C., and Ioannou, P. (1994). A comparision of spacing and headway control laws for automatically controlled vehicles. *Vehicle System Dynamics*, 23(1):597–625.

Tanaka, O. (1992). Forming a circle by distributed anonymous mobile robots. *Bachelor thesis, Hiroshima University.*

Tanenbaum, A. S. and Van Steen, M. (2007). *Distributed systems: Principles and Paradigms.* Pearson Prentice Hall.

Tsugawa, S. (2002). Inter-vehicle communications and their applications to intelligent vehicles: An overview. In *IEEE Intelligent Vehicle Symposium*, volume 2, pages 564–569, Versailles, France.

Vicsek, T., Czirók, A., Jacob, E. B., Cohen, I., and Schochet, O. (1995). Novel type of phase transitions in a system of self-driven particles. *Physical Review Letters*, 75(6):1226–1229.

Walton, K. and Marshall, J. E. (1987). Direct method for TDS stability analysis. In *IEE Proceedings D – Control Theory and Applications*, pages 101–107.

Wang, H. (2016). Second-order consensus of networked thrust-propelled vehicles on directed graphs. *IEEE Transactions on Automatic Control*, 61(1):222–227.

Wang, J. and Beni, G. (1988). Cellular robotic systems: Self-organizing robots and kinetic pattern generation. In *IEEE International Workshop on Intelligent Robots (IROS)*, pages 139–144, Tokyo, Japan.

Wang, P. K. C., Hadaegh, F. Y., and Lau, K. (1999). Synchronized formation rotation and attitude control of multiple free-flying spacecraft. *Journal of Guidance, Control, and Dynamics*, 22(1):28–35.

Wang, X., Yu, C., and Lin, Z. (2012). A dual quaternion solution to attitude and position control for rigid-body coordination. *IEEE Transactions on Robotics*, 28(5):1162–1170.

Wentzell, A. D., Chomet, S., and Chung, K. L. (1981). *Introduction to time-delay systems: Analysis and control.* McGraw-Hill International, New York.

Wieland, P., Kim, J. S., Scheu, H., and Allgöwer, F. (2008). On consensus in multi-agent systems with linear high-order agents. In *Proceedings of the IFAC World Congress*, pages 1541–1546, Seoul, Korea.

Winkler, R. L. (1968). The consensus of subjective probability distributions. *Management Science*, 15(2):B–61–B–75.

Xi, J., Li, H., Cai, N., and Zhong, Y. (2013). Consensus of swarm systems with time delays and topology uncertainties. *IET Control Theory & Applications*, 7(8):1168–1178.

Xia, C., Geng, Q., Gu, X., Shi, T., and Song, Z. (2012). Input–output feedback linearization and speed control of a surface permanent-magnet synchronous wind generator with the boost-chopper converter. *IEEE Transactions on Industrial Electronics*, 59(9):3489–3500.

Xiao, L. and Boyd, S. (2004). Fast linear iterations for distributed averaging. *Systems & Control Letters*, 53(1):65–78.

Xiao, L. and Gao, F. (2011). Practical string stability of platoon of adaptive cruise control vehicles. *IEEE Transactions on Intelligent Transportation Systems*, 12(4):1184–1194.

Xiong, J. and Lam, J. (2009). Robust H_2 control of Markovian jump systems with uncertain switching probabilities. *International Journal of Systems Science*, 40(3):255–265.

Xiong, J., Lam, J., Gao, H., and Ho, D. W. C. (2005). On robust stabilization of Markovian jump systems with uncertain switching probabilities. *Automatica*, 41(5):897–903.

Xu, S. and Lam, J. (2005). Improved delay-dependent stability criteria for time-delay systems. *IEEE Transactions on Automatic Control*, 50(3):384–387.

Yang, B. (2013). Stability switches of arbitrary high-order consensus in multiagent networks with time delays. *The Scientific World Journal*, 2013.

Yu, W., Chen, G., and Cao, M. (2010). Some necessary and sufficient conditions for second-order consensus in multi-agent dynamical systems. *Automatica*, 46(6):1089–1095.

Zhang, L. and Boukas, E. (2009). Stability and stabilization of Markovian jump linear systems with partly unknown transition probabilities. *Automatica*, 45(2):463–468.

Zhang, L., Boukas, E., and Lam, J. (2008). Analysis and synthesis of Markov jump linear systems with time-varying delays and partially known transition probabilities. *IEEE Transactions on Automatic Control*, 53(10):2458–2464.

Zhang, Q., Niu, Y., Wang, L., Shen, L., and Zhu, H. (2011). Average consensus seeking of high-order continuous-time multi-agent systems with multiple time-varying communication delays. *International Journal of Control, Automation and Systems*, 9(6):1209–1218.

Zhao, H., Xu, S., and Yuan, D. (2011). An LMI approach to consensus in second-order multi-agent systems. *International Journal of Control, Automation and Systems*, 9(6):1111–1115.

Zheng, Y., Li, S. E., Wang, J., Cao, D., and Li, K. (2016). Stability and scalability of homogeneous vehicular platoon: Study on the influence of information flow topologies. *IEEE Transactions on Intelligent Transportation Systems*, 17(1):14–26.